AL/EQ-TR-1996-0027

EVALUATION OF NATURAL ATTENTUATION OF ORGANIC TRACERS AT THE MADE SITE USING THE BIOPLUME II TRANSPORT MODEL

James Beach, Dennis Fryar, Hanadi Rifai,
Kevin Appling, Thomas B. Stauffer

INTERA Inc.
6850 Austin Center Boulevard
Suite 300
Austin TX 78731

ENVIRONICS DIRECTORATE
139 Barnes Drive, Suite 2
Tyndall AFB FL 32403-5323

March 1996

Final Technical Report for Period May 1995 - March 1996

ARMSTRONG LABORATORY

AIR FORCE MATERIEL COMMAND
TYNDALL AIR FORCE BASE, FLORIDA 32403-5323

NOTICES

This report was prepared as an account of work sponsored by an agency of the United States Government. Neither the United States Government nor any agency thereof, nor any employees, nor any of their contractors, subcontractors, or their employees, make any warranty, expressed or implied, or assume any legal liability or responsibility for the accuracy, completeness, or usefulness of any privately owned rights. Reference herein to any specific commercial products, process, or service by trade name, trademark, manufacturer, or otherwise, does not necessarily constitute or imply its endorsement, recommendation, or favoring by the United States Government or any agency, contractor, or subcontractor thereof. The views and opinions of the authors expressed herein do not necessarily state or reflect those of the United States Government or any agency, contractor, or subcontractor thereof.

When Government drawings, specifications, or other data are used for any purpose other than in connection with a definitely Government-related procurement, the United States Government incurs no responsibility or any obligation whatsoever. The fact that the Government may have formulated or in any way supplied the said drawings, specifications, or other data, is not to be regarded by implication, or otherwise in any manner construed, as licensing the holder or any other person or corporation; or as conveying any rights or permission to manufacture, use, or sell any patented invention that may in any way be related thereto.

This technical report has been reviewed by the Public Affairs Office (PA) and is releasable to the National Technical Information Service, where it will be available to the general public, including foreign nationals.

This report has been reviewed and is approved for publication.

FOR THE COMMANDER:

Thomas B. Stauffer

THOMAS B. STAUFFER, PhD
Chief, Environmental Chemical Processes

JIMMY C. CORNETTE, PhD
Chief, Environmental Research Division

REPORT DOCUMENTATION PAGE

Form Approved
OMB No. 0704-0188

1. AGENCY USE ONLY *(Leave blank)*	2. REPORT DATE	3. REPORT TYPE AND DATES COVERED
	March 15, 1996	Final -- May 1995 to March 1996

4. TITLE AND SUBTITLE

Evaluation of Natural Attenuation of Organic Tracers at the MADE Site Using the Bioplume II Transport Model

5. FUNDING NUMBERS

6. AUTHOR(S)

James Beach, Dennis Fryar, Hanadi Rifai, Kevin Appling, and Thomas B. Stauffer

7. PERFORMING ORGANIZATION NAME(S) AND ADDRESS(ES)

INTERA Inc.
6850 Austin Center Boulevard
Suite 300
Austin, Texas 78731

Rice University
Houston, Texas

8. PERFORMING ORGANIZATION REPORT NUMBER

9. SPONSORING/MONITORING AGENCY NAME(S) AND ADDRESS(ES)

AL/EQC
139 Barnes Drive, Suite 2
Tyndall AFB, Florida 32403-5323

10. SPONSORING/MONITORING AGENCY REPORT NUMBER

AL/EQ-TR-1996-0027

11. SUPPLEMENTARY NOTES

For further information, contact Dr. Thomas B. Stauffer (904) 283-6059

12a. DISTRIBUTION/AVAILABILITY STATEMENT

12b. DISTRIBUTION CODE

13. ABSTRACT *(Maximum 200 words)*

This report describes the results of implementing the flow-and-transport code Bioplume II to simulate the field tracer test known as the MADE-2 experiment. MADE-2 was initiated in June 1990 and completed in September 1991 (Stauffer et al., 1994). The MADE-2 experiment consisted of injecting several aromatic hydrocarbons and a nonreactive tracer into an uncontaminated shallow aquifer system to characterize the flow-and-transport characteristics of the system. This was achieved by monitoring an expansive network of multilevel samplers on a regular basis for about 16 months. The data collected from the MADE-2 experiment were used to calibrate Bioplume II in an effort to evaluate the appropriateness and applicability of this model. The results of the modeling indicate that the assumption of instantaneous aerobic biodegradation used in Bioplume II may not be appropriate in regions of the fuel hydrocarbon plumes that exhibit relatively low concentrations. Simulations incorporating the instantaneous oxygen reaction resulted in too much degradation at the front edge of the plume and underestimated the extent of the down gradient plume when compared to field observations. It was found that implementing first-order decay with little or no instantaneous aerobic degradation provided the best model for simulating plume fate and transport during the MADE-2 experiment. Based on the available data and modeling evaluation, it is impossible to decipher exactly which biodegradation processes were most active during the MADE-2 experiment.

14. SUBJECT TERMS

Natural Attenuation, MADE-2, Bioplume II, Numerical Modeling, In Situ Biodegradation

15. NUMBER OF PAGES

16. PRICE CODE

17. SECURITY CLASSIFICATION OF REPORT	18. SECURITY CLASSIFICATION OF THIS PAGE	19. SECURITY CLASSIFICATION OF ABSTRACT	20. LIMITATION OF ABSTRACT

NSN 7540-01-280-5500

Standard Form 298 (Rev. 2-89)
Prescribed by ANSI Std 239-18
298-102

(The reverse of this page is blank.)

PREFACE

This report was prepared by INTERA Inc. and Rice University for the Armstrong Laboratory Environics Directorate (AL/EQC), 139 Barnes Drive, Suite 2, Tyndall Air Force Base, Florida 32403-5323. The work, which was funded under contract F08637-94-R-6002, was performed between June 1995 and March 1996 under the direction of AL/EQC project manager Dr. Thomas B. Stauffer.

(The reverse of this page is blank.)

EXECUTIVE SUMMARY

A. OBJECTIVE

The purpose of this project was to implement the Bioplume II flow and transport code to simulate the results of the MADE-2 experiment and evaluate the appropriateness and applicability of the Bioplume II code at similar sites. The MADE-2 experiment was a controlled field experiment involving the injection of several aromatic hydrocarbons and a nonreactive tracer into an uncontaminated aquifer (Stauffer *et al.*, 1994). Bioplume II is a numerical computer model that simulates groundwater flow, as well as fate and transport of contaminants in groundwater. Of particular interest in this study is the ability of Bioplume II to simulate the fate and transport of organic contaminants under the influence of biologic and abiotic degradation.

This objective has evolved from observations at many sites that indicate natural attenuation plays a significant role in the fate and transport of organic compounds (Stauffer *et al.*, 1994, Wiedemeier *et al.*, 1995). Natural attenuation is the term describing the *in situ* reduction in contaminant concentration and mass by biologic and/or abiotic mechanisms which may result in delayed plume migration or, in some cases, may result in plume stabilization or reduction of plume size.

B. BACKGROUND

Groundwater at many Department of Defense (DOD) sites is contaminated by organic compounds such as JP-4, gasoline, and diesel, as well as chlorinated solvents such as trichloroethylene (TCE) and tetrachloroethylene (PCE). Many of these chemical compounds are regulated by the Environmental Protection Agency (EPA) as hazardous substances, and often it is necessary for the DOD to characterize and remediate groundwater that has been contaminated by these organic compounds. Characterizing the nature and extent of contamination through field studies has proven to be a difficult task at many facilities due to the complexities and uncertainties of (1) the source, (2) the flow dynamics of the hydrogeologic system, and (3) the behavior and fate of the contaminants in the subsurface. In general, the reliability of remediation plans is related directly to how well the system can be characterized.

Mackay and Cherry (1989) documented the poor performance of typical pump-and-treat technologies in cases where non-aqueous phase liquids (NAPLs) provide a contaminant source that continues to produce dissolved phase plumes with concentrations greater than regulatory limits for many years. These authors document the challenge that stems from a fundamental lack of understanding of the physical phenomena governing NAPL movement in the subsurface and the

challenge of implementing effective remedial strategies at improperly characterized sites. Although the persistence of NAPLs in aquifers has been well established, controlled field experiments like MADE-2 confirm the observations at many other contaminated sites that indicate natural attenuation processes are a powerful phenomenon that should be considered when designing cost-effective characterization and remediation programs.

The ability to properly simulate the fate and transport of dissolved contaminants in groundwater through modeling techniques is vital in developing an understanding of the action required to minimize risks to human health and the environment. Modeling is a valuable tool for evaluating remedial options and designing cost-effective and protective strategies to deal with contaminated groundwater. Using data bases like MADE-2 in the model validation process is critical in developing reliable tools that serve to balance remediation expenditures and protection of human health and the environment.

C. SCOPE

The scope of this study is to evaluate the ability of an existing flow-and-transport code (Bioplume II) to simulate the results of the MADE-2 experiment. The ability to appropriately simulate natural attenuation processes is important in (1) understanding the characteristics and factors at a site that affect the fate and transport of a contaminant plume as related to the risk associated to human health and the environment, (2) evaluating the need for active remediation, and, if necessary (3) designing and optimizing long-term monitoring and remediation programs. The ability to identify, verify, and characterize the natural attenuation process in the field is an important subject that is beyond the scope of this study. However, this modeling study has identified several factors that are important in developing an appropriate field characterization investigation to document natural attenuation.

D. METHODOLOGY

The first objective in simulating fate and transport processes is to develop appropriate groundwater velocity estimates that can be incorporated into the contaminant transport equations. As discussed by Boggs *et al.* (1992), the shallow aquifer at the MADE site in which the tracer test was completed is very heterogeneous. The tracer test consisted of injecting a nonreactive tracer (tritium) and four organic compounds (benzene, naphthalene, p-xylene, and o-dichlorobenzene). Tracer monitoring indicated that the plume developed an irregular shape, evidently caused by preferential flow through high-permeability zones. The Bioplume II model assumes that the flow system can be modeled as one layer and averaged in the vertical direction (e.g., flow and transport characteristics are represented by a one-layer model that does not account for vertical variation in hydraulic conductivity, concentration, etc.). Therefore, a significant effort was put forth to develop a vertically

integrated (one-layer) flow model for the aquifer that approximates the gross behavior of the observed flow dynamics. In general, the main goal was to develop an areal groundwater velocity distribution throughout the transport domain that would closely mimic the velocity distribution estimated by monitoring the nonreactive tracer plume during the MADE-2 experiment. The flow model was calibrated through a trial-and-error deterministic approach. This method was selected because a significant amount of detailed vertical characterization information (hydraulic conductivity and tracer concentration) was "lost" through the vertical averaging required by Bioplume II. The loss of information through the vertical averaging of a very heterogeneous system negates much of the benefit derived from using more sophisticated approaches to flow model calibration.

One unique aspect of the MADE-2 experiment data is the controlled nature in which the experiment was performed. Source conditions and length of time which the source had been active were well known and modeling efforts could focus more on how the transport parameters affected the fate of the tracer plumes. Stauffer *et al.* (1994) describe tracer monitoring through a series of sampling events called "snapshots". A snapshot event consisted of collecting samples from most of the multilevel samplers (MLS) in the area where the plume was assumed to have been transported. Five snapshots were completed over a 16-month period. The data collected during these snapshots served as the basis for transport model calibration, verification, and prediction. To make a direct comparison to Bioplume II results, the concentration data were first corrected according to the suggestions of Stauffer *et al.* (1994). In addition, because Bioplume II can simulate only one organic contaminant at a time, the concentrations of all four organic tracers were summed at each sample location to determine a total organic tracer concentration for that location. Finally, all the concentration data from each MLS were vertically averaged to accommodate comparison to Bioplume II results.

The flow model calibration was based on the estimated center of mass of the tritium plume during the study period. Center-of-mass estimates for the tritium plume were available for the first four snapshots. Snapshots 2, 3, and 4 were used to calibrate the flow model. The hydraulic conductivity distribution was adjusted to affect the velocity distribution so that a conservative particle tracked from the tracer injection location would move at the same rate as the observed plume (based on the center-of-mass calculations). Because the main objective of the project was to evaluate the Bioplume II model, the goal of the flow model calibration was to provide a steady-state velocity distribution that mimicked the gross behavior of the observed velocity distribution as closely as possible. The reliability of the flow model predictions is discussed in detail in Section 4.

A three-stage process was used to calibrate the model and test the reliability of the model's predictions. The concentration data collected during the second snapshot (132 days after injection) were used to calibrate the model. Then, the third snapshot (224 days after injection) was used to verify the calibration and make minor adjustments to model parameters to calibrate the model more appropriately. The fourth snapshot (328 day after injection) was then used to compare the predicted plume to the observed plume to evaluate the reliability of the transport model.

E. RESULTS

The results of the flow modeling indicated that a simple vertical average of the hydraulic conductivity data from all the wells resulted in significantly smaller groundwater velocities than those observed during the MADE-2 experiment (based on tracer tritium movement). This result indicated that the high-permeability zones played a key role in the transport of the tracers. Calibration of the model required the implementation of a hydraulic conductivity distribution skewed toward the highest hydraulic conductivity measurements collected in the field. In addition, minor modifications to the hydraulic conductivity distribution were necessary to simulate the appropriate groundwater velocities required to calibrate the flow model according to the center-of-mass estimates for the tritium plume.

When observed groundwater elevations were extrapolated to the boundaries of the model to serve as prescribed head boundary conditions, the simulated groundwater flow direction was significantly different from that indicated by the observed plume movement. This occurred in the steady-state and transient flow simulations. This is an important implication because this methodology is often employed to predict future conditions without the advance knowledge of tracer movement. In the MADE-2 case, without antecedent knowledge of tracer movement, the reliability of the flow model would have been greatly reduced and the prediction of the plume movement would have been significantly different from that observed during the experiment. This difficulty has been documented at other well-characterized sites such as the Borden experimental site (Wilson and Linderfelt, 1994).

Comparison of the simulated and observed plumes at Snapshot 4 indicates that, in general, the Bioplume II model is capable of approximating the transport processes observed during the MADE-2 experiment. However, incorporating instantaneous aerobic biodegradation to the degree suggested by field data (i.e., providing 3 mg/L of dissolved oxygen for instantaneous reaction) does not adequately predict the fate and transport of organic tracers observed during the MADE-2 experiment. The model incorporating only first-order decay (without instantaneous aerobic degradation) was the best model for predicting long-term plume development. The size and shape of the plume simulated with the model incorporating instantaneous aerobic degradation did not mimic the observed plume. Because the model was two-dimensional, it did not reproduce the fingering and highly heterogeneous plume dimensions that were measured from the extensive three-dimensional sampling network. The simulated plume from the model incorporating only first-order decay did exhibit the same asymmetric distribution as the observed plume.

F. CONCLUSIONS

The appropriateness of applying the Bioplume II model at the MADE-2 site depends largely on the objective of the modeling. Although limitations of the MADE-2 data base precludes a *complete* assessment of the adequacy of Bioplume II for simulation of natural attenuation processes,

the following conclusions can be stated.

1. One limit of the Bioplume II code identified by using the MADE-2 data set is the instantaneous aerobic degradation assumption. Results from this study indicate that this assumption may not be appropriate for the MADE-2 experiment because of the relatively low concentrations of organics at the front edge of the plume. This conclusion is drawn from the results of the model incorporating instantaneous aerobic degradation that indicated premature degradation of the organics plume.

2. If the objective of a modeling evaluation is to develop a tool to evaluate the general movement and behavior of the contaminant plume, Bioplume II may be able to simulate observed conditions. However, this does not mean that the natural attenuation processes are being handled appropriately or that predictions far in time from the calibration period will be accurate. This conclusion is made from the observation that the measured dissolved oxygen concentration was never reduced to levels that are believed necessary for anaerobic biodegradation to occur. However, the model incorporating only first-order decay (representing anaerobic biodegradation) and not aerobic biodegradation provided the best calibration.

3. If the objective of the modeling is to evaluate how the heterogeneity of the site affects the fate and transport of the plume (especially in the vertical direction) and to develop a more complete understanding of the intricate details of the plume, Bioplume II may not be appropriate because of the two-dimensional, vertical-average conceptualization of the model. This conclusion is drawn from recognizing the basic flow dynamics of the system and the flow modeling calibration, which indicated incorporation of vertically averaged hydraulic conductivity estimates was not appropriate for simulating contaminant transport.

4. Although the MADE-2 data base represents one of the most comprehensive controlled field experiments to date, weaknesses of the data base include (a) the lack of field characterization data concerning anaerobic degradation, and (b) inadequate spatial characterization of the aerobic and anaerobic biodegradation processes in the aquifer that may be caused by the extremely heterogeneous velocity distribution.

5. The initial flow model based on observed heads and hydraulic conductivity measurements would have produced groundwater flow vectors (direction and magnitude) that were not consistent with tracer movement observed during the MADE-1 and 2 experiments. This result demonstrates an elementary fact that is sometimes overlooked in fate and transport modeling — the flow dynamics of a system must be understood to develop reliable predictive models for any site.

In general, the results indicate that Bioplume II could be used to model the MADE-2 experiment with some degree of accuracy by incorporating only first-order decay with little or no aerobic biodegradation. This type of approach does not require Bioplume II because many transport

codes have the ability to model the loss of contaminants through first-order decay and a full gamut of flow and transport models could have been used to achieve the same results. In this study, the model could be used only as a tool to indicate how the system will respond in the future based on historical observations. This study indicates that the conceptual model has a significant impact on the predictive capability of the MADE-2 site model. Anderson and Woesnner (1992) point out that findings from post audits of modeling studies indicate that inaccurate predictions were caused by (1) errors in the conceptual model of the system, or (2) failure to use appropriate values for future system stresses. The model incorporating instantaneous aerobic biodegradation was not reliable in predictive mode because the assumption of instantaneous aerobic biodegradation is not representative for the MADE-2 experiment. The main "system stresses" for this type of model that may cause prediction errors include (1) rates and ratio of aerobic and anaerobic biodegradation, (2) spatial and temporal distribution of these processes throughout the system, (3) reaeration rates, and (4) retardation coefficients. The sensitivity analysis section discusses how some of these variables affect the model results.

G. RECOMMENDATIONS

This modeling study has provided insight into both the field and the modeling aspects of the MADE-2 experiment. The limitations of the MADE-2 data set with respect to explicitly modeling each degradation process became apparent during model development. In addition, limitations of the Bioplume II model became apparent when applied to the highly heterogeneous MADE-2 site.

Significant data are required to properly characterize contaminant plumes, especially when the effort is aimed at demonstrating and verifying natural attenuation processes such as biodegradation. Of special importance is the challenge in estimating the extent of the dissolved-phase plume. Estimating the extent of the plume is inherently associated with the detection limit of the methods used to analyze the groundwater samples. In general, it is best to implement a methodology that provides the lowest detection limits feasible for oxygen and organic contaminants. Understanding the contaminant and oxygen concentrations is critical to characterizing and verifying the extent of aerobic biodegradation and developing an understanding of potential anaerobic and abiotic processes that may be active. Future tests should focus on characterizing anaerobic degradation processes as well as aerobic biodegradation. In addition, future natural attenuation studies at the MADE-2 site should attempt to describe spatial heterogeneity in the aerobic and anaerobic biodegradation processes. In other words, the study should decipher the types of processes that are active in the low- and high-permeability zones (and if they are different) so that a more accurate conceptual model can be developed at heterogeneous sites.

Several limitations were discovered in applying Bioplume II at the MADE-2 site. Perhaps the most important was the inability to implement Bioplume II to simulate the flow and transport processes in three dimensions. In applying Bioplume II, it is assumed that variations in flow and

transport processes in the vertical direction are negligible and can be appropriately represented by a vertically integrated model. Hydraulic conductivity and concentration distributions documented by Stauffer *et al.* (1994) and Boggs *et al.* (1990) indicate that this assumption may not be appropriate at the MADE-2 site. At sites where there is significant heterogeneity in the hydraulic properties of the aquifer, three-dimensional models may be more appropriate. Another limitation was the inability to incorporate the hydraulic anisotropy associated with the buried stream channel on a gridblock-by-gridblock basis. Bioplume II only allows anisotropy to be incorporated for the entire aquifer, and it does not allow an irregularly spaced grid. Gridblock size can be different in the x and y directions, but the same gridblock size must be maintained in each respective direction. This restriction could be limiting in cases where the model should be extended to important hydraulic boundaries that are a significant distance from the area of transport. Therefore, more robust models should be developed to provide options not currently available in biodegradation models.

Another limitation of Bioplume II is the inability to simulate anaerobic biodegradation explicitly. Wiedemeier *et al.* (1995) point out the potential significance of anaerobic processes for bioremediation of fuel hydrocarbons. Monitoring and characterizing the degradation of the organics was only a secondary objective of the MADE-2 experiment. Therefore, the extensive chemical analyses required to quantify and document anaerobic degradation processes were not completed to the extent required to develop a reliable model of these processes during the MADE-2 experiment. As stated, all the degradation processes other than oxygen limited biodegradation were simulated by incorporating a first-order decay term. At many sites, it may be necessary to understand and quantify the importance of each anaerobic biodegradation process in order to build a reliable transport model to evaluate natural attenuation and remediation strategies and provide reliable long term predictions. Therefore, transport models that explicitly incorporate anaerobic biodegradation processes should be developed.

(The reverse of this page is blank.)

TABLE OF CONTENTS

TABLE OF CONTENTS (continued)

TABLE OF CONTENTS (concluded)

LIST OF FIGURES

LIST OF FIGURES (continued)

LIST OF FIGURES (continued)

LIST OF FIGURES (continued)

LIST OF FIGURES (continued)

LIST OF FIGURES (continued)

LIST OF TABLES

SECTION I
INTRODUCTION

A. OBJECTIVES OF THE STUDY

The purpose of this project was to implement the Bioplume II flow and transport code to simulate the results of the MADE-2 experiment and to evaluate the appropriateness and applicability of the Bioplume II code, especially with respect to other Air Force sites. The MADE-2 experiment was a controlled field experiment involving the injection of several aromatic hydrocarbons and a nonreactive tracer into an uncontaminated aquifer (Stauffer et al., 1994). Bioplume II is a numerical computer model that simulates groundwater flow as well as fate and transport of contaminants in groundwater. Of particular interest in this study is the ability of Bioplume II to simulate the removal of organic contaminants through natural attenuation processes.

The need to characterize and document flow-and-transport properties has evolved from observations at many sites which indicate that natural attenuation of organic compounds plays a significant role in the fate and transport of contaminants (Stauffer et al., 1994, Wiedemeier et al., 1995). Natural attenuation is the term describing the *in situ* reduction in contaminant concentration and mass by biologic and/or abiotic mechanisms which may result in delayed plume migration or, in some cases, may result in plume stabilization or reduction of plume size.

The MADE-2 experiment was designed to provide data on those properties which significantly control the propagation of dissolved contaminants in groundwater systems. A secondary objective was to measure the *in situ* degradation rates of the selected organic compounds (Stauffer *et al.*, 1994). The most interesting result of the MADE-2 experiment was the documented observation of significant organic tracer loss through natural degradation processes. Although monitoring and characterizing each of the biological and abiotic degradation processes was beyond the scope of the MADE-2 experiment, substantial evidence was collected during the test to verify that hydrocarbon losses were due to chemical degradation rather than physical losses (Stauffer *et al.*, 1994).

B. BACKGROUND

Groundwater at many Department of Defense (DOD) sites is contaminated by organic compounds such as JP-4, gasoline, diesel (e.g., BTEX), as well as chlorinated solvents such as trichloroethylene (TCE) and tetrachloroethylene (PCE). Many of these chemical compounds are regulated by the Environmental Protection Agency (EPA) as hazardous substances and, in many cases, it is necessary for the DOD to characterize and remediate groundwater systems that have been contaminated by these organic compounds. Characterization of the nature and extent of

contamination through field studies has proven to be a difficult task at many facilities due to the complexities and uncertainties of (1) the source, (2) the flow dynamics of the hydrogeologic system, and (3) the behavior and fate of the contaminants in the subsurface. In general, the reliability of remediation plans is directly related to how well the system can be characterized. Mackay and Cherry (1989) document the poor performance of typical pump-and-treat technologies in cases where non-aqueous phase liquids (NAPLs) provide a contaminant source that continues to produce dissolved phase plumes with concentrations greater than regulatory limits for many years. These authors document the challenge that stems from a fundamental lack of understanding of the physical phenomena governing NAPL movement in the subsurface, as well as the challenge of implementing effective remedial strategies at sites that are improperly characterized. On the other hand, controlled field experiments like MADE-2 confirm the observations at many other contaminated sites that indicate natural attenuation processes are powerful phenomena that should be considered when designing cost-effective characterization and remediation programs.

The ability to properly evaluate the fate and transport of dissolved contaminants in groundwater through modeling techniques is vital in developing an understanding of the action required to minimize risks to human health and the environment. Modeling is a valuable tool for evaluating remedial options and designing cost-effective and protective strategies to deal with contaminated groundwater. Using data bases like MADE-2 in the model validation process is critical in developing reliable tools that serve to balance remediation expenditures and protection of human health and the environment.

C. SCOPE

The scope of this study is to evaluate the ability of an existing flow-and-transport code (Bioplume II) to simulate the results of the MADE-2 experiment. The ability to appropriately simulate natural attenuation processes is important in (1) understanding the characteristics and factors at a site that affect the fate and transport of a contaminant plume as related to the risk associated to human health and the environment, (2) evaluating the need for active remediation and, if necessary, (3) designing and optimizing remediation systems and long-term monitoring programs. The ability to identify, verify and characterize the range of natural attenuation processes in the field is an important subject which is beyond the scope of this study. However, this modeling study has identified several factors that are important in developing an appropriate field characterization investigation to document natural attenuation.

SECTION II
LITERATURE REVIEW

A. NATURAL ATTENUATION OF ORGANIC CONTAMINANTS IN GROUNDWATER

Natural attenuation is the reduction of the total contaminant mass in groundwater due to non-engineered processes. Fuel hydrocarbon contamination is one of the most prevalent types of groundwater contamination. When these two facts are examined together, possible natural attenuation of fuel-hydrocarbon contamination is of great interest to regulatory authorities, environmentalists, researchers, industry, and other related parties. If contamination is undergoing natural attenuation, active remediation may not be required. This can result in significant cost savings when the price of a monitoring system alone is compared with the combined cost of a monitoring system and a remediation system.

Hydrocarbon contaminant concentrations can be decreased through both abiotic and biotic means. The abiotic processes include dilution, sorption, volatilization, abiotic oxidation, and hydrolysis. However, in the cases of dilution, sorption, and volatilization, the original pollutant is not destroyed. In contrast, abiotic oxidation and hydrolysis result in a change in the chemical structure of the contaminant and may serve as a more permanent solution with respect to protecting human life and the environment.

Similarly, biotic processes typically result in a chemical change in the contaminant. These processes typically consist of either aerobic microbial respiration or anaerobic hydrocarbon utilization. Types of anaerobic degradation include denitrification, ferric iron reduction, sulfate reduction, and methanogenesis. Other types of biotic attenuation, including cometabolism and plant uptake may be important at some sites and are being studied further. However, at this time they are beyond the scope of this review.

In general, the process of aerobic respiration (the use of O_2 as an electron acceptor in the biodegradation reaction) is the pathway for hydrocarbon fuel biodegradation that is preferred over any of the anaerobic processes. Aerobic microbes tend to be more robust than anaerobes and will out-compete the anaerobes for the available nutrients. When aerobic respiration is no longer viable due to lack of oxygen or some other inhibition, anaerobic degradation will take over. The standard preferential order of anaerobic electron acceptor use (from most preferred to least) is: (1) NO_3^-, (2) Fe^{3+}, (3) SO_4^{2-}, and (4) CO_2. However, the groundwater chemistry (pH, temperature, alkalinity, etc.) at any specific site may inhibit any of the degradation reactions. This can result in a different preferential order for a specific site.

As mentioned, aerobic micro-organisms use dissolved oxygen as the electron acceptor. The fuel hydrocarbon provides the bulk of the raw material for cell growth and reproduction. The fuel hydrocarbon is called the primary substrate. In addition, the primary substrate is the electron donor and provides the energy needed by the cell. Using benzene as the primary substrate, an aerobic biodegradation reaction is:

$$C_6H_6 + 7.5O_2 \Rightarrow 6CO_2 + 3H_2O$$

In this reaction, 3.1 grams of oxygen are required to degrade one gram of benzene. This results in a stoichiometric mass ratio of 3.1 : 1.

Denitrification involves the conversion of nitrogen containing compound to nitrogen gas. Typically, the nitrogen source in the ground water at a site is nitrate (NO_3). The denitrification reaction based upon nitrate and benzene is:

$$C_6H_6 + 6H^+ + 6NO_3^- \Rightarrow 6CO_2 + 3N_2 + 6H_2O$$

The stoichiometric mass ratio of nitrate to benzene is 4.8 : 1. In some instances, nitrite (NO_2) may be found at a site. In this case, it is possible that a similar reaction to the one above may occur, providing another source of nitrogen for the denitrification process.

Following denitrification, ferric iron reduction becomes the dominant biodegradation mechanism. Ferric iron is typically insoluble and is often present as ferric hydroxide. During iron reduction, ferric iron (Fe^{3+}) is reduced to soluble ferrous iron. It is difficult to determine exactly how much iron is available for biodegradation. This type of reaction is usually monitored by determining the amount of ferrous iron (Fe^{2+}) present in solution. The corresponding reaction is:

$$C_6H_6 + 30Fe(OH)_3 + 60H^+ \Rightarrow 6CO_2 + 30Fe^{2+} + 78H_2O$$

The stoichiometric mass ratio of ferric hydroxide to benzene is 41.1 : 1.

During sulfate reduction, sulfate is reduced to hydrogen sulfide. The sulfate is typically present as a background contaminant in the groundwater. The stoichiometric mass ratio of sulfate to benzene is 4.6 : 1. The corresponding reaction is :

$$C_6H_6 + 7.5H^+ + 3.75SO_4^{2-} \Rightarrow 6CO_2 + 3.75H_2S + 3H_2O$$

Methanogenesis gets its name due to the methane produced during this reaction. The electron acceptor is carbon dioxide. The only additional reactant required for this process is water. The stoichiometric relationship reported for this reaction is the mass ratio of methane to benzene; 0.77:1.

The corresponding reaction is:

$$C_6H_6 + 4.5H_2O \Rightarrow 2.25CO_2 + 3.75CH_4$$

Godsy (1994) listed conditions that must be met for contaminants to be removed from groundwater by bacteria.

1. The bacteria must be in the immediate vicinity of the contaminant.
2. The contaminant must be available to the bacteria.
3. The bacteria must have the capacity to participate in some part of the degradation or transformation process.

In addition to the electron acceptor and hydrocarbon, microbial growth requires other trace nutrients. These nutrients include sulfur, nitrogen, and phosphorus. Sufficient sulfur is usually available, but the lack of nitrogen and phosphorus can be growth limiting. Godsy (1994) states that an ideal carbon/nitrogen/phosphorus ratio is usually around 300 to 100/10/1 to 0.05, depending on the contaminant of interest. In this paper, Godsy also mentions that biodegradation proceeds best at near neutral pH and that the rate of degradation approximately doubles for every 10°C increase in ambient temperature.

Wiedemeier *et al.* (1994) presented an overview of a "technical protocol . . . for data collection, ground water modeling, and exposure assessment in support of intrinsic remediation (natural attenuation) with long-term monitoring for restoration of fuel hydrocarbon contaminated ground water." In this protocol, Wiedemeier *et al.* outline the following seven steps to determine the viability of intrinsic remediation at a site.

1. Review existing site data.
2. Develop a preliminary conceptual model for the site, and assess the potential significance of intrinsic remediation.
3. Perform site characterization in support of intrinsic remediation.
4. Refine the conceptual model based on site characterization data, complete premodeling calculations, and document indicators of intrinsic remediation.
5. Model intrinsic remediation using numerical data and transport models that allow incorporation of a biodegradation term.
6. Conduct an exposure assessment.
7. Prepare a long-term monitoring plan, long-term monitoring wells at the site, and point of compliance wells.
8. Present findings to regulatory agencies, and obtain approval for the intrinsic remediation with long-term monitoring option.

Wiedemeier *et al.* suggest that the soil and groundwater at the site be analyzed for the parameters listed in Table 1 below..

TABLE 1
PARAMETERS FOR DEMONSTRATING NATURAL ATTENUATION

Soil	
Total volatile hydrocarbons	Total extractable hydrocarbons
Aromatic hydrocarbons	Total organic carbon
Groundwater	
Dissolved oxygen	Sulfide
Oxidation-reduction potential	Ferrous iron
pH	Carbon dioxide
Temperature	Methane
Conductivity	Chloride
Alkalinity	Total petroleum hydrocarbons
Nitrate	Aromatic hydrocarbons
Sulfate	

In general, Wiedemeier *et al.* state that by comparing concentration contour plots of the electron donors (dissolved oxygen, sulfate, etc.), degradation by-products (methane, carbon dioxide, etc.), and the fuel hydrocarbon, one can locate areas of probable natural attenuation. In areas where biodegradation is occurring, there should be a decrease in the available amount of electron acceptors. For example, in areas where aerobic respiration is taking place, the concentration of dissolved oxygen is decreased. In addition, concentrations of degradation by-products are elevated. In areas where methanogenesis is taking place, elevated levels of methane should be found. However, Wiedemeier *et al.* say that this is not sufficient evidence to demonstrate natural attenuation is occurring at a site. These indicators should be supported by microcosm studies, tracer studies, and biodegradation modeling showing probable natural attenuation.

Another methodology was presented by Novick *et al.* in 1995. This evaluation technique was developed by Mobil Oil Corporation "for the demonstration of natural attenuation of petroleum hydrocarbons in groundwater." This approach consists of three levels of assessment called tiers. A Tier I approach is the easiest to accomplish, and if it is accepted, no further work is required. If a Tier I approach is not accepted, the analysis progresses to Tier II and continues to Tier III, if required. The following summary of the three tiers is taken from *Novick et al.* (1995).

Tier I assessment categorizes the plume as stable, expanding or shrinking, estimates plume migration distance, with and without natural attenuation, and establishes the rate of natural attenuation . . .

Tier II requires collecting monitoring data on indicators specific to intrinsic bioremediation. This may include measurements of dissolved oxygen, sulfate, nitrate, soluble iron (Fe^{+2}) and manganese (Mn^{+2}), methane and inorganic carbon.

A **Tier III** approach, if necessary, uses microcosm studies and detailed groundwater modeling to further demonstrate the significance of natural attenuation at a given site.

This approach provides several different levels of detail that are not as rigidly defined in the protocol given by Wiedemeier et al. 1994. McAllister and Chiang (1994) also present an approach to determining the natural attenuation occurring at a site which is similar to those given by both Novick et al (1995) and Wiedemeier et al. (1994).

Table 2 lists some of the field studies that have been performed at sites that show existing fuel-hydrocarbon contamination.

TABLE 2
FIELD STUDIES OF HYDROCARBON CONTAMINATION

Reference	Contaminant	Location
Barker *et al.*, 1995	BTEX	Denver Basin, Colorado
Butler and Bartlett, 1995	Volatile organic compounds (VOCs)	Central New Jersey
Davis *et al.* 1994	Benzene	U.S. eastern seaboard
Eganhouse *et al.*, 1994	Petroleum hydrocarbons	Bemidji, Minnesota
Ginn *et al.*, 1995	Polycyclic aromatic hydrocarbons (PAHs)	New York
Nelson *et al.*, 1994	BTEX	Denver, Colorado
Toze *et al.*, 1995	BTEX	Perth, Australia
Wilson *et al.*, 1994	BTEX, JP-4	Eglin Air Force Base (AFB), Hill AFB
Wilson *et al.*., 1994	BTEX	Traverse City, Michigan
Wilson *et al.*, 1995	BTEX	George AFB
Wiedemeier *et al.*, 1995	Petroleum hydrocarbons	Phoenix, Arizona
Wiedemeier *et al.*, 1995	Benzene, toluene, ethylbenzene, and xylenes (BTEX)	Hill AFB and Patrick AFB

Governmental agencies have begun to set guidelines for the acknowledgment of natural attenuation as a viable remediation technique (AFCEE, 1994; Florida Bureau of Waste Management, October 1990; and Wisconsin Department of Natural Resources, February 1993). AFCEE reviewed the regulations for Delaware, Florida, Iowa, Michigan, North Carolina, Ohio, Wisconsin, and the District of Columbia. The regulatory authorities of these areas currently require the removal of both the source of the contamination and the free product before natural attenuation is considered as a remediation option. All these entities require continual monitoring of the natural attenuation to ensure that no future health risk occurs because of contaminant migration. Each regulatory authority differs in its requirements for demonstrating natural attenuation, the period between permit approvals, and the requirements for the permit approvals. In some cases, contaminant release which results in concentrations that exceed the water quality standards for an area are allowed if sufficient natural attenuation is occurring (AFCEE, 1994). In all cases, groundwater quality must be monitored at some receptor location downgradient from the source of contamination. If the contaminant levels at this point exceed the water quality standards, more active remediation will be required.

Natural attenuation is gaining acceptance as a final measure of remediation at a site. After an active remediation system (typically a pump-and-treat system) has been in place and operating for some time, the rate of contaminant mass removal decreases. If the effectiveness of the system decreases substantially, the pump-and-treat program may be discontinued. After the system is stopped, the monitored levels of contaminant within the aquifer often rebound to some higher level. If the active treatment system is then restarted, the contaminant levels will decrease quickly, but will probably rebound when the system is switched off again. Continued remediation through a pump-and-treat system may be extremely inefficient at such sites. Natural attenuation monitoring may provide a low-cost alternative to allow such sites to be closed. A regulatory approach, a case study, and mathematical modeling of this type of site are discussed by Walker and Weers (1994), Maresco *et al.* (1995), and Illangasekare *et al.* (1994), respectively.

A major consideration in allowing natural attenuation to remediate contaminated sites is the risk to possible receptors. Risk determination continues to be studied intensively. As risk assessment becomes more reliable, natural attenuation may become a more accepted remedial alternative at qualified sites. Ultimately, enhancing natural attenuation through oxygen injection, slurry walls, and other techniques will play a vital role in remediating groundwater contamination.

B. PREVIOUS INVESTIGATIONS AT THE MADE SITE

The MADE site is located at Columbus Air Force Base, Mississippi, USA. The acronym MADE stands for macrodispersion experiment. Two field experiments were conducted at the site, namely, MADE-1 and MADE-2. The shallow hydrogeology of the site can be described as an unconfined, heterogeneous alluvial aquifer that is underlain by a relatively impermeable clay. The alluvial terrace deposits average 11 meters in thickness. Boggs *et al.* (1990), Boggs *et al.* (1992a), Rehfeldt *et al.* (1992), and Stauffer *et al.* (1994) document the intensive effort undertaken to

characterize the hydraulic conductivity distribution of the aquifer, as well as soil mineralogy, water chemistry, and other hydraulic properties.

The MADE-1 natural gradient field experiment was conducted between October 1986 and June 1988. The test entailed injection of a bromide tracer. The experiment methodology and results are fully described in a set of papers by Boggs *et al.* (1992a), Adams *et al.* (1992), Rehfeldt *et al.* (1992), and Boggs *et al.* (1992b). The overall goal of the field experiment was to test the validity and practicality of stochastic theories describing field-scale dispersive mixing in very heterogeneous aquifers (Adams *et al.*, 1992). One reason the MADE site was selected for this experiment is because of the large-scale variations in hydraulic conductivity. The MADE-1 experiment indicated that these large-scale hydraulic conductivity variations may produce extreme nonuniformity in flow.

The MADE-2 natural gradient field experiment was conducted to investigate the transport and degradation of four dissolved aromatic organic compounds (benzene, naphthalene, p-xylene, and o-dichlorobenzene) and one nonreactive tracer (tritium) in an aquifer (Stauffer *et al.*, 1994). The study was completed over a 16-month period. The tracer mixture was injected over a 48.5-hour period beginning on June 26, 1990, at a constant rate of 3.3 liters per minute. The plume development was monitored using 328 multilevel samplers and 56 BarCad samplers. Five complete sample sets (called "snapshots") were collected during the 16-month period. Degradation rates of the organic tracers were determined, but no attempt was made to classify or quantify the microbial populations.

Results of the MADE-2 experiment indicated that the tritium plume was extremely skewed in the longitudinal direction as a result of the highly heterogeneous flow field and the high velocity zone that exists downgradient from the tracer injection zone. Degradation kinetics indicated that the data were approximately first-order and that the degradation processes were a major factor in the overall attenuation of the plume as compared to sorption. The disappearance and transformation of the organic solutes during the MADE-2 experiment demonstrated that the natural degradation processes were able to effectively reduce organic concentrations over a reasonable time frame (Stauffer et al. 1994).

C. PREVIOUS APPLICATIONS OF BIOPLUME I AND BIOPLUME II

Bioplume has been applied to a variety of sites by industry, academic institutions, consultants, and governmental agencies. At all the sites, aerobic biodegradation was considered to be the primary degradation mechanism. These applications of the Bioplume model have resulted in the development of new modeling techniques and the improvement of existing methods of biodegradation modeling. The first case study - United Creosoting Company Inc. in Conroe, Texas - is the only study described here that used the Bioplume I model. All other studies used Bioplume II. The UCC site is included for completeness as the governing biodegradation equations are the same in all versions of Bioplume.

1. UCC Site - Conroe, Texas

Borden and Bedient (1986, 1987) and Borden *et al.* (1986) applied the Bioplume I model to the United Creosoting Company Inc. (UCC) site. This site is located in Conroe, Texas where UCC operated a wood-preserving facility from 1946 to 1972. The wastes from this treatment process were placed into two on-site, unlined ponds. The wastes were composed primarily of polycyclic aromatic hydrocarbons and pentachlorophenol. Elevated levels of these compounds and chlorine were discovered in the groundwater beneath the site.

Borden and Bedient (1986) injected known amounts of chlorine, napthalene, and p-dichlorobenzene to study the probable fate and transport of the original contaminants at this site. Based on the field work, laboratory studies carried out at Rice University, and a review of the applicable literature, Borden and Bedient (1986) selected the following parameters for use in the model.

TABLE 3
BIOPLUME PARAMETERS FOR THE UCC SITE - CONROE, TEXAS

Parameter	Symbol	Value
Velocity	υ	0.015 m/d
Longitudinal dispersivity	α_l	9.1 m
Transverse dispersivity	α_t	1.8 m
Maximum hydrocarbon utilization rate	k	1.7 day
Ratio of oxygen to hydrocarbon consumed	F	3.0
Microbial yield coefficient	Y	0.5 g cell/g H
Hydrocarbon half saturation constant	K_h	0.13 mg/L
Oxygen half saturation constant	K_o	0.10 mg/L
Microbial decay coefficient	b	0.01 day
Background hydrocarbon concentration	H_b	0.0 mg/L
Background oxygen coefficient	O_b	3.0 mg/L
Background microbial biomass	M_b	0.001 mg/L
Background organic carbon	C	750 mg/L
Influent hydrocarbon concentration	H_i	4.5 mg/L
Influent oxygen concentration	O_i	3.0 mg/L
Influent microbe concentration	M_i	0.001 mg/L
Organic carbon utilization rate	k_c	2.7×10^{-6} day
Hydrocarbon retardation factor	R_h	1.0
Microbial retardation factor	R_m	100

Sensitivity analyses using a one-dimensional model indicated that the microbial parameters (K_h, K_o, k, Y, and F) had little effect on the distribution of hydrocarbon within the plume or with the travel time of the hydrocarbon. This led Borden and Bedient (1986) to the instantaneous reaction assumption discussed in the review of the Bioplume equations in Section V. Using this assumption, along with the established biodegradation and transport parameters, Borden and Bedient (1986) performed a series of two-dimensional simulations. The background concentrations were used to establish boundary and initial conditions, and influent concentrations were implemented to describe the contaminant source.

Based on these simulations, Borden and Bedient (1986) drew several conclusions. Three conclusions pertinent to simulating natural attenuation by using the Bioplume I model were:

1. When exchange of oxygen with the hydrocarbon plume is rate limiting, the consumption of oxygen and hydrocarbon by micro-organisms may be approximated as an instantaneous reaction between oxygen and hydrocarbon. This greatly simplifies the mathematical analysis but may not be applicable for slowly degradable hydrocarbons in situations where the native microbial population has not yet adapted to the foreign hydrocarbon.

2. Transverse mixing will be the dominant source of oxygen for most hydrocarbon plumes when adsorption is not significant. Longitudinal mixing appears to have little effect on hydrocarbon biodegradation.

3. Vertical exchange of oxygen and hydrocarbon within the unsaturated zone may significantly enhance the rate of biodegradation. Preliminary simulations indicate that vertical exchange will result in a first-order decay in the vertically averaged hydrocarbon concentration. The first-order decay rate is strongly dependent on the saturated thickness and the vertical dispersion coefficient.

2. Traverse City, Michigan

Several researchers have applied the Bioplume II model to the Traverse City, Michigan, site. (Alder-Schaller, 1989; Miller, 1989; Rifai and Bedient, 1987, 1989, and 1992; Rifai *et al.* 1988; and Ward *et al.*, 1989.) In 1969, a substantial quantity of aviation fuel leaked from a flange on an underground storage tank at the U.S. Coast Guard Air Station in Traverse City, Michigan. Between 37,850 and 75,700 liters of fuel were released accidentally, which most likely formed a pool of a non-aqueous phase liquid (NAPL) within the aquifer. The NAPL provided a continuous source of contaminant for a plume in a shallow drinking water aquifer underneath a nearby residential area. The plume consisted primarily of benzene, toluene, ethyl-benzene, and the xylenes (BTEX). To prevent further migration of the contaminants, an interdiction field (i.e., a row of extraction wells) was established downgradient.

Rifai *et al.* (1988) applied Bioplume II to this site during development of the Bioplume II model. The parameters that were used in modeling the site are given in Table 4.

TABLE 4
BIOPLUME II PARAMETERS FOR THE TRAVERSE CITY, MICHIGAN, SITE

Parameter	Value
Grid size	16 x 38
Cell size	30 m. x 20 m.
Porosity	0.3
Longitudinal dispersivity	3 m.
Hydraulic conductivity	50 m/day
Dissolved oxygen concentration	8.0 mg/L
Reaeration decay coefficient	0.003 day^{-1}
Recharge	1.14×10^{-3} m/day

The contaminant source was represented by seven injection wells with a total flow rate of 6.85 m^3/day. The average injection concentration was approximately 1,380 mg/L. Prescribed head cells were used to establish the boundary conditions. Natural recharge of oxygen across the boundaries was set at 8.0 mg/L. No hydrocarbon was considered to enter the grid across the boundaries.

Rifai *et al.* (1988) determined that more investigation was necessary at the Traverse City site to define the source area. However, they concluded from this study's results that the coefficient of reaeration, the coefficient of anaerobic decay, and the hydraulic conductivity had the most influence on the amount of mass lost due to biodegradation. Rifai *et al.* (1988) also concluded that more research was necessary to understand anaerobic biodegradation and to provide a better definition of the vertical exchange of oxygen from the unsaturated zone to the saturated zone. Finally, they stated that more advanced numerical techniques for simulating biodegradation were needed.

3. Amoco Sites, Florida

Caldwell *et al.* (1992) used Bioplume II to model the fate and transport of BTEX (as a group) and benzene (individually) at a service station. Amoco performed field studies using both shallow and deep wells to determine the amount of BTEX, methyl tert-butyl ether and total recoverable petroleum hydrocarbons present in the soil and groundwater at three service stations in

Broward County, Florida. Caldwell *et al.* chose to model one of these sites using the following parameters:

TABLE 5
BIOPLUME II PARAMETERS FOR THE AMOCO SITE, FLORIDA

Parameter	Value
Grid size	12 x 12
Cell size	15 ft x 30 ft
Flow velocity	0.34 ft/day
Infiltration oxygen concentration	4.0 mg/L
Infiltration rate	30 in/yr
F ratio	3.0
Benzene retardation factor	1.7
BTEX retardation factor	2.7
Longitudinal dispersivity	7.5 ft
Transverse dispersivity	2.5 ft
Anaerobic degradation coefficient	0.00012 day^{-1}
Reaeration coefficient	0.005 day^{-1}

The source of the contamination was unknown. Caldwell *et al.* (1992) assumed that the contaminant source had been a continual release over several years that had gradually decreased. Four injection wells were used to simulate the source, with the maximum initial injection rate being slightly over 3 gallons of gasoline per year. The gasoline was assumed to contain 2 percent benzene and 8.6 percent BTEX.

Caldwell *et al.* (1992) also assumed that the plume only impacted the upper portion of the groundwater aquifer (the portion of the aquifer sampled by a series of shallow wells). This assumption allowed them to reduce the thickness of the modeled aquifer. During the benzene modeling, Caldwell *et al.* (1992) considered 1 percent of the background oxygen to be available for biodegradation. For the BTEX simulations, this value was raised to 4 percent.

The plume simulated by incorporating aerobic degradation matched the monitor-well data for both benzene and BTEX. Next, the biodegradation and oxygen coefficients were set to zero and the model was run again. This plume indicated the possible extent of the hydrocarbon plume assuming no biodegradation. The plume extended up to 100 feet beyond the boundaries of the biodegraded plume. By comparing these plumes, Caldwell *et al.* concluded that biodegradation processes were probably limiting the extent of the plume migration.

4. Michigan Gas Plant

Chiang *et al.* (1990) modeled a plume consisting of benzene, toluene, and xylene (BTX) contained in a sandy aquifer beneath a gas plant facility in Michigan. The sources of contamination were an on-site flare pit and a slop oil tank area. Examination of field data revealed that a decrease in the amount of BTX in the groundwater corresponded to a decrease in the amount of available dissolved oxygen. Two models, a MOC code (modified to include first-order decay) and Bioplume II, were used to model natural attenuation at the site.

The field data were used to set the initial conditions for both dissolved oxygen and BTX. The following parameters were also used in modeling the site.

TABLE 6
BIOPLUME II PARAMETERS FOR THE MICHIGAN GAS PLANT

Parameter	Value
Grid size	10 x 17
Cell size	Not reported
Hydraulic conductivity	1.1×10^{-1} cm/s
F ratio	3.0
Longitudinal dispersivity	80 cm
Transverse dispersivity	30 cm

Chiang *et al.* (1990) noted that the Bioplume II simulation was highly sensitive to variations in the transverse and longitudinal dispersivities. They were able to calibrate Bioplume II and obtain similar results for the observed and predicted BTX plumes. However, they were unable to appropriately model the dissolved oxygen plume.

Chiang *et al.* (1990) suggested two possibilities for this discrepancy. The first was their difficulty in accurately determining the oxygen recharge through the flare pit and the unsaturated zone. The second was that the F ratio in Bioplume II did not account for the hydrocarbon used in cell growth. If cell growth is taken into account, less oxygen is needed to degrade the same amount of hydrocarbon.

5. Denver Fuel Spill

Wiedemeier *et al.* (1993) modeled a plume at a jet fueling facility near Denver, Colorado. The plume source was Jet-A fuel leaking from on-site underground storage tanks. Both dissolved contaminant and non-aqueous phase liquids (NAPLs) were present within the aquifer. The NAPLs were present in the vadose zone and provided a continuous source of BTEX contamination.

Field data were used as model input for the initial BTEX plume. Wiedemeier *et al.* (1993) used the following additional parameters in modeling the site:

TABLE 7
BIOPLUME PARAMETERS FOR THE DENVER FUEL SPILL

Parameter	Value
Grid size	20 x 24
Cell size	75 ft x 75 ft
Hydraulic conductivity	1.0×10^{-3} cm/s
F ratio	3.1
Longitudinal dispersivity	10 ft
Transverse dispersivity	1 ft
Reaeration coefficient	0.0 day^{-1}
Anaerobic degradation coefficient	0.0 day^{-1}

The initial oxygen plume was also determined from site data. To ensure a conservative simulation, Wiedemeier *et al.* (1993) allowed no oxygen transfer across the prescribed head boundaries.

The Bioplume II results indicated that the maximum travel for the center of mass of the plume was less than one half mile. The nearest receptors were located approximately 2.5 miles downgradient. Using this worst-case scenario of no oxygen transfer across the prescribed head boundaries, Wiedemeier *et al.* (1993) showed that no active remediation was required. A bioventing system was later installed to remove the NAPL in the vadose zone.

6. Houston/Florida Underground Storage Tanks

Evans (1995) used Bioplume II to develop a risk-based approach to remediation. Evans considered two sites in Texas (sites A and B) and one site in Florida (site C) that were contaminated by leaking underground storage tanks. These tanks had been used to store gasoline and had released an unknown amount of BTEX into the surrounding groundwater.

Evans used the parameters in Table 8 to model the three sites.

TABLE 8
BIOPLUME PARAMETERS FOR THE HOUSTON/FLORIDA SITES

Parameter	Site A	Site B	Site C
Grid size	20 x 75	40 x 75	40 x 75
Cell size	20 ft x 20 ft	20 ft x 20 ft	20 ft x 30 ft
Hydraulic conductivity	1.4×10^{-3} cm/s	2.4×10^{-4} cm/s	1.0×10^{-3} cm/s
Porosity	0.45	0.40	0.30
Longitudinal dispersivity	5 ft	5 ft	5 ft
Transverse dispersivity	0.5 ft	0.5 ft	0.5 ft
Source concentration	25, 35, 70, 85 mg/L	30, 50, 100 mg/L	4-150 mg/L
Source recharge rate	2.0×10^{-7} ft/s	5.0×10^{-9} ft/s	5.0×10^{-9} ft/s
Background dissolved oxygen	0.0 mg/L	0.0 mg/L	0.0 mg/L

A steady-state model was used to evaluate the following remediation techniques:

1. No action taken.
2. Source removal only.
3. Oxygen injection with source removal.
4. Pump and treat with source removal.
5. Pump and treat combined with oxygen injection and source removal.

Evans also used the results of these simulations to evaluate the current clean-up standards with respect to exposure of possible receptors at the three sites. This study demonstrated that immediately removing the source of the contamination gave the most significant risk reduction. Based on this work, Evans concluded that, in specific cases, "the wisest course of action may be to implement an initial corrective action . . . and then pursue a risk-based assessment to determine an appropriate endpoint for remediation."

7. USAF — Risk-Based Studies

Parsons Environmental Services (Parsons ES) used Bioplume II in the development of a risk-based approach to remediation. The U.S. Air Force contracted Parsons ES to "perform intrinsic remediation demonstrations at 31 United States Air Force (USAF) bases and conduct risk-based approach remediation at eight USAF bases nationwide" (D. Moutox, personal communication 1995). The overall purpose of these studies was to "develop a systematic process for scientifically investigating and documenting naturally occurring attenuation processes that can be factored into overall site remediation plans". Two specific goals of this program were to:

1. ". . .provide defensible evidence that intrinsic remediation of dissolved-phase hydrocarbons can be used to develop an effective groundwater remediation strategy."

2. ". . . provide a series of regional case studies demonstrating that natural degradation often reduces contaminant concentrations in groundwater to below acceptable clean up standards completion of possible exposure pathways."

The contaminants of interest at these sites were benzene, toluene, ethylbenzene and xylene (BTEX). This risk-based approach considered reducing the concentrations of these contaminants to be more important than reducing the total concentration of petroleum hydrocarbons due to the relative toxicities of the two groups. By accounting for the benefit from natural attenuation, a significant cost savings can be obtained.

SECTION III
HYDROGEOLOGIC SETTING

A. GEOLOGIC ENVIRONMENT

The MADE site is located on Columbus Air Force Base in northeastern Mississippi (Figure 1) near the confluence of the Buttahatchee and Tombigbee Rivers, approximately 6 km east of the Tombigbee River and 2.5 km south of the Buttahatchee River (Boggs *et al.*,1990). The site is about 25 hectares in size and lies above the 100-year floodplain of both rivers (Young *et al.*, 1994; Boggs *et al.*, 1992). Topography at the site is relatively flat with a gentle slope to the north. The shallow unconfined aquifer at the site is an alluvial terrace deposit of Quaternary age associated with the Buttahatchee River. The aquifer, which averages approximately 11 meters in thickness, is composed of generally unconsolidated, poorly-sorted to well-sorted sandy gravel and gravelly sand, with minor amounts of silt and clay (Boggs *et al.*, 1992). The deposit is highly heterogeneous, with facies occurring in discontinuous lenses and layers. The facies generally have horizontal dimensions on the order of 8 meters or less and vertical dimensions of less than 1 meter (Boggs *et al.*, 1990; Boggs *et al.*, 1992).

Boggs *et al.* (1990) state that, based on facies mapping in gravel pits near the site, the depositional setting for the shallow aquifer was a braided stream environment. However, a former river meander observed on aerial photographs (Young *et al.*, 1994; Boggs *et al.*, 1992) indicates at least some deposition by meandering streams. The meander cuts across the middle of the MADE site with a southwest to northeast trend. Rehfeldt *et al.* (1992) note that the edges of the meander are poorly defined, both at the land surface and in the subsurface, and that the channel corresponds to a zone of higher hydraulic conductivity.

The terrace deposits are unconformably underlain by the Cretaceous marine Eutaw formation, which consists of interbedded clays, silts, and sands. Boggs *et al.* (1990) state that the Eutaw surface beneath the terrace deposit at the MADE site is composed of dense clay, except for one region in which fine-grained sands form the upper surface. In the region where the sand unit is present, it is underlain by the clay aquitard. For modeling purposes, the upper Eutaw sand was included with the terrace deposits as part of the aquifer. The top of the Eutaw clay was considered the base of the aquifer.

B. SUMMARY OF PREVIOUS HYDRAULIC TESTING AT THE MADE SITE

Numerous hydrogeological investigations have been conducted at the MADE site to characterize aquifer properties, hydraulic head distribution, and boundary conditions which affect head distribution. Determination of hydraulic conductivity at the site was the principle emphasis of many of the investigations. The following information describing these tests is drawn from Boggs *et al.* (1990), who present a detailed description of hydraulic tests conducted at the MADE site.

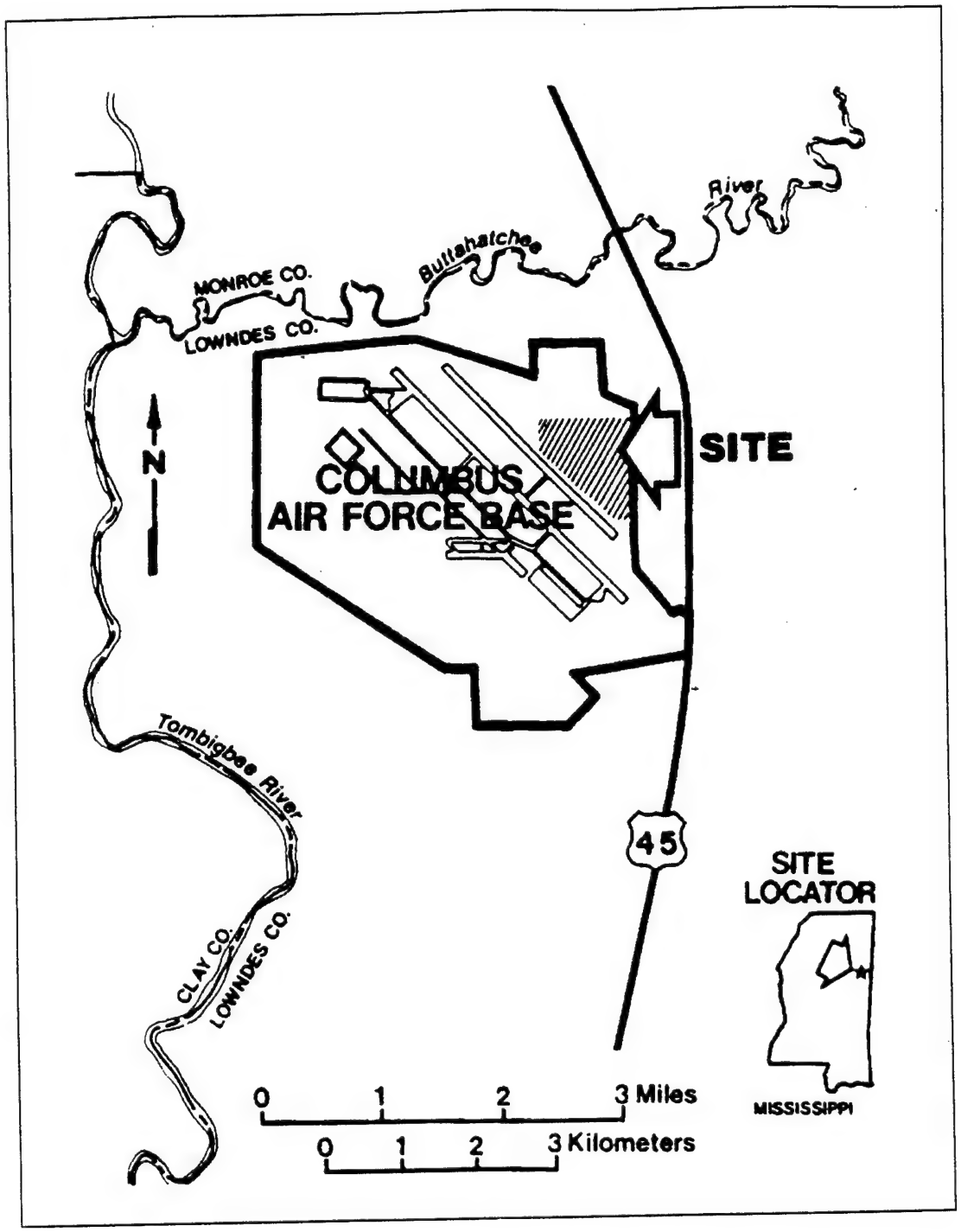

Figure 1. Site Location Map. (After Boggs et al., 1990)

1. Aquifer Tests

Two large-scale aquifer tests were conducted at the site in 1985, one southeast and one north of the MADE-2 injection site. These tests employed a central pumping well and several observation wells. The production wells were pumped at a constant rate, and water-level responses for the pumping and observation wells were monitored during pumping and recovery. The Neuman-type curve method for anisotropic unconfined aquifers was used to analyze the results of both tests. Estimates for transmissivity, specific yield, and the ratio of vertical hydraulic conductivity to horizontal hydraulic conductivity were determined by averaging the values for individual wells. Also, during tracer injection for the first MADE experiment, water levels in the injection wells and nearby monitor wells were recorded and analyzed using the Theis solution for nonsteady pumping.

Aquifer test AT1, conducted in March 1985, was located approximately 80 meters southeast of the MADE-2 injection site. Pumping lasted for 3 days, followed by 5 days of recovery measurements. An average transmissivity of 1.8 cm^2/s was obtained for the AT1 site, yielding an average horizontal hydraulic conductivity of 2.2×10^{-3} cm/s. The average specific yield was 0.04. Non-circular shaped drawdown contours for test AT1 indicated horizontal variability of the aquifer properties.

In July 1985, aquifer test AT2 was conducted at a location approximately 60 meters north of the MADE-2 injection site. This test is more pertinent to flow-and-transport modeling because it took place in the region traversed by the plume. The production well was pumped for 8 days and recovery was monitored for an additional 8 days. The test yielded an average transmissivity of 20.1 cm^2/s, an average hydraulic conductivity of 2.0×10^{2} cm/s, and an average specific yield of 0.10. Drawdown contours for AT2 are elliptical in shape, indicating either anisotropy or large-scale transmissivity variations. Boggs *et al.* (1990) give an estimated horizontal hydraulic conductivity ratio, K_{11}/K_{22}, of 2.6, based on an analysis of the final drawdown cone configuration.

Tracer injection for the MADE-1 experiment began on October 28, 1986 and lasted for 48.5 hours. Water levels in the injection wells and seven nearby observation wells were monitored. The average transmissivity calculated was 2.13 cm^2/s and the average horizontal hydraulic conductivity was 2.5×10^{-3} cm/s.

2. Borehole Flowmeter Tests

At the MADE site, 58 wells were installed for borehole flowmeter testing for the MADE-1 experiment, and an additional 11 wells were installed for the MADE-2 experiment. The borehole flowmeter measures flow into a pumping well at discrete elevation intervals. Hydraulic conductivities, which are proportional to flow, are calculated from the measured flow rates using the Cooper-Jacob well equation. Key assumptions for the borehole flowmeter method are that the

aquifer is layered and each layer is homogeneous and of uniform thickness, the storage coefficient of each layer is linearly related to the layer transmissivity, and the well losses for each layer can be estimated (Boggs *et al.*, 1990). Vertical spacing of the flowmeter measurements within each well was 15.24 cm (6 inches) (Rehfeldt *et al.*, 1992). For a more detailed description of the borehole flowmeter technique, see EPRI Report EN-6511 by Rehfeldt *et al.* (1989).

Figure 2(a) shows the aerial and side view of the borehole flowmeter measurement locations. Figure 2(b) shows the interpolated hydraulic conductivity distribution at five elevations in the transport region. This figure illustrates the extreme variability of conductivity, both vertically and horizontally. Hydraulic conductivity obtained from borehole flowmeter measurements varies from two to four orders of magnitude within individual wells and can even vary two orders of magnitude or more from sample to sample. A detailed analysis of the spatial variability of hydraulic conductivity at the site and hydraulic conductivity profiles for some of the wells are presented by Boggs *et al.* (1990).

3. Other Tests

Slug tests were conducted at 22 of the monitor wells and five of the tracer injection wells. These tests consisted of instantaneously increasing the water level in a well, followed by monitoring the water-level decline over time using a pressure transducer and data-logging system (Rehfeldt *et al.*, 1992). Boggs *et al.* (1990) present a table of the hydraulic conductivity estimates for each well. The geometric mean hydraulic conductivity based on these estimates was 1.2×10^{-2} cm/s, which compares well with the hydraulic conductivity estimate obtained from aquifer test AT2.

Another method evaluated for directly measuring variation in hydraulic conductivity was the double packer test. This method consists of injecting water at a constant flowrate or at a constant pressure into a section of the aquifer which has been isolated by pneumatic packers above and below the test section. Flowrates and pressures were monitored and used to estimate hydraulic conductivity. Only one well was tested using the double packer method. Boggs *et al.* (1990) state that hydraulic conductivities estimated from the packer tests were consistently higher than those from the flowmeter tests and showed less variation. They suggest that this may be due to vertical flow in the well annulus, since packer tests are more susceptible to annulus effects than the flowmeter method.

Laboratory permeameter tests were conducted on nine minimally disturbed cores from a single sample hole (Boggs *et al.*, 1990). Because the sediments at the site were generally cohesionless and therefore could not be trimmed without disturbing the core, a laboratory permeameter was designed to allow testing of the core while it remained in its field tube. Boggs *et al.* (1990) state that although there are some regions where hydraulic conductivities estimated by permeameter testing are comparable to flowmeter conductivity estimates, differences of up to three

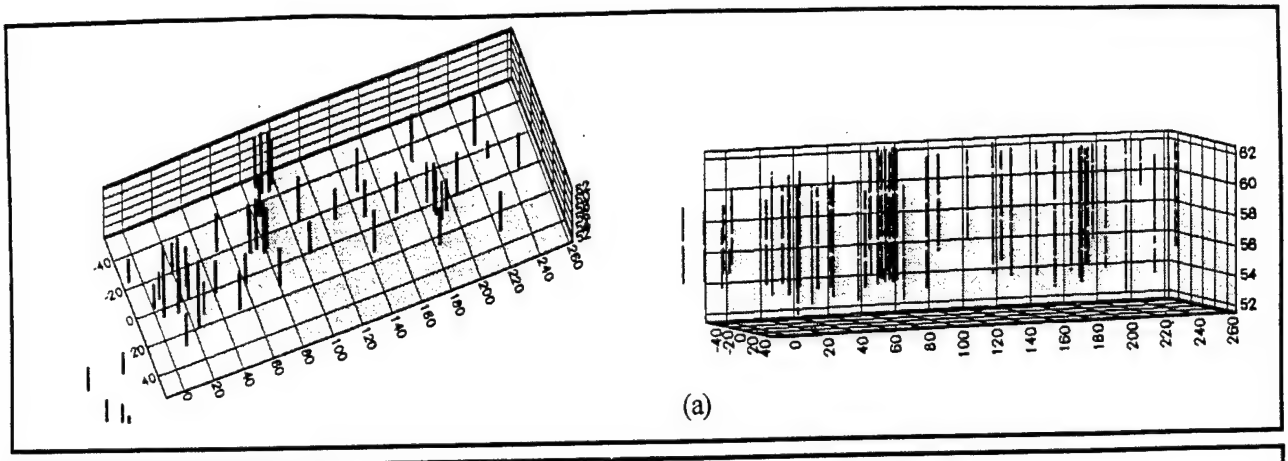

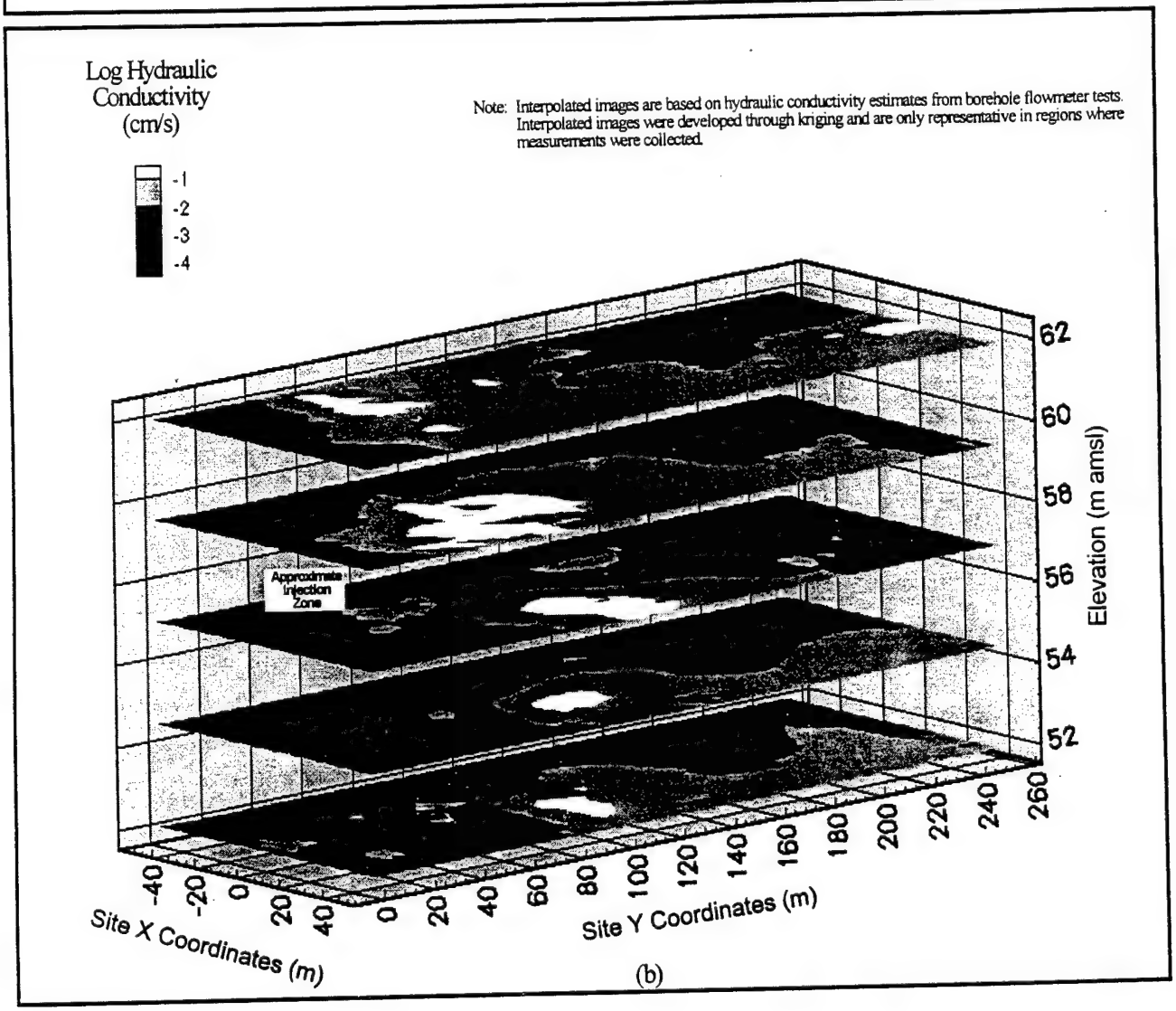

Figure 2. (a) Two Viewpoints Illustrating Location of Borehole Hydraulic Conductivity Measurements.
(b) Interpolated Hydraulic Conductivity Distribution at Five Elevations in the Transport Region.

orders of magnitude were indicated for other intervals. As an explanation for the lower estimates obtained from the permeameter tests, Boggs *et al.* (1990) suggest that the vertical conductivity measurements from the permeameter tests cannot be meaningfully compared to the horizontal conductivity estimates obtained from the flowmeter method due to the presence of low conductivity layers within the core samples.

Several indirect methods for estimating the spatial variability of the hydraulic conductivity field were tested at the site, including grain-size analysis, surface geophysical surveys, and downhole geophysical logging. Results of the grain-size analysis indicate a mean hydraulic conductivity of 4.3×10^{-2} cm/s. A detailed description of the geophysical methods and results is presented by Boggs *et al.* (1990).

4. Comparison of Results

Table 9 summarizes the hydraulic conductivity estimates obtained from each of the direct measurement methods tested at the MADE site. Because flow-and-transport modeling used a single-layer areal model, methods which sampled multiple discrete sections of a well were vertically averaged at each well for comparison. The average hydraulic conductivity obtained from the flowmeter measurements shows relatively good agreement with aquifer test AT2, the slug tests, and the double packer tests. However, it should be noted that the double packer tests were conducted at only one well, K12. The vertically averaged flowmeter hydraulic conductivity estimate for well K12 was 1.33×10^{-2} cm/s, only about one third of the estimated conductivity based on the double packer tests. As noted, this difference in the hydraulic conductivity estimates for the two methods may be due to vertical flow in the well annulus during the packer tests. The average flowmeter estimate was slightly higher than the AT2 estimate, and about the same as the value obtained from the slug tests. Aquifer test AT1, the tracer injection test, and the laboratory permeameter tests all yield hydraulic conductivity estimates over one order of magnitude less than the average flowmeter estimate. The location of these tests in areas of relatively low hydraulic conductivity probably accounts for the lower estimates. The vertically averaged hydraulic conductivity estimate for the flowmeter well closest to sample hole C11 (source of the core used for the laboratory permeameter tests) was 3.81×10^{-3} cm/s, slightly over three times higher than the average permeameter value. One possible explanation for this difference is the different measurement orientation of these two methods. The permeameter measures vertical flow, and the flowmeter measures predominantly horizontal flow.

TABLE 9
HORIZONTAL HYDRAULIC CONDUCTIVITIES (AVERAGE AND RANGE) OBTAINED FROM THE VARIOUS DIRECT MEASUREMENT METHODS

Test Description	Number of Wells Used for Avg.	Minimum Hydraulic Conductivity (cm/s)	Maximum Hydraulic Conductivity (cm/s)	Arithmetic Average Hydraulic Conductivity (cm/s)
Aquifer Test AT1	12	8.0×10^{-4}	4.6×10^{-3}	2.2×10^{-3}
Aquifer Test AT2	16	8.2×10^{-3}	7.7×10^{-2}	2.0×10^{-2}
Tracer Injection Test	7	1.5×10^{-3}	3.7×10^{-3}	2.5×10^{-3}
Borehole Flowmeter Tests	67	8.7×10^{-4}	2.3×10^{-1}	3.1×10^{-2} (1)
Slug Tests	27	7.0×10^{-4}	1.8×10^{-1}	3.1×10^{-2}
Double Packer Tests	1	4.2×10^{-2}	4.2×10^{-2}	4.2×10^{-2}
Lab. Permeameter Tests	1	1.2×10^{-3}	1.2×10^{-3}	1.2×10^{-3}

(1) Represents the arithmetic average of the thickness-weighted vertical averages for 67 boreholes.

C. GROUNDWATER

1. Flow Dynamics

A network of piezometers at the site (Figure 3) was used to monitor the groundwater levels approximately monthly throughout the 16-month duration of the MADE-2 experiment. Additionally, eight pairs of staged piezometers were equipped with continuous water-level recorders. Wells denoted by a well name followed by a letter suffix (A, B, C, or D) are multistaged and consist of individual piezometers screened over different vertical intervals. Type "A" piezometers are screened at an average elevation of 61.1 meters, and type "B" piezometers are screened at an average elevation of 56.3 meters (Boggs *et al.*, 1993). Potentiometric surface maps from data collected each month during the experiment are presented in Appendix A. Potentiometric surfaces were generated for both the shallow (Type "A") and deep (Type "B" and no suffix) wells.

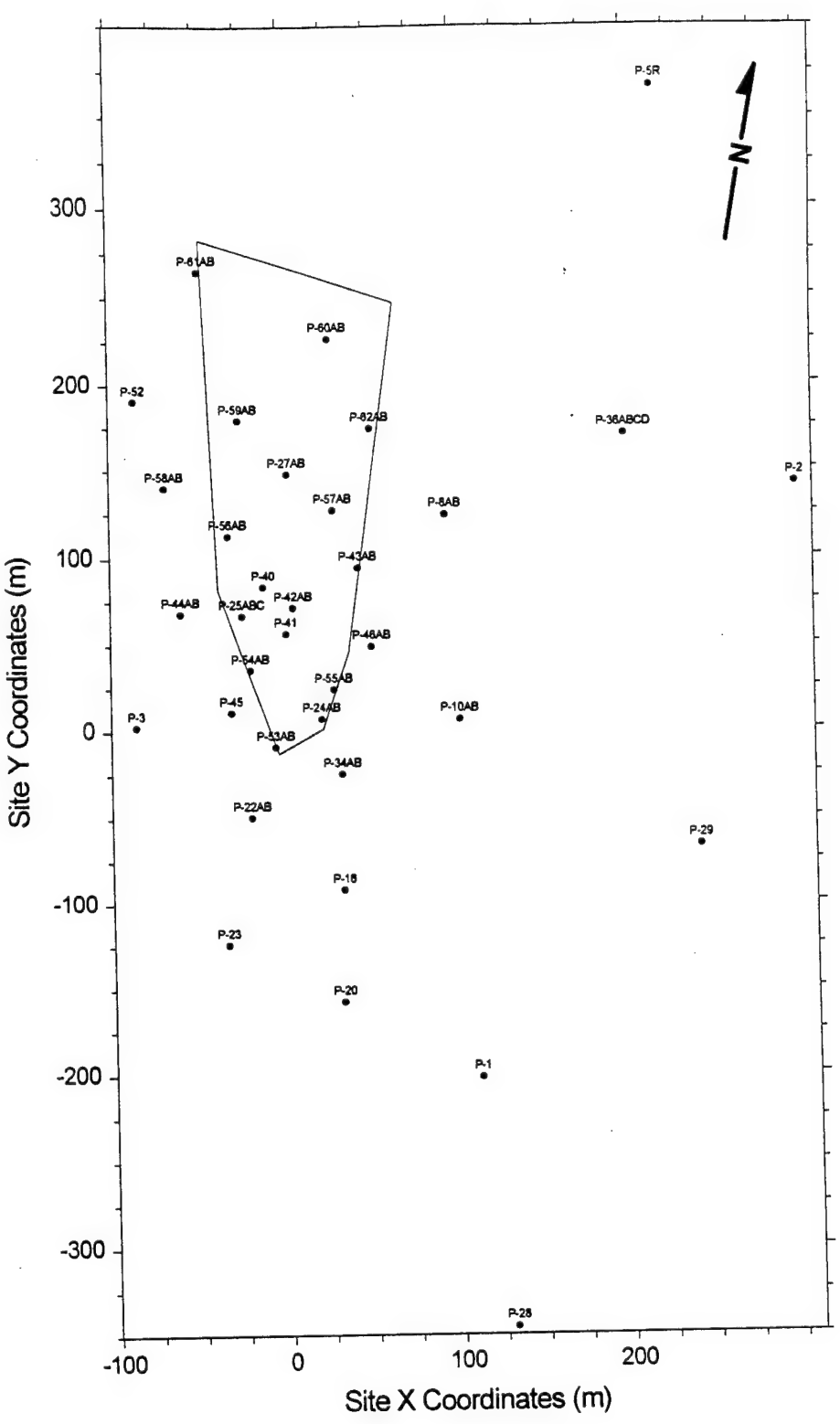

Figure 3. MADE-2 Groundwater Observation Wells.

Examination of the potentiometric surface maps in Appendix A reveals a generally northward gradient which varies in both magnitude and direction through time. Seasonal fluctuations in the water table range from 2 to 3 meters, resulting in a 20 to 30 percent variation in the saturated thickness of the aquifer (Boggs *et al.*, 1992). Figure 4, a plot showing the difference between the shallow and deep potentiometric surfaces (based on data collected January 8, 1991), indicates strong vertical gradients throughout much of the model area, particularly in areas of relatively low permeability. Boggs *et al.* (1992) state that vertical hydraulic gradients at the site were of the same magnitude or larger than the horizontal gradient in some places.

2. Chemistry

For the ambient groundwater at the site, Boggs *et al.* (1992) and Stauffer *et al.* (1994) report a low total dissolved solids content averaging 43 mg/L, an ionic composition dominated by sodium, silica, and chloride, and a pH averaging 4.8. Boggs *et al.* (1990) report that the average groundwater redox (Eh) level is 543 mV, indicating oxidizing conditions. They state that the following four factors probably contribute to this condition: (1) a high rate of recharge containing a high oxygen content and a high redox buffering capacity; (2) high groundwater velocity and short residence times; (3) low concentrations of organic matter in the aquifer; and (4) the presence of other redox buffers. For a more detailed summary of the chemical characteristics of the groundwater, see Boggs *et al.* (1992) and Stauffer *et al.* (1994).

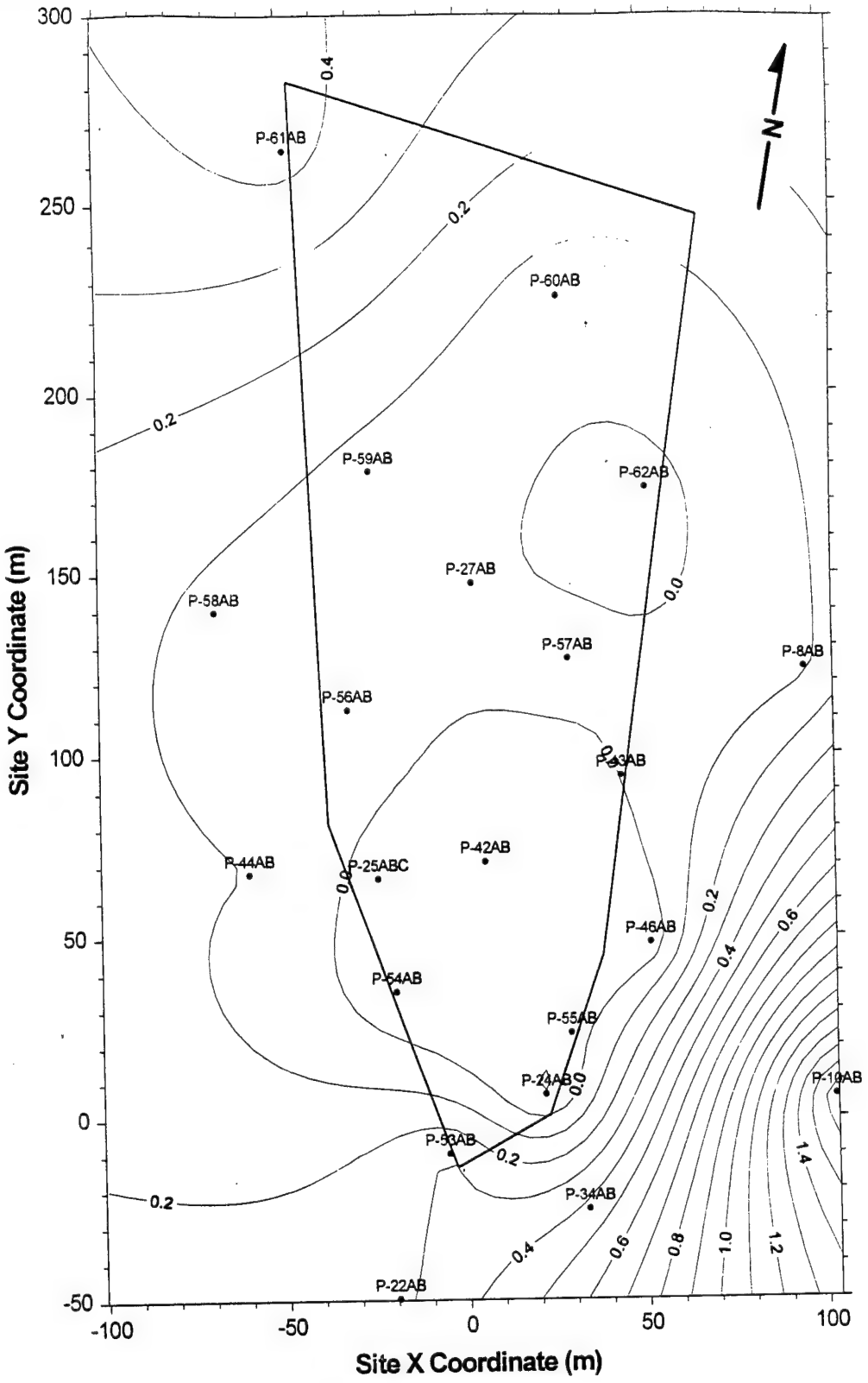

Figure 4. Contour Plot of the Difference Between the Shallow and Deep Potentiometric Surfaces for January 8, 1991.

SECTION IV
SITE GROUNDWATER FLOW MODEL

A. CODE SELECTION AND DESCRIPTION

MODFLOW was selected for development of a flow model in this study. MODFLOW (McDonald and Harbaugh, 1988) is a three-dimensional, finite-difference flow model that is based on a block-centered approach. Hydrogeologic layers can be simulated as confined, unconfined, or a combination of both. External stresses such as wells, areal recharge, evapotranspiration, drains, and streams can also be simulated. For this study, the finite-difference flow equations were solved using a preconditioned conjugate-gradient method. The code is written in FORTRAN 77 and is well documented. The code is in the public domain, is well accepted by regulatory agencies, and has been used extensively to simulate groundwater flow under field conditions. The code MODPATH (Pollock, 1989) was used to track particles during the calibration of the flow model. MODPATH is a particle-tracking, post-processing package for computing three-dimensional path lines using output from steady-state simulations of MODFLOW.

B. MODEL FRAMEWORK AND PARAMETERIZATION

1. Finite-Difference Grid

Since the results of the flow modeling were used as input to Bioplume II, the design of the groundwater flow model finite-difference grid was determined by the Bioplume II model requirements. A single-layer areal flow model was necessary because Bioplume II is a two-dimensional contaminant transport model. Bioplume II required a constant grid spacing in the x and y directions, although the constant grid spacing in the two directions can be different. This eliminated the possibility of using a telescoping grid with refinement in the area of the source, making it necessary to use a relatively small constant grid spacing. This small grid spacing, coupled with the need to limit the total number of grid cells in order to maintain acceptable run times for Bioplume II, limited the size of the modeled area.

The original grid design had a total of 1947 grid blocks: 33 grid blocks in the x direction (perpendicular to flow) and 59 grid blocks in the y direction (parallel to flow). The grid spacings were 6.096 meters (20 feet) and 7.62 meters (25 feet) for the x and y directions, respectively. The area covered by this grid extended more than 30 meters in all directions beyond the area sampled by the five snapshots (Figure 5). Initial Bioplume II simulations indicated that grid refinement was required near the source to avoid excessive numerical dispersion. A second refined grid was developed (Figure 6) with a grid spacing of 1.524 meters (5 feet) in both directions. To limit the total number of grid cells, the dimensions of the model area were reduced. There are 92 and 205 grid cells in the x and y directions, respectively, yielding a total of 18860 grid blocks.

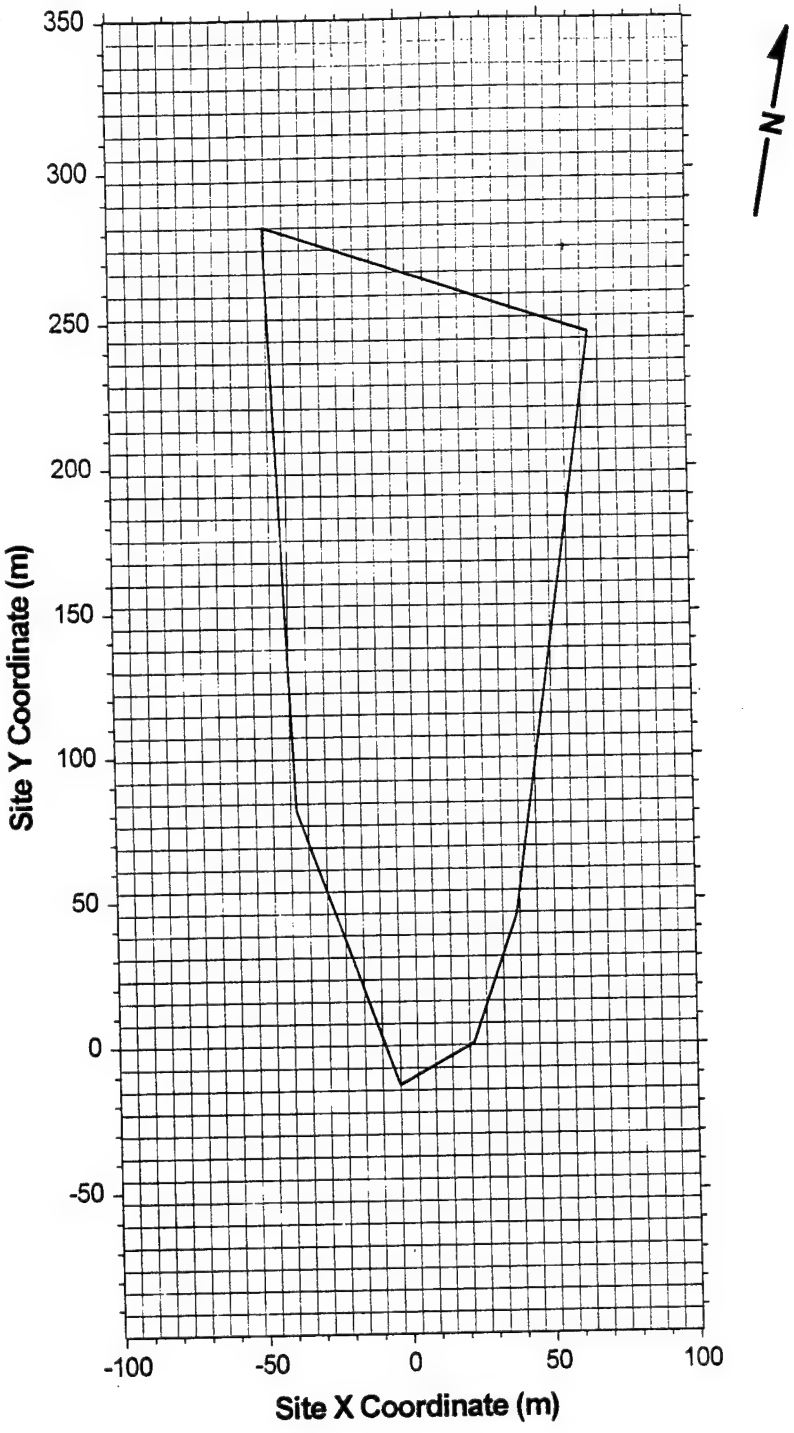

Figure 5. Original Finite-Difference Grid with Cell Dimensions of 6.096 m (20 ft) and 7.62 m (25 ft) in the X and Y Coordinate Directions (Specified Head Cells Are Shaded).

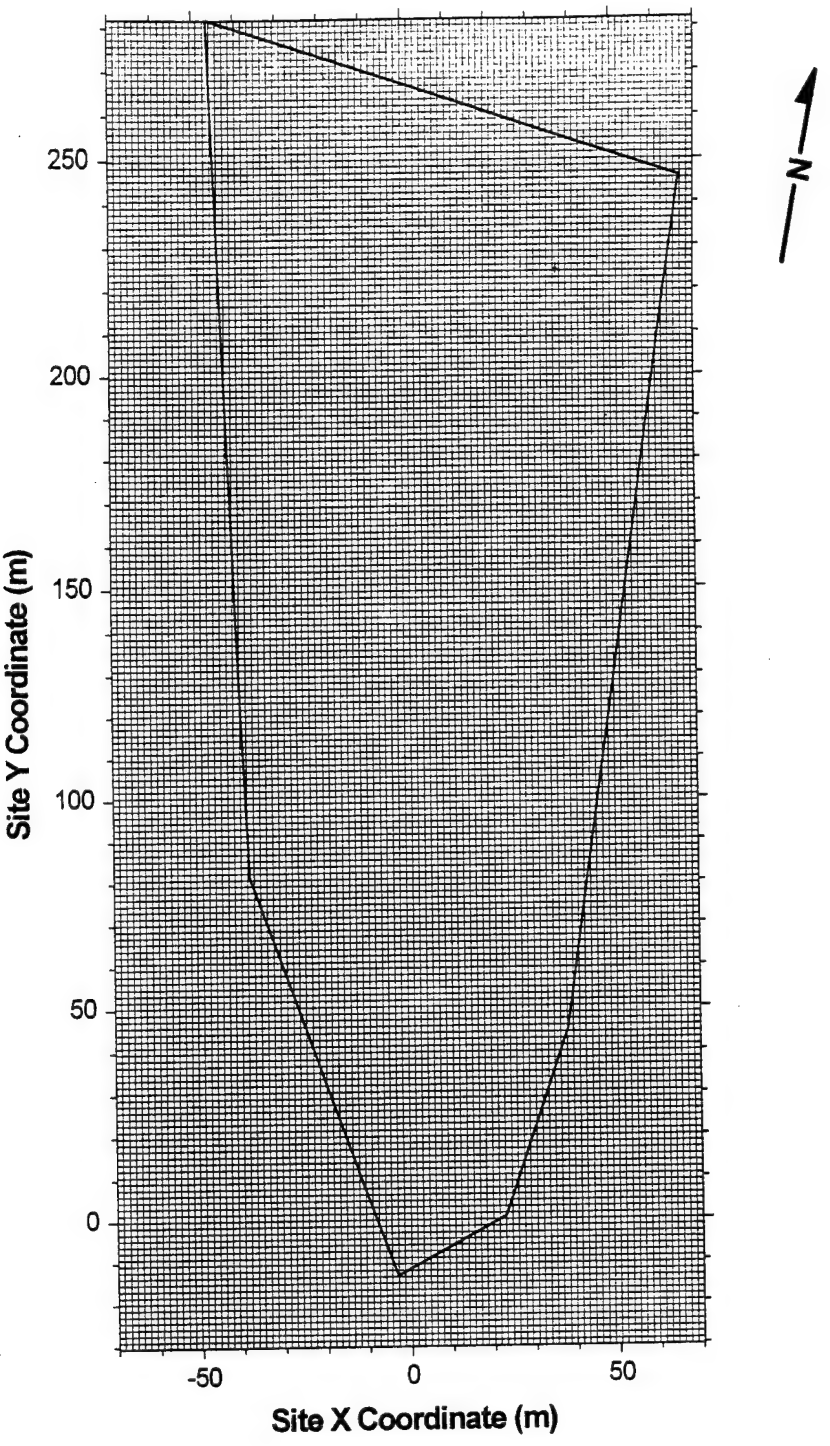

Figure 6. Refined Finite-Difference Grid with Cell Dimensions of 1.524 m (5 ft) in both X and Y Coordinate Directions (Specified Head Cells Are Shaded).

2. Hydraulic Parameterization

a. Hydraulic Conductivity

Hydraulic conductivities used for flow modeling are based on borehole flowmeter conductivity estimates. Boggs et al. (1993) document hydraulic conductivity values derived from the borehole flowmeter measurements collected at the MADE site. The three-dimensional data base includes hydraulic conductivity measurements in 56 wells tested for the MADE-1 experiment and 11 new wells tested for MADE-2. Vertical spacing of measurements was approximately 15 cm. Figure 7 shows the location of all flowmeter wells. Rehfeldt *et al.* (1989) describe the details of the borehole flowmeter method for determining hydraulic conductivity.

FORTRAN code was developed to vertically average conductivities from the data base. The following algorithm was used to estimate the horizontal conductivity for each well, treating each vertical sample as a separate layer of a layered system:

$$K_{avg} = \sum_I (m_i \cdot K_i) / \sum_I m_i$$

in which:

m_i is the vertical thickness of an individual layer, and
K_i is the hydraulic conductivity of an individual layer.

A kriging algorithm was then used to estimate conductivity values at each grid cell for input to the flow modeling routine. A map of the vertically averaged conductivities compares well with the depth averaged hydraulic conductivity plot shown by Rehfeldt et al (1992).

b. Recharge

Precipitation data for the 16-month period of the MADE-2 experiment was provided by Boggs (personal communication, 1995). Boggs *et al.* (1990) state that work by GeoTrans indicated that net recharge to the aquifer from local infiltration is approximately 40 percent of total precipitation. However, they also state that the recharge estimate should be considered only an order of magnitude estimate.

For the steady-state model, a recharge value of 17 inches/year, approximately 25 percent of yearly precipitation based on the 16-month MADE-2 test period, was used. The transient model used a time varying percentage of precipitation which was based on well hydrographs for wells equipped with continuous water-level recorders. Recharge varied from 0 percent of precipitation in the summer up to 100 percent during March.

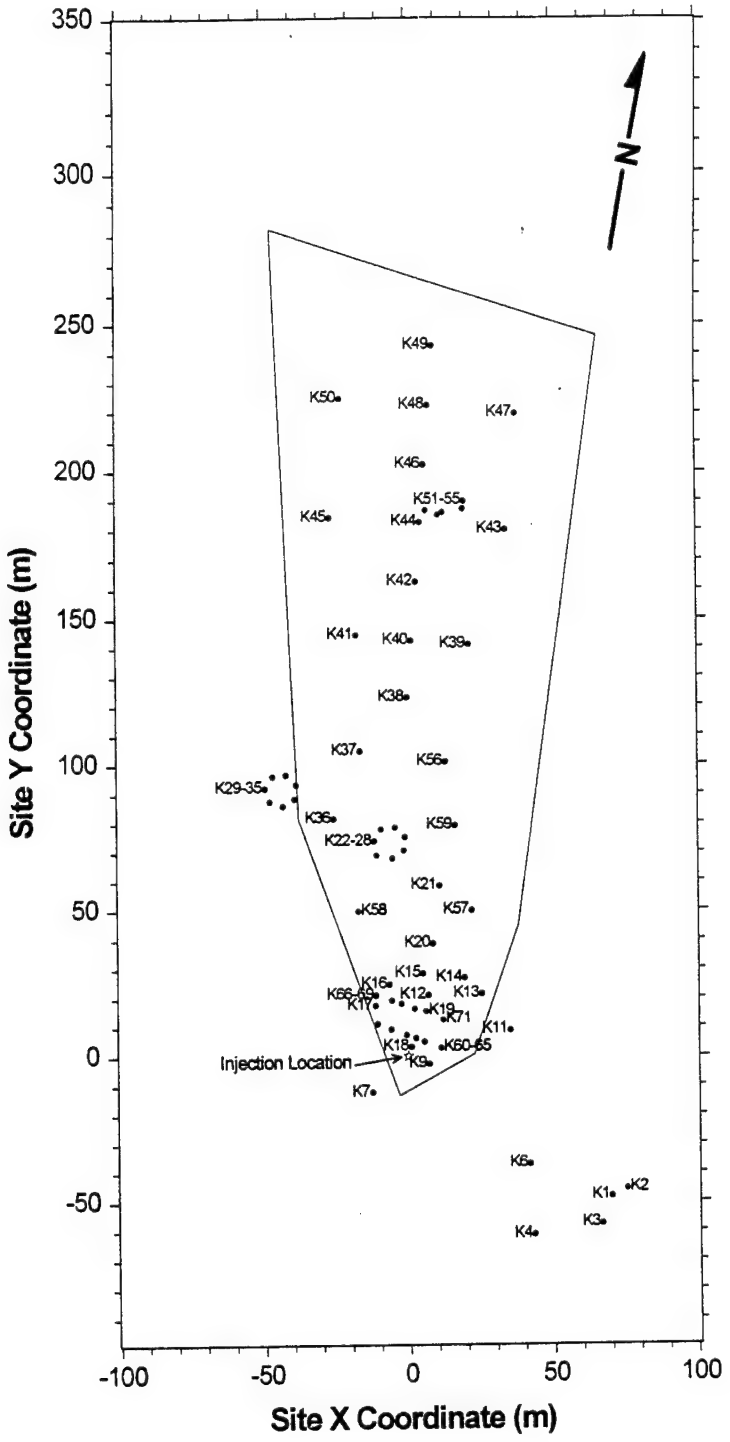

Figure 7. MADE-2 Borehole Flowmeter Test Well Locations.

3. Boundary Conditions

Since the MADE site is located about 2.5 km upgradient from the Buttahatchee River, the river is too far away to use as a boundary for the model. Likewise, there are no well-defined hydraulic boundaries upgradient of the site. Therefore, it was necessary to estimate hydraulic head conditions that would provide suitable boundary conditions for the flow domain represented by the finite-difference grid. Since the grid was aligned along the center line of the plume and therefore not exactly orthogonal to the flow direction, no-flow boundaries could not be used. All external boundaries had to be modeled as prescribed head boundaries.

4. Model Calibration

Calibration is the process of refining the hydraulic parameters of a flow model (hydraulic conductivity, system stresses, recharge rates, and boundary conditions) until an acceptable correspondence between the model simulation and field observations can be obtained. A model is considered calibrated when a set of hydraulic parameters produces model results which match observed values within a pre-determined range. Field-measured heads and estimated center of mass location of the conservative tracer were used to calibrate the flow model.

Flow model calibration was achieved through a trial and error deterministic approach. This method was selected because a significant amount of vertical characterization information (hydraulic conductivity and tracer concentration) was "lost" through the vertical averaging required by Bioplume II. The loss of information resulting from vertically averaging a system that is known to be highly heterogeneous negates much of the benefit derived from using more sophisticated approaches to flow model calibration.

A brief description of the calibration process is documented in the following section. For a more detailed description of the flow model calibration, see Appendix B.

a. Steady-State Calibration

(1) *Calibration Methodology.* For a steady-state estimate of the head field, water-level measurements collected during the 16-month test period were averaged for each of the piezometers shown in Figure 8. Because of the small area being modeled and the use of prescribed heads for all boundaries, the residual error was relatively small for all the calibration simulations.

Because the results of the flow model were used as input to the Bioplume II contaminant transport model, groundwater velocity (magnitude and direction) was extremely important. Therefore, the primary focus of the flow model calibration was on developing a groundwater velocity distribution that would closely mimic the velocity distribution estimated by

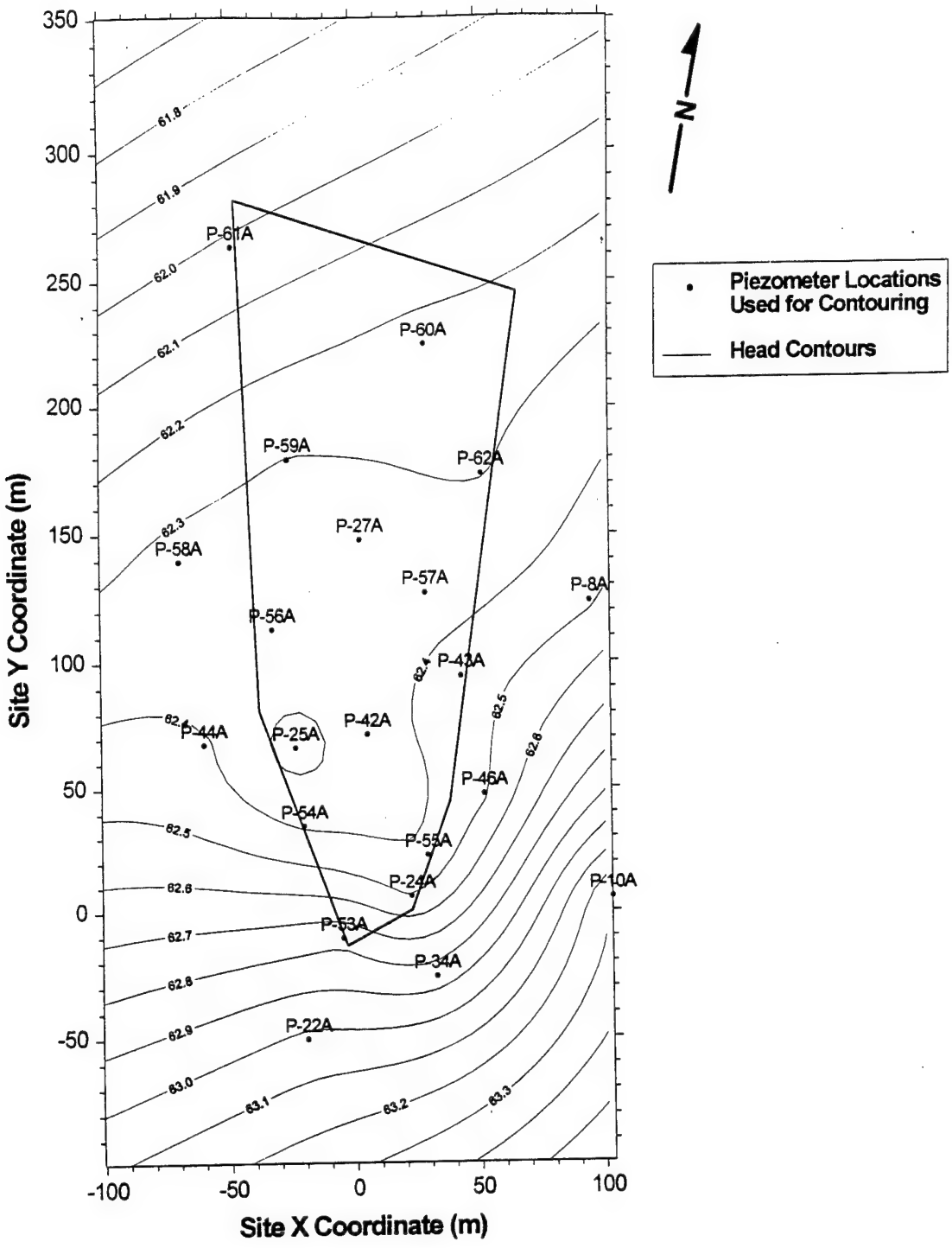

Figure 8. Contour Plot of the 16 Month Average Water Level Measurements.

monitoring the tritium plume during the MADE-2 experiment. Particle tracking was used to determine how well the simulated flow velocity compared to observed flow based on the center of mass locations for the tritium plume. Stauffer *et al.* (1994) list the center of mass locations for the tritium plume during Snapshots 1, 2, 3, and 4. A comparison of observed and simulated center of mass locations for Snapshot 2 was used for calibration. Then, snapshots 3 and 4 were used for verification and further model calibration. Calibration was achieved by adjusting to the hydraulic conductivity distribution and boundary heads so the conservative particle movement was comparable to the estimated center of mass for the observed tritium plume.

(2) *Hydraulic Parameters.* The initial hydraulic conductivity field was developed by vertically averaging conductivity measurements using the method described in Section IV.B.2.a. Particles tracked through the resulting steady-state velocity field showed that plume velocities were much too low when compared to observed velocities based on measured tritium plume advance. Preferential movement of the tracer through higher conductivity zones is probably the source of this difference.

To preserve the higher hydraulic conductivity zones in the model, a different approach was taken to calculate the vertical average. Instead of vertically averaging every measurement collected in a well, the aquifer thickness was divided into even increments with conductivity measurements vertically averaged for each increment. The hydraulic conductivity for the well was then set equal to the largest vertically averaged hydraulic conductivity calculated from the increments. Vertical increments of 0.5 meters, 1 meter, 2 meters, and 3 meters were evaluated, with 0.5 meters giving the best results with respect to travel time comparisons. Plots of these conductivity fields and the model results obtained using them are shown in Appendix B. To achieve a better match between modeled and observed plume velocities, other minor adjustments were made to the conductivity field. The final conductivity field, shown in Figure 9, is strongly skewed toward the highest observed field measurements.

For a steady-state estimate of groundwater elevations along the model boundaries, water-level measurements collected during the 16-month test period were averaged for each well. Extrapolating to the boundaries using a kriging routine provided the initial prescribed head boundary conditions for the model. The kriging routine implemented a linear drift to account for the natural gradient at the site, which was assumed to provide better head estimates at the boundaries. Particle tracking of model results using these boundary conditions revealed that the simulated groundwater flow direction was significantly different from that indicated by the observed tritium plume. Several iterations of minor boundary adjustments were made to properly orient the flow direction so that it would agree with that of the observed plume.

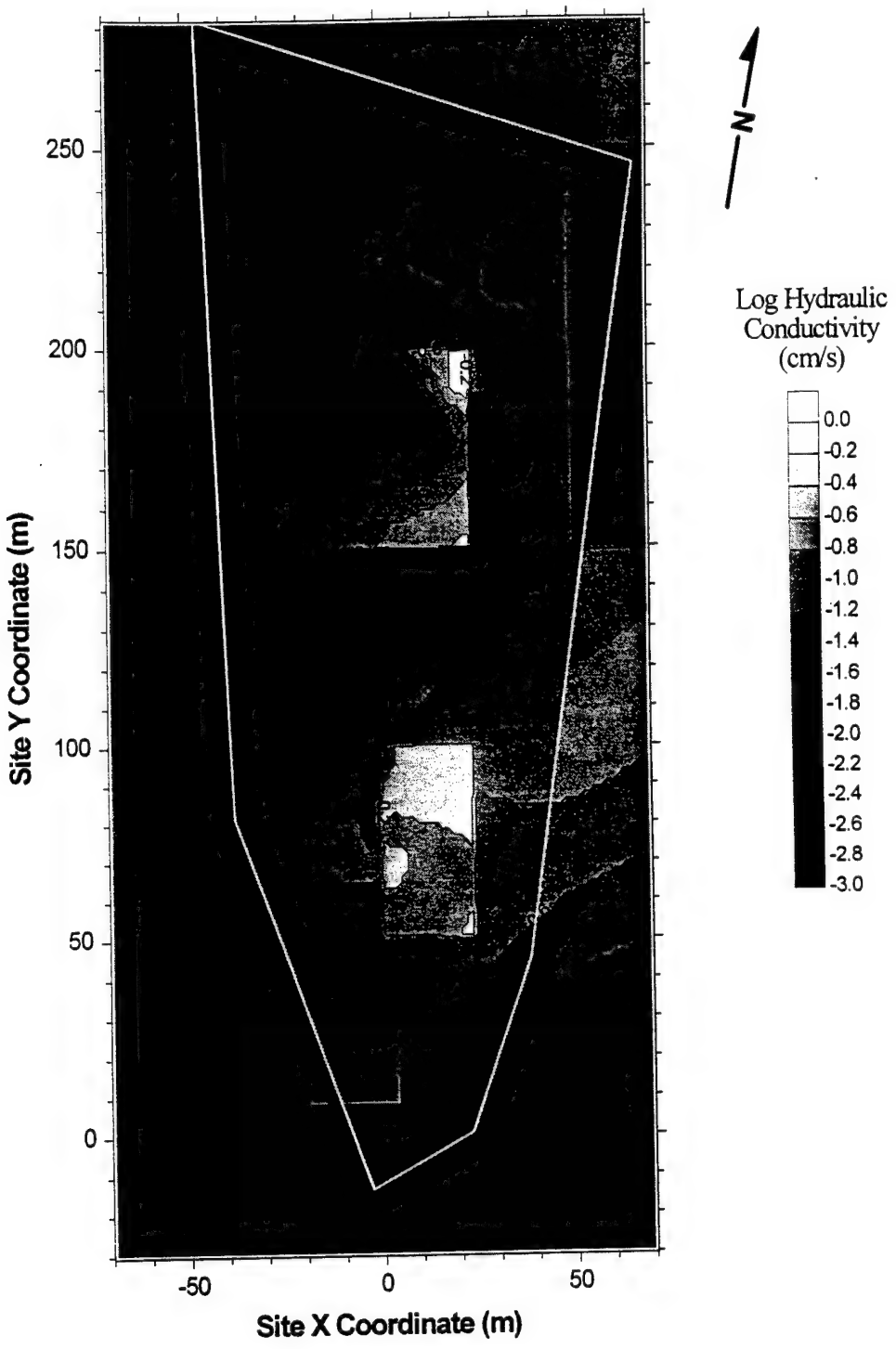

Figure 9. Final Calibrated Hydraulic Conductivity Field.

The initial estimate for recharge due to precipitation was 10 in/yr (approximately 15 percent of total recharge based on measured precipitation during the MADE-2 test). This was later increased to 17 inches/year (approximately 25 percent of precipitation). Due to the small size of the modeled area, changes in recharge have a relatively minor effect on model results as compared to changes in hydraulic conductivity or boundary heads. The Bioplume II model allows modification of the reaeration coefficient, regardless of the volumetric recharge rate.

(3) *Calibration Results.* Figure 10 shows initial model results using a weighted vertical average hydraulic conductivity field and prescribed head boundaries based on time averaged head estimates. The behavior of a conservative particle tracked from the injection location demonstrates that these assumptions did not yield a velocity distribution which could have produced the observed tritium plume. Simulated groundwater velocity is significantly different from that indicated by the observed plume in both direction and speed.

Model results incorporating the changes mentioned in the previous section are shown in Figure 11. Figures 12 and 13 show the histogram and scattergram for the head residuals. The residuals are fairly normally distributed, with few outliers. Particle tracking demonstrates that simulated flow closely follows the center of the observed tritium plume out to about 200 meters (MADE-2 coordinates), where the observed plume starts to curve more sharply to the east than the simulated particle. The main goal of calibration for this flow model was to develop a groundwater velocity distribution throughout the transport domain that would closely mimic the velocity distribution estimated by monitoring the tritium plume during the MADE-2 experiment. The calibration methodology employed herein met this criterion in the region of interest for transport modeling.

b. Transient Calibration

(1) *Calibration Methodology.* The transient flow model was developed to determine if a steady-state model was sufficient to meet the study objectives. As with the steady-state model, particle tracking was used to evaluate how well the simulated velocity compared to observed flow based on the center of mass locations for the tritium plume. Center of mass locations for Snapshots 2, 3, and 4 were used to evaluate the results. Adjustments to the transient boundary heads were used to match the movement of a conservative particle to that of the observed plume.

(2) *Hydraulic Parameters.* The hydraulic conductivity field used for transient modeling was developed by vertically averaging conductivity measurements over six vertical increments of two meters each using the method described in Section IV.B.2.a. The maximum conductivity thus calculated for each well was then assigned as the hydraulic conductivity at the well location. An interpolation algorithm was then used to estimate conductivity values at each grid cell. Prescribed head boundaries for transient modeling were obtained by extrapolation of water-level measurements

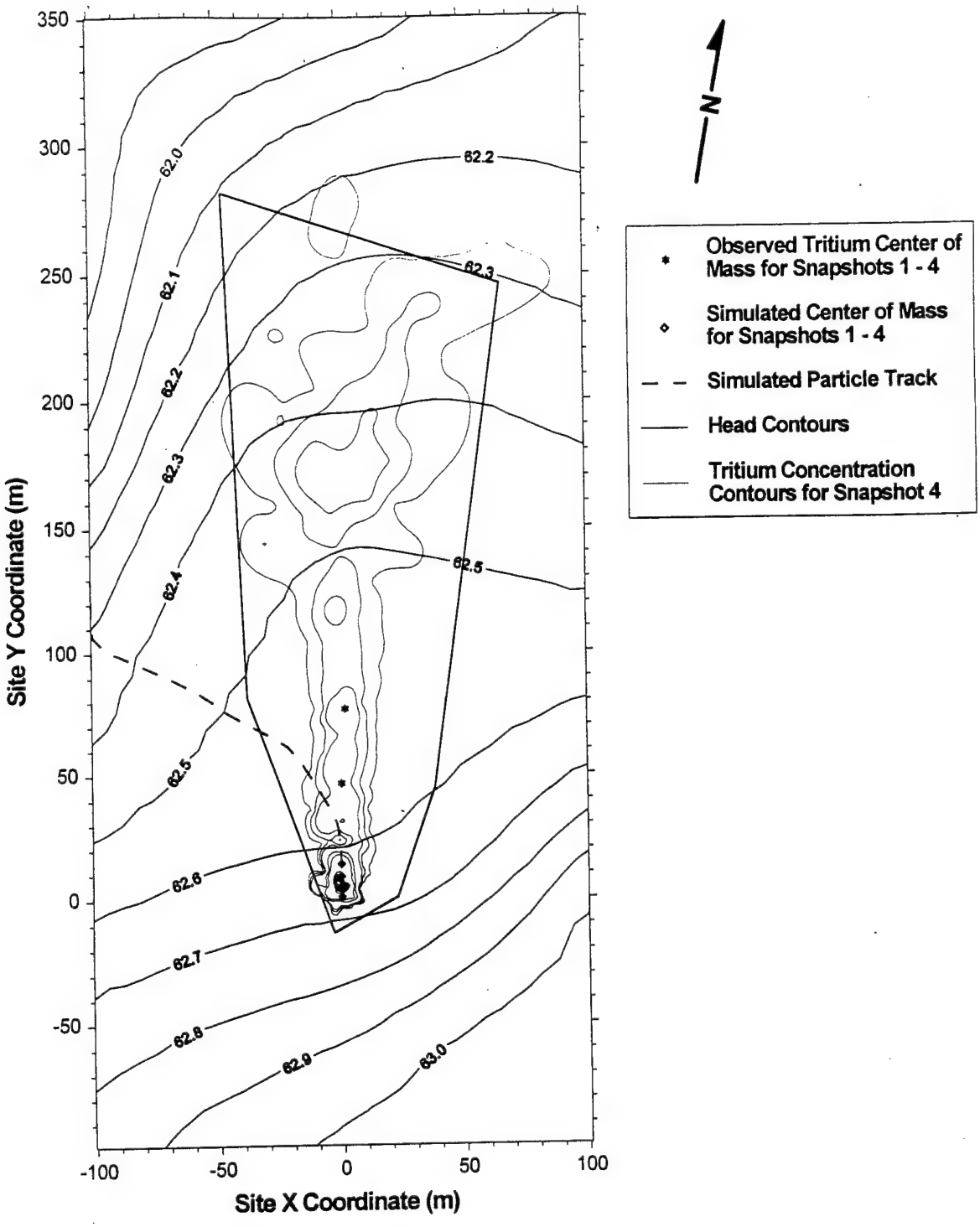

Figure 10. Steady-State Simulated Heads (m amsl) Based on Initial Assumptions for Hydraulic Conductivities and Boundary Conditions.

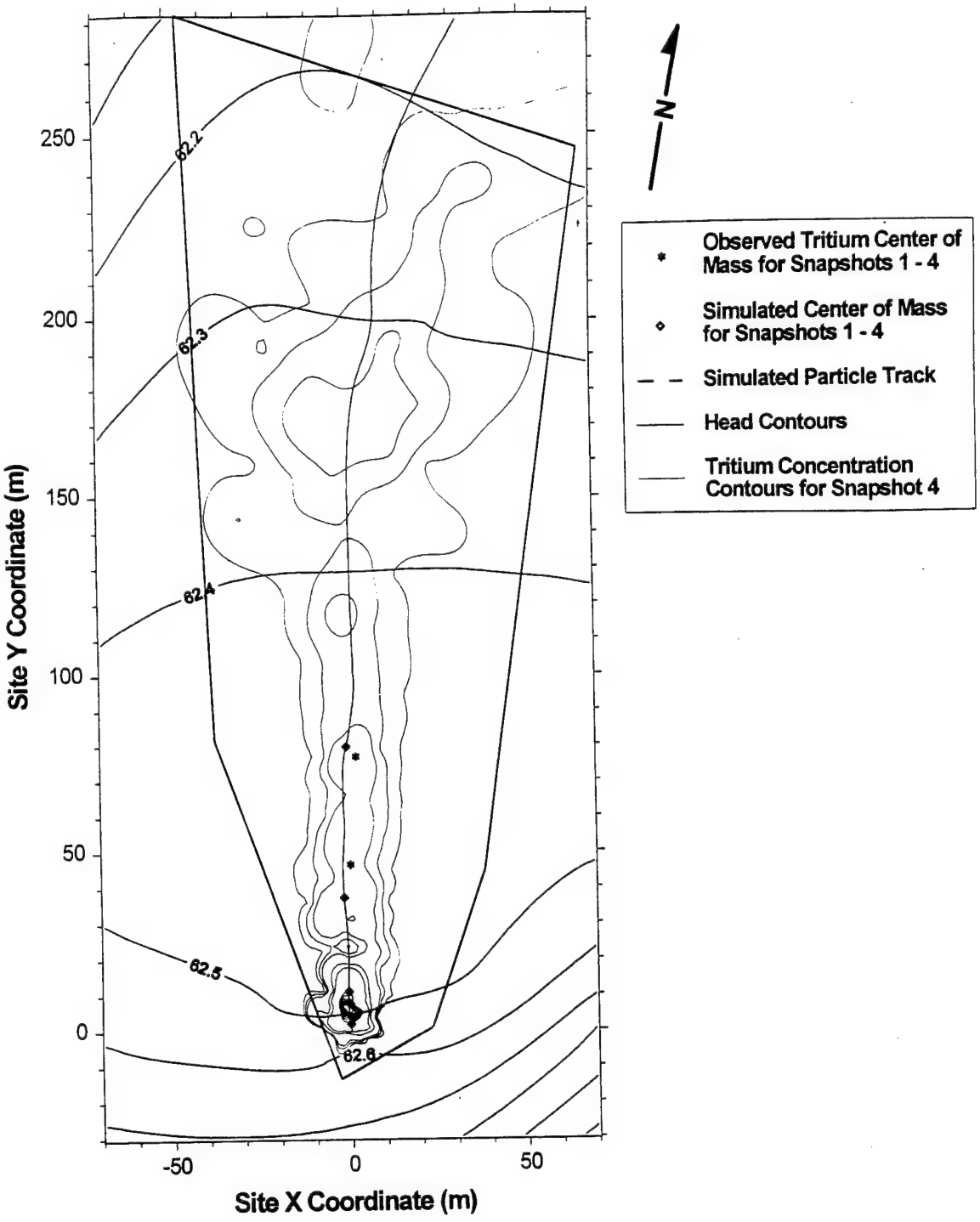

Figure 11. Final Calibrated Steady-State Simulated Heads (m amsl).

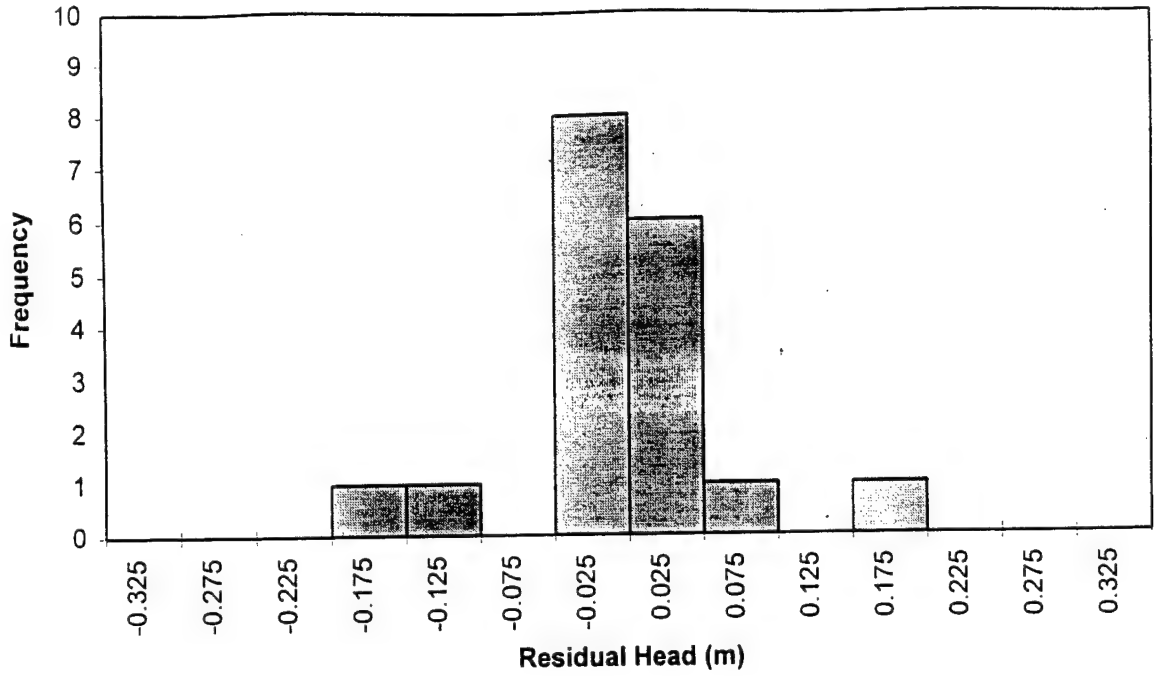

Figure 12. Histogram of Head Residuals for the Final Calibrated Flow Model.

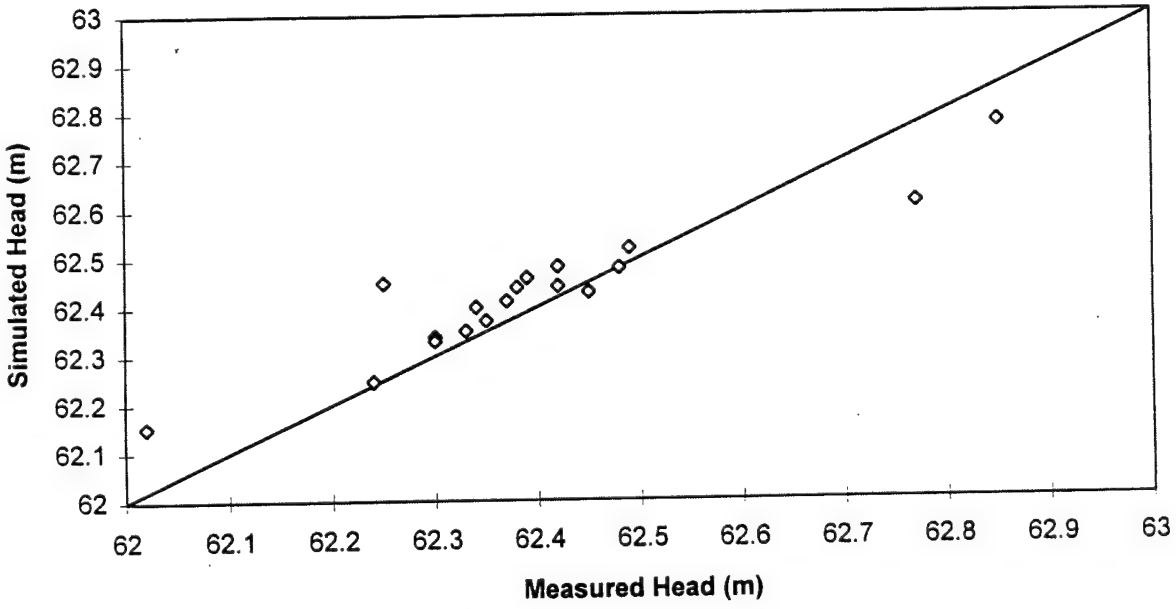

Figure 13. Scattergram of Head Residuals for the Final Calibrated Flow Model.

to the boundaries for each of the monthly sampling events, followed by interpolation to the 7- to 10-day stress periods used. The transient model used a time varying percentage of precipitation which was based on the response shown by well hydrographs to precipitation events. Wells equipped with continuous water-level recorders were used to gather these data. Based on evaluation of the data, simulated recharge varied from 0 percent of precipitation in the summer up to 100 percent during March.

(3) *Calibration Results.* Figure 14 shows the initial transient model results. A conservative particle tracked from the injection location moves toward the northwest, away from the centerline of the observed tritium plume. Comparison of this particle track with that for the initial steady-state simulation (Figure 10) shows very similar results. This result is important because it indicates that the groundwater flow directions estimated by a standard approach to transient modeling were not reliable without further calibration based on *a priori* knowledge of the tracer movement. The same conclusion was reached for the steady-state modeling.

Figure 15 shows the results of a transient simulation in which the prescribed head boundaries were adjusted to alter the flow direction and match observed plume behavior. It was also noted from this simulation that the simulated particle only moved about half as far as the estimated tritium plume center of mass. Because the results of the steady-state and transient flow modeling were very similar in that both models required similar parameter modifications for calibration, the steady-state model was selected for transport modeling. The steady-state model was also selected because it was sufficient to simulate the overall observed velocity distribution and required much less computer runtime during the transport simulation phase.

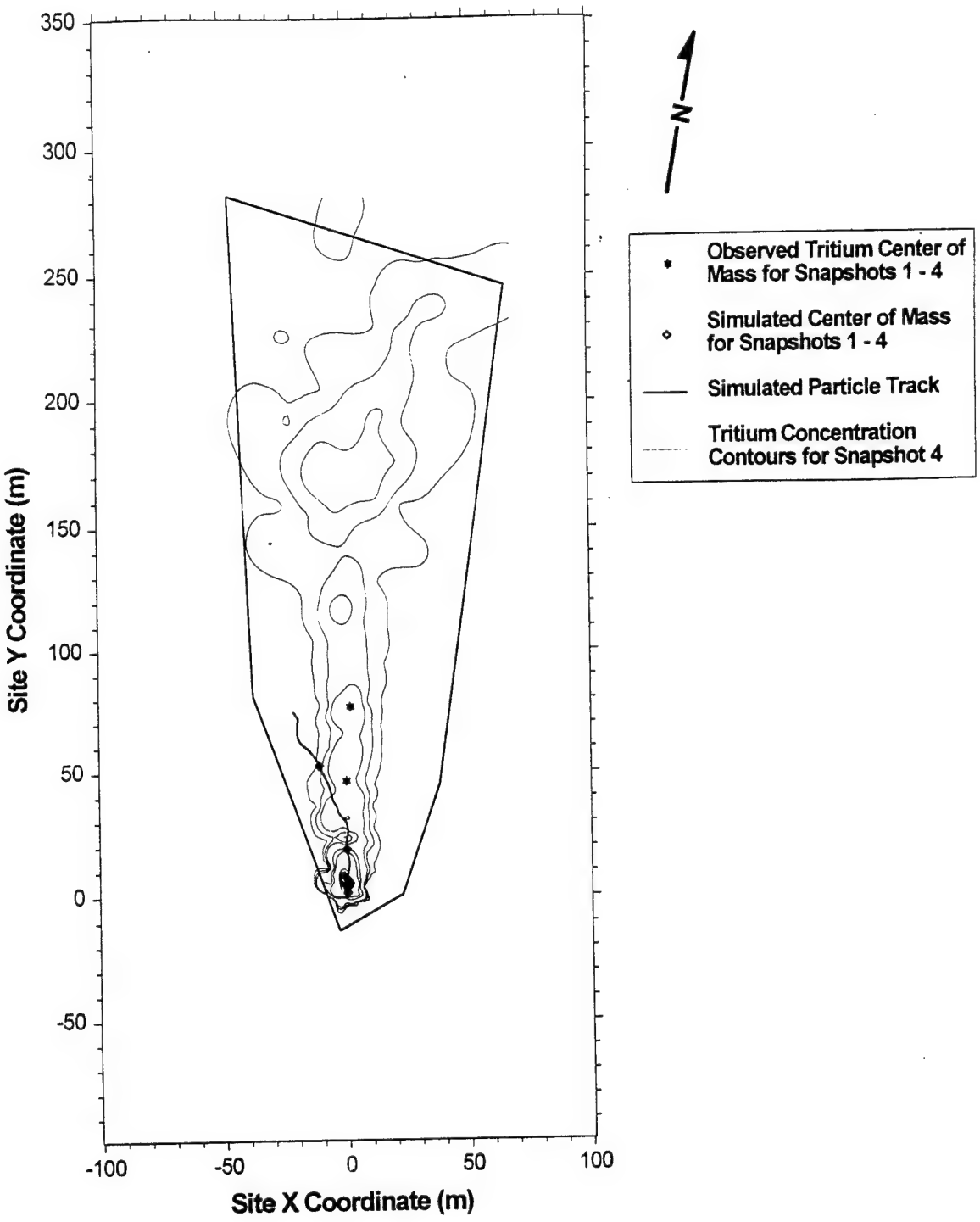

Figure 14. Initial Transient Model Results.

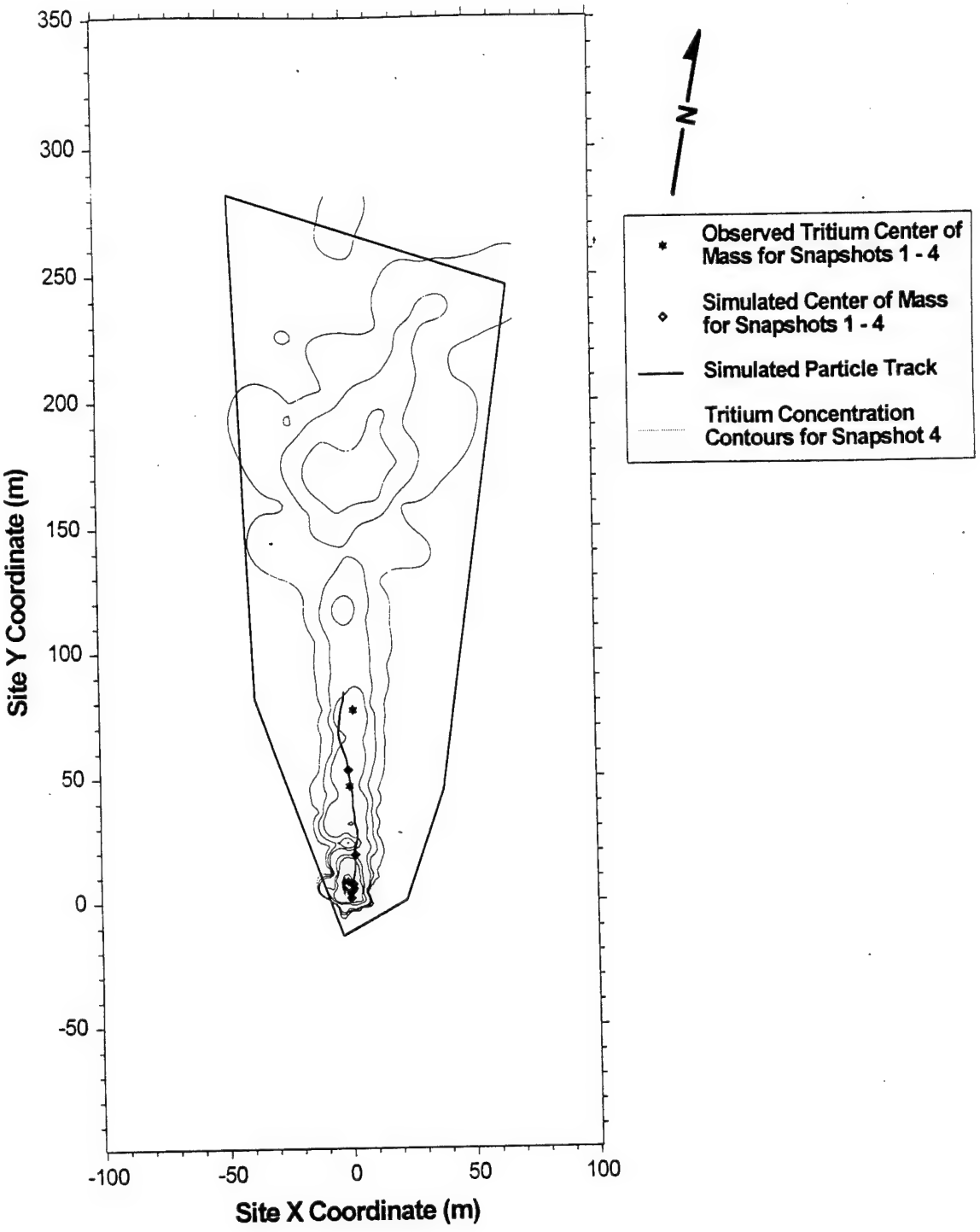

Figure 15. Transient Model Results with Modified Prescribed Head Boundaries.

SECTION V
BIOPLUME II TRANSPORT MODELING

A. CONCEPTUAL MODEL

The original Bioplume model was developed by Borden and Bedient (1986, 1987), Borden *et al.* (1986), and Borden *et al.* (1989), based on studies performed at the United Creosoting Company, Inc. (UCC) site in Conroe, Texas. Bioplume relies on the concept that hydrocarbon biodegradation in groundwater is often limited by the available dissolved oxygen. Borden and Bedient (1986) combined Monod kinetics with the advection-dispersion equation to create an aerobic degradation simulator. This simulator was later modified by replacing the Monod kinetics with a simplifying assumption. With this modification, the hydrocarbon degradation is considered an instantaneous reaction that follows a stoichiometric relationship between hydrocarbon and oxygen. For example, for every mg of BTEX removed, 3.1 mg of oxygen must be removed. By comparing the difference between the time required for groundwater movement and the time required for aerobic biodegradation (roughly months to days), this assumption was shown to be reasonable in most cases.

Bioplume II integrated the concepts from the original Bioplume developed by Borden and Bedient (1986) into the two-dimensional USGS solute transport model, better known as the method of characteristics (MOC) model (Konikow and Bredehoeft, 1978). Bioplume II tracks two plumes: contaminant and oxygen. These plumes are superimposed and the instantaneous reaction assumption is applied at each time step to determine the new hydrocarbon and oxygen concentrations. Bioplume II's development is documented in Rifai (1989), Rifai and Bedient (1987), and Rifai *et al.* (1988, 1989).

Bioplume II provides all the functionality of the USGS model as related to sources, sinks, and boundary conditions. Bioplume II allows the simulation of in-situ bioremediation so that bioreclamation schemes can be examined before implementation. Bioplume II is limited because oxygen is the only terminal electron acceptor. Rifai (1995) discussed the ongoing development of Bioplume III, which allow nitrate, iron, sulfate, and carbon dioxide as electron acceptors. Bioplume III also provides the option of simulating the hydrocarbon degradation with Monod kinetics or the instantaneous reaction assumption.

B. CODE DESCRIPTION

The biodegradation equations used in all versions of Bioplume are those developed by Borden and Bedient (1986). Modified Monod functions described hydrocarbon removal, oxygen removal, and microorganism growth as follows:

$$\frac{\partial H}{\partial t} = -M_t \cdot k \frac{H}{(K_h + H)} \frac{O}{(K_o + O)} \quad (1)$$

$$\frac{\partial O}{\partial t} = -M_t \cdot k \cdot F \frac{H}{(K_h + H)} \frac{O}{(K_o + O)} \quad (2)$$

$$\frac{\partial M_t}{\partial t} = -M_t \cdot k \cdot Y \frac{H}{(K_h + H)} \frac{O}{(K_o + O)} + K_C \cdot Y \cdot OC - b \cdot M_t \quad (3)$$

where:

H = hydrocarbon concentration
O = oxygen concentration
M_t = total microbial concentration
K = maximum hydrocarbon utilization rate per unit mass organism
Y = microbial yield coefficient (g cells/g hydrocarbon)
K_h = hydrocarbon half saturation constant
K_o = oxygen half saturation constant
K_c = first order decay rate of natural organic carbon
OC = natural organic carbon concentration
b = microbial decay rate
F = ratio of oxygen to hydrocarbon consumed

After combining equations (1) and (2) with the advection-dispersion equation, Borden and Bedient (1986) obtained the following system of equations:

$$\frac{\partial H}{\partial t} = \frac{\nabla(D\nabla H - vH)}{R_H} - \frac{M_t \cdot k}{R_H} \frac{H}{(K_h + H)} \frac{O}{(K_o + O)} \quad (4)$$

where:

D = dispersion tensor

v = groundwater velocity vector

$$\frac{\partial O}{\partial t} = \nabla(D\nabla O - vH) - M_t \cdot k \cdot F \frac{H}{(K_h + H)} \frac{O}{(K_o + O)} \qquad (5)$$

R_h = retardation factor for hydrocarbon

The transfer of organisms from the soil surface to the groundwater and back was assumed to be related to total microorganism concentration and to follow a linear relationship. This transfer was simulated using a retardation factor approach given in Freeze and Cherry (1979):

$$\frac{\partial M_s}{\partial t} = \frac{\nabla(D\nabla M_s - vM_s)}{R_m} + M_s \cdot k \cdot Y \frac{H}{(K_h + H)} \frac{O}{(K_o + O)} + K_c \cdot Y \cdot \frac{OC}{R_m} - b \cdot M_s \qquad (6)$$

where:

M_s = concentration of microbes in solution

M_a = concentration of microbes attached to solids

K_m = ratio of microbes attached to microbes in solution

$M_a = K_m \cdot M_s$

$M_t = M_s \cdot M_a$

$= (1+K_m) \cdot M_s$

$= R_m \cdot M_s$

Using the assumption that the removal of hydrocarbon and oxygen is instantaneous and independent of the microbial parameters, the loss of oxygen and hydrocarbon in explicit finite-difference form is written as follows:

$$H(t+1) = H(t) - O(t)/F \qquad (7)$$
$$O(t+1) = 0$$

where $H(t) > O(t)/F$

$$O(t+1) = O(t) - H(t) \cdot F \qquad (8)$$
$$H(t+1) = 0$$

where $O(t) > H(t) \cdot F$

where:

$H(t)$ = hydrocarbon concentration at time t
$O(t)$ = oxygen concentration at time t
$H(t+1)$ = hydrocarbon concentration at time t+1
$O(t+1)$ = oxygen concentration at time t+1

Equations (7) and (8) were used to simplify the Monod kinetics in Equations (4) and (5) giving the following:

$$\frac{\partial H}{\partial t} = \frac{1}{R_h}\left(D_l \frac{\partial^2 H}{\partial x^2} + D_l \frac{\partial^2 H}{\partial y^2} - v\frac{\partial H}{\partial x} \right) - \frac{\delta}{R_h} \pm W_h \qquad (9)$$

$$\frac{\partial O}{\partial t} = \left(D_l \frac{\partial^2 O}{\partial x^2} + D_l \frac{\partial^2 O}{\partial y^2} - v\frac{\partial O}{\partial x} \right) - \delta F \pm W_o \qquad (10)$$

where:

R_h = retardation factor for hydrocarbon
F = ratio of oxygen to hydrocarbon consumed
δ = $\min(R_h H, O/F)$
D_l = longitudinal dispersion coefficient
α_l = longitudinal dispersivity
$D_l = \alpha_l v$
D_t = transverse dispersion coefficient
α_t = transverse dispersivity
$D_t = \alpha_t v$
W_h = hydrocarbon source or sink
W_o = oxygen source or sink

These two equations are solved by Bioplume II. Since the reactions are assumed to be instantaneous, microbial growth is no longer a factor.

The parameters required for Bioplume II to solve the flow-and-transport equations can be divided into three major categories, as shown in Table 10.

TABLE 10
REQUIRED BIOPLUME PARAMETERS

Basic Problem Set-Up	
Simulation time	(years)
Grid Size	(unitless)
Cell Size	(feet)
Location of all injection/extraction wells	(unitless)
Injection/extraction rate at all wells	(cubic feet/second)
Half life of the contaminant	(seconds)
Anaerobic decay coefficient for the contaminant	(1/day)
Node values	
Leakance	(unitless)
Contaminant concentration	(mass/volume)
Oxygen concentration	(mass/volume)
Diffuse recharge/discharge	(cubic feet/second)
Initial water table	(feet)
Hydrogeologic Parameters	
Porosity	(unitless)
Longitudinal dispersivity	(feet)
Horizontal dispersivity	(feet)
Transmissivity in the x direction	($feet^2$/second)
Transmissivity in the y direction	($feet^2$/second)
Aquifer thickness	(feet)
Hydraulic gradient	(unitless)
Bulk density of the soil	(mass/volume)
Biodegradation Parameters	
Concentration of oxygen in injected water	(mass/volume)
Concentration of hydrocarbon in injected water	(mass/volume)
Initial oxygen plume concentrations	(mass/volume)
Initial hydrocarbon plume concentrations	(mass/volume)
Recharge concentration of oxygen	(mass/volume)
Distribution coefficient of the contaminant	(volume/mass)
Reaeration coefficient	(1/day)

(Rifai *et al.*, 1987, Appendix A)

C. MODEL FRAMEWORK AND PARAMETERIZATION

1. Finite-Difference Grid

The initial model considered the entire MADE-2 site by utilizing a 33 by 59 grid consisting of cells that were 20 feet by 25 feet. This grid worked relatively well for modeling the tritium plume. At this resolution, the calibration simulations were completed in approximately 5 minutes on a Sun Sparc 20. However, initial simulations indicated that this would not provide sufficient detail for calibration of the organic plume transport.

A more refined model grid was then established which consisted of a grid of 92 by 205 cells which had dimensions of 5 feet by 5 feet. The refined grid incorporated a smaller portion of the MADE-2 site. Coordinates of the rectangular grid domain were -230.0 feet, -100.0 feet. for the lower left corner and 230.0 feet, 925.0 feet for the upper right (see Figure 16). In meters, these coordinates are -70.1, -30.5 and 70.1, 281.9, respectively. The new finite-difference grid incorporates most of the sampling network and only excludes three of the sampling points (M253, M289, and M279). The run time of this model was on a scale of hours rather than minutes, with the longest runs (hydrocarbon predictive runs) taking approximately 9 hours.

2. Simulation of Combined Organic Tracers

Two adjustments were applied to the field data per Boggs *et al.*, (1993). These adjustments were based on the idea that the relative concentration of degrading organic contaminant (benzene, napthalene, p-xylene, o-dichlorobenzene) should never be higher than the relative concentration of non-degrading contaminant (tritium). These adjustments were only applied to those samples that failed to meet this criterion.

$$\text{I} \qquad \text{If } C_i(^3H) = 0 \quad \text{then} \quad C^*_i(\text{org}) = 0 \tag{11}$$

$$\text{II} \qquad C^*_i(\text{org}) = C_o(\text{org}) C_i(^3H) / C_o(^3H) \tag{12}$$

where

C^* = adjusted concentration

C_o = injection concentration

I = 1 to # of samples

To generate the data sets for data visualization, all samples that shared the same x, y coordinates were vertically averaged to determine a single value for that coordinate. If all measurements in the multilevel sampler were below the detection limit, a zero value was assigned at that location. In addition, because Bioplume II can only simulate the transport and fate of one

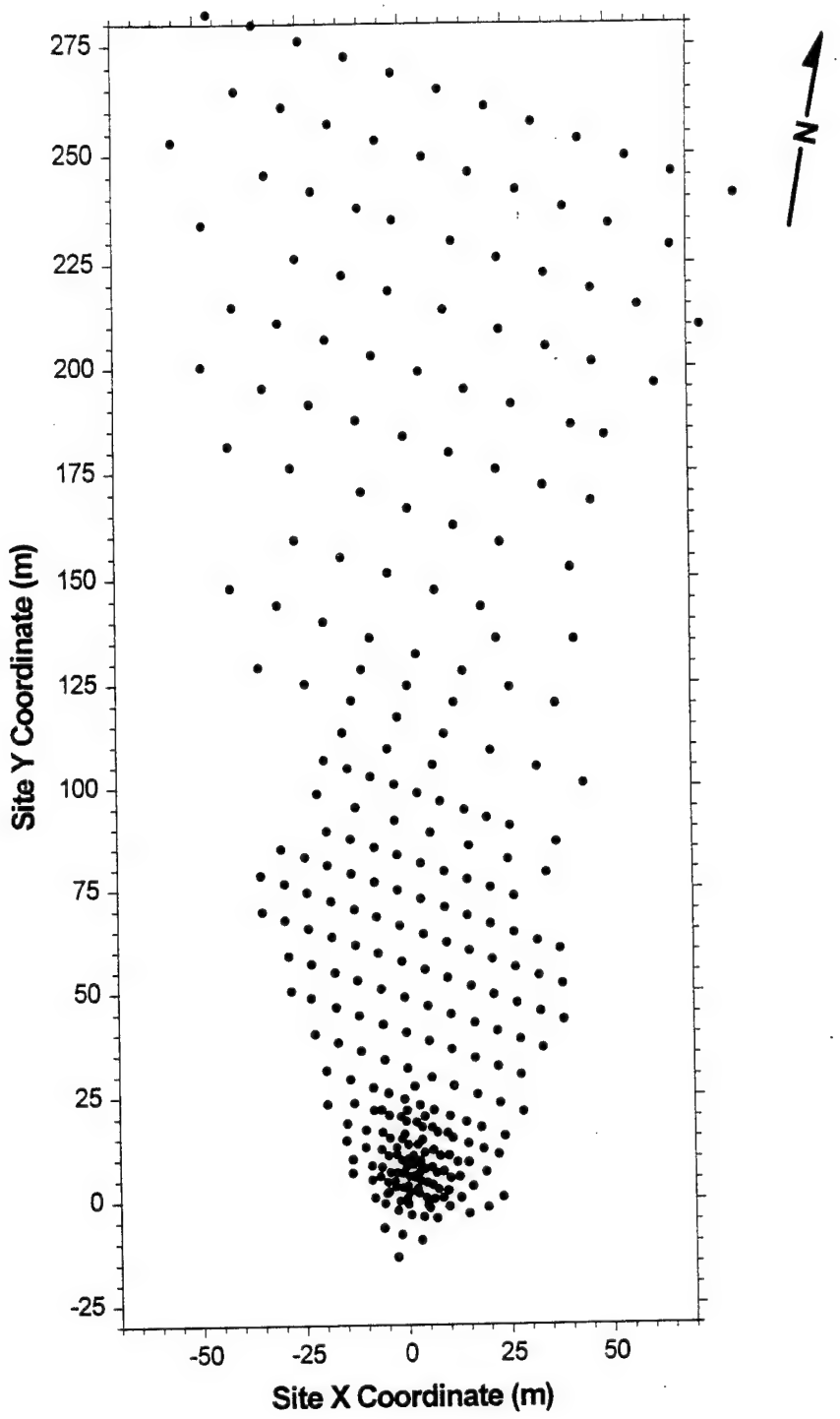

Figure 16. Sample Collection Locations Used to Monitor Tracers.

organic compound, the four organic tracers were summed at each sampling point and averaged over all vertical sampling points in the vertical. This produced an estimate of the vertical average of the combined concentration of all organic tracers. The value of this estimate is referred to as the "combined organic concentration" in this report. The vertically averaged concentrations for the tritium and the combined organics were then contoured using the SURFER software package for visual comparison with the Bioplume II model output. SURFER interpolated the concentrations onto a regular Cartesian grid using the geostatistical method of kriging (see Figures 17, 18, 19, 20, 21, and 22). Figures 17 through 19 illustrate the non-Gaussian shape of the tritium plume, especially at Snapshots 3 and 4. The movement of the majority of the injected mass away from the injection zone is very slow, as noted by the relatively high percentage of mass surrounding the injection zone at Snapshots 3 and 4. The low conductivity zone near the injection location restricts the movement of a large percentage of the pulse injection. The portion of the plume that does move down gradient moves to a higher conductivity zone and is quickly moved down gradient by the relatively fast groundwater velocity that occurs down gradient. The apparent separation of the plume may be caused by a lack of sampling points, or it may be a real development caused by the extreme velocity increases that occur in that area. The velocity increases could be amplified by rainfall events, which result in even larger velocity variations throughout the aquifer.

3. Source Implementation and Initial Conditions

The basic transport assumptions were (1) steady-state flow, (2) constant recharge, and (3) uniform aquifer thickness. Bulk density and porosity were assumed to be spatially homogeneous and were assigned values of 1.77 g/cm^3 and 0.35, respectively (Boggs *et al.*, 1993). The contaminant source was originally treated as a pulse injection over a 48.5-hour period. In later runs, a continuous source model was considered. A weighted average based on the relative percentage of each organic contaminant injected was used to determine both the F ratio (mass oxygen consumed/ mass hydrocarbon degraded) and the retardation factor for the combined organic. The retardation factor and bulk density were then used to calculate the distribution coefficient used by Bioplume II for determining sorption of the hydrocarbon on the aquifer media. These calculations are detailed in Table 11, with the retardation values and injected masses taken from EPRI report TR-101998.

4. Oxygen Conditions

Boggs *et al.*, (1993) includes dissolved oxygen data for 6/18/90, 8/13/90, 10/15/90, 12/4/90, 3/7/91, and 5/22/91. These data were contoured and examined to determine the initial estimate for the dissolved oxygen concentrations across the site. As is common at many sites, some dissolved oxygen was usually present in the heart of the hydrocarbon plume. By arbitrarily subtracting the approximate average minimum value of 3.6 mg/L from the approximate average maximum value of 6.6 mg/L, an initial dissolved oxygen concentration of 3.0 mg/L was estimated. This value was implemented as the initial dissolved oxygen concentration for each gridblock in the model.

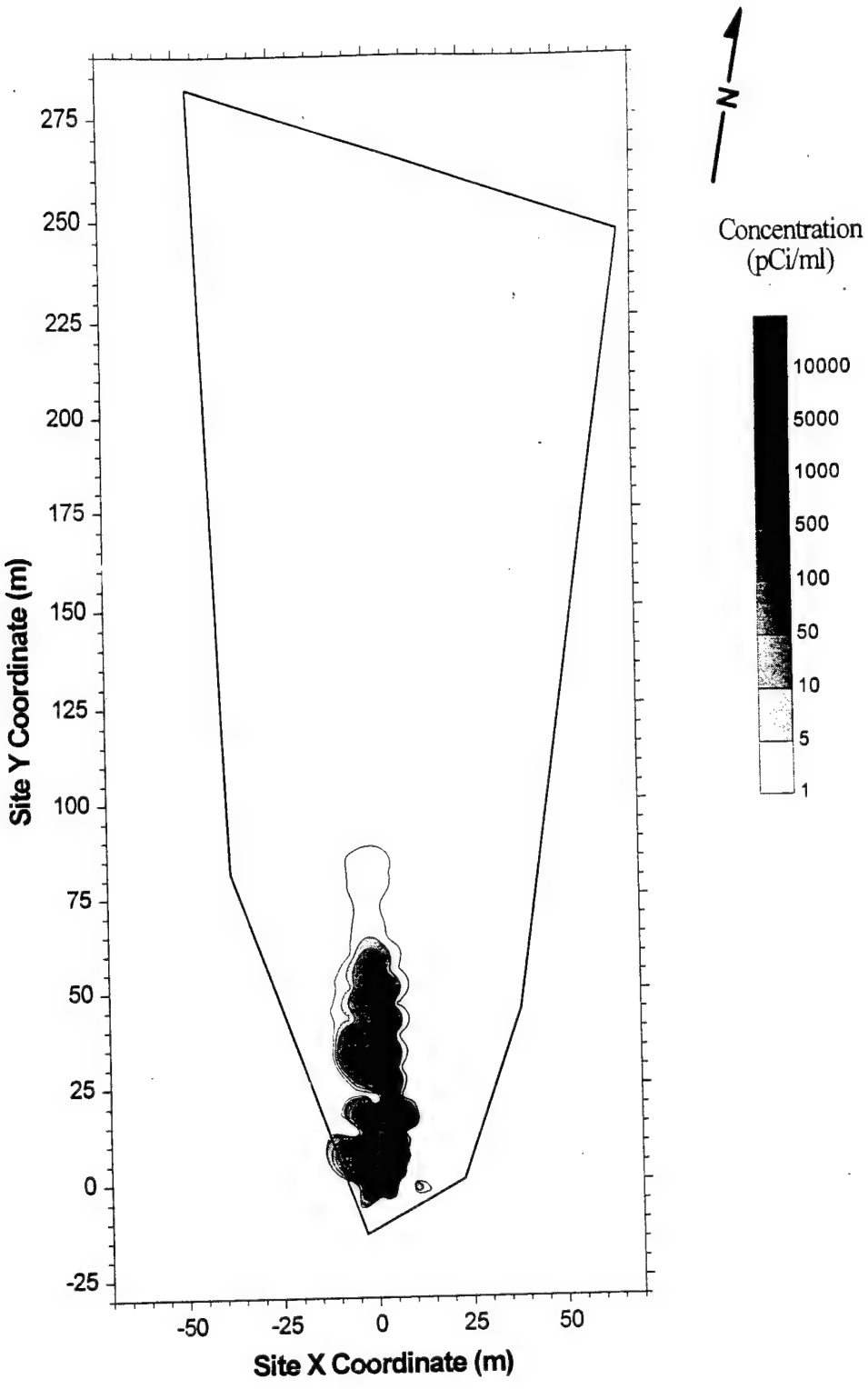

Figure 17. Vertically Averaged Observed Tritium Concentration for Snapshot 2 (132 Days After Injection).

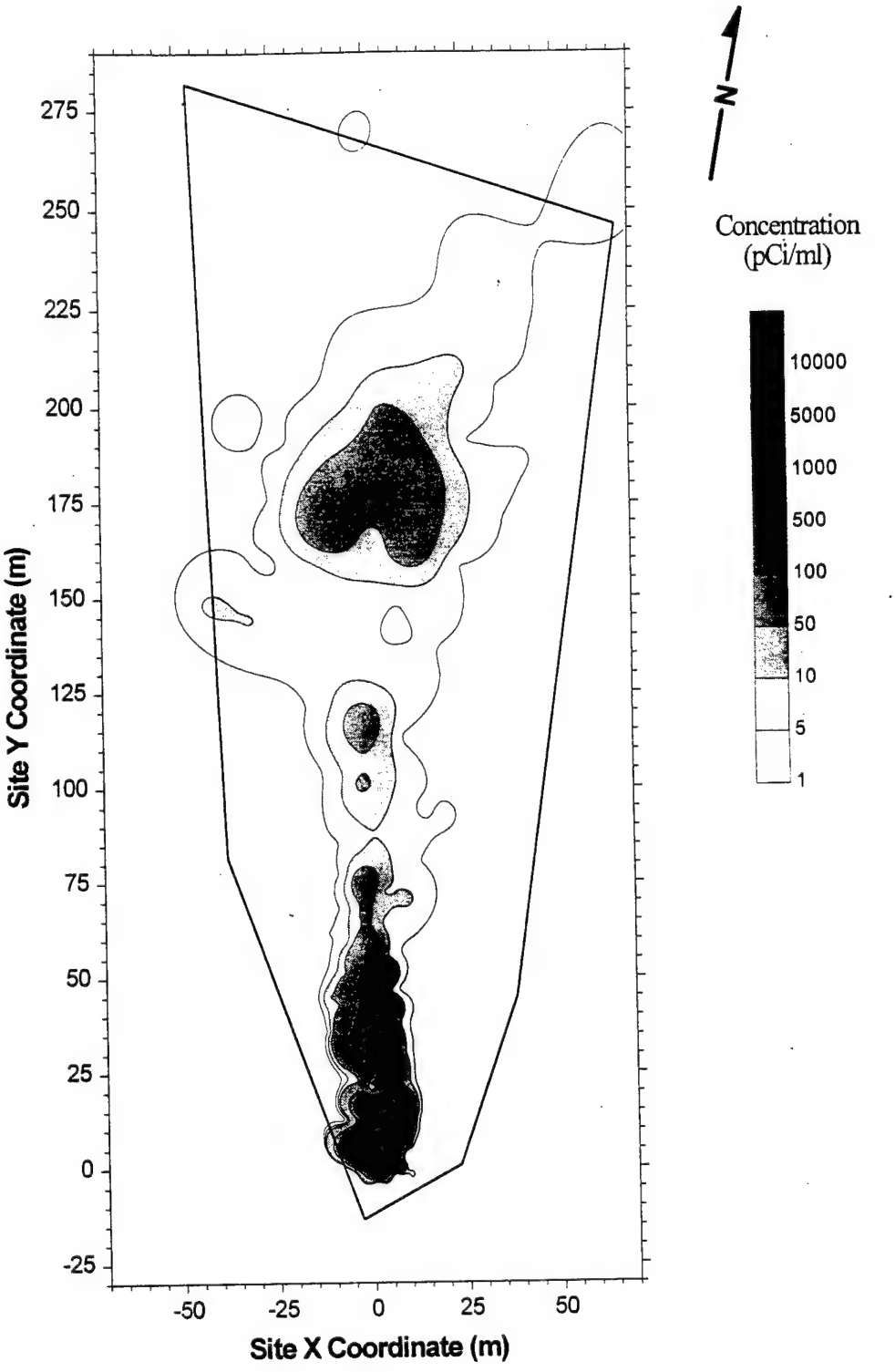

Figure 18. Vertically Averaged Observed Tritium Concentration for Snapshot 3 (224 Days After Injection).

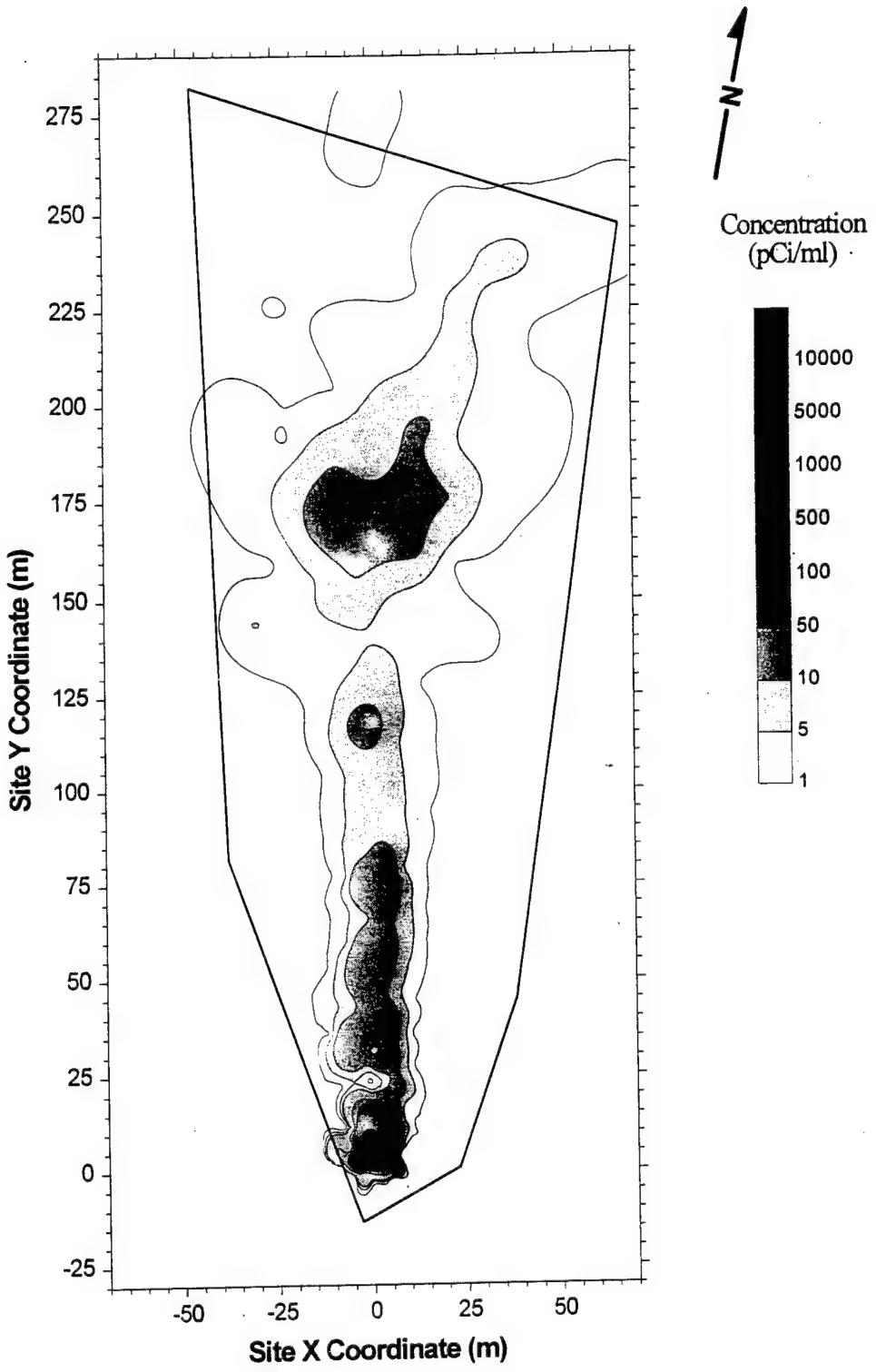

Figure 19. Vertically Averaged Observed Tritium Concentration for Snapshot 4 (328 Days After Injection).

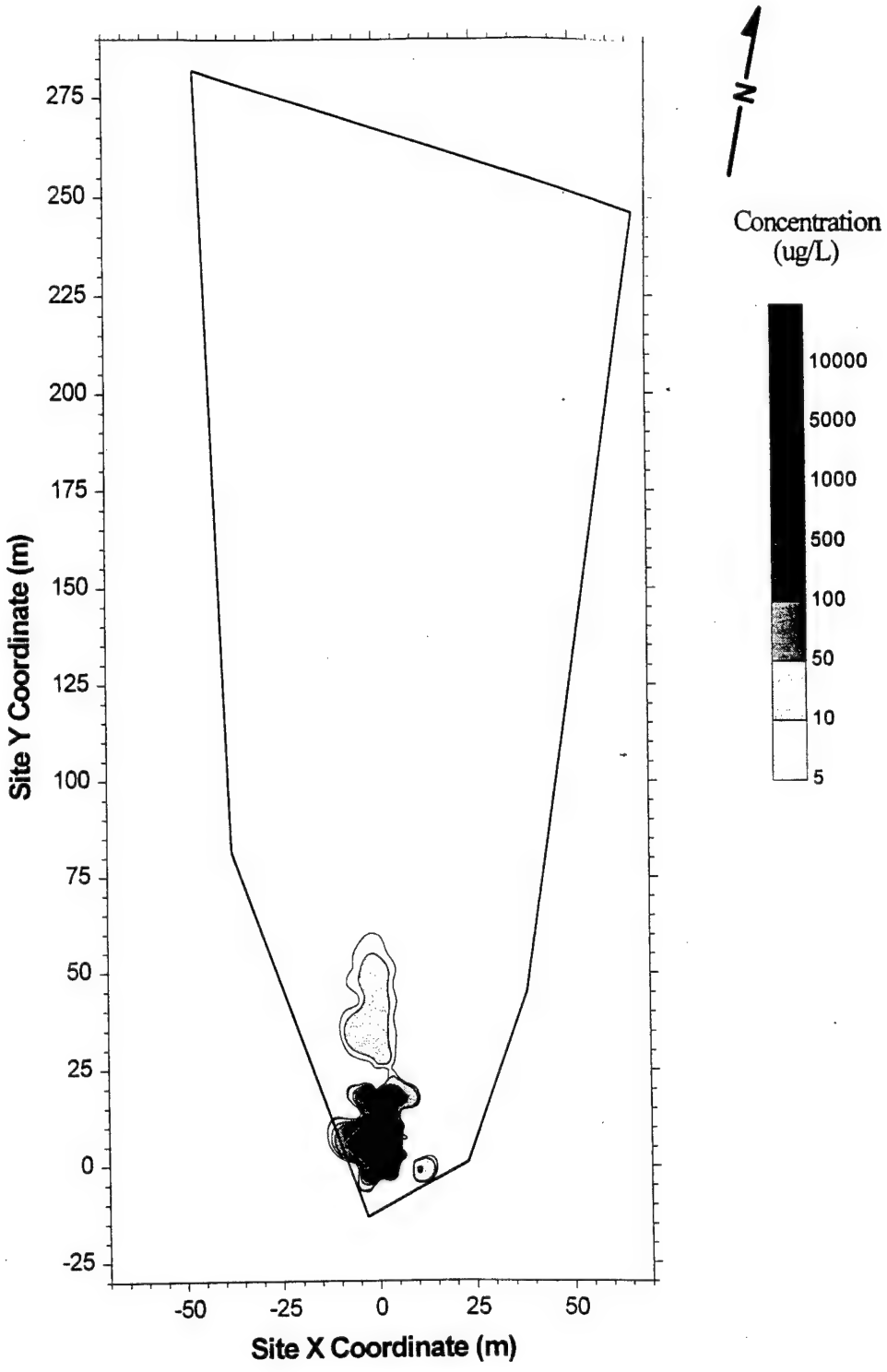

Figure 20. Vertically Averaged Observed Combined Organic Concentration for Snapshot 2 (132 Days After Injection).

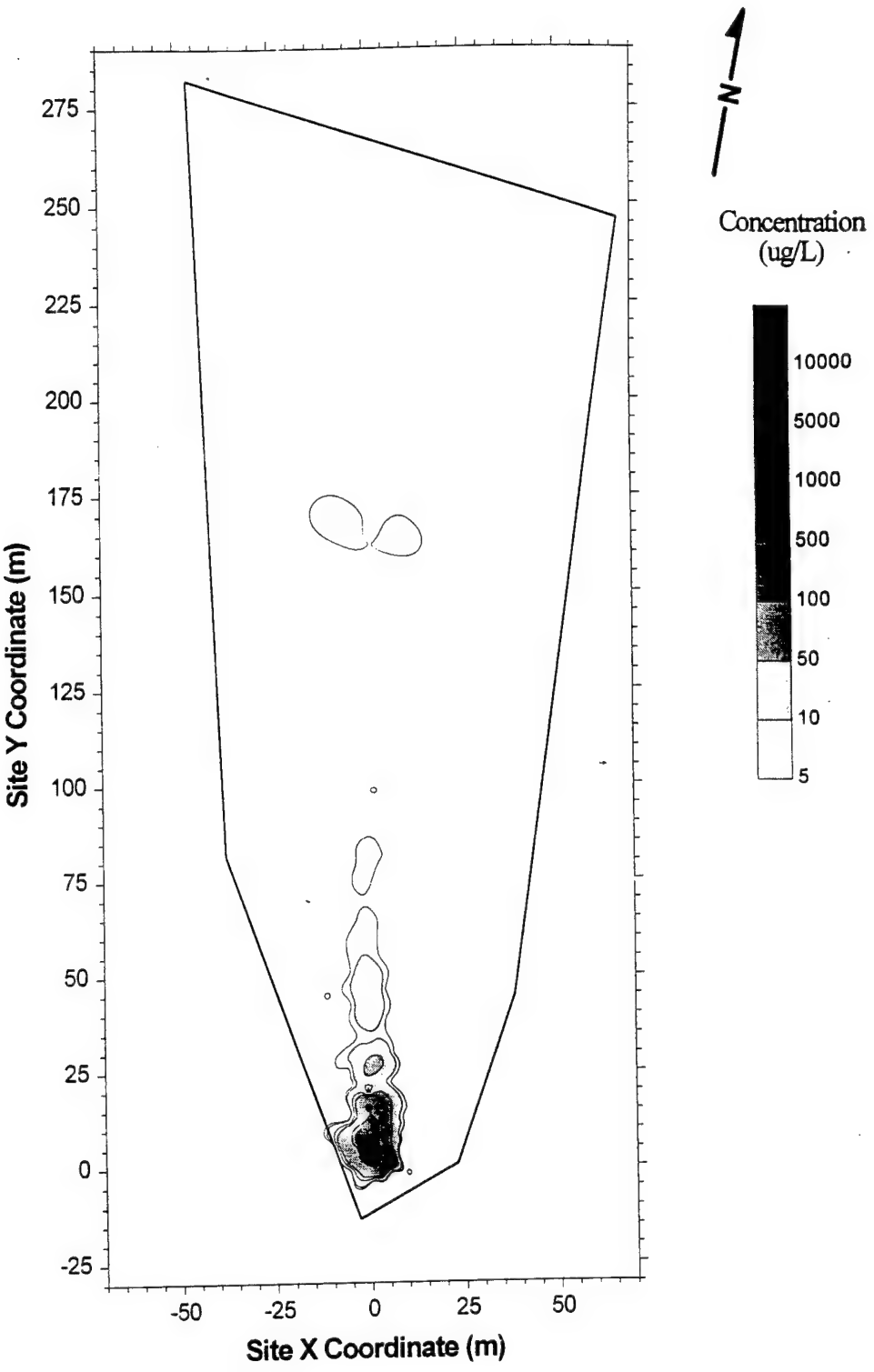

Figure 21. Vertically Averaged Observed Combined Organic Concentration for Snapshot 3 (224 Days After Injection).

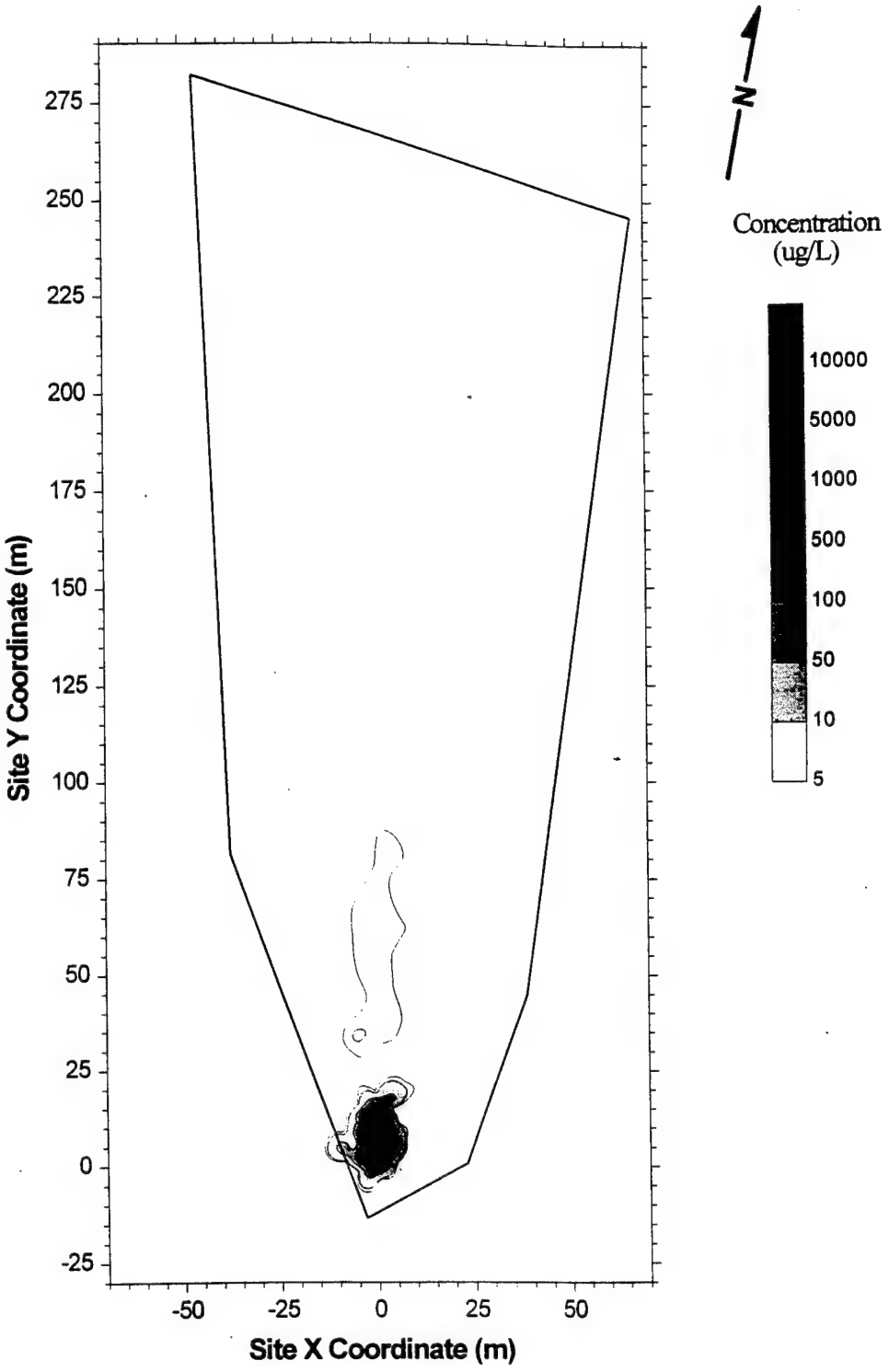

Figure 22. Vertically Averaged Observed Combined Organic Concentration for Snapshot 4 (328 Days After Injection).

TABLE 11
F RATIO AND RETARDATION CALCULATIONS

Combined Organic Concentration F Ratio Calculations					
Contaminant	**Inj. Mass (g)**	**% Mass**	**Mol. Wt.**	**F Ratio**	**% Mass * F**
Benzene	659.7	45.52%	78.113	3.072	1.398
p-Xylene	402.0	27.74%	106.167	3.165	0.878
Napthalene	70.0	4.83%	128.173	2.996	0.145
o-DCB	317.7	21.92%	147.004	1.415	0.310

Total Mass = 1449.4 g	
Mol. Wt. O_2 = 31.999	

Average F = 2.731

Contaminant	**Stoichiometric Equation**
Benzene	$2\ C_6H_6 + 15\ O_2 \rightarrow 12\ CO_2 + 6\ H_2O$
p-Xylene	$2\ C_8H_{10} + 21\ O_2 \rightarrow 16\ CO_2 + 10\ H_2O$
Napthalene	$C_{10}H_8 + 12\ O_2 \rightarrow 10\ CO_2 + 4\ H_2O$
o-DCB	$C_6H_4Cl_2 + 6.5\ O_2 \rightarrow 6\ CO_2 + 1\ H_2O + 2\ Cl^- + 2\ H^+$

Combined Organic Concentration Retardation Calculations				
Contaminant	**Inj. Mass (g)**	**% Mass**	**Retardation**	**% Mass * R**
Benzene	659.7	45.52%	1.200	0.546
p-Xylene	402.0	27.74%	1.450	0.402
Napthalene	70.0	4.83%	1.160	0.056
o-DCB	317.7	21.92%	1.330	0.292

Total Mass = 1449.4 g

Average R = 1.296

Porosity (n) = 0.35
Aquifer bulk density (p_b) = 1.77g/cm^3
Distribution coefficient K_d = (R-1)n/p_b = 0.0585g/cm^3

5. Dispersion

Boggs *et al.*, (1993) estimates longitudinal dispersivity as 10 meters at the MADE-2 site. Similarly, transverse dispersivity is estimated at 2.2 meters. However, Boggs *et al.* (1993) state that 2.2 meters is probably higher than the actual value. The Boggs *et al.* transport model had a convergent flow field near the injection point, and required a relatively high value to model the transverse spread of the plume. Based on these considerations, the initial longitudinal dispersivity and ratio of longitudinal to transverse dispersivity in the Bioplume II model were set at 32.8 and 0.22 feet, respectively.

6. Biodegradation Rates

Initial biodegradation rates were determined by taking a weighted average of the values given in Boggs *et al.*, (1993). This report gives separate values for biodegradation of each tracer in the near field and for overall biodegradation throughout the site. The resulting average values were 0.0075 day^{-1} and 0.001 day^{-1}. Initially the value .001 day^{-1} was used to represent the first order decay rate for the combined organic contaminant at the site.

D. SELECTION OF DATA SUB-SETS FOR MODEL CALIBRATION

Numerous samples were collected in the 16 months after tracer injection. Two strategies were implemented in an attempt to characterize the fate and transport of the tracers. The first strategy was to sample "fencelines" that were oriented perpendicular to flow. The second was to sample each multilevel sampler in the area where the plume was thought to have moved. These data sets are known as "snapshots."

The fenceline data were taken from 56 Barcad samplers that were sampled at 13, 48, 83, 111, 160, 195, and 281 days after injection. These samplers were arranged in two parallel rows aligned orthogonal to the direction of groundwater flow, approximately 6 meters and 16 meters down gradient from the injection points. These are useful in time series analysis of the contaminant transport. A snapshot event consists of measurements from the fenceline samplers plus an array of 328 multilevel samplers. These events give the most complete three-dimensional representation of the contaminant plume and as such are the events used to calibrate and validate the Bioplume II model.

During the initial data examination, it became clear that simple vertical averaging of all of the data points within a snapshot gave inconsistent results between locations that were near to each other. Closer examination showed that vertical averaging of the samples taken from the Barcad samplers did not match the averaging from the multilevel samplers. This was mainly due to the differences in the number of samples collected from each type of device. In particular, the multilevel samplers provide greater definition with regard to depth than the Barcad samplers do. In general, only two

vertical samples were collected from the Barcad samples. This resulted in more points being averaged for a single x, y location for a multilevel sampler than for a Barcad device. Because of the preferential flow paths in the aquifer caused by the extreme heterogeneity of the porous media, there was a lower probability of finding tracer in a Barcad sample. To achieve consistency across this site, all data from the Barcad samplers were disregarded.

Five snapshots were available for calibration, validation, and prediction steps. These snapshots occurred 27, 132, 224, 328, and 442 days after injection. Snapshot 5 (442 days after injection) was inconsistent with the previous snapshots because only the multilevel samplers near the injection zone were sampled. Snapshot 1 was too soon after injection (27 days) to be very meaningful. Therefore Snapshots 2, 3, and 4 were used for calibration, validation, and prediction, respectively.

E. FATE AND TRANSPORT CALCULATIONS WITH BIOPLUME II

All the vertically averaged concentrations in each Bioplume II grid block were averaged. If there was no data in a particular grid block, this grid block was not used to calculate calibration statistics. This resulted in a total of six sets of observed data for comparison, three sets of tritium data, and three sets of organic data (Snapshots 2, 3, and 4 for each). These data were used to check the validity of the model. After each run, the simulated plume concentrations were compared with the corresponding snapshot and the percent root mean squared (% RMS) error was calculated.

The root mean squared error was calculated as follows:

$$\mathbf{RMS} = \sqrt{\frac{\sum_{i=1}^{n} (c_o - c_p)_i^2}{n}} \tag{13}$$

$$\%\mathrm{RMS} = \frac{\mathrm{RMS}}{(c_{O_{max}} - c_{O_{min}})} \times 100 \tag{14}$$

where:

c_o = observed concentration
c_p = predicted concentration
n = number of observations

In this procedure, concentration values below 62 µg/L in the observed organic data sets were set to 62 µg/L. This provides a conservative percent RMS error calculation since it is probable that the concentration within that grid block is below 62 µg/L. In general, the RMS error is more sensitive to the simulated and observed concentrations in the higher concentration areas and is less meaningful in defining errors in the low concentrations regions. For this reason, the RMS estimate may not be a good indicator of the model's ability to simulate the extent of the plume as defined by relatively low concentrations at the front edge of the plume.

Two source configurations were considered. The first, a pulse source, was configured to closely mimic the actual injection at the site. The second, a continuous source, was configured to improve the predictive ability of the model. All transport and biodegradation parameters were determined from the pulse source simulations and were not modified in the continuous source model. First, tritium was calibrated and validated. All physical transport parameters estimated from the tritium calibration were then fixed for the organic modeling. Thus, dispersivity, injection rate, injection concentration, and transmissivity were adjusted solely on the basis of the calibration and validation simulations performed with the pulse source tritium model. Initial oxygen concentration and first-order decay rates were determined from the pulse source hydrocarbon simulations.

1. Calibration of the Pulse Source Model

For the pulse source model, the injection concentration and injection rate were the first parameters calibrated. Snapshot 2 (132 days after injection) was used for model calibration. Initially, a total injection rate and tracer concentration identical to that used at the MADE-2 site were used in the Bioplume II simulations. This injection rate caused significant simulated hydraulic mounding at the injection points. This result is partially caused by the reduction in the number of injection wells from the five used at the site to the two simulated in Bioplume II. The resultant gradient caused the contaminants to spread too quickly during the injection period. New injection rates and concentrations were established by scaling the injection rates and injection concentrations such that the total injected mass was constant, but the injection volume and rate decreased. For example, it the injection rate was reduced by a factor of two, the injection concentration was increased by a corresponding factor of two. By trial and error, a factor of nine was determined to give the best estimate. This resulted in a simulated injection rate of 1.08×10^{-4} cfs, and a simulated tritium injection concentration of 504,800 pCi/ml. The actual tritium injection concentration was 55,620 pCi/ml.

The hydraulic conductivity determined in the MODFLOW modeling was converted to transmissivity for the Bioplume II simulations. This transmissivity field showed the plume moving in the correct direction and at a reasonable velocity. However, the field data showed an area of high concentration remained near the injection points that the model was not accurately simulating. To improve the model calibration, the transmissivity immediately around the injection zone was reduced

from 8.83 x 10^{-3} ft^2/s to 1.00 x 10^{-3} ft^2/s. This helped to retain the area of high concentration and to decrease the transverse spreading of the plume.

To further reduce the transverse spreading of the tracers, the ratio of longitudinal to transverse dispersivity was decreased. Boggs *et al.*, (1993) reported that the transverse dispersivity was initially estimated at 0.22 feet. By reducing this value to 0.10 feet, a better correlation was obtained between the model calibration results and the field data. Figure 23 illustrates the calibration simulation results for the tritium plume. Comparison of Figure 23 and 17 indicate that the simulated plume was more dispersed in the transverse and longitudinal direction than the observed plume. The relatively non-dispersed nature of the observed tritium plume may be due to the convergent flow field observed in the field that could not be recreated with the vertically-averaged flow model used in this study.

Snapshot 3 (224 days after injection) was used to validate the results of the different source scenarios. During this step it was noted that the leading edge of the modeled plume was not traveling the distance observed during the MADE-2 experiment. This result was different than observed during the calibration simulation, which indicated that the simulated plume had traveled farther than the observed plume. This is probably caused by the extreme groundwater velocity increase in the region beyond about 100 meters down gradient from the source. Again, because of the vertically-averaged model developed herein, the groundwater velocity in the high conductivity regions were probably underestimated. The apparent increase in dispersivity with increased plume size is consistent with finding of many other plume characterization studies as summarized by Gelhar (1985). To provide for better predictive capability (i.e., appropriate prediction of Snapshot 4 tritium plume) in the calibrated model, the longitudinal dispersivity was increased to 37.0 feet. Changes were not made to the flow and transport parameters; i.e., dispersivity, injection rate, injection concentration and transmissivity. Figures 24 and 25 illustrate the validation and prediction simulation results for the tritium plume.

Two techniques were used to simulate the organic decay. For both of these techniques, the scaling of the injection rate and injection concentrations determined the simulated combined organic injection concentration of 1,358.4 mg/L. (The actual organic injection concentration was 159.6 mg/L). The first model simulated degradation by incorporating first-order decay only. Calibration simulations (i.e., Snapshot 2) showed the best results were obtained when the rate of decay was set to 0.0 (no decay) . This was obviously incorrect overall, since the combined organic concentrations decrease with time, but resulted in the best comparison for the period considered (days 1 through 132). The estimated first-order decay rate was arbitrarily left at 0.01 day^{-1} until the validation simulations (i.e., Snapshot 3) were completed.

During these simulations, RMS errors were minimized when the first-order decay rate was set to 0.0165 day^{-1}. The calibration (i.e., Snapshot 2) simulation was then repeated. The results from the repeated calibration step were poor, but it was determined that this rate (of 0.0165 day^{-1}) gave

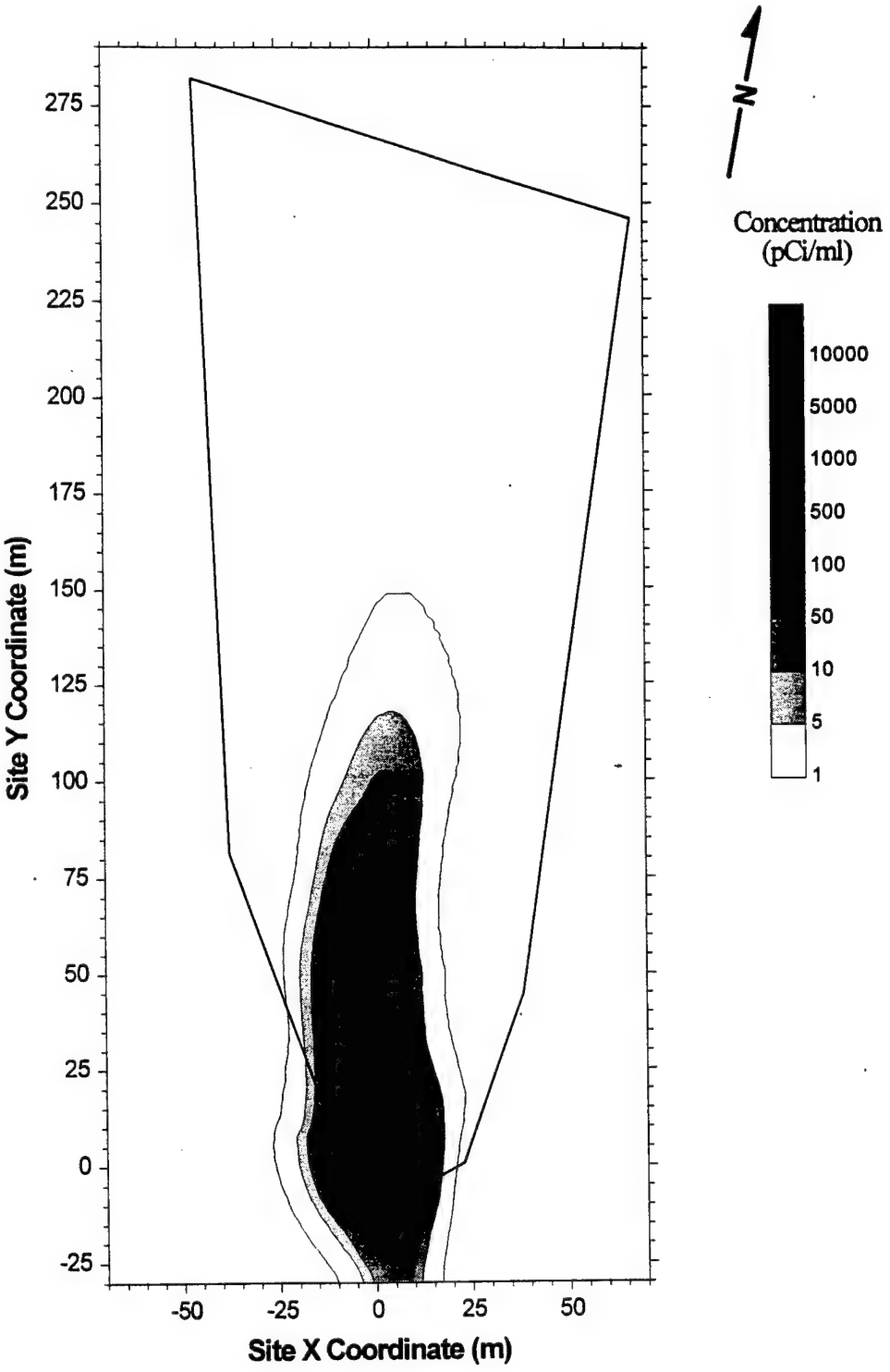

Figure 23. Simulated Tritium Concentration for Snapshot 2 (132 Days After Injection, Pulse Injection Model).

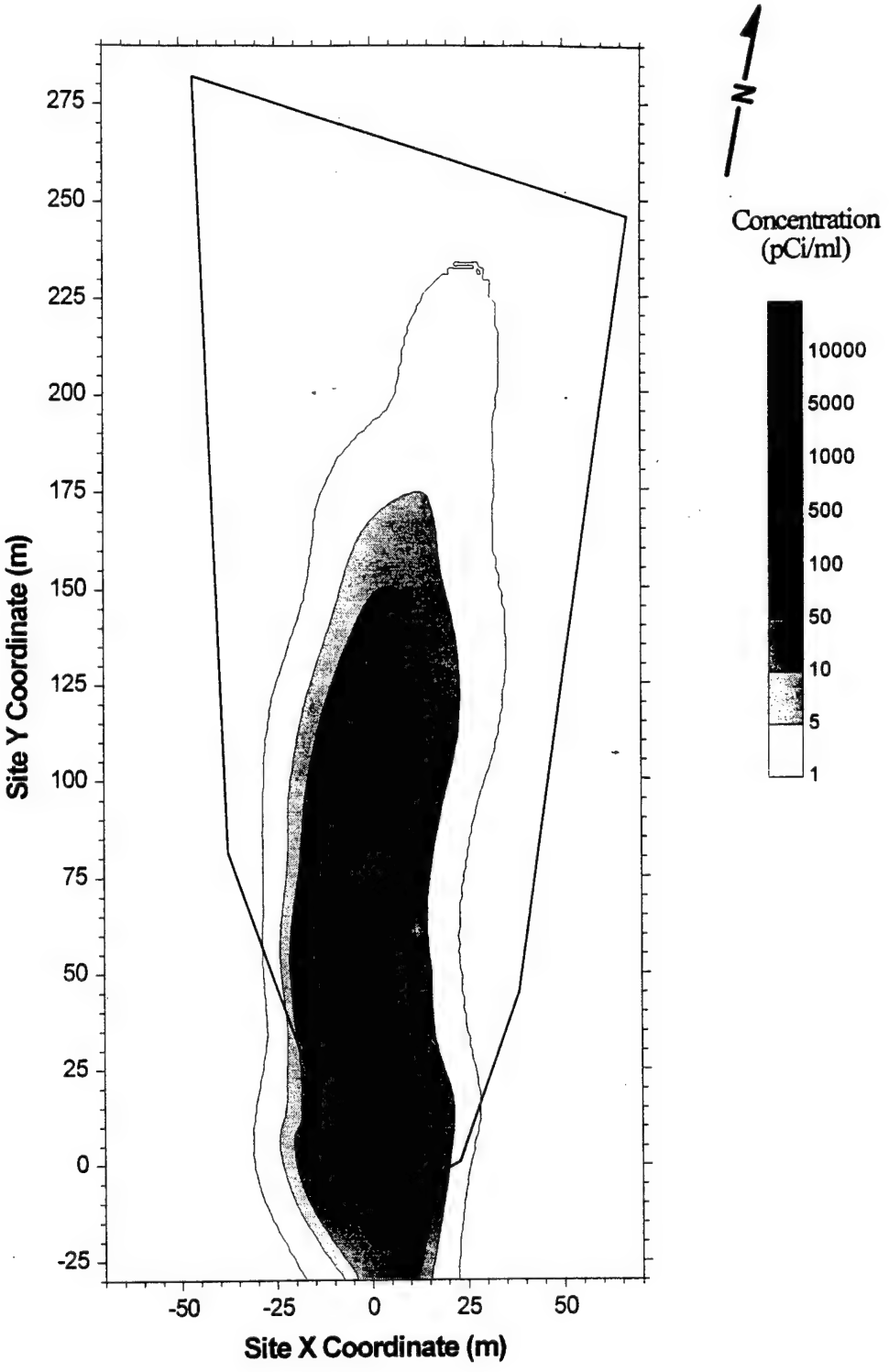

Figure 24. Simulated Tritium Concentration for Snapshot 3 (224 Days After Injection, Pulse Injection Model).

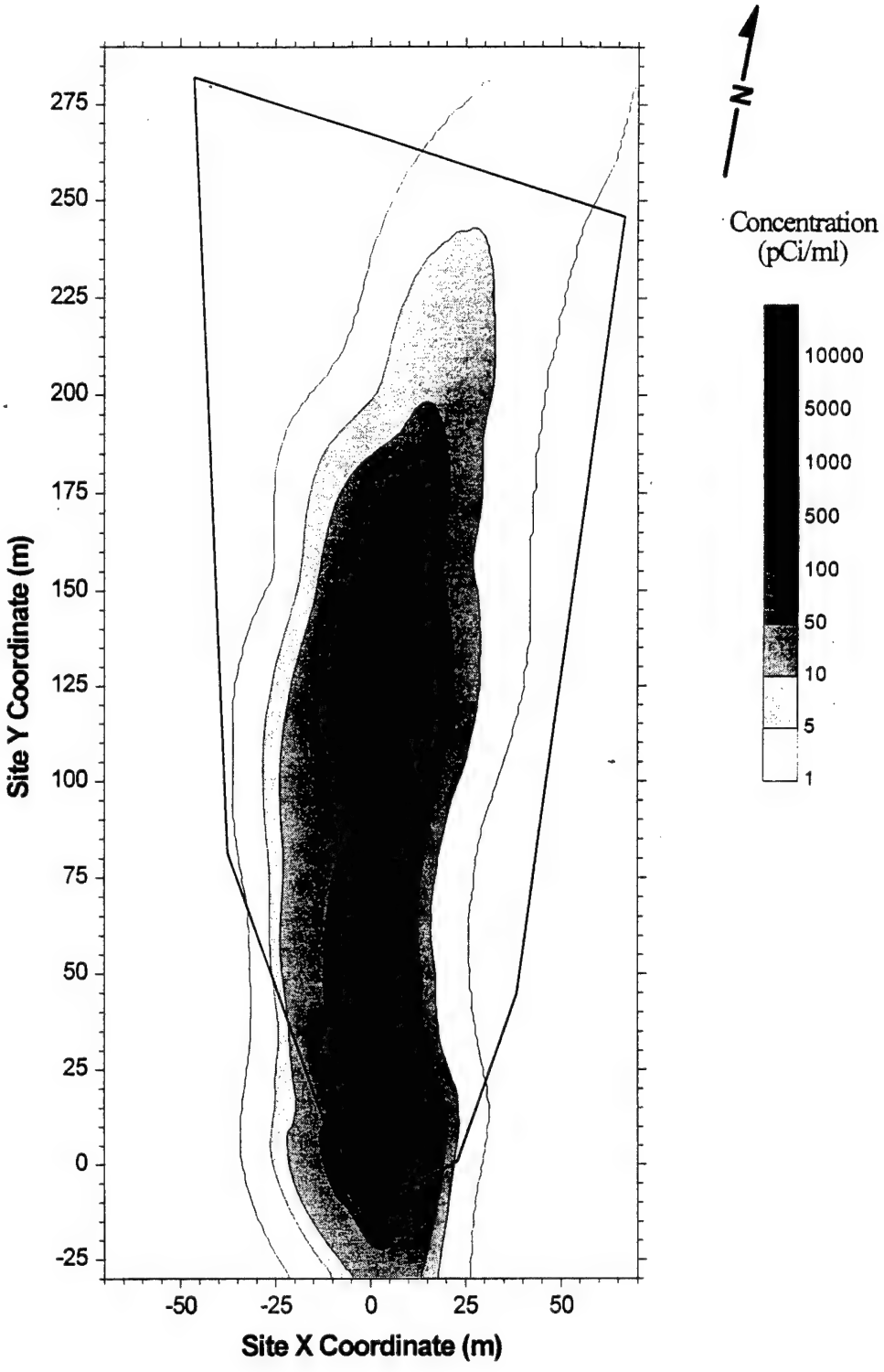

Figure 25. Simulated Tritium Concentration for Snapshot 4 (328 Days After Injection, Pulse Injection Model).

the best overall results for the experiment as a whole. Figures 26, 27, and 28 show the results of the calibration, validation and prediction simulations for the pulse injection model that incorporates first-order decay only.

The second technique used to simulate the organic decay was a combination of instantaneous degradation and first-order decay. The initial oxygen concentration across the site was set at 3,000 ug/L. With the reaeration rate set to zero, this value was varied in numerous simulations to see if a better estimate could be obtained. After testing values from 0 ug/L to 8,000 ug/L it was determined that lowering the initial oxygen concentration to 2,600 ug/L gave the best fit when the model results were compared to the field data for Snapshot 2. Then the reaeration rate was set to 0.01 day^{-1} and increased until the best estimate for this parameter was found to be between 0.011 day^{-1} and 0.013 day^{-1} (this first-order decay rate only applies to the simulations that implemented instantaneous degradation and first-order decay simulations). The best estimate was determined in the validation step and the results were contoured (see Figure 5-10) with first-order decay.

In the combined oxygen and first-order decay model, the initial oxygen concentration was again varied. The best overall results were obtained when the initial oxygen concentration estimation was 3,000 ug/L (the original estimate). The range of values for the first-order decay rate (reaeration rate) determined in the calibration step were simulated. The best results occurred when a value of 0.0125 day^{-1} was used. Again, the calibration simulations were repeated with these new estimates and found to be acceptable based on RMS errors and comparisons of plume extent. Figures 29, 30, and 31 show the results of these simulations.

2. Calibration of the Continuous Source Model

After examining the contoured field data, a second conceptual model was considered. It appeared that the source might be better represented by treating a portion of the total mass as a pulse injection during the first 48.5 hours and the remainder of the total mass as a continuous source throughout the remainder of the time experiment. This conceptualization was based on the observation that the measured plumes appeared very non-Gaussian in shape and did not appear to move as an instantaneous injection. Evidently, this is the result of the low conductivity zone that surrounds the injection location. All the transport and biodegradation parameters estimated from the pulse injection model were used in this scenario. The ratio of mass injected as pulse mass injected continuously was varied by 5-percent steps, ranging from 0 percent pulse, 100 percent continuous to 100 percent pulse, 0 percent continuous. Three configurations (0 percent pulse, 100 percent continuous, 5 percent pulse, 95 percent continuous, and 10 percent pulse, 90 percent continuous) gave the best results and no significant difference was found in the % RMS error of these three configurations. During the validation step, the best results were obtained using a 5 percent pulse injection, 95 percent continuous injection. This injection ratio was found to give the best results for the tritium and combined organic plumes and was determined independently for both plumes.

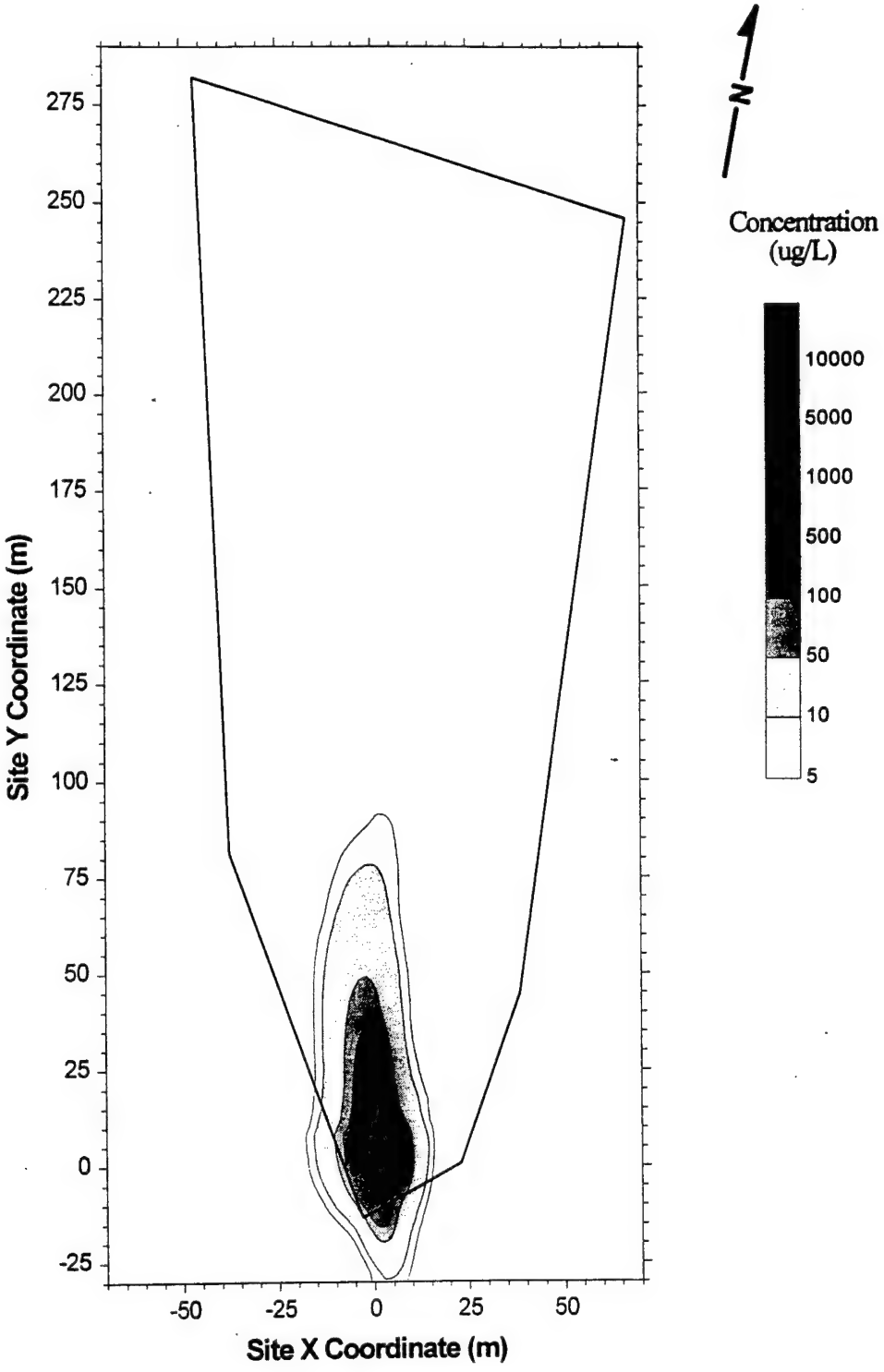

Figure 26. Simulated Combined Organic Concentration for Snapshot 2 (132 Days After Injection, Pulse Injection Model with First-Order Decay).

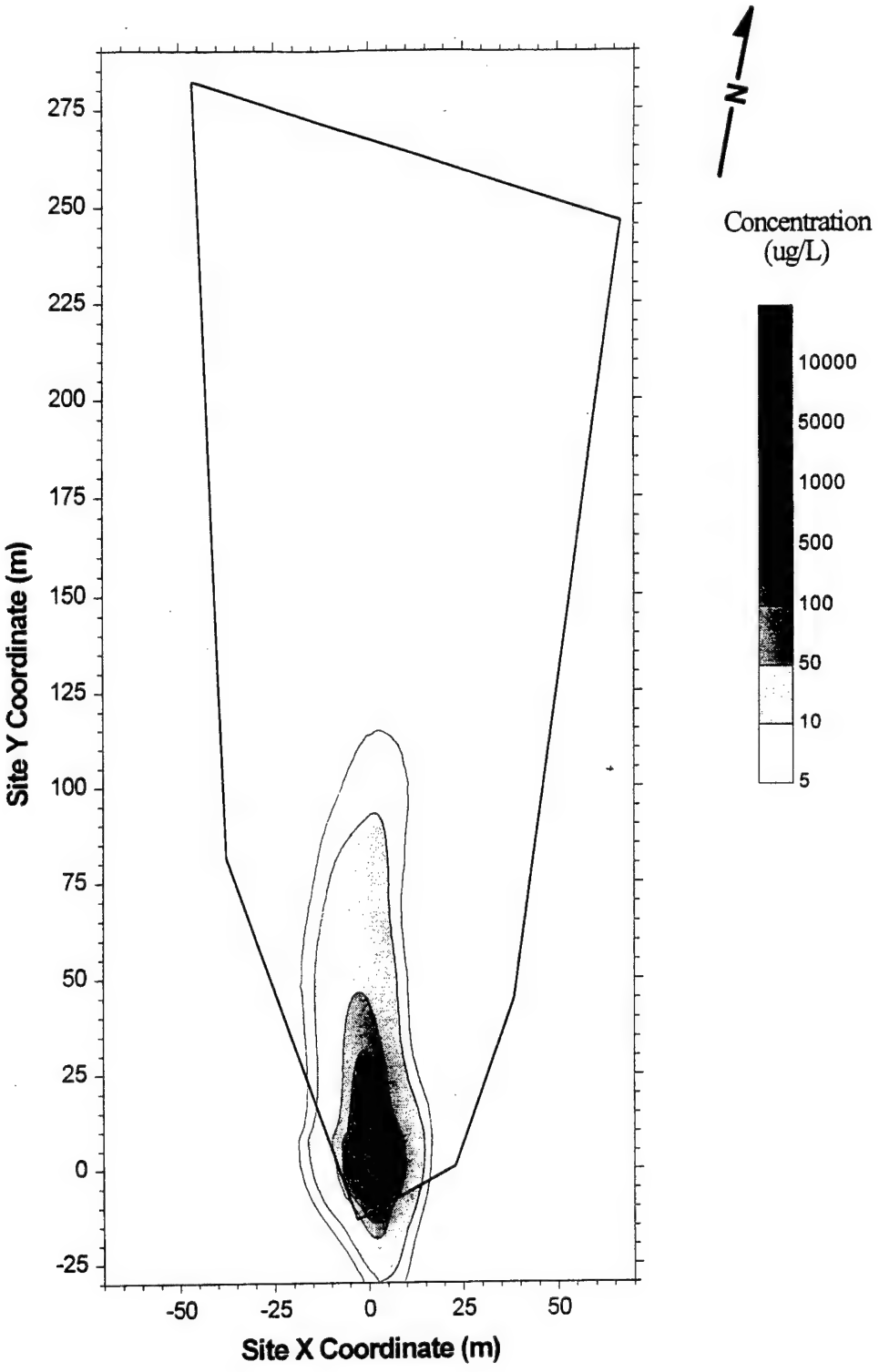

Figure 27. Simulated Combined Organic Concentration for Snapshot 3 (224 Days After Injection, Pulse Injection Model with First-Order Decay).

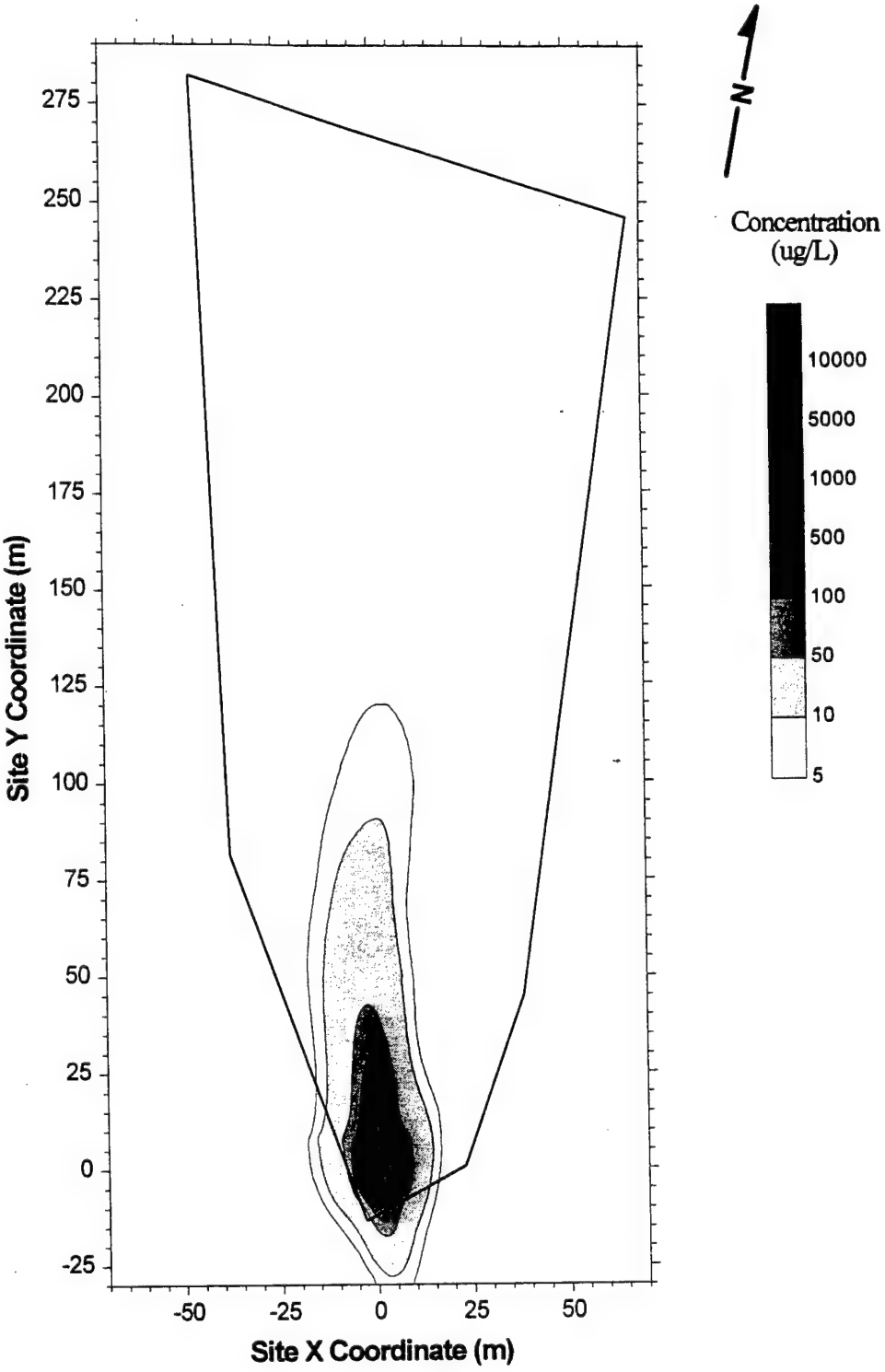

Figure 28. Simulated Combined Organic Concentration for Snapshot 4 (328 Days After Injection, Pulse Injection Model with First-Order Decay).

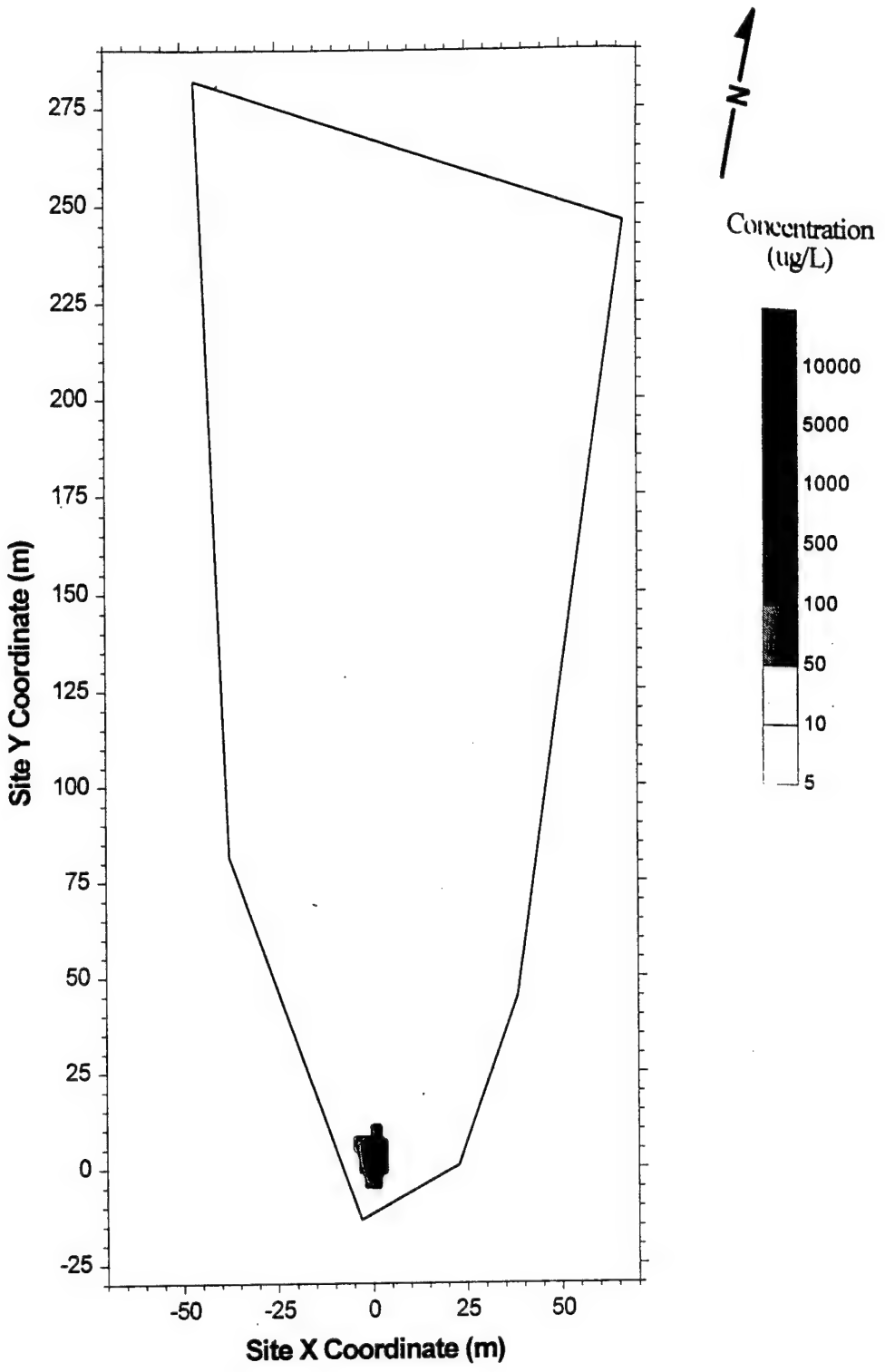

Figure 29. Simulated Combined Organic Concentration for Snapshot 2 (132 Days After Injection, Pulse Injection Model with Aerobic Degradation and First-Order Decay).

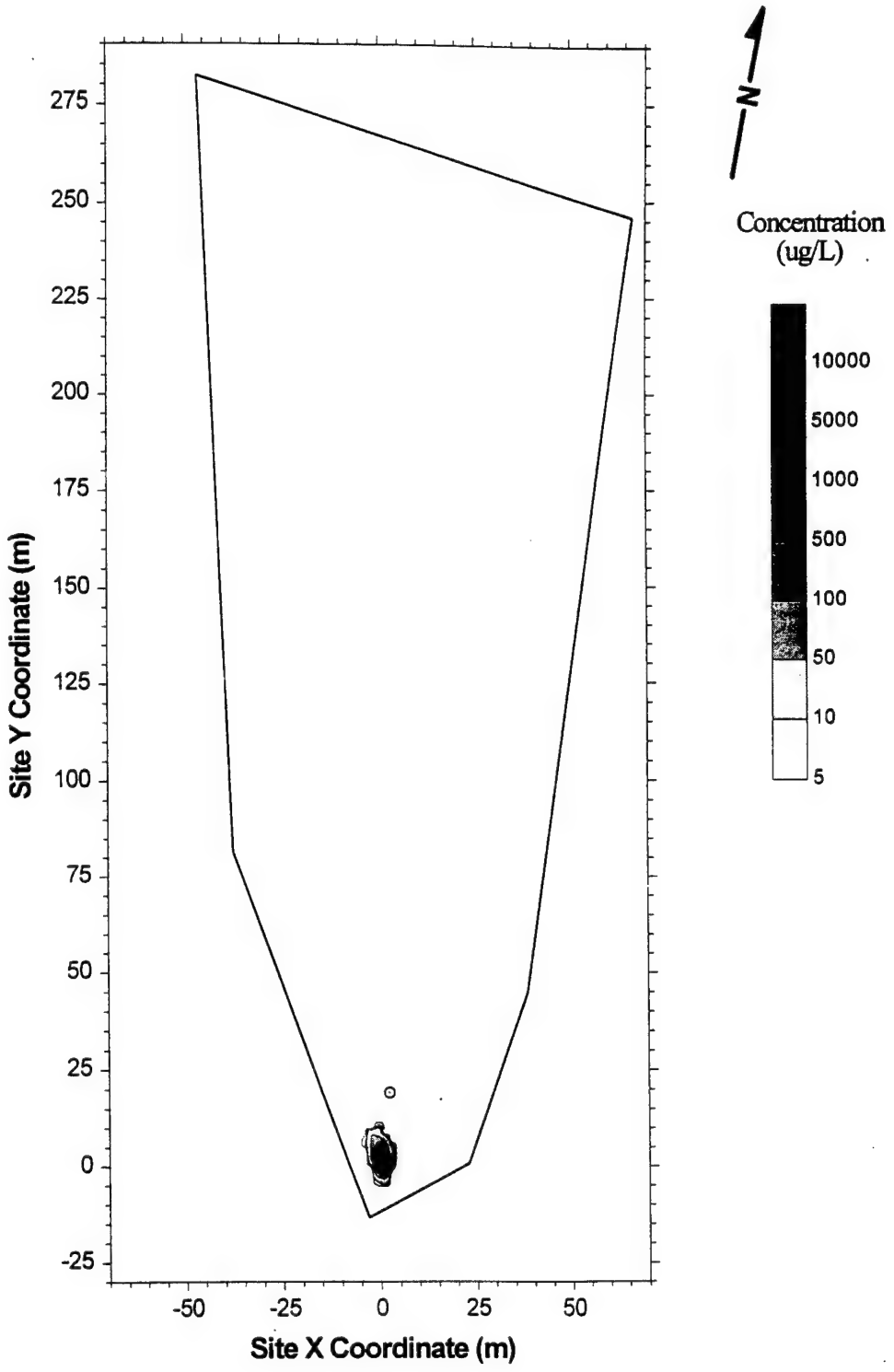

Figure 30. Simulated Combined Organic Concentration for Snapshot 3 (224 Days After Injection, Pulse Injection Model with Aerobic Degradation and First-Order Decay).

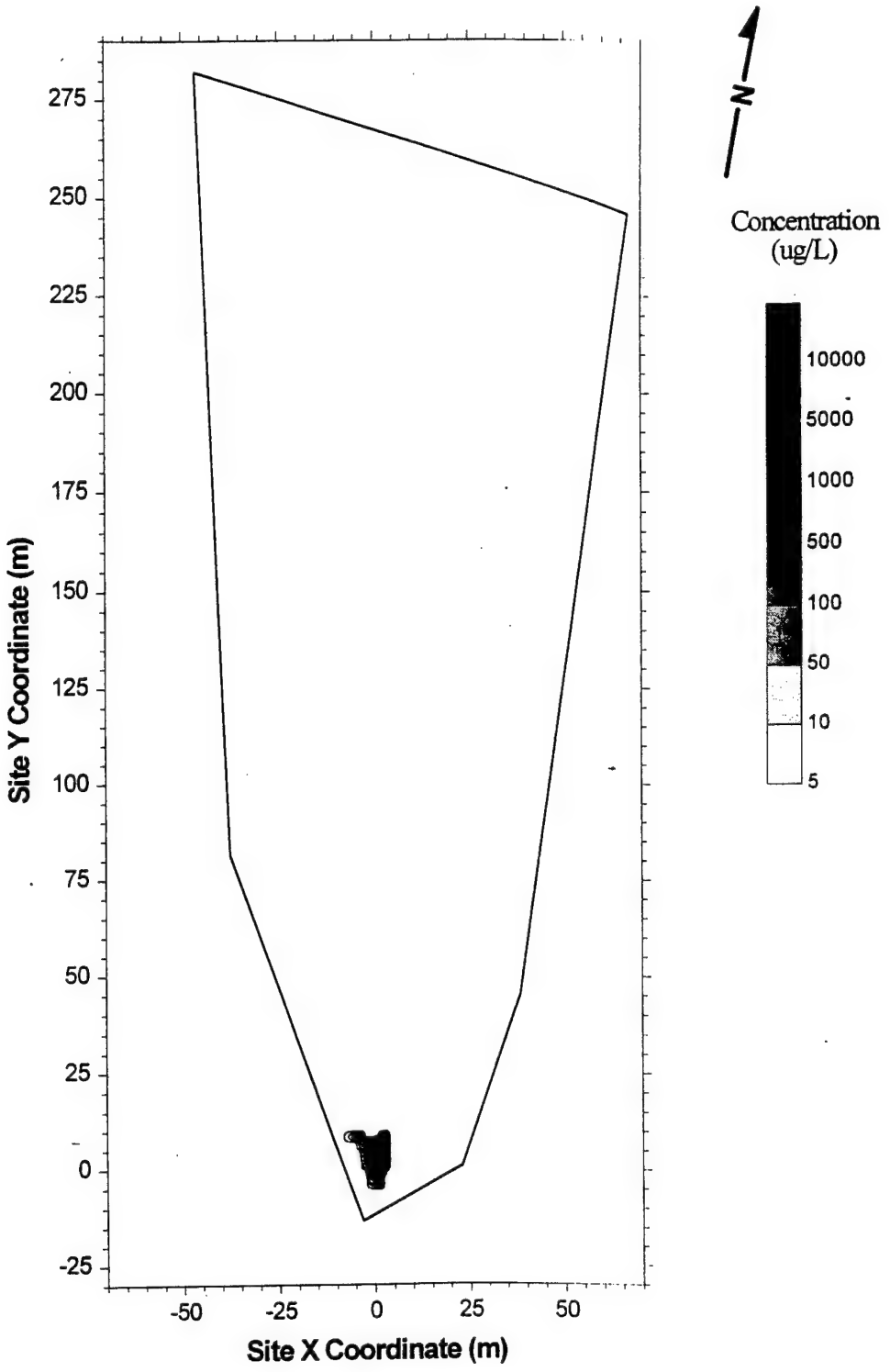

Figure 31. Simulated Combined Organic Concentration for Snapshot 4 (328 Days After Injection, Pulse Injection Model with Aerobic Degradation and First-Order Decay).

Figures 32, 33 and 34 show the tritium plumes resulting from the calibrated continuous injection model for Snapshots 2, 3, and 4, respectively. Comparison of these figures to the observed tritium plumes in Figures 17 through 19 indicates one difference — the peak concentration at the source area. This is probably due to the inability of the model to adequately approximate the injection process. This hypothesis is confirmed by observing Figure 26, which shows that the pulse injection model results indicate the same inadequacy. Comparing the observed tritium plume (Figure 18) at Snapshot 3 with that simulated by the continuous source model (Figure 33) illustrates that the simulated plume does not move as far as the observed plume. This is the same observation that was gleaned from the pulse source model. In both cases, the inadequacy of the model is probably the velocity distribution in the far-field region. The vertically averaged flow model underestimates the ground-water velocity in the far-field because it does not account explicitly for the high permeability zones. Figure 34 indicates that the simulated tritium plume from the continuous source model does not match the observed tritium plume (Figure 19) as well as the pulse source model (Figure 25) on the basis of far-field plume extent.

Figures 35, 36, and 37 show the combined organic plumes resulting from the calibrated continuous injection model for Snapshots 2, 3, and 4, respectively. Comparing these figures to the observed organic plumes in Figures 20 through 22 indicates that the simulated peak concentration at the source area is smaller than the peak concentration observed for the tritium simulations. Figure 35 shows that the extent of the simulated organic plume matches the extent of the observed organic plume relatively well at Snapshot 2 (and better than the pulse source model shown in Figure 26) even though the RMS errors shown in Table 13 would indicate that the overall error is relatively the same for both models. The same conclusion can be drawn for Snapshots 3 and 4 shown in Figures 36 and 37.

Figures 38, 39, and 40 show the simulated plume from the continuous source model incorporating aerobic degradation and first-order decay for Snapshots 2, 3, and 4, respectively. The most evident feature of the simulated plumes when compared to the observed plumes is the difference in the location of the front edge of the plume. The simulated plumes from this model are relatively small because the aerobic reaction instantaneously degrades much of the plume. Based on comparison to the observed results, the instantaneous aerobic degradation assumption does not appear appropriate for the MADE-2 experiment conditions. This may be due to the fact that the combined organic concentration was not high enough at the front edge of the plume to provide enough primary substrate to enhance microbial growth to a level that would provide instantaneous degradation of the available organics. This may be why the model incorporating first-order decay gives better results than the model incorporating instantaneous aerobic degradation and first-order decay. The limitation of the instantaneous degradation reaction may be partially corrected by incorporation of Monod-type kinetics.

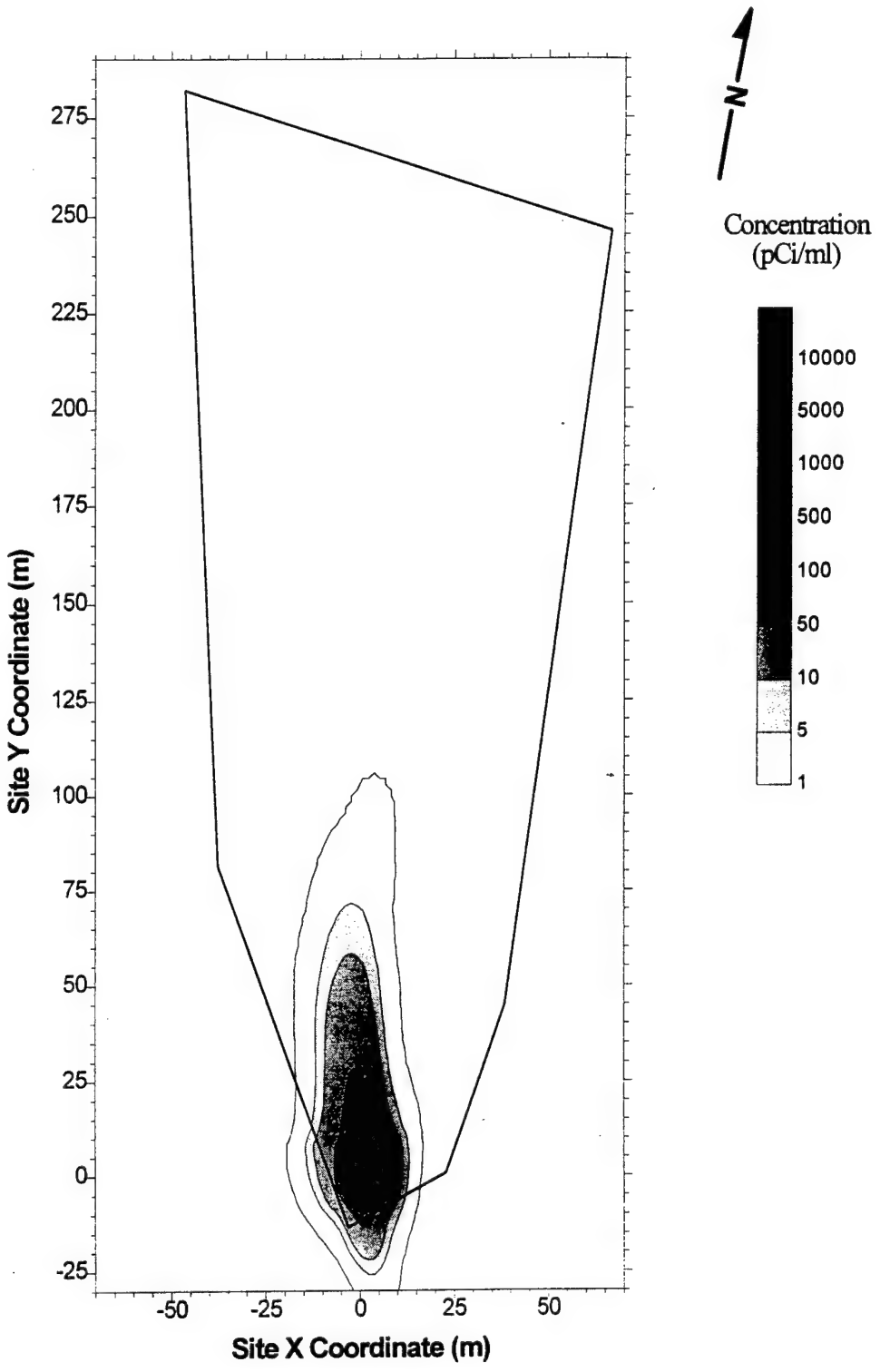

Figure 32. Simulated Tritium Concentration for Snapshot 2 (132 Days After Injection, Continuous Injection Model).

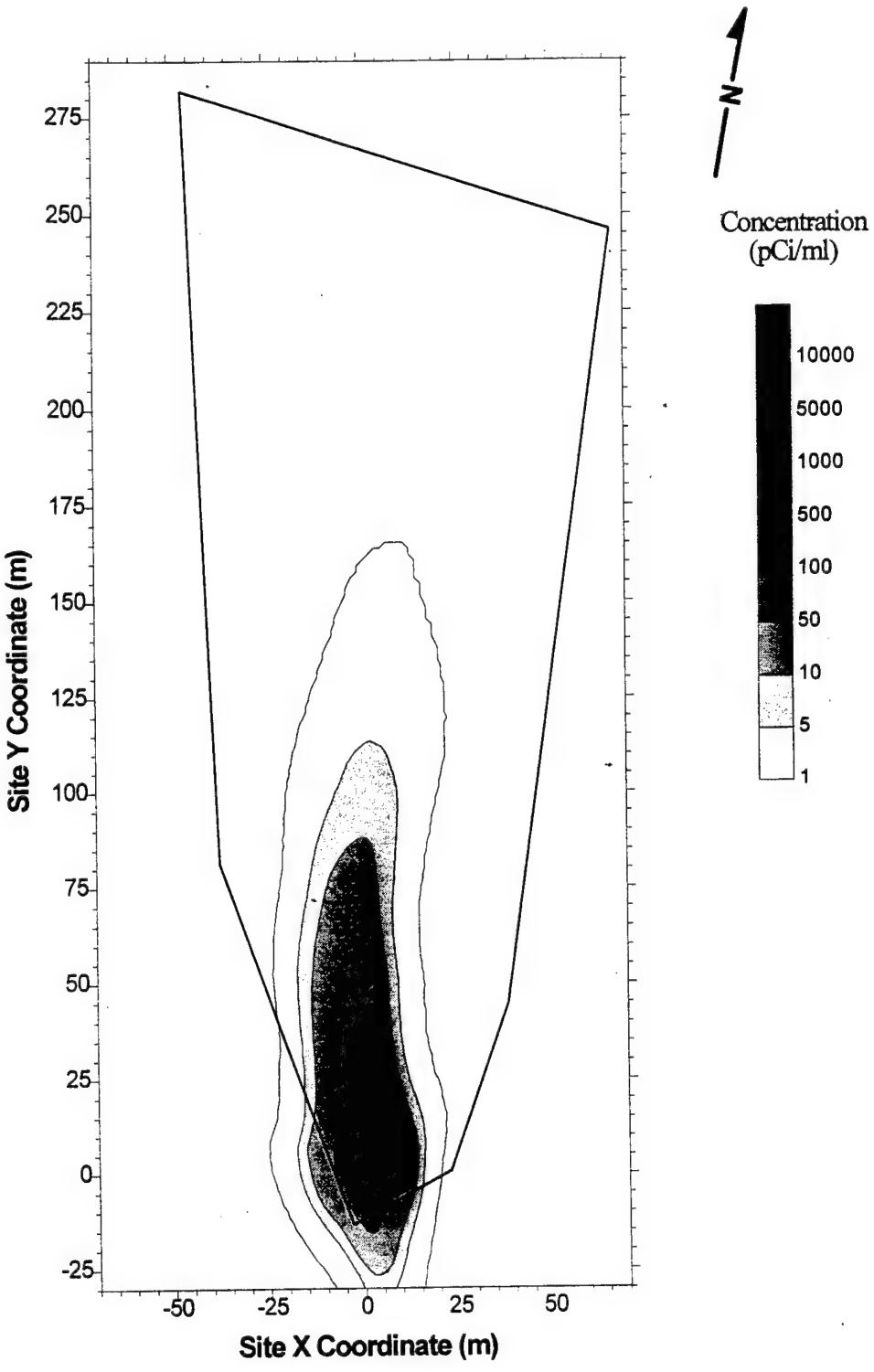

Figure 33. Simulated Tritium Concentration for Snapshot 3 (224 Days After Injection, Continuous Injection Model).

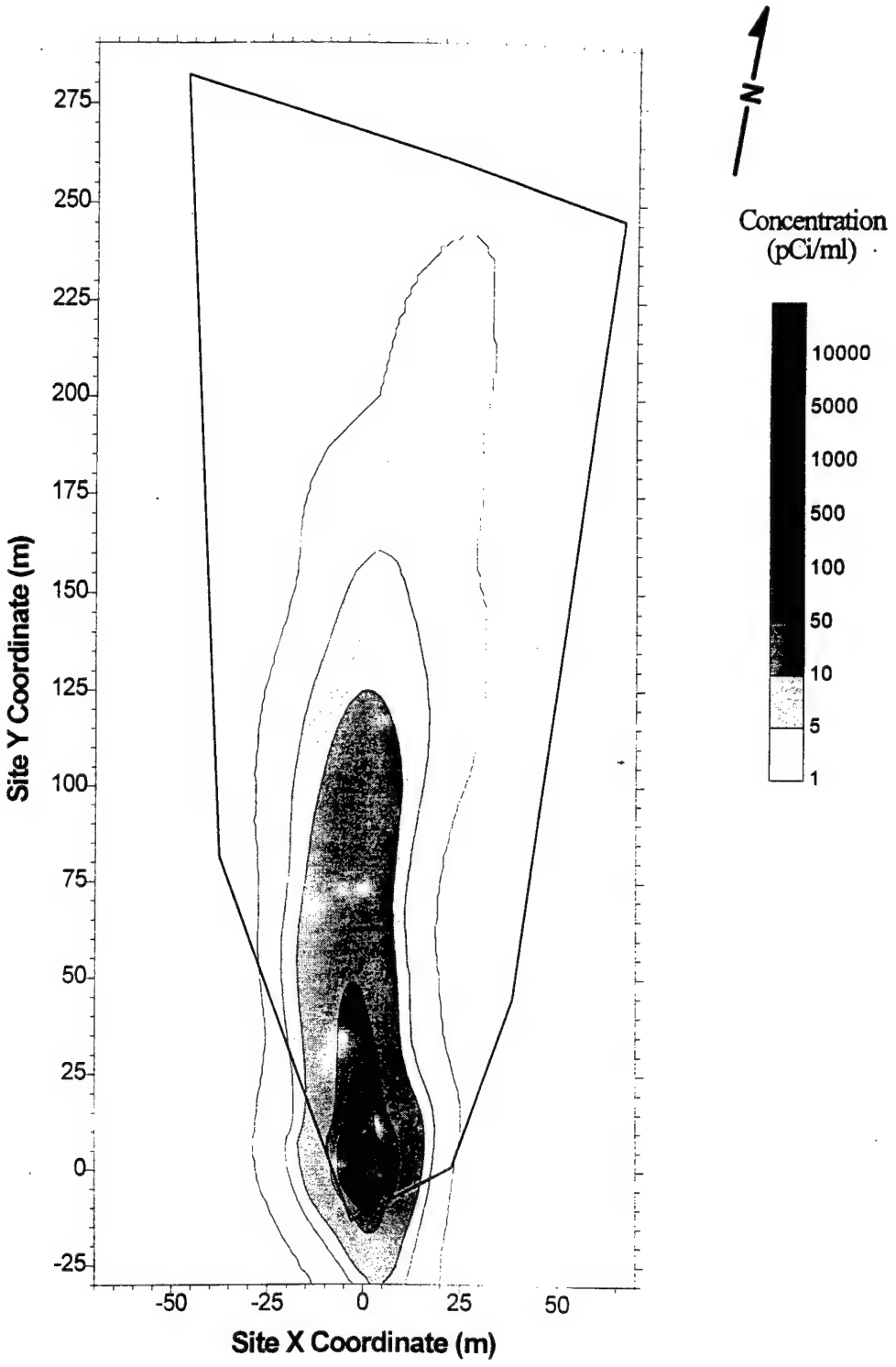

Figure 34. Simulated Tritium Concentration for Snapshot 4 (328 Days After Injection, Continuous Injection Model).

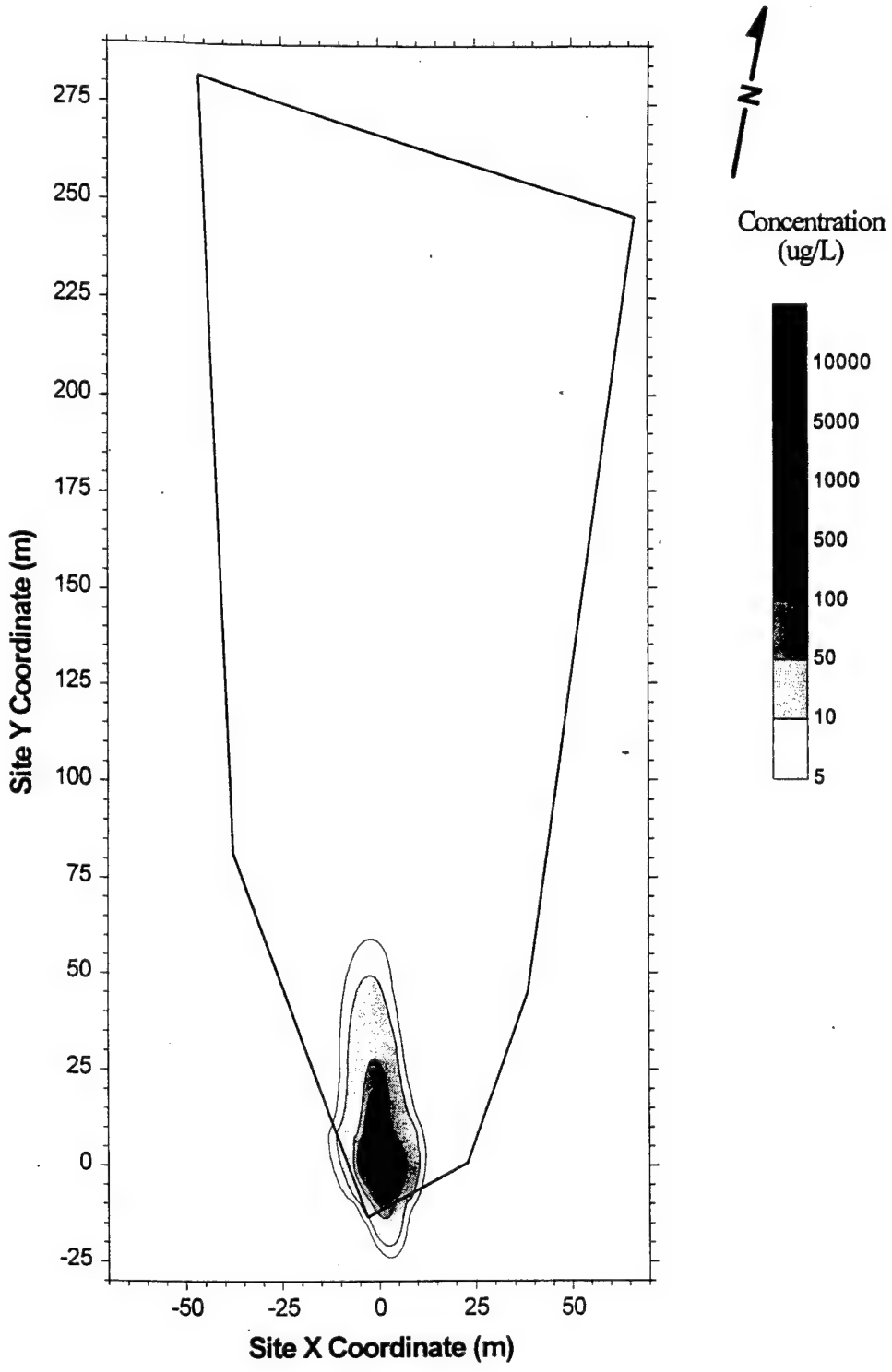

Figure 35. Simulated Combined Organic Concentration for Snapshot 2 (132 Days After Injection, Continuous Injection Model with First-Order Decay).

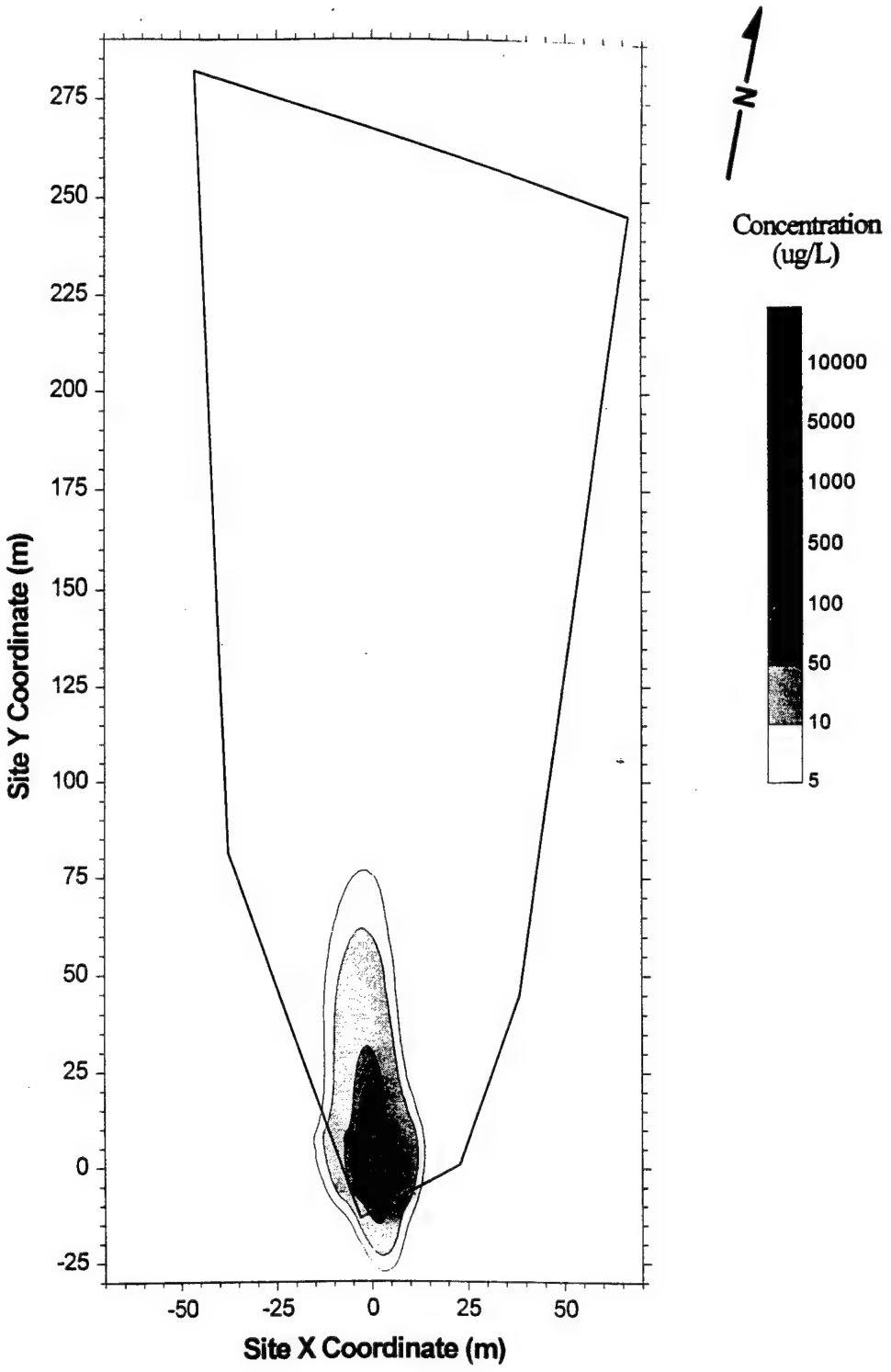

Figure 36. Simulated Combined Organic Concentration for Snapshot 3 (224 Days After Injection, Continuous Injection Model with First-Order Decay).

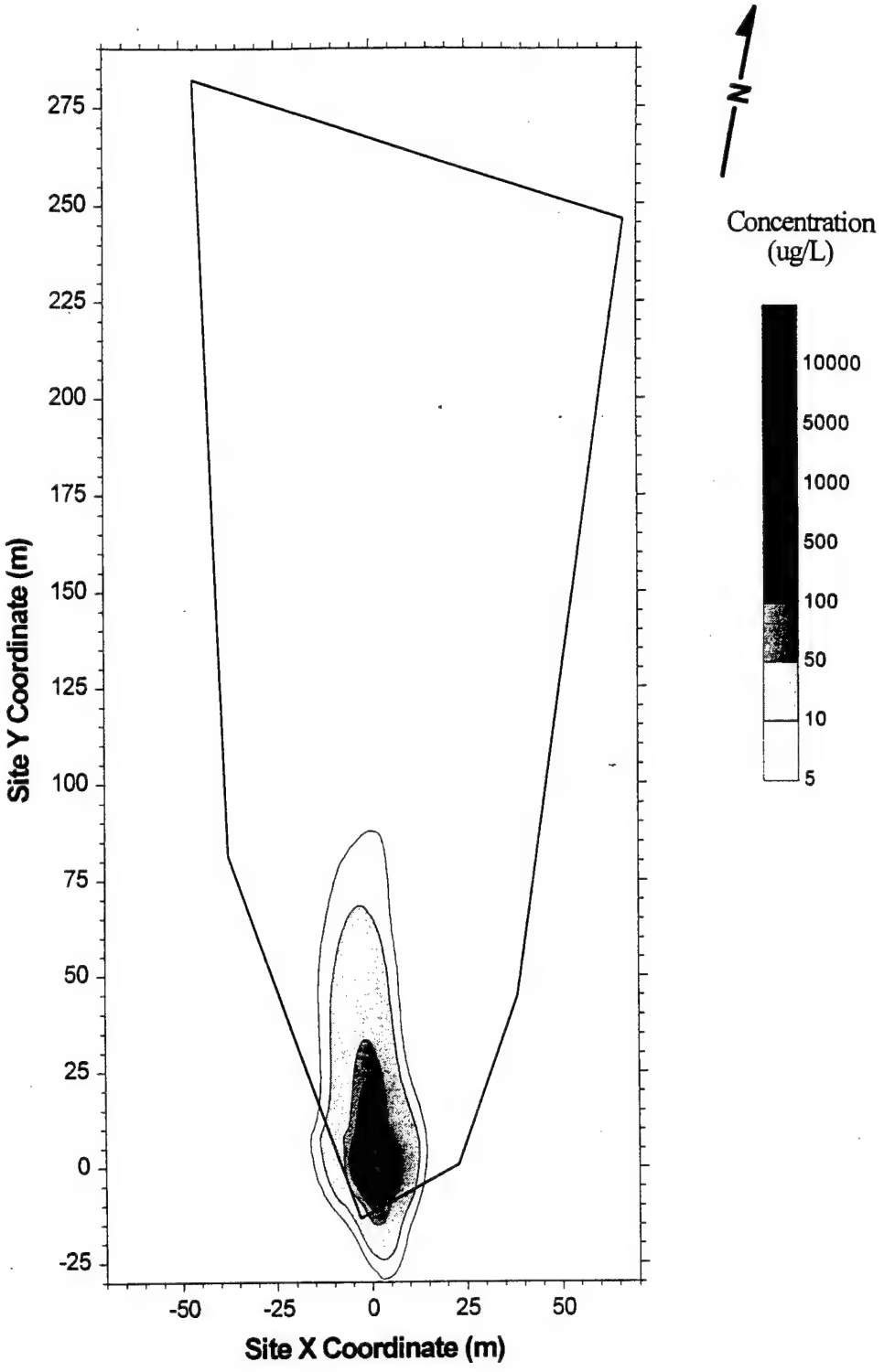

Figure 37. Simulated Combined Organic Concentration for Snapshot 4 (328 Days After Injection, Continuous Injection Model with First-Order Decay).

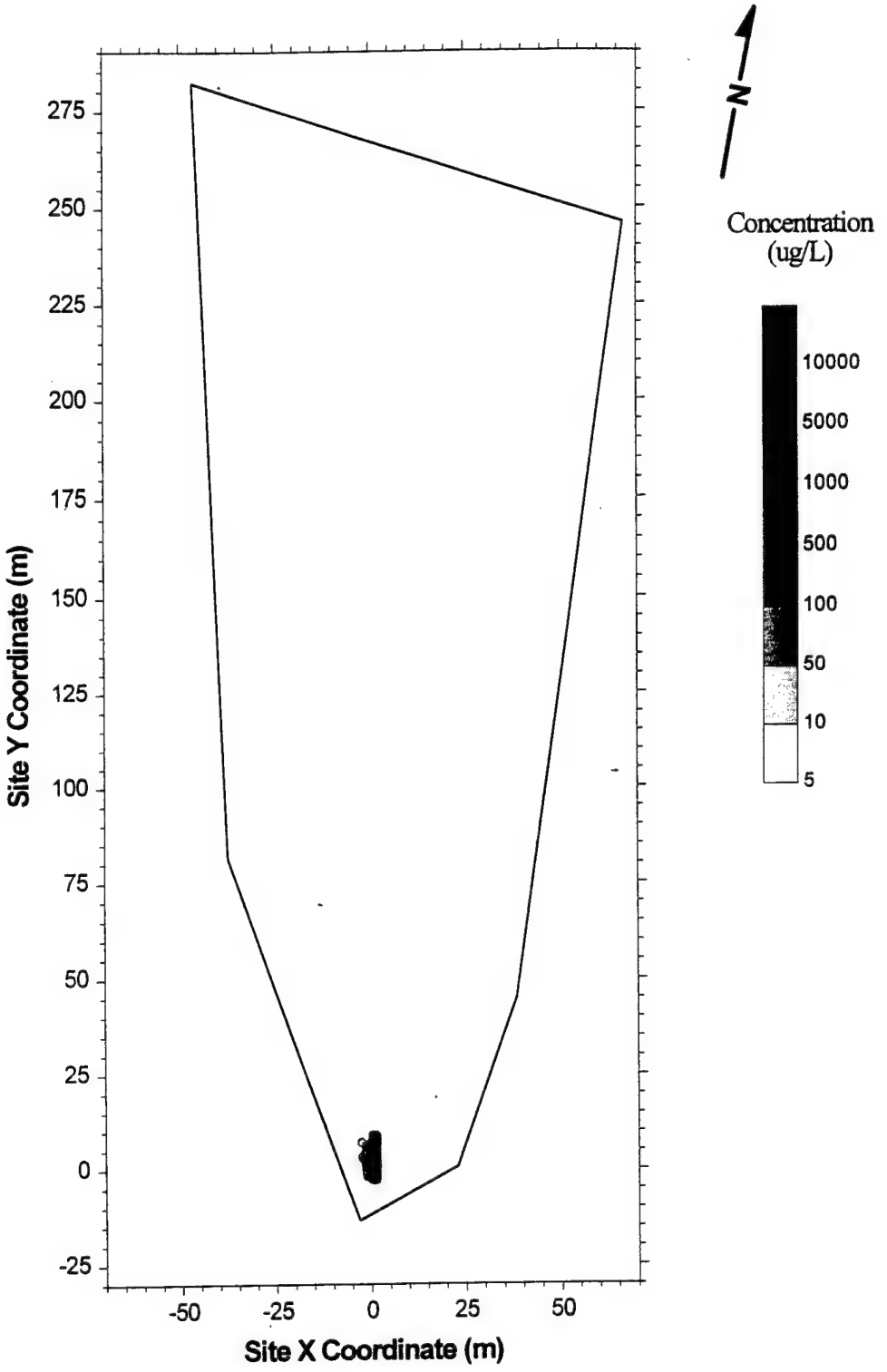

Figure 38. Simulated Combined Organic Concentration for Snapshot 2 (132 Days After Injection, Continuous Injection Model with Aerobic Degradation and First-Order Decay).

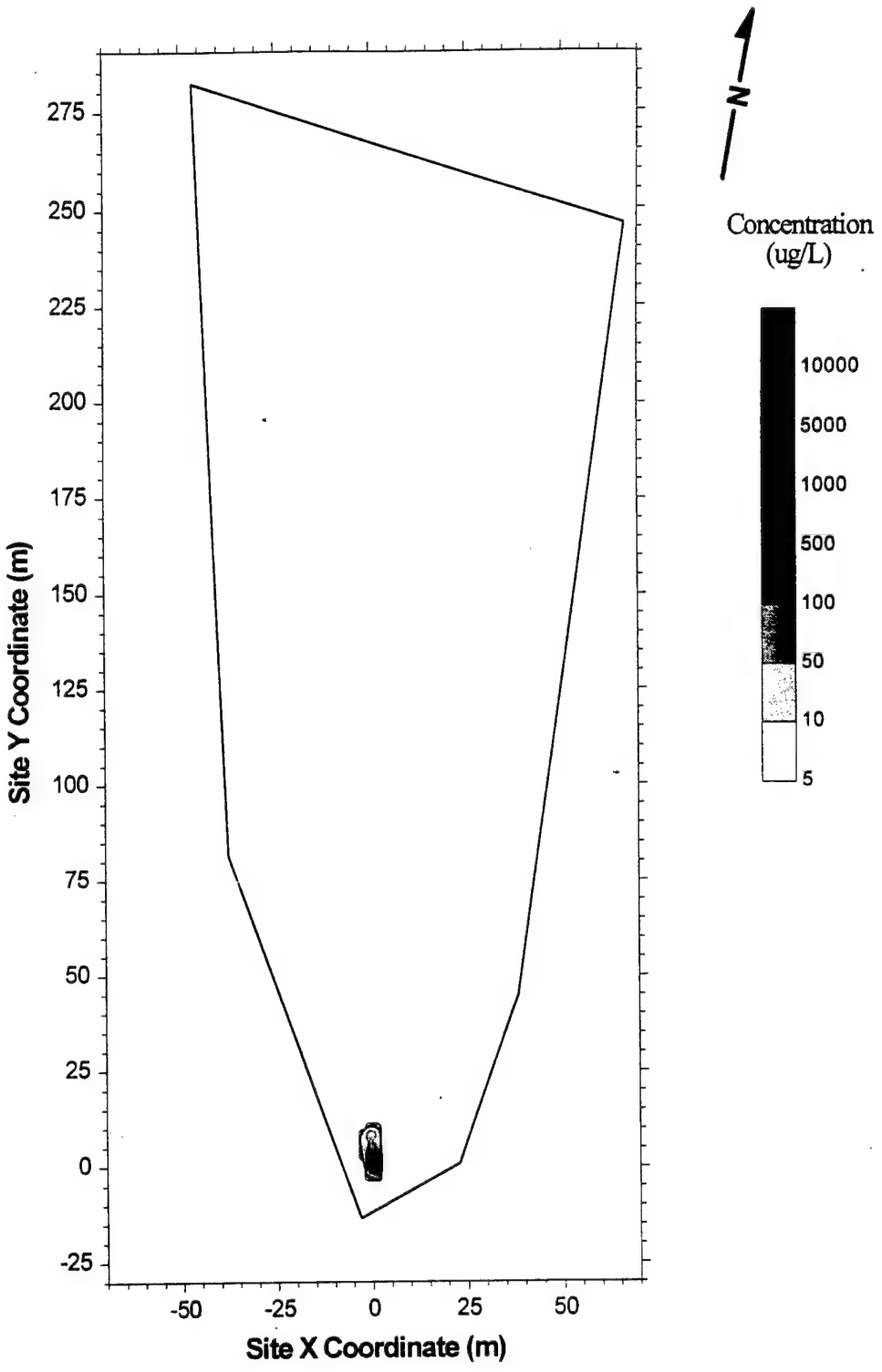

Figure 39. Simulated Combined Organic Concentration for Snapshot 3 (224 Days After Injection, Continuous Injection Model with Aerobic Degradation and First-Order Decay).

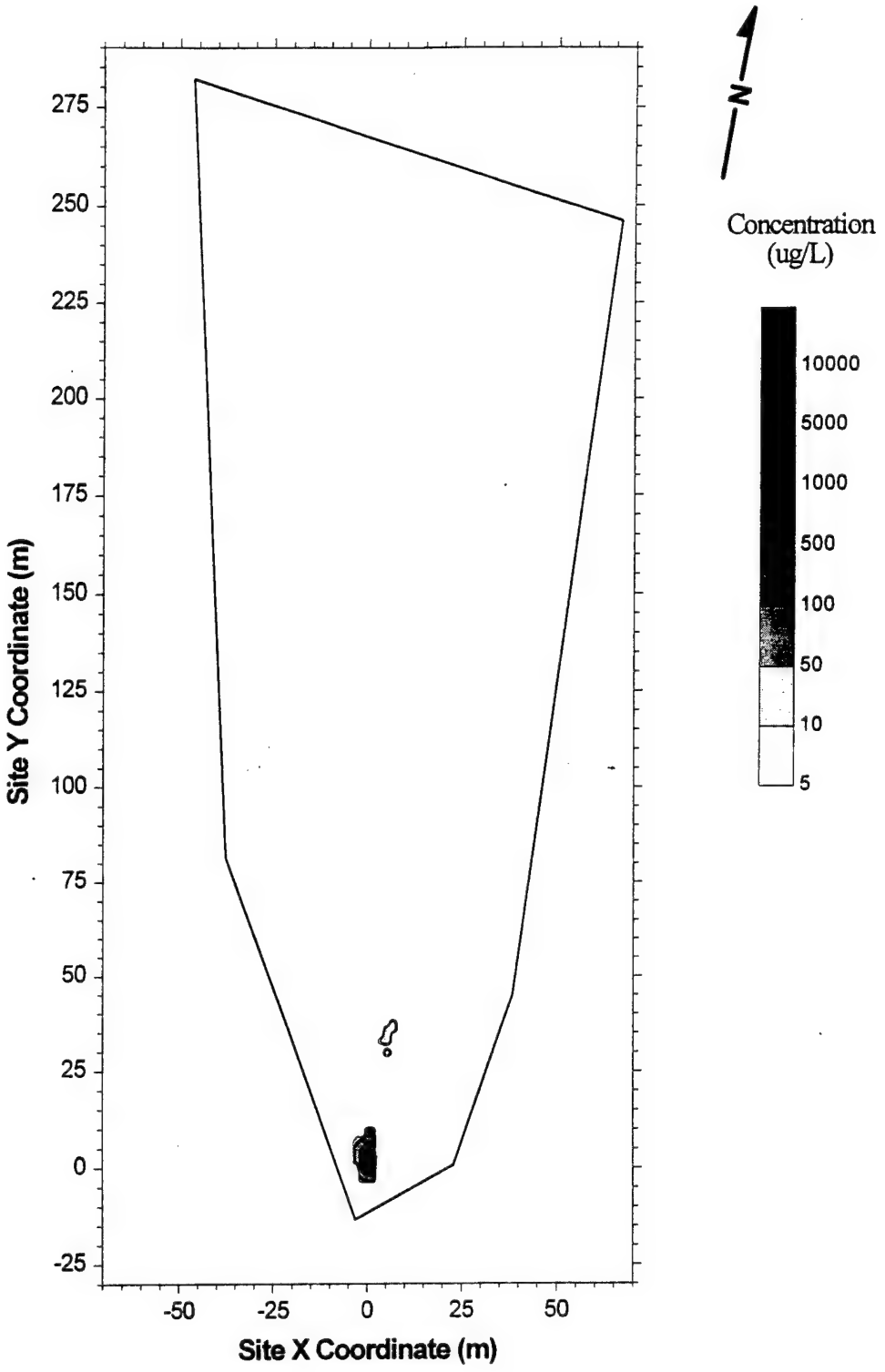

Figure 40. Simulated Combined Organic Concentration for Snapshot 4 (328 Days After Injection, Continuous Injection Model with Aerobic Degradation and First-Order Decay).

F. ANALYSIS AND COMPARISON OF RESULTS

After completing the calibration and validation process, the calibrated model parameters were used for the prediction simulations (Snapshot 4, 328 days after injection). A summary of the calibrated model parameters is shown in Table 12.

TABLE 12
BIOPLUME II PARAMETERS FOR THE MADE-2 SITE

Variable	Actual or Estimated from Observed Data	Modeled
All Simulations		
Porosity	0.31	0.35
Time		
— Calibration (snapshot 2)	132 days (0.3616 years)	0.3616 years
— Validation (snapshot 3)	224 days (0.6137 years)	0.6137 years
— Prediction (snapshot 4)	328 days (0.8986 years)	0.8986 years
Number of injection wells	5	2
Pulse Injection Only		
Injection concentration		
— Tritium	55,610 pCi/ml	504,873 pCi/ml
— Hydrocarbon	159.63 mg/L	1,358.40 mg/L
Injection rate (per well)	0.67 L/min (3.92E-04 cfs)	1.08E-04 cfs
Longitudinal dispersivity	10 m (32.8 ft)	37.0 ft
Transverse dispersivity	2.2 m (7.22 ft)	3.7 ft
Initial oxygen concentration	4.2 mg/L	3.0 mg/L
1st order decay rate		
— Only first-order decay	0.01 day^{-1}	0.0165 day^{-1}
— O_2 and first-order decay	n/a	0.0125 day^{-1}
Pulse and Continuous Injection		
Pulse injection concentration		
— Hydrocarbon	n/a	1,358.40 mg/L
Continuous injection concentration		
— Hydrocarbon	n/a	149.4 mg/L
Injection rate (per well)		
— Pulse (48.5 hours)	n/a	5.40 E-06 cfs
— Continuous (~ 328 days)	n/a	5.77 E-06 cfs

Table 13 shows the percent RMS error and center of mass location for all calibration and validation simulations. Burgess (1993) suggests that a percent RMS error of less than 15 percent should be considered acceptable. Based on this criterion, the continuous source simulations more accurately represent the MADE-2 experiment results. From examining only Table 13, it would appear that the first-order decay simulations and the aerobic biodegradation with first-order decay simulations are roughly equivalent. However, visual inspection demonstrates that the first-order decay simulation results more appropriately mimic the extent of the observed plume edges. Therefore, the percent RMS error values were used only as a rough gauge for model calibration.

TABLE 13
PERCENT RMS ERROR AND CENTER OF MASS OF SIMULATED PLUMES

Variable	RMS Error (%)	Center of Mass (m)
Pulse Injection Only		
Calibration results (snapshot 2)		
— Tritium	14.8	0.12, 16.75
— Organic (1st-order decay)	14.5	0.35, 9.49
— Organic (1st-order + O_2)	15.4	0.61, 2.07
Validation results (snapshot 3)		
— Tritium	7.5	0.04, 33.01
— Organic (1st-order decay)	7.5	0.36, 14.14
— Organic (1st-order + O_2)	7.9	0.53, 2.01
Prediction results (snapshot 4)		
— Tritium	10.5	1.12, 52.05
— Organic (1st-order decay)	18.7	0.50, 16.57
— Organic (1st-order + O_2)	19.4	0.52, 2.06
Continuous Injection		
Calibration results (snapshot 2)		
— Tritium	17.3	0.33, 9.89
— Organic (1st-order decay)	16.6	0.50, 5.53
— Organic (1st-order + O_2)	18.2	0.71, 1.94
Validation results (snapshot 3)		
— Tritium	7.9	0.79, 20.58
— Organic (1st-order decay)	7.5	0.41, 8.90
— Organic (1st-order + O_2)	7.6	0.51, 2.85
Prediction results (snapshot 4)		
— Tritium	8.6	0.62, 35.32
— Organic (1st-order decay)	13.1	0.42, 12.02
— Organic (1st-order + O_2)	13.0	0.65, 2.18

1. Pulse Injection

Visual comparison between the tritium contours of the Bioplume II simulations (Figures 23, 24, and 25) and the tritium contours of the field data show that the progress of the leading edge of the simulated plume and the progress of the leading edge of the actual tritium plume are similar. In the near field, the simulated plume is much wider than the actual plume. This is most likely caused by the high concentration gradient resulting from the simulated pulse injection. This causes the plume to disperse much faster than is likely to occur in the field. The simulated plumes show the leading edge of all contours greater than 50 µg/L significantly farther down gradient than is evidenced by the field tritium data. This could also be caused by excessive dispersion in the Bioplume II simulation. It is most likely caused by a combination of dispersion and inexact modeling of the transmissivity in the near field.

As expected, the simulated tritium plume does not show the fingering and separation evident in the observed plumes. This is probably due to the high velocity zones and tortuous flow paths that exist at the MADE-2 site. Channels of high hydraulic conductivity allow the contaminants to follow a tortuous path and could cause plume separation. This is most evident in Figures 18 and 19, which show vertically averaged tritium plumes at times corresponding to Snapshots 3 and 4, respectively. The vertically integrated flow and transport equations do not allow the type of vertical plume separation that was observed in the field. The observed plume separation may also be caused by increased groundwater velocity (in the high permeability zone about 50-100 meters down gradient of the source zone, see Figure 2) associated with infiltration from rainfall events. Heavy infiltration could cause an influx of water that converges from the low conductivity zones into the high conductivity zone (see convergent flow field in Figure 8) that could serve to pinch off the plume from the source zone and push the front edge of the plume down gradient.

Figures 20, 21, and 22 show vertically averaged combined organic plumes, at times corresponding to Snapshots 2, 3, and 4. Examination of Figures 20, 21, and 22 shows that the combined organic plume appears to achieve a quasi-steady-state or actually to be receding, unlike the tritium field data, where the front edge of the tracer continually moves down gradient. This may be caused by aerobic degradation at the edges of the organic plume. However, the first-order decay simulations do not show this effect. In these simulations, the leading edge of the plume progresses slowly, as shown in Figures 26, 27, and 28. The extent of the simulated organic plumes is greater than observed in field. As with the tritium plume, dispersion and transmissivity play an important role in the transport of the organic tracers.

When aerobic degradation and first-order decay are considered simultaneously, the organic plumes reach a steady-state situation. However, the area of the plume resulting from this model is much smaller than observed in the field, based on the implementation of 3 mg/L initial oxygen concentration (see Figures 29, 30, and 31). As the simulation progresses, the available oxygen continually degrades the edges of the simulated organic plume. However, the concentrations

in the center of the plume remain relatively constant after snapshot 2 because all the oxygen has been depleted. After the initial oxygen is depleted in the heart of the plume, only first-order decay (representing anaerobic degradation) decreases the combined organic concentrations. This results in organic concentrations above 1,000 µg/L in the heart of the simulated plumes. These high concentrations remain relatively constant throughout the simulations for Snapshots 2, 3, and 4. This result does not match the field observations, which show a reduction in concentration at all points within the plume as time progresses.

2. Continuous Injection

The continuous injection model does not simulate the peak tritium concentrations as accurately as the pulse injection model. This is most apparent in snapshots 2 and 3 (Figures 32 and 33). However this difference is much smaller in the simulation representing Snapshot 4 (Figure 34). In general, the continuous source model provides better predictive capability than the pulse source model at later times (and in the far-field) and the pulse source model are more representative in the early stages of the plume.

The continuous source model incorporating only first-order decay provides the best overall representation of organic tracer fate and transport during the MADE-2 experiment. This model provides the best correlation to field data as evidenced in both the percent RMS error and visual inspection (see Figures 35, 36, and 37). The continuous source model overpredicts the area of contamination, but results in better results when compared to the contoured field data than the model incorporating aerobic degradation and first-order decay (shown in Figures 29, 30, and 31). Plumes from the model incorporating first-order decay only show little change in concentrations in the heart of the plume and are continually transported down gradient over time. The simulated data for Snapshots 2 and 3 and field Snapshots 2 and 3 show good visual correlation. The field data for Snapshot 4 show a smaller plume than the simulated data. This indicates that aerobic degradation may play a role in natural attenuation during the MADE-2 experiment. However, the simulations incorporating 2.6 mg/L oxygen probably overestimate the amount of oxygen used in the aerobic degradation processes at the site. A model incorporating first-order decay and aerobic degradation would probably provide a better visual correlation if aerobic degradation was allowed to degrade a smaller amount of organics instantaneously. This would be accomplished by lowering the initial oxygen concentration and adjusting the reaeration rate. In this way, the aerobic degradation would act to stabilize the growth of the plume without prematurely degrading the entire plume. Sensitivity simulations were completed to look at these scenarios and are discussed below.

The continuous source simulations of aerobic degradation with first-order decay show a slight reduction in the internal contaminant concentration through time for Snapshots 2, 3, and 4, respectively (see Figures 38, 39, and 40). As mentioned above, the extent of the simulated plumes does not accurately represent the plume that was measured during the MADE-2 experiment. In fact, the continuous source model gives a worse result than the pulse source model. One anomaly appears

in the simulated Snapshot 4 plume (Figure 40). A simulated slug of organic contaminant moves down gradient between Snapshots 3 and 4. This does not appear in the previous snapshots but corresponds roughly to a down gradient slug of contaminant observed in the field (see Figure 22). The results of the continuous source model may have more closely mimicked the observed results if the initial oxygen concentration and reaeration rate were lowered.

3. General Observations

One of the considerations that arose during model calibration was the justification for modeling aerobic degradation and first-order decay simultaneously. Examination of the dissolved oxygen data for the near-field sampling points (D010, M041, and M066) from Boggs *et al.* (1993) shows that the lowest dissolved oxygen concentration collected during the study in the area where degradation is occurring is 2.6 mg/L. (The corresponding maximum in this area is 6.8 mg/L.) These measurements were collected before tracer injection (June 18, 1990). The next measurements were collected on August 13, 1990. During this time, the measured oxygen actually increased at some sample locations (2.4 mg/L at M041, port 10) and did not decrease substantially overall. This indicates either that significant recharge of dissolved oxygen is occurring at the site, or that there is some inconsistency or inaccuracy in the reported data. If significant reaeration was occurring at the site, then the simulated first-order decay could effectively represent decay resulting from the oxygen reaeration. It is simply a way of accounting for the suspected introduction of dissolved oxygen into the groundwater from the vadose zone or though infiltrating rain water.

In addition, since there are some very low permeability zones near the injection zone, it is possible that pockets of low dissolved oxygen (and thus anaerobic biodegradation) may have developed during the experiment. The dissolved oxygen monitoring in the near field was relatively sparse. Three multilevel samplers were sampled at three ports, approximately every two or three months. These samples may not have been collected from zones exhibiting anaerobic biodegradation. In this case, the first-order decay term would account for any anaerobic biodegradation that occurred in these zones.

The model incorporating instantaneous aerobic biodegradation (with 3 mg/L available dissolved oxygen) always degraded too much of the low concentration organic plume. The results of these simulations indicate that the aerobic biodegradation of the organics may be rate-limited by the amount of available hydrocarbon. In the physical system, the microbe colonies may not increase activity and growth immediately when the organic concentration is only increased slightly. As concentrations continue to increase and the "lag" time passes, microbe activity increases to match the increased nutrient supply, assuming all other conditions support increased growth. The instantaneous aerobic biodegradation assumption in Bioplume II does not simulate this process. It assumes that available oxygen and nutrients are brought into a reaction instantaneously, regardless of microbe activity. This may be a good assumption under certain conditions, but appears to be weak in simulating microbe response in regions of the aquifer where microbe activity has not yet increased

due to limited nutrient increase or other activity-limiting factors. It is possible that the organic tracers were the limiting substrate during the MADE-2 experiment, not the available oxygen, especially at the edges of the plume. Odencrantz *et al.*, (1990) state that ". . . when the substrate concentration is small with respect to K_s, the kinetics are first-order, when it is high with respect to K_s, they are zero order." (K_s is the half-saturation or half-velocity constant.) Tabak *et al.* (1990) give a K_s value of 22 and 67 mg/L for benzene and p-xylene respectively, based upon their studies. The largest portion of the organic plumes during the MADE-2 experiment had a lower concentration than these reported K_s values. If the indications from Odencrantz *et al.*, (1990) are correct, that would explain why the model incorporating only first-order decay produces the best simulated results when compared to observed plumes. Potentially the best model would describe aerobic biodegradation with rate-limited reactions (Monod kinetics) and anaerobic biodegradation with first-order decay. Monod kinetics (used in Bioplume and available in Bioplume III, but not Bioplume II) account for rate-limited aerobic biodegradation, based on availability of all the required substrates (Rifai and Bedient, 1990). This study indicates that because the instantaneous aerobic biodegradation assumption may be especially weak for modeling the movement of the front edge of the plume (i.e., relatively low concentration), the potential impacts of this assumption should be carefully considered when using models to develop remediation systems and long-term monitoring plans.

G. SENSITIVITY ANALYSIS OF TRANSPORT PARAMETERS

A sensitivity analysis was performed to determine what effect various parameters had on contaminant transport and on mass loss due to biodegradation and adsorption. The parameters considered were transmissivity, longitudinal dispersivity, the ratio of transverse to longitudinal dispersivity, retardation, first-order decay, and initial oxygen concentration. All sensitivity estimates were developed by evaluating the simulated plume at snapshot 2 (132 days after injection). The base-case parameters used in the sensitivity analysis are the estimates developed in the calibration and validation process. These are shown in Table 14.

Simulated tritium plumes were used to study the sensitivity of model results to transmissivity and dispersivity. The calibrated transmissivity distribution was multiplied by a scaling factor (M) to decrease and increase the transmissivity by an order of magnitude. Figure 41(a) and (b) show the tritium concentration along the centerline of the plume for the pulse source and continuous source models. In these figures, peak concentrations and extent of the plumes vary significantly. In general, as the transmissivity increased, the peak concentrations decreased while plume areas increased.

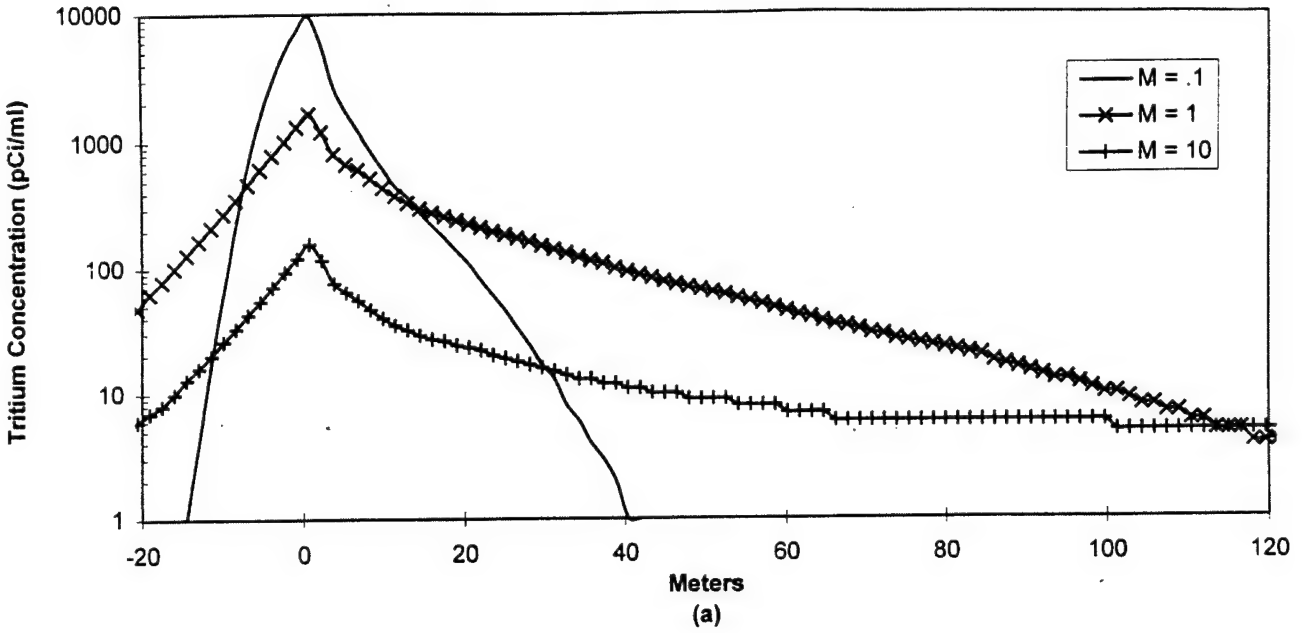

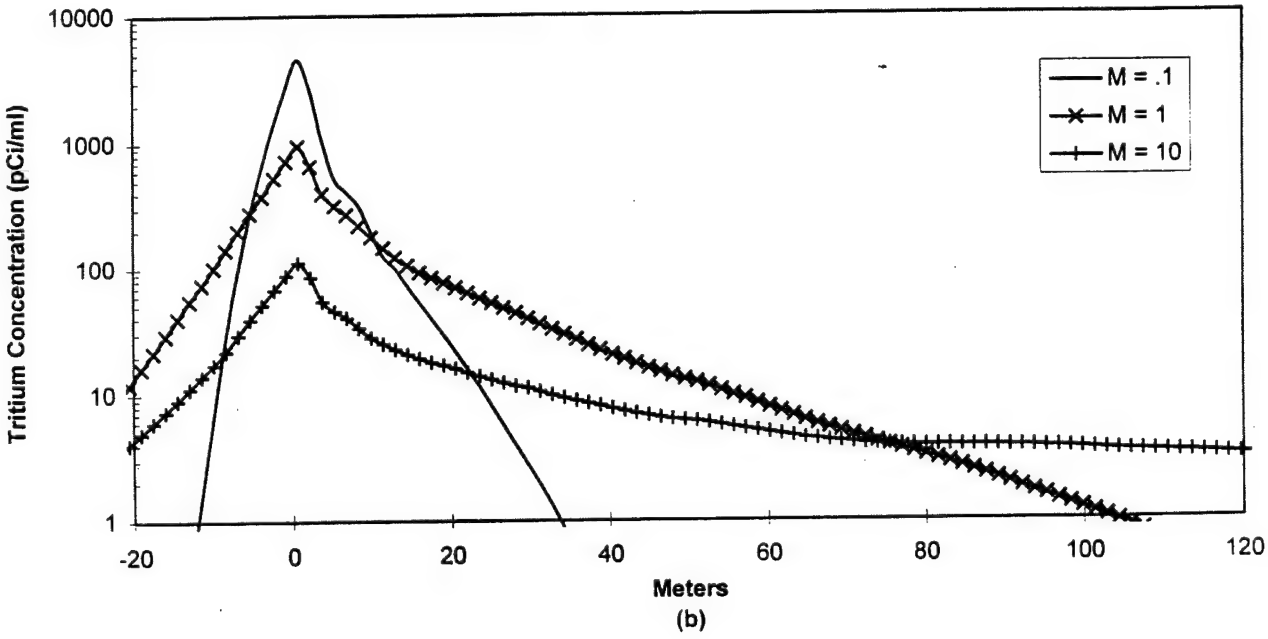

Figure 41. Effect of Transmissivity Scaling Factor (M) on Simulated Centerline Tritium Concentrations for (a) the Pulse Source Model and (b) the Continuous Source Model.

TABLE 14
BASE-CASE PARAMETERS FOR SENSITIVITY ANALYSIS

Parameter	Base-Case Estimate
Transport Parameters	
Transmissivity scaling factor	1
Longitudinal dispersivity	37 ft
Dispersivity ratio	0.1
Biodegradation Parameters (First-order decay only)	
First-order decay rate	0.0165 day^{-1}
Retardation	1.296
Biodegradation Parameters (First-order decay and Aerobic Degradation)	
First-order decay rate	0.0125 day^{-1}
Initial oxygen concentration	3,000 µg/L
Retardation	1.296

The effects of longitudinal dispersivity are shown in Figure 40. The longitudinal dispersivity was varied from 15 to 45 feet for both source types. The concentration profiles shown in (a) and (b) are similar for all simulations, regardless of source configuration. As the dispersivity was increased, peak concentration decreased and plume extent increased. The response of the system to increased dispersivity was much smaller than the response due to increased transmissivity.

The tritium concentration along the center line and across a transect of the plume are shown in Figures 43 and 44. Increasing the ratio of transverse to longitudinal dispersivity ratio (RD) has little effect on the shape of the plume. In the center of the plume, the peak concentrations decreased with an increase in the dispersivity ratio. Additionally, the width of the plume increased slightly with an increase in RD.

The relative magnitude of the effects resulting from changing the values of transmissivity and dispersivity indicate that advective transport dominates this system. Increasing the transmissivity depleted the contaminant in the heart of the plume more than increasing longitudinal dispersivity and dispersivity ratio. This was also evident during the calibration and validation process. Major plume characteristics were controlled through the transmissivity field, while modifications to the dispersion parameters were used to effect small changes at the edges of the plume.

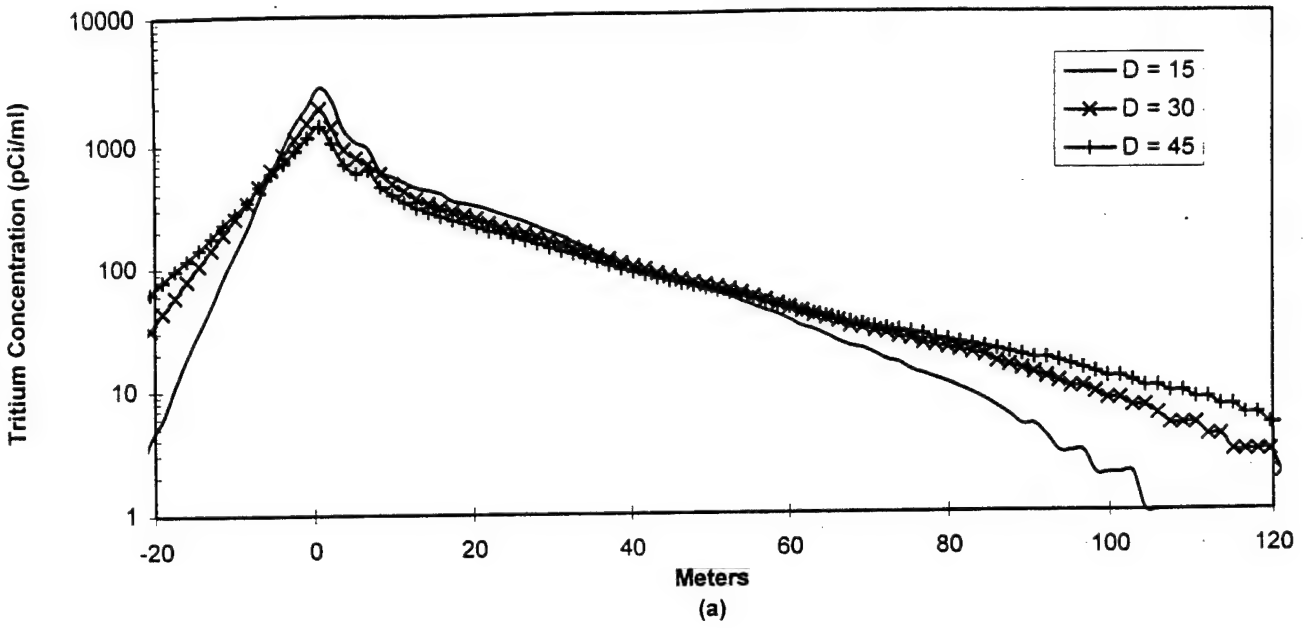

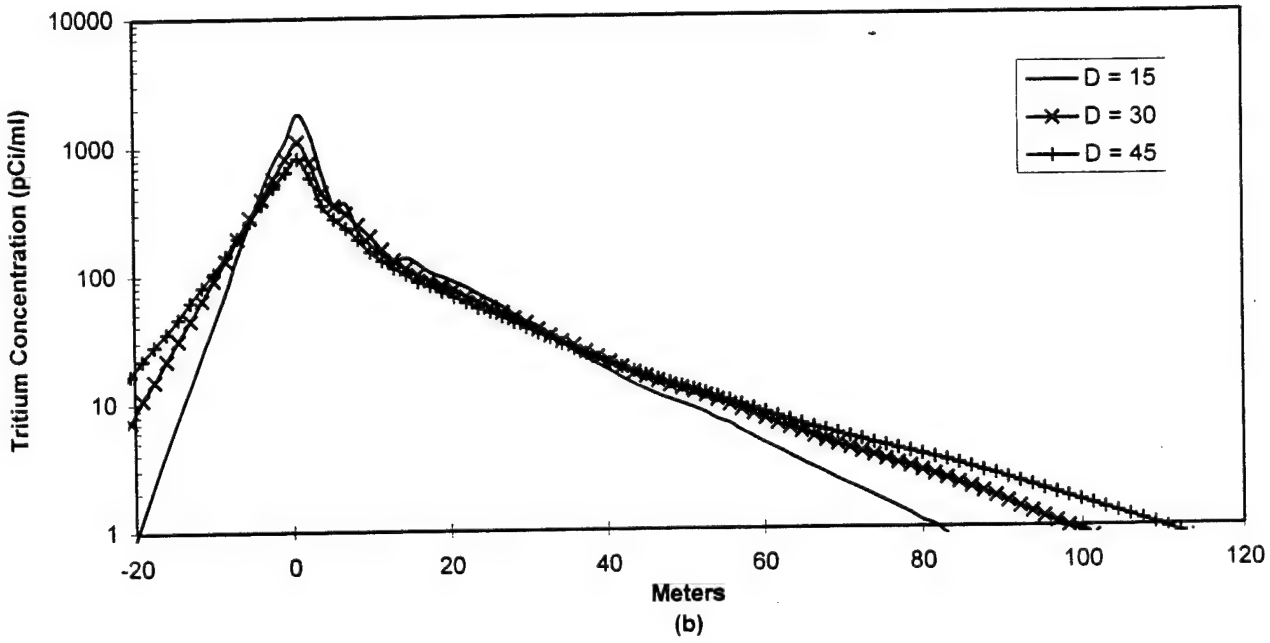

Figure 42. Effect of Longitudinal Dispersivity on Simulated Centerline Tritium Concentrations for (a) the Pulse Source Model and (b) the Continuous Source Model.

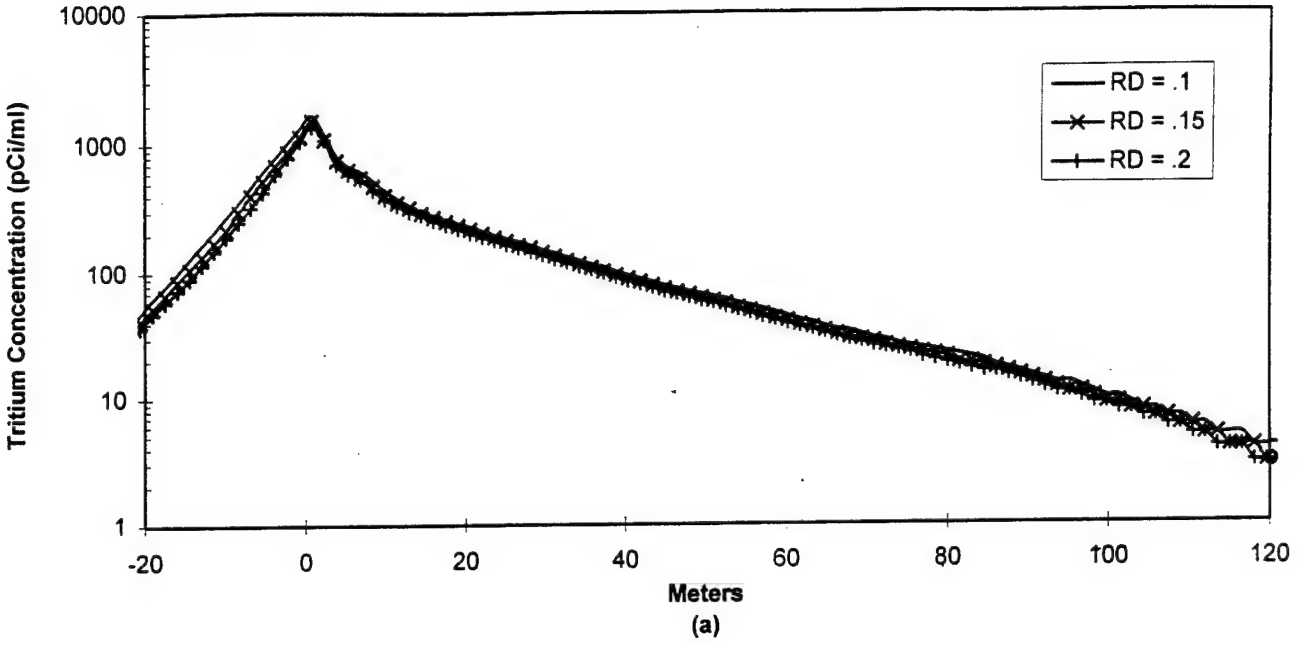

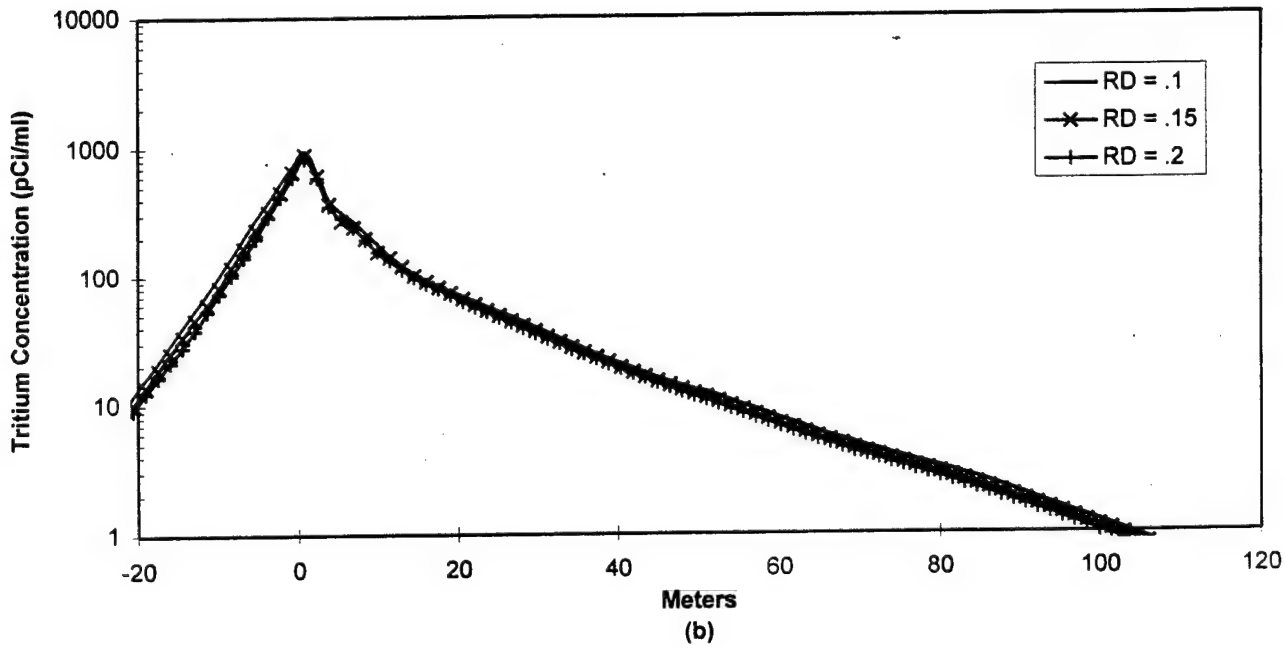

Figure 43. Effect of the Ratio of Transverse / Longitudinal Dispersivity on Simulated Centerline Tritium Concentrations for (a) the Pulse Source Model and (b) the Continuous Source Model.

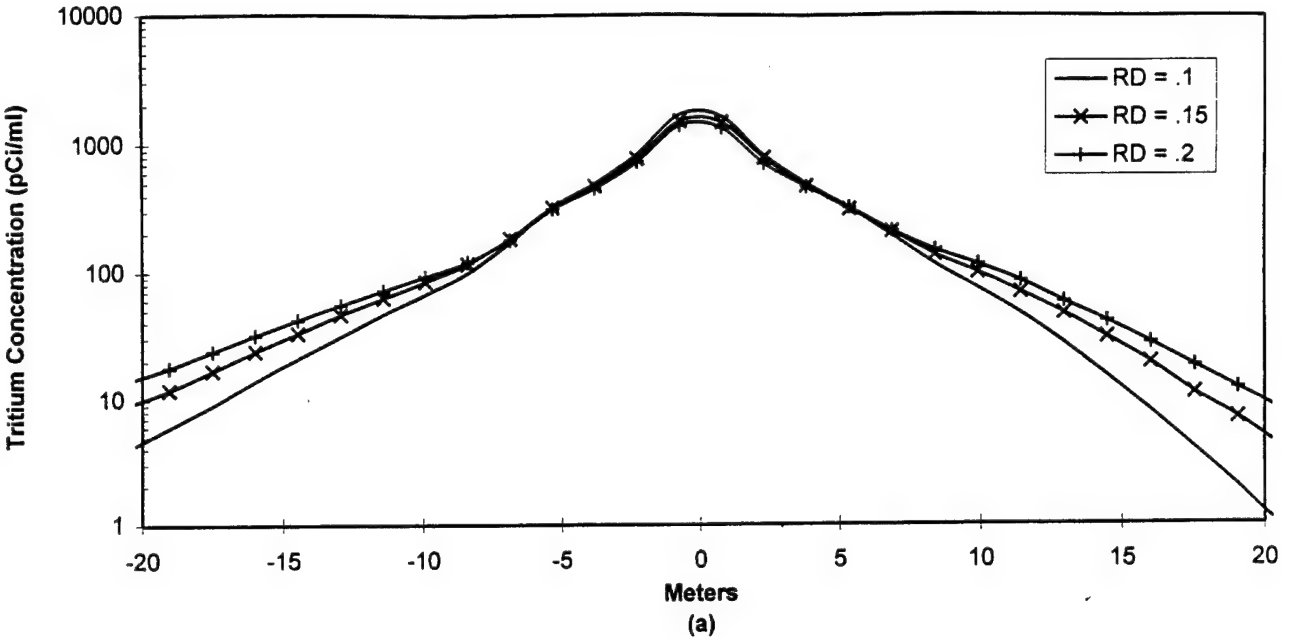

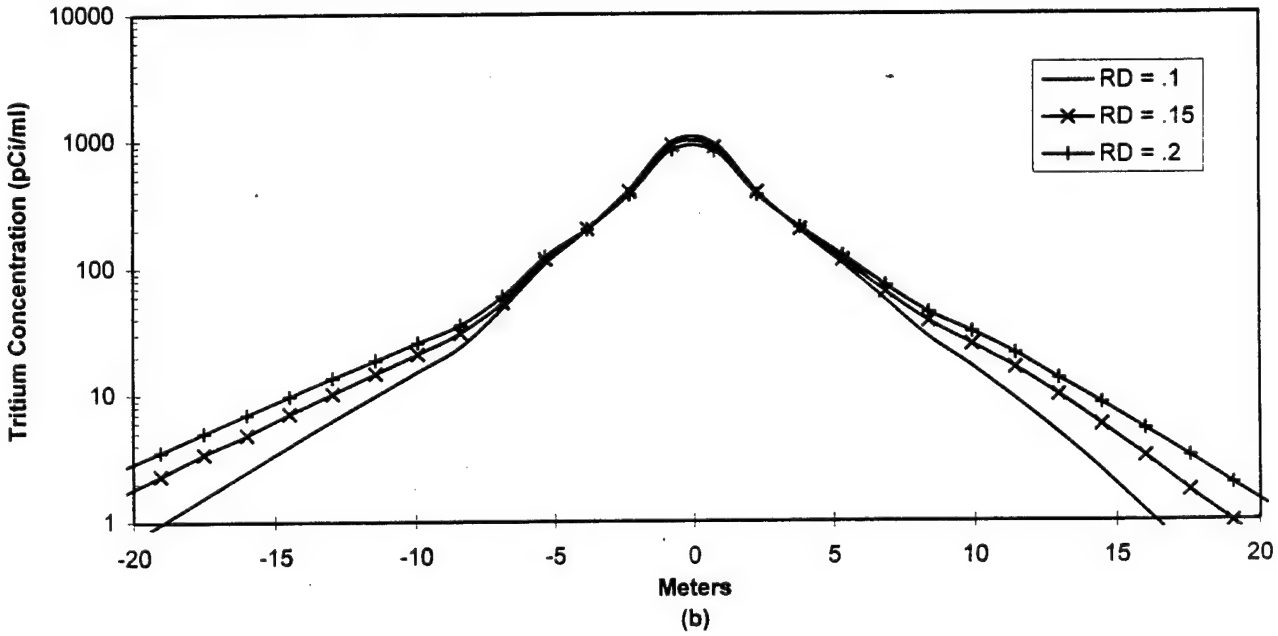

Figure 44. Effect of the Ratio of Transverse / Longitudinal Dispersivity on Simulated Transect Tritium Concentrations for (a) the Pulse Source Model and (b) the Continuous Source Model.

Sensitivity to retardation and biodegradation parameters were studied by simulating the combined organic plumes with both the pulse source and continuous source models. The type and magnitude of the plume response was almost identical for both source types.

Combined organic concentration along the center line of the plume for three retardation values ranging from 1.114 to 1.447 are shown in Figures 45(a) and (b), respectively, for pulse and continuous source models. These values are taken from Boggs *et al.* (1993) as the limits of the 95% confidence interval for the retardation factor. Because these values are relatively close to unity, there was no significant impact in the simulated plumes due to changes in this value. Results indicate that plume extent and peak concentration are almost identical.

Figures 46 and 47 show the combined organic concentration along the plume center line for first-order decay rates between 0.0068 day^{-1} and 0.0132 day^{-1}. Figures 46(a) and (b) show this concentration for the first-order decay only scenario, and Figures 47(a) and (b) show this concentration profile for the aerobic degradation with first-order decay scenario. From these figures, it is difficult to assess the impact of first-order decay but the affect of incorporating aerobic degradation is clearly illustrated by comparing Figures 47(a) and (b) to Figures 45(a) and (b).

This sensitivity analysis indicates that the most important biodegradation parameter in the Bioplume II modeling was the initial oxygen concentration. Figures 48(a) and (b) show the simulated center line organic concentration for initial dissolved oxygen rates of 0, 4, and 8 mg/L. Figures 49(c) and (d) show the corresponding percent dissolved mass remaining with the addition of the data points for 1 and 2 mg/L initial oxygen concentration. The slope of the percent mass remaining vs. initial oxygen concentration is very steep between values of 0 and 1 mg/L, after which the slope decreases. As the initial oxygen concentration is increased, the edges of the contaminant plume are immediately degraded, which is the same result observed in Figures 38 through 40 when an initial oxygen concentration of 3 mg/L was incorporated. Figure 44(a) shows the relatively low concentrations at the transverse edges of the plume. These relatively low concentrations are due to the area of low transmissivity surrounding the injection point which restricts the movement of the contaminant following injection. When the initial concentration of oxygen is increased to a level sufficient to degrade all of the contaminant present in the edges of the plume, the amount of mass degraded per increase in initial concentration decreases significantly. This occurs at approximately 2 mg/L, indicating that the most appropriate Bioplume II model for the MADE-2 experiment would incorporate a lower initial oxygen concentration than indicated during model calibration. Based on the sensitivity simulations, the initial dissolved oxygen concentration value is between 0.5 and 2.0 mg/L instead of the 3.0 mg/L estimated by using % RMS error as a criterion to calibrate the model.

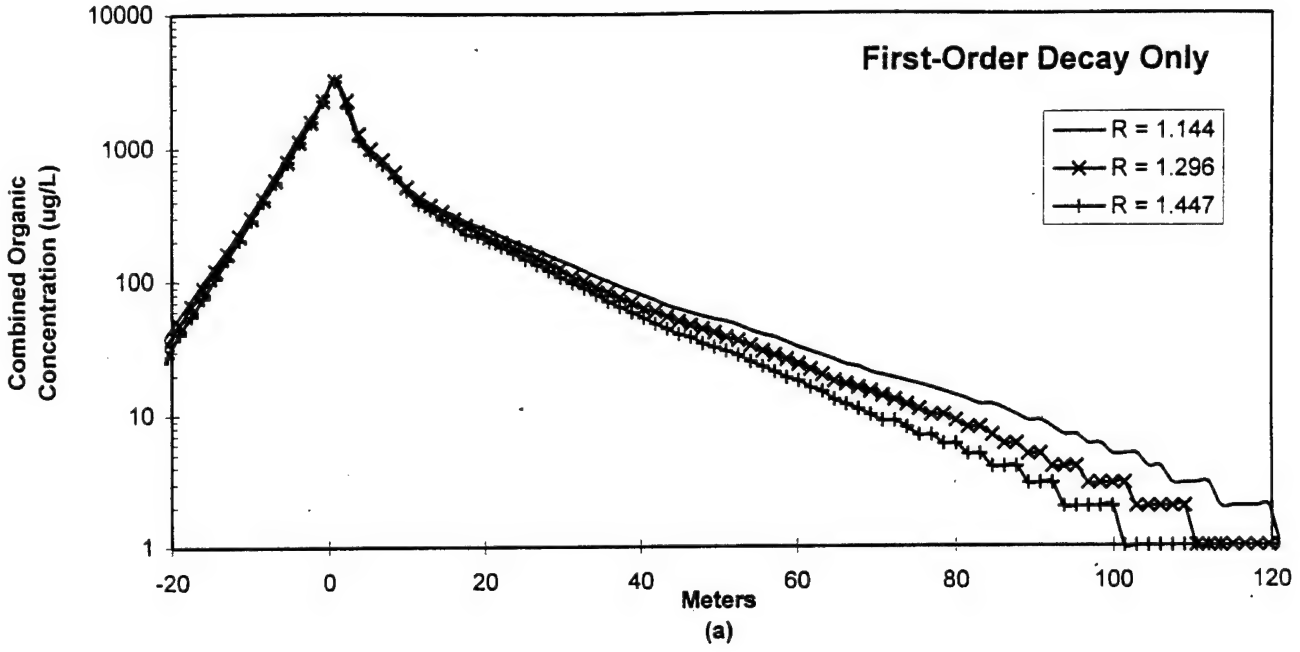

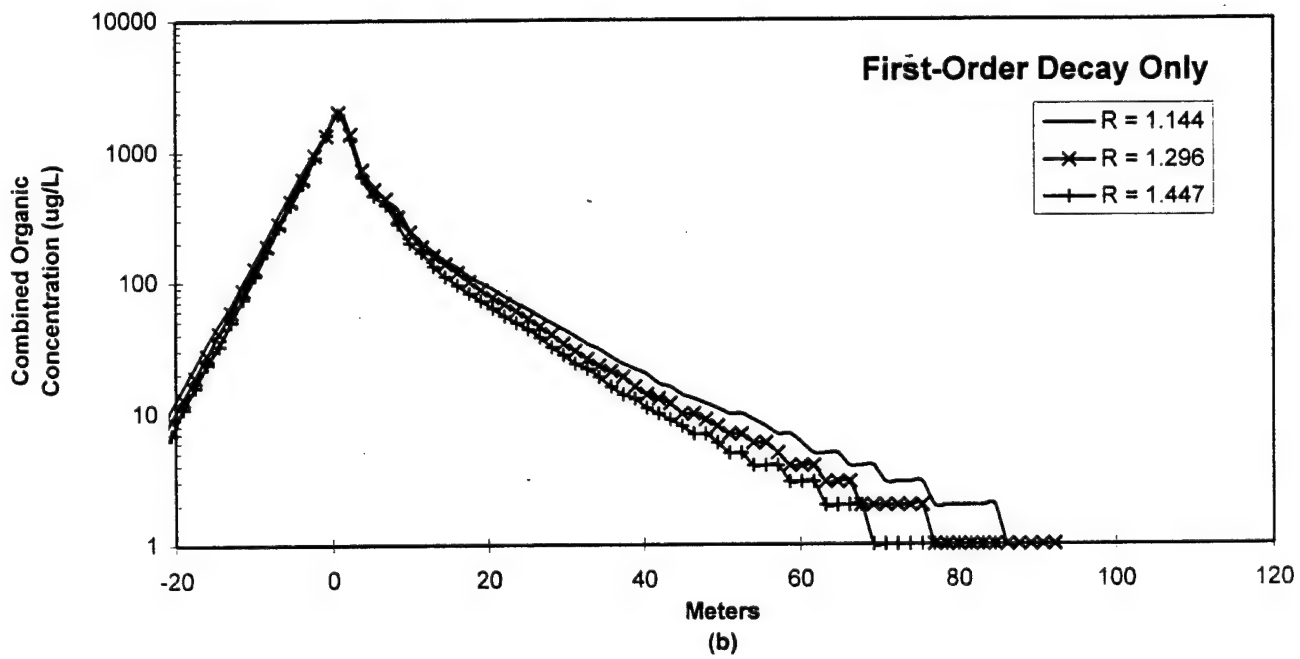

Figure 45. Effect of Retardation on the Simulated Centerline Combined Organic Concentrations for (a) the Pulse Source Model and (b) the Continuous Source Model.

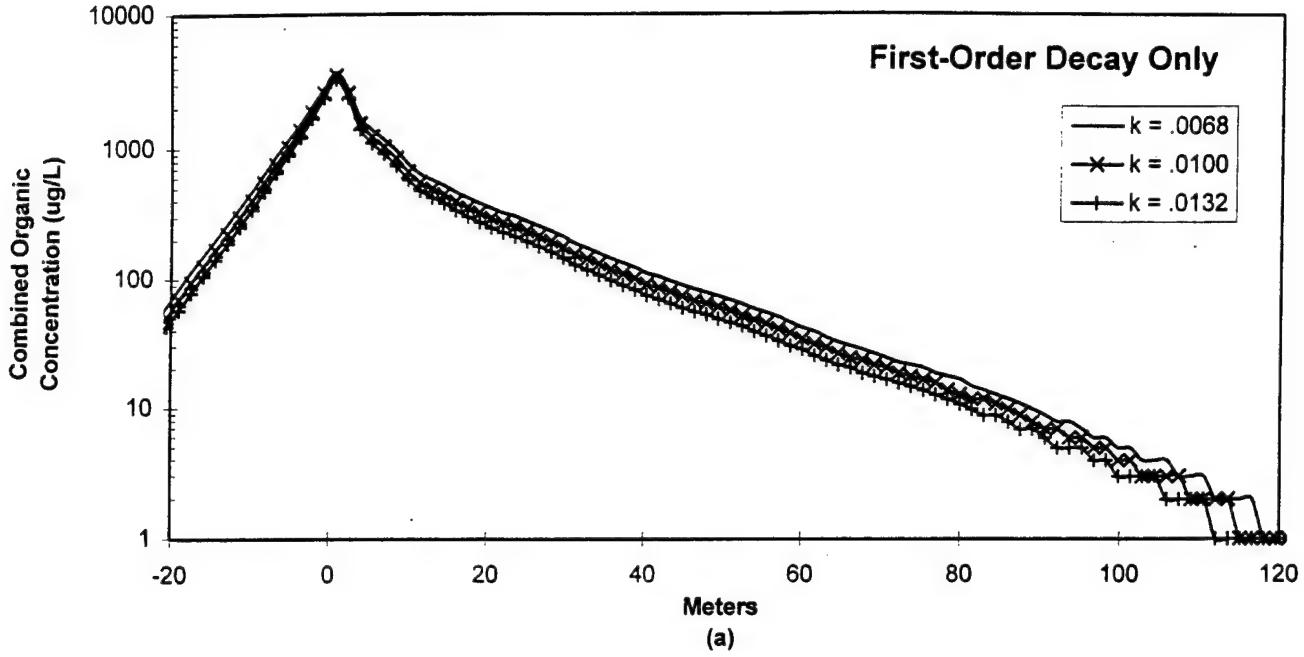

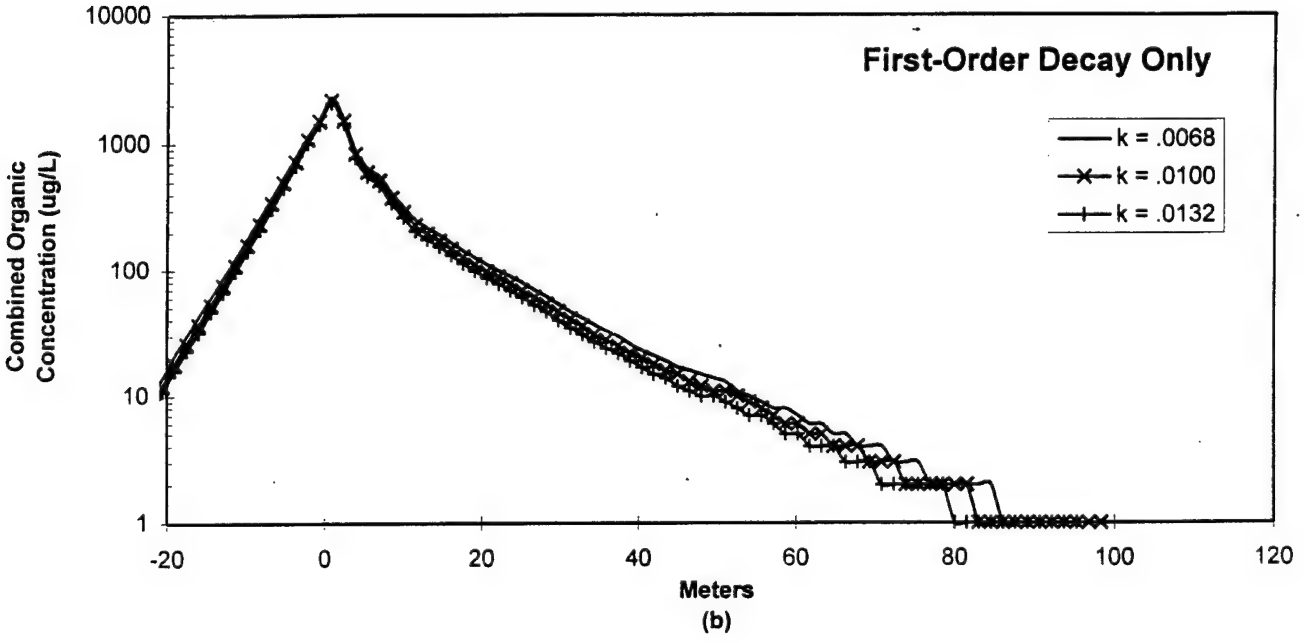

Figure 46. Effect of First-Order Decay Rate on the Simulated Centerline Combined Organic Concentrations for (a) the Pulse Source Model and (b) the Continuous Source Model.

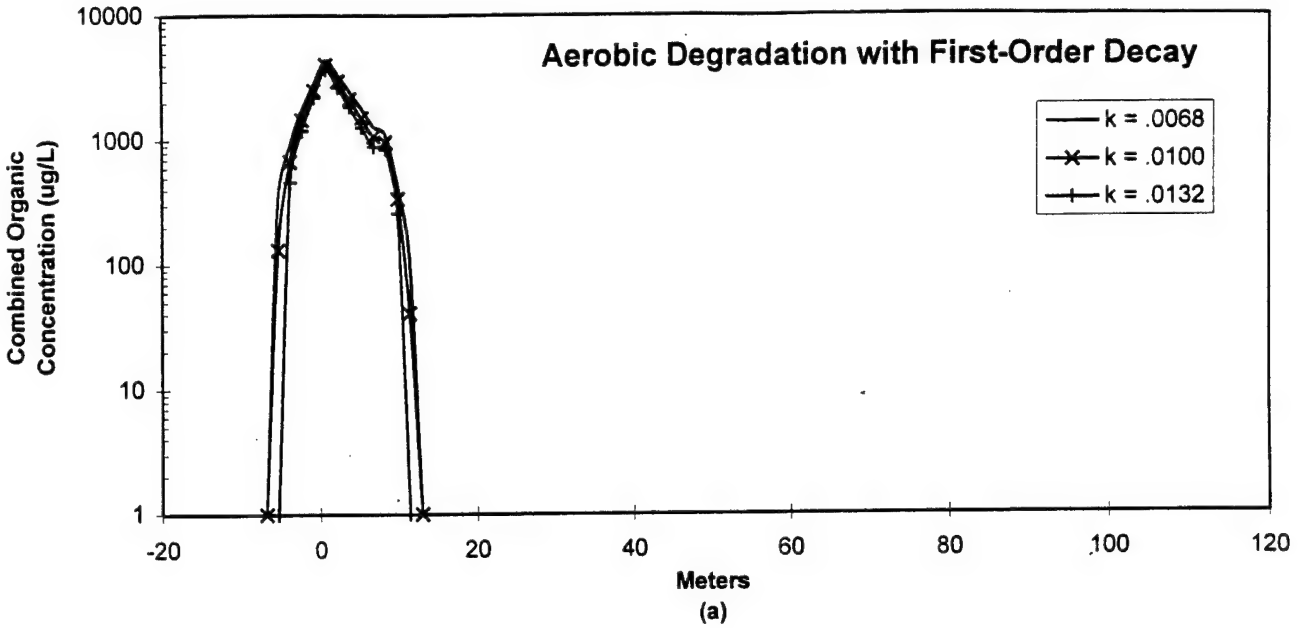

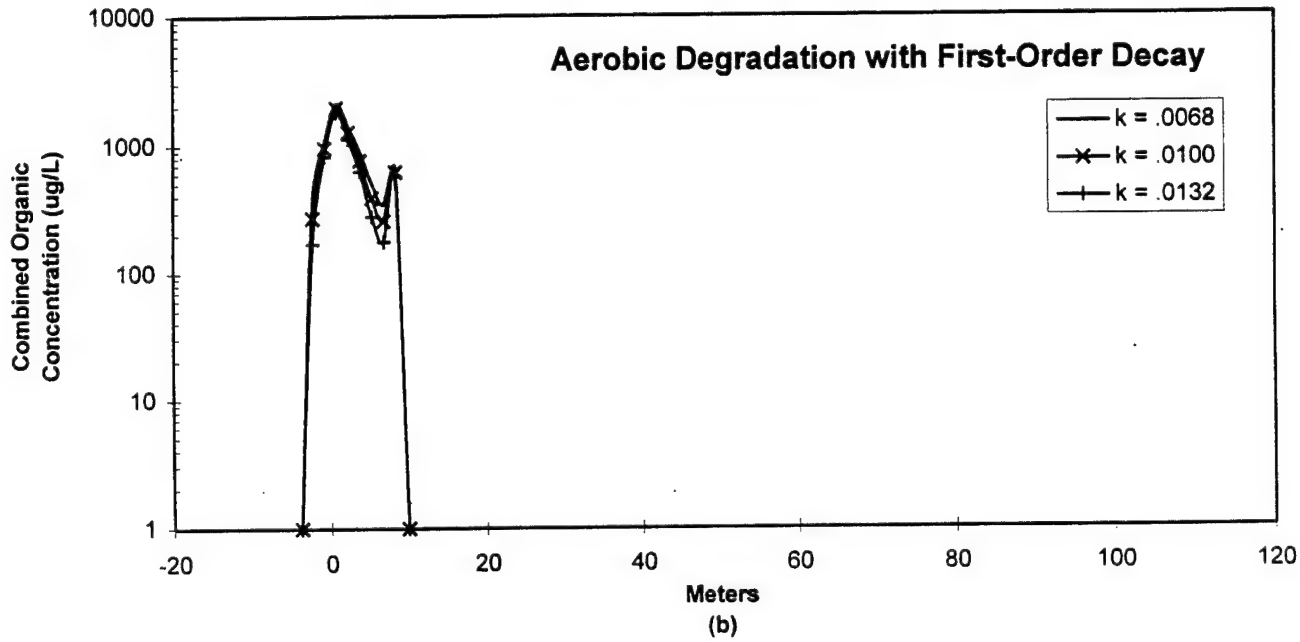

Figure 47. Effect of First-Order Decay Rate on the Simulated Centerline Combined Organic Concentrations for (a) the Pulse Source Model and (b) the Continuous Source Model.

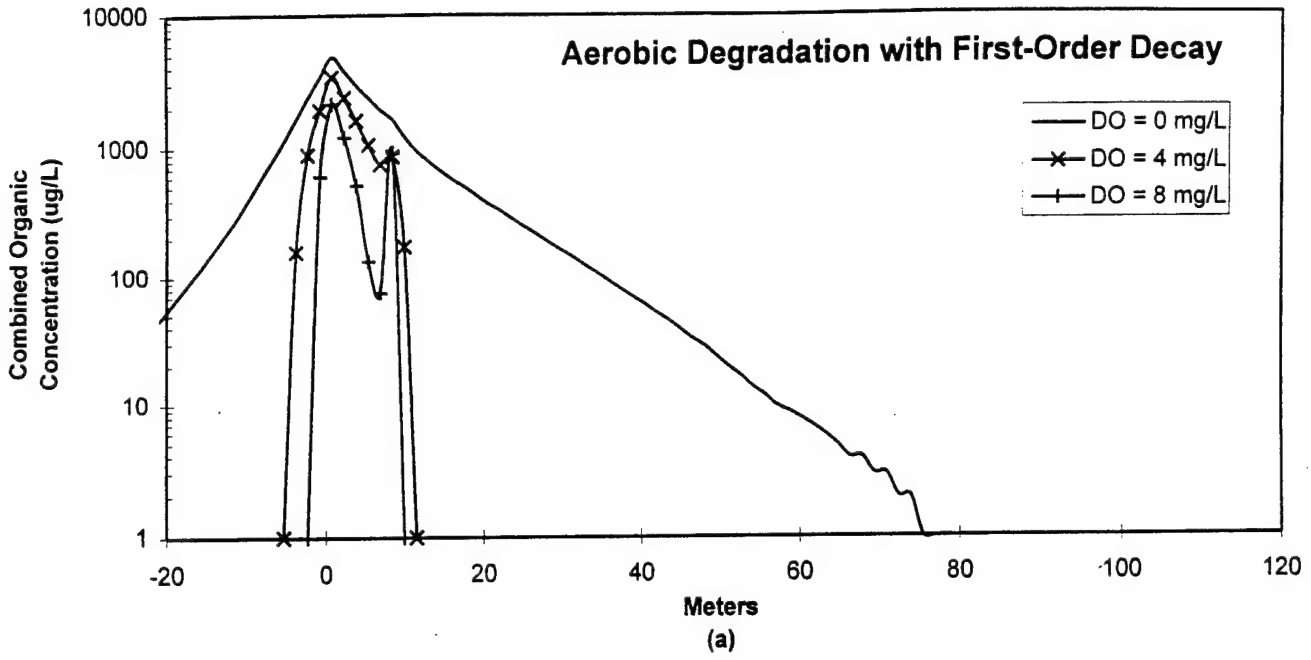

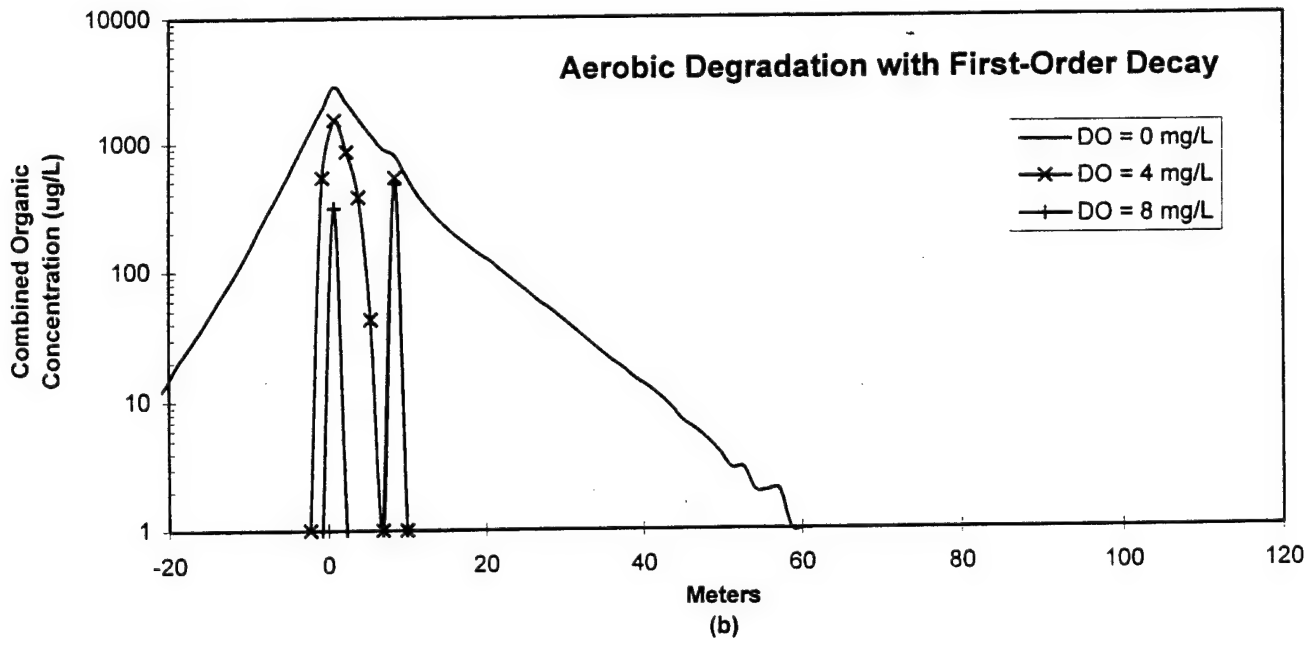

Figure 48. Effect of Initial Dissolved Oxygen on the Simulated Centerline Combined Organic Concentrations for (a) the Pulse Source Model and (b) the Continuous Source Model.

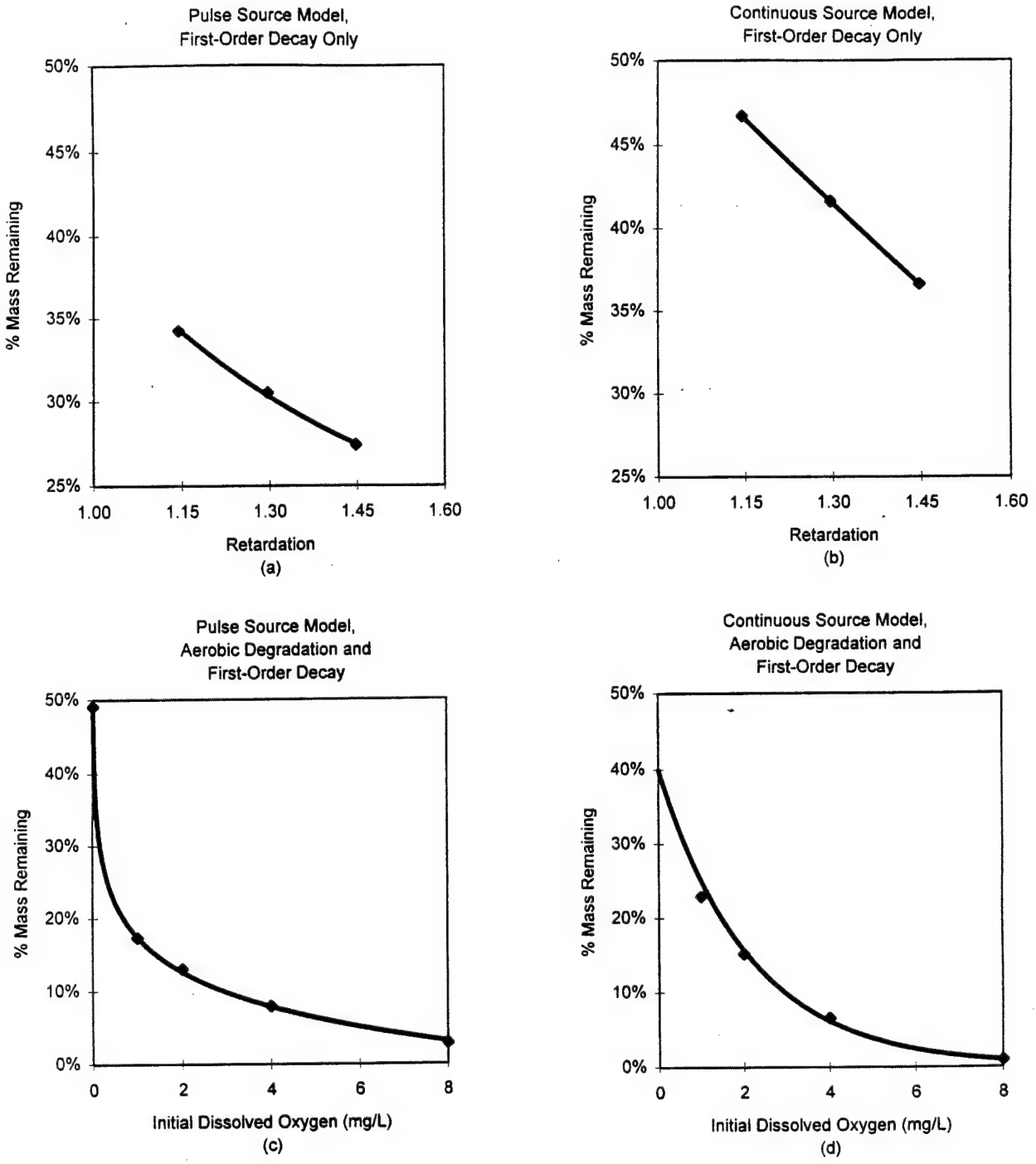

Figure 49. The Effect of Retardation on the Percent Mass Remaining for (a) the Pulse Source Model and (b) the Continuous Source Model. The Effect of Initial Dissolved Oxygen on the Percent Mass Remaining for (c) the Pulse Source Model and (d) the Continuous Source Model.

Figures 49(a) and (b) present the percent mass remaining in the dissolved-phase as a function of the retardation factor. As the retardation factor increases, more contaminant adsorbs to the aquifer media, resulting in a decrease in percent mass remaining in the groundwater. This appears to be an approximately linear relationship for the range of retardation values evaluated here.

Figure 50 illustrate the remaining percent mass as a function of the first-order decay rate. Figures 50(a) and (b) show the results for the model incorporating first-order decay only. Figures 50(a) and (b) indicate that increasing the first-order decay rate decreased the percent mass remaining by approximately 6 and 10 percent (pulse and continuous sources, respectively.) The overall percentage of mass remaining in the system is greater for the continuous source model because the first-order decay mechanism does not have as much time to degrade the mass that is injected continuously as it does for the pulse injection scenario.

Figures 50(c) and (d) show effects of varying the first-order decay rate in the model incorporating aerobic degradation and first-order decay. As expected, the percentage of mass remaining is much smaller when aerobic degradation is incorporated. An increase in the decay rate from 0.0068 day^{-1} to 0.0132 day^{-1} resulted in a decrease in the percent dissolved mass remaining of approximately 4 percent for the continuous source model, and approximately 5 percent for the pulse source model.

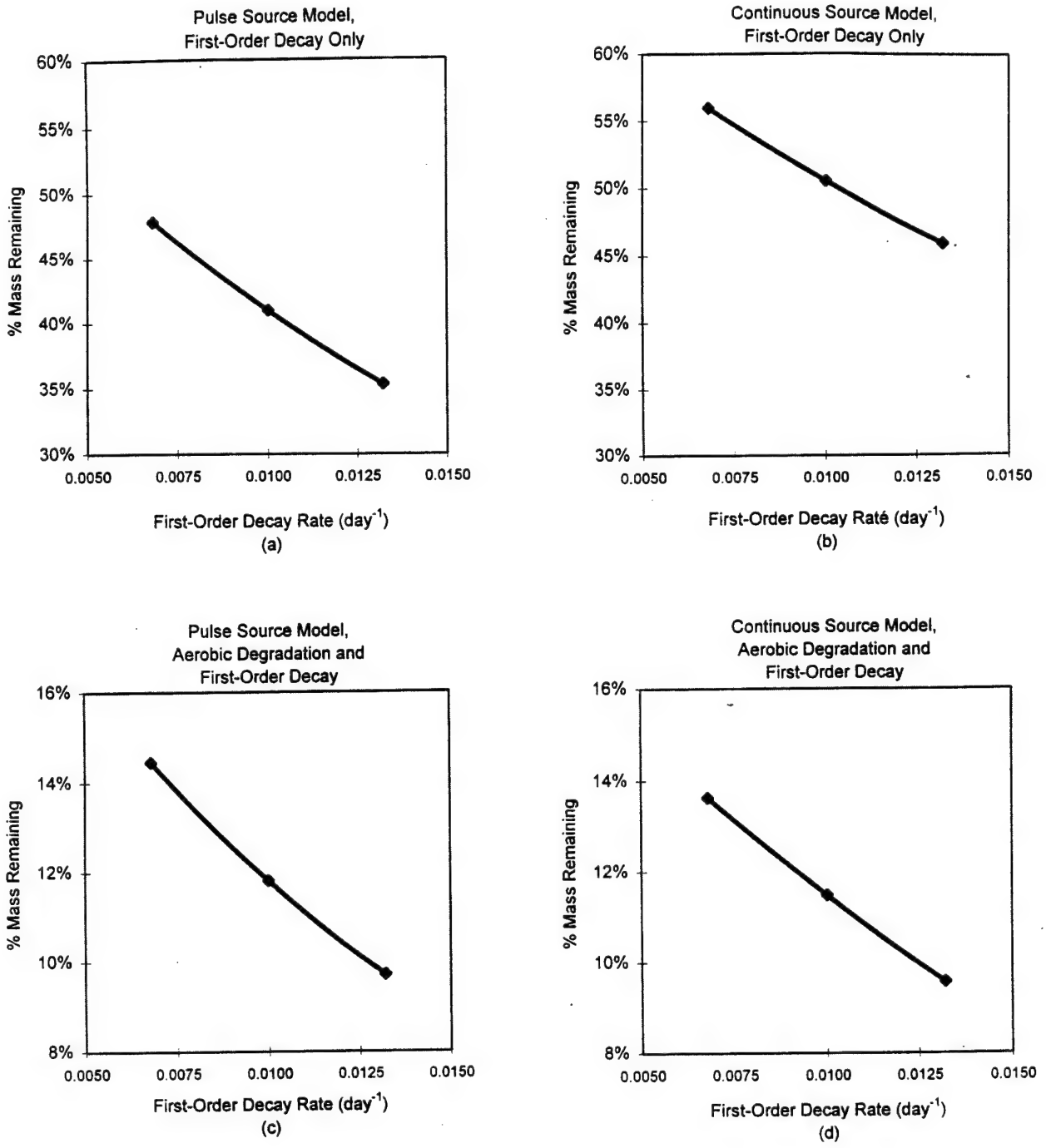

Figure 50. The Effect of First Order Decay Rate on the Percent Mass Remaining for (a) the Pulse Source Model with First-Order Decay Only; (b) the Continuous Source Model with First-Order Decay Only; (c) the Pulse Source Model with Aerobic Degradation and First-Order Decay; and (d) the Continuous Source Model with Aerobic Degradation and First-Order Decay.

SECTION VI
LIMITATIONS AND POSSIBLE SOLUTIONS

A. IDENTIFICATION OF LIMITATIONS

Several limitations were identified while modeling the MADE-2 experiment with BIOPLUME II. These limitations can be classified as field- or model-related. These limitations are discussed to provide insight for future field and modeling activities related to natural attenuation.

1. Field Aspects

All the initial data-collection objectives of the MADE-2 experiment were accomplished satisfactorily during the 16-month field monitoring period. However, since the completion of the MADE-2 experiment, developments in the area of natural attenuation characterization have provided significant insight for future experiments. Although most of these shortcomings could not be anticipated and/or avoided during the MADE-2 experiment, future experiments should consider the following points when developing a field characterization program to build a data base that can be used to validate flow-and-transport models. Following is a list of limitations.

a. Incomplete sampling/characterization of the sampling network at the last snapshot.

b. The relatively high laboratory detection limit of benzene, which resulted in the lack of edge data for the combined organic plume.

c. Incomplete characterization of anaerobic degradation processes.

d. Uncertainty as to how well the data collected by the continuous monitoring devices represent actual potentiometric levels in the aquifer.

2. Model Aspects

During the modeling process, the following limitations were realized.

a. Assumption of instantaneous aerobic biodegradation without the option to model rate-limited aerobic biodegradation kinetics.

b. Using a two-dimensional vertically integrated model to represent a three-dimensional heterogeneous flow system.

c. Inability to explicitely simulate anaerobic biodegradation.

d. Inability to use a nonuniform grid.

e. Difficulty in properly representing source injection wells.

f. Instabilities in the boundary conditions with respect to contaminant mass balance.

g. Uncertainty in implementing the transient conditions at the site.

h. Inability to implement anisotropic hydraulic conductivity on a block-by-block basis to represent the buried stream channel at the site.

B. POSSIBLE SOLUTIONS TO CURRENT LIMITATIONS

1. Field Aspects

The simplest way to avoid incomplete sampling of the plume is to decrease the time in which the last snapshot is collected to ensure that the plume is still surrounded by the sampling network. Better analytical methods could be implemented to lower the detection limit for benzene, preferably to a maximum of 5 ppb. Because approximately 45% of the injected mass was benzene, a better defined plume extent with respect to benzene would increase reliability in the model calibration.

Evaluation of the precipitation data and continuous water-level data creates some doubt about how well the continuous water-level measurements represent actual potentiometric water levels in the aquifer. The hydrographs of the continuous water-level measurements indicate very quick responses to precipitation during the winter months. The water level in the wells tends to increase promptly after a precipitation event and then to decline exponentially. This behavior is evident in many wells across the site. The release of water from storage (which lowers the potentiometric levels in an aquifer) under natural conditions typically does not result in an exponential decline in water levels. This would be expected if the aquifer was being pumped or artificially stressed in some way. However, there is no evidence of these activities during the test. Therefore, the validity of the water-level increase after winter precipitation events is suspect. The apparent sharp increase and exponential decrease in water levels may be explained by a pressurization of the water table caused by a saturated infiltration pulse moving downward that prevents the air in the unsaturated zone from escaping. Therefore, the water levels may increase in the wells for a period until the pressure is relieved as the saturated pulse redistributes in the vadose zone and allows air to escape through the partially saturated soil. More detailed monitoring of potentiometric surfaces after periods of heavy precipitation may provide enough information to reveal the cause of this phenomenon.

The lack of characterization data for anaerobic biodegradation processes limits the conclusions that can be drawn from the modeling. Without field data to substantiate the level of anaerobic biodegradation, it is difficult to interpret how well different degradation mechanisms in the model are representing field processes. The Air Force Intrinsic Remediation Protocol provides a

good foundation for developing a fundamental characterization plan to document anaerobic biodegradation processes.

2. Model Aspects

The modeling results indicate that the instantaneous aerobic biodegradation assumption in Bioplume II may be inappropriate for some systems. This issue is discussed fully in Section V. Based on the results from this study, the assumption of instantaneous aerobic biodegradation may be inappropriate for the MADE-2 experiment because of the reatively low concentrations of the organics down gradient from the injection zone. When instantaneous aerobic biodegradation was included in the model to simulate the removal of organics from the aquifer, the simulated organics plumes were much too small compared to the observed plumes. The findings from this study are confirmed by other studies that indicate first-order reactions are more appropriate under conditions similar to those during the MADE-2 experiment. One possible solution to this limitation is to use models that have the option of including rate-limited aerobic biodegradation reactions as opposed to only instantaneous aerobic biodegradation. This allows the user to incorporate field observations and information from previous work to develop a model most appropriate for the conditions at a particular site.

A big assumption in developing the flow model was that a vertically integrated two-dimensional model represents a complex three-dimensional flow system. Careful selection of the hydraulic conductivity values for each grid block may decrease the impact of this assumption. However, the ability to account for vertical heterogeneity in the hydraulic properties and the contaminant distribution by using a truely three-dimensional model may be crucial at somes sites. In applying Bioplume II, it is assumed that variations in flow and transport processes in the vertical direction are negligible and can be represented appropriately by a vertically integrated model. Hydraulic conductivity and concentration distributions documented by Stauffer *et al.* (1994) and Boggs *et al.* (1990) indicate that this assumption may not be appropriate at the MADE-2 site. At sites where there is significant heterogeneity in the hydraulic properties of the aquifer, three-dimensional models may be more appropriate. As discussed previously, the appropriateness of a vertically integrated two-dimensional model will depend on the modeling objectives.

Another limitation of Bioplume II is the inability to simulate anaerobic biodegradation explicitly. Wiedemeier *et al.* (1995) and Newell *et al.* (1995) discuss the potential significance of anaerobic processes for natural attenuation of fuel hydrocarbons. Monitoring and characterizing the degradation of the organics was only a secondary objective of the MADE-2 experiment. Therefore, the intensive chemical analyses required to quantify and document anaerobic degradation processes were not completed to the extent required to develop a reliable model of these processes during the MADE-2 experiment. As stated above, all of the degradation processes other than oxygen limited biodegradation were simulated by incorporating a first-order decay constant. At many sites, it may

be necessary to understand and quantify the importance of each anaerobic biodegradation process to build a reliable transport model to evaluate natural attenuation and remediation strategies.

In the field, the MADE-2 contaminants were injected through a series of five wells spaced approximately 1 meter apart in a line perpendicular to groundwater flow. In the Bioplume II model, the location of injection wells is related to grid selection since the injection wells must be located at the center of a cell. Because of Bioplume II's constraints, the best injection scenario was determined to be injection through 2 wells, approximately 1.5 meters apart. This necessitated a reduction in the injected volume and an increase in the injection concentration to prevent mounding. The degree of discetization (i.e., the size of the finite-difference grid blocks) can greatly influence the simulation results of a model, especially with an MOC code like Bioplume II. In some field-scale problems, it may be more practical to use a nonuniform or telescoping grid, especially if numerous wells are being simulated to evaluate remedial alternatives. If possible, this capability should be added to Bioplume II and Bioplume III.

Initially, the steady-state water table was defined by placing constant head boundaries on all sides of the Bioplume grid. During the biodegradation simulations, this caused a cumulative numerical error which eventually caused severe numerical challenges. The problem was overcome by relaxing the constraints on two of the four sides. Originally, in the node identification section of the Bioplume II input file, the water table was fixed on the two long sides of the grid. By allowing Bioplume II to determine the water table on these grid boundaries (the water table along the short sides are still fixed) the numerical error was overcome. This resulted in slightly less control over the hydraulic gradient, but allowed the model to run to completion.

In publicly available versions, Modflow and Bioplume II have the ability to implement anisotropic hydraulic conductivity for a complete layer, but neither code allows block-by-block definition of anisotropy. At the MADE site, this limitation is important because it limits the ability to represent the effects of the suspected buried stream channel. Calibration simulations indicate that incorporating a hydraulic anisotropy of 3 will significantly improve the direction of flow estimates without modification to the boundary conditions. However, the model user will have more flexibility if the models allow for block-by-block assignment of hydraulic anisotropy.

SECTION VII
CONCLUSIONS AND RECOMMENDATIONS

A. CONCLUSIONS

The appropriateness of applying the Bioplume II model at a site contaminated with fuel hydrocarbons depends largely on the (1) objectives of the modeling study, (2) the complexity of the flow system, and (3) and the type of natural attenuation processes active at the site. All these factors should be considered when developing a strategy for modeling any site, and especially when developing a modeling approach and selecting a flow-and-transport model.

The results of the flow modeling indicated that a simple vertical average of the hydraulic conductivity data from all the wells resulted in significantly smaller groundwater velocities than those observed during the MADE-2 experiment (based on non-reactive tracer movement). This result indicated that the high-permeability zones played a key role in the transport of the tracers. Calibration of the model required the implementation of a hydraulic conductivity distribution skewed toward the highest hydraulic conductivity measurements collected in the field. In addition, minor modifications to the hydraulic conductivity distribution were necessary to simulate the appropriate groundwater velocities required to calibrate the flow model according to the center-of-mass estimates for the tritium plume. In addition, assuming that groundwater flow is perpendicular to the interpolated potentiometric surfaces (either on a monthly basis or on average) produces flow directions inconsistent with observed flow directions based on tracer migration. This result indicates that the complexity of the heterogeneous flow system can not be completely represented by a vertically-averaged flow model. Therefore, implementation of a vertically-averaged flow model in a heterogeneous flow system should be undertaken only when the limitations and ramifications of the assumptions are understood. In addition, the uncertainty associated with the model assumptions should be accounted for in drawing conclusions from the model.

If the objective of the flow-and-transport modeling is to develop a tool to evaluate general movement and behavior of the contaminant plume in a flow system that is relatively uniform in the vertical direction (i.e., with respect to permeability, velocity, and contaminant and electron acceptor characteristics), then a vertically integrated model like Bioplume II may be appropriate. However, since vertical heterogeneity in the flow system can greatly affect the fate and transport of the contaminants, a fully three-dimensional model may be warranted if the data are available to quantify this heterogeneity.

Bioplume II can only model instantaneous aerobic biodegradation explicitily. Rate-limited aerobic biodegradation can not be simulated and anaerobic biodegradation and abiotic processes are

lumped into a first-order decay term. This methodology may be appropriate in situations where (1) limited field data are available to quantify individual attenuation mechanisms, and/or
(2) the objectives of the modeling do not require explicit mathematical description of each attenuation mechanism. However, as pointed out by Newell *et al.* (1995), recent research at numerous sites indicates that anaerobic processes, especially sulfate reduction and methanogenesis, may dominate the biodegradation of dissolved petroleum hydrocarbons. In those cases where the natural attenuation processes are not properly represented by a first-order decay term, the model's prediction reliability is limited. In addition, results from this study indicate that the assumption of instantaneous aerobic biodegradation is not valid for the MADE-2 study results.

The simulations completed in this study indicate that the most appropriate model (with respect to matching measured organic tracers) to simulate observed natural attenuation processes during the MADE-2 experiment used first-order decay and very limited instantaneous aerobic degradation. This finding indicates that the aerobic biodegradation is probably not instantaneous, as assumed in the Bioplume II model. Therefore, any transport model incorporating a first-order decay reaction may have been used to reproduce results comparable to those obtained with the Bioplume II model. However, if a first-order decay term does not adequately simulate the complex kinetics which govern biodegradation processes, then this simplified approach will not be adequate.

Simulations that incorporated instantaneous aerobic degradation (assuming that 3 mg/L dissolved oxygen was available for reaction with the contaminant) resulted in much smaller contaminant plumes than those observed in the field. In these scenarios, almost 1,100 ug/L of contaminant could be instantaneously degraded with the oxygen initially present in the groundwater as predicted by the Bioplume II model. This biodegradation capacity led to substantially reduced plume dimensions as compared to observed plumes. The simulations that incorporated only first-order decay resulted in plumes that were more similar to the observed plumes in areal extent (e.g., the front edge of the plume). This finding is contradictory to the accepted understanding of the relationship between aerobic and anaerobic biodegradation processes. It is generally accepted that aerobic reactions dominate "the system" until oxygen is depleted, after which anaerobic biodegradation governs the system. Observations during the MADE-2 experiment indicated that dissolved oxygen was never completely depleted (or even significantly reduced) in any monitored region of the plume. However, the Bioplume II model, which incorporated only first-order decay and is normally implemented to represent anaerobic biodegradation reactions, provided the best results when compared to the observed organic plume. Because dissolved oxygen was not depleted, conventional models would assume that anaerobic biodegradation was not active. The question, then, is why the model incorporating only a first-order reaction simulates the MADE-2 experiment results better than the model incorporating instantaneous aerobic biodegradation. Based on the findings of this study, the following explanations are presented.

1. The instantaneous aerobic biodegradation assumption is not valid for the MADE-2 experiment.

2. The heterogeneous aquifer at the MADE-2 site allows low permeability pockets of anaerobic biodegradation to exist amongst higher permeability zones of aerobic biodegradation.

The arguement against the validity of instantaneous aerobic biodegradation is fully discussed in Section V. However, it is important to reiterate one important ramification of this conclusion here. Regulations often require that concentrations at downgradient receptors be maintained below some maximum limit. In many of these cases, the focus of transport modeling is to define the frontal position and concentration of the contaminant plume. With this objective, it is especially important to appropriately define the natural attenuation processes in the model so that the outer extent of the plume is simulated properly. If a model assumes instantaneous aerobic biodegradation is occurring when it is not, the model could greatly underpredict the downgradient extent of the plume. The heterogeneous nature of the aquifer may permit low permeability pockets to retain groundwater for long enough to produce anaerobic conditions, while the higher permeability zones can be replenished with oxygen from infiltration. However, based on the information gathered during the MADE-2 experiment, it is impossible to prove or disprove this hypothesis.

B. RECOMMENDATIONS

Future work in the area of natural attenuation should include controlled field experiments that focus on quantifying all natural attenuation processes. These field experiments should also serve as the setting for developing and/or verifying field methodologies to characterize natural attenuation processes. The Air Force has developed a protocol for demonstrating intrinsic bioremediation (AFCEE, 1995) that is largely based on observation from sites that had uncontrolled contaminant releases. Controlled experiments can (1) help to verify and improve the AF protocol, (2) help fine-tune field methodologies for characterizing natural attenuation processes, and (3) serve as an environment to develop complete data bases to verify models.

This modeling study has provided insight into both the field and the modeling aspects of the MADE-2 experiment. Future tests should focus on characterizing anaerobic degradation processes as well as aerobic biodegradation. In addition, future natural attenuation studies at the MADE-2 site should attempt to describe spatial heterogeneity in the aerobic and anaerobic biodegradation processes. In other words, the study should decifer what types of processes are active in the low and

high permeability zones (and if they are different) so a more accurate conceptual model can be developed at heterogeneous sites.

Several limitations discovered in applying Bioplume II at the MADE-2 site should be addressed to provide a more comprehensive tool for other sites. Although it is not always necessary, the ability to simulate natural attenuation processes in three dimensions should be developed. A transport model for simulating natural attenuation processes should have the option of incorporating rate-limited aerobic biodegradation and anaerobic biodegradation reactions.

SECTION VIII
REFERENCES

Adams, E.E., and L.W. Gelhar, 1992. Field study of dispersion in a heterogeneous aquifer. 2. Spatial moments analysis. *Water Resources Research,* 28(12), 3293-3307.

Air Force Center for Environmental Excellence, 1995. Technical Protocol for Implementing Intrinsic Remediation with Long-Term Monitoring for Natural Attenuation of Fuel Contamination Dissolved in Groundwater. Air Force Center for Environmental Excellence, Technology Transfer Division, Brooks AFB, San Antonio, Texas.

Air Force Center for Environmental Excellence, 1994. Review of State Regulations Regarding Natural Attenuation as a Remedial Option. Technology Transfer Division, Brooks AFB, San Antonio, Texas.

Alder-Schaller, S. E., 1989. Comparison of Analytical and Numerical Biodegradation Models with Application to Aquifer Remediation. Masters Thesis, Rice University. Houston, Texas.

Anderson, M.P., and W.W. Woessner, 1992. Applied Groundwater Modeling. Academic Press, Inc. 381 p. San Diego, California 92101

Barker, G.W., K.T. Raterman, J.B. Fisher, J.M. Corgan, G.L. Trent, D.R. Brown, and K.L. Sublette, 1995. Assessment of Natural Hydrocarbon Bioremediation at Two Gas Condensate Production Sites. In R. E. Hinchee, J. T. Wilson, & D. C. Downey (Ed.), *Intrinsic Bioremediation* (pp. 181-188). Columbus, Ohio: Battelle Press.

Barker, J.F., G.C. Patrick, and D. Major, 1987. Natural Attenuation of Hydrocarbons in a Shallow Sand Aquifer. *Ground Water Monitoring Review*, 7(4), 64-71.

Bedient, P.B., and H.S. Rifai, 1992. Ground Water Contaminant Modeling for Bioremediation: A Review. *Journal of Hazardous Materials*, **32**(2-3), 225-243.

Boggs, J.M., L.M. Beard, S.E. Long, M.P. McGee, W.G. MacIntyre, C.P. Antworth, and T.B. Stauffer, 1993a. Database for the Second Macrodispersion Experiment (MADE-2) (TR-102072). Electric Power Research Institute. Palo Alto, California 94304

Boggs, J.M., L.M. Beard, W.R. Waldrop, T.B. Stauffer, W.G. MacIntyre, and C.P. Antworth, 1993b. Transport of Tritium and Four Organic Compounds During a Natural Gradient Experiment (MADE-2) (TR-101998). Electric Power Research Institute. Palo Alto, California 94304

Boggs, J.M., S.C. Young, L.M. Beard, L.W. Gelhard, K.R. Rehfeldt, and E.E. Adams, 1992. Field study of a dispersion in a heterogeneous aquifer. 1. Overview and Site Description. *Water Resources Research,* **28**(12), 3281-3291.

Boggs, J.M., and E.E. Adams, 1992. Field study of dispersion in a heterogeneous aquifer. 4. Investigation of Adsorption and Sampling Bias. *Water Resources Research*, 28(12), 3325-3336.

Boggs, J.M., S.C. Young, D.J. Benton, Y.C. Chung, 1990. Hydrogeologic Characterization of the MADE Site. Electric Power Research Institute (EPRI) Report EN-2485-5.

Borden, R. C., and P.B. Bedient, 1987. In Situ Measurement of Adsorption and Biotransformation at a hazardous Waste Site. *Water Resources Bulletin*, **23**(4), 629-636.

Borden, R.C., 1986. Influence of Adsorption and Oxygen Limited Biodegradation on the Transport and Fate of a Creosote Plume: Field Methods and Simulation Techniques. Doctoral Dissertation, Rice University.

Borden, R.C., and P.B. Bedient, 1986. Transport of Dissolved-Phase Hydrocarbons Influenced by Oxygen-Limited Biodegradation, 1. Theoretical Development. *Water Resources Research,* **22**(13), 1973-1982.

Borden, R.C., P.B. Bedient, M.D. Lee, C.H. Ward, and J.T. Wilson, 1986. Transport of Dissolved Hydrocarbons Influenced by Oxygen-Limited Biodegradation, 2. Field Application. *Water Resources Research*, **22**(1983-1990).

Borden, R.C., M.D. Lee, M. Thomas, P.B. Bedient, and C.H. Ward, 1989. In Situ Measurement and Numerical Simulation of Oxygen Limited Biotransformation. *Ground Water Monitoring Review*, **9**(1), 83-91.

Brown, R.A., P.M. Hicks, R.J. Hicks, and M.C. Leahy, 1995. Postremediation Bioremediation. In R.E. Hinchee, J.T. Wilson, and D.C. Downey (Ed.), *Intrinsic Bioremediation* (pp. 77-84). Columbus, Ohio: Battelle Press.

Burgess, K. S. 1993. Flow and Transport Modeling of a Heterogeneous Field Site Contaminated with Dense Chlorinated Solvent Waste. Masters, Rice University.

Butler, W.A., and C.L. Bartlett, 1995. Taking Advantage of Natural Biodegradation. In R.E. Hinchee, J.T. Wilson, and D.C. Downey (Ed.), *Intrinsic Bioremediation* (pp. 59-65). Columbus, Ohio: Battelle Press.

Caldwell, K.R., D.L. Tarbox, K.D. Barr, S. Fiorenza, L.E. Dunlap, and S.B. Thomas, 1992. Assessment of Natural Bioremediation as an Alternative to Traditional Active Remediation at Selected Amoco Oil Company Sites, Florida. In: *Proceedings of the 1992 Petroleum Hydrocarbons and Organic Chemicals in Ground Water: Prevention, Detection, and Restoration*, Houston, Texas, (pp. 509-524). Water Well Journal Publishing Co.

Chiang, C., P. Petkovsky, M. Beltz, S. Rouse, T. Boyd, C. Newell, and T. McHugh, 1992. An Enhanced Aerobic Bioremediation System at a Central Production Facility - System Design and Data Analysis. In: *Proceedings of the NGWA Conference on Petroleum Hydrocarbons*, Houston, Texas.

Chiang, C.Y., J.P. Salanitro, E.Y. Chai, J.D. Colthart, and C.L. Klein, 1989. Aerobic Biodegradation of Benzene, Toluene, and Xylene in a Sandy Aquifer - Data Analysis and Computer Modeling. *Ground Water*, **27**(6), 823-834.

Davis, J.W., N.J. Klier, and C.L. Carpenter, 1994. Natural Biological Attenuation of Benzene in Ground Water Beneath a Manufacturing Facility. *Ground Water*, **32**(2), 215-226.

Eganhouse, R.P., M.J. Baedecker, and I.M. Cozzarelli, 1994. Biogeochemical Processes in an Aquifer Contaminated by Crude Oil: An Overview of Studies at the Bemidji, Minnesota, Research Site. *Proceedings of the Symposium on Intrinsic Bioremediation of Ground Water*, Denver, CO, EPA/540/R-94/515 (pp. 111-119). U.S. Environmental Protection Agency.

Evans, K. L. (1994). A Transient Methodology for Evaluating Risk Reduction Associated with Ground Water Remediation at Leaking Underground Storage Tank (LUST) Sites. Masters Thesis, Rice University.

Florida Department of Environmental Regulation, 1990. No Further Action and Monitoring Only Guidelines for Petroleum-Contaminated Sites (FDER-10/90).

Ginn, J.S., R.C. Sims, and I.P. Murarka, 1995. In Situ Bioremediation (Natural Attenuation) at a Gas Plant Waste Site. In R. E. Hinchee, J. T. Wilson, & D. C. Downey (Ed.), *Intrinsic Bioremediation* (pp. 153-162). Columbus, Ohio: Battelle Press.

Godsy, E.M., 1994. Microbiological and Geochemical Degradation Processes. *Proceedings of the Symposium on Intrinsic Bioremediation of Ground Water*, Denver, Colorado, EPA/540/R-94/515 (pp. 35-40). U.S. Environmental Protection Agency

Illangasekare, T. H., Szlag, D. C., & Wilson, J. T. (1994). The Role of Intrinsic Bioremediation in Closure of Sites After Cleanup Through In Situ Bioremediation: The Role of Mathematical Models. Proceedings of the Symposium on Intrinsic Bioremediation of Ground Water in Denver, Colorado, EPA/540/R-94/515. (pp. 53-59). U.S. Environmental Protection Agency.

King, M.W.G., J.F. Barker, and K.A. Hamilton, 1995. Natural Attenuation of Coal Tar Organics in Groundwater. In R.E. Hinchee, J.T. Wilson, and D.C. Downey (Ed.), *Intrinsic Bioremediation* (pp. 171-179). Columbus, Ohio: Battelle Press.

Klecka, G.M., J.W. Davis, D.R. Gray, and S.S. Madsen, 1990. Natural Bioremediation of Organic Contaminants in Ground Water: Cliffs-Dow Superfund Site. *Ground Water*, **28**(4), 534-543.

Konikow, L.F., and J.D. Bredehoeft, 1978. Computer Model of Two-Dimensional Solute Transport and Dispersion in Ground Water Automated Data Processing and Computations Techniques of the U.S. Geological Society.

Long, H.P., 1992. Modeling Natural Biodegradation: Theory and Field Application. Masters Thesis, Rice University.

MacDonald, M.G., and Harbaugh, A.W., 1988. A Modular Three-Dimensional Finite-Difference GroundWater Flow Model: U.S. Geological Survey Techniques of Water Resources Investigations, Book 6, Chapter A1, 14 ch.

MacIntyre, W.G., M. Boggs, C.P. Antworth, and T.B. Stauffer, 1993. Degradation kinetics of aromatic organic solutes introduced into a heterogeneous aquifer. *Water Resources Research*, 29(12), 4045-4051.

Maresco, V.S., A. Kearns, T.R. Byrnes, D.J. Bender, and M.A. Troy, 1995. Evidence for Natural Attenuation of BTEX After Termination of a Groundwater Pump-and-Treat System - A Case Study. *Proceedings of the 1995 Petroleum Hydrocarbons and Organic Chemicals in Ground Water: Prevention, Detection, and Remediation Conference and Exposition*, Houston, Texas (pp. 509-525). Water Well Journal Publishing Co.

McAllister, P.M., and C.Y.Chiang, 1994. A Practical Approach to Evaluating Natural Attenuation of Contaminants in Ground Water. *Ground Water Monitoring Review*, **14**(1), 161-173.

McAllister, P.M., C.Y. Chiang, J.P. Salanitro, I.J. Dortch, and P. Williams, 1995. Enhanced Aerobic Bioremediation of Residual Hydrocarbon Sources. In R.E. Hinchee, J.T. Wilson, and D.C. Downey (Ed.), *Intrinsic Bioremediation* (pp. 67-75). Columbus, Ohio: Battelle Press.

Mackay D.M., and J.A. Cherry, 1989. Groundwater contamination: Pump-and-treat remediation. Environ. Sci. Technol., Vol. 23, No. 6.

Miller, K.M., 1989. Application of Bioplume II to Simulate Biodegradation, a Study of an Aviation Fuel Spill from a Leaking Underground Storage Tank in Traverse City, Michigan. Masters Thesis, Rice University.

Nelson, C., 1994. In Situ Bioremediation at the Seventh Avenue Site in Denver: Remediation of Soils and Ground Water. *Proceedings of the Symposium on Intrinsic Bioremediation of Ground Water,* Denver, CO, EPA/540/R-94/515 (pp. 47-48). U.S. Environmental Protection Agency.

Newell, C.J., J.A. Winters, H.S. Rifai, R.N. Miller, J. Gonzales, and T.H. Wiedemeier, 1995. Modeling Intrinsic Remediation with Multiple Electron Acceptors: Results from Seven Sites. *Proceedings of the 1995 Petroleum Hydrocarbons and Organic Chemicals in Ground Water: Prevention, Detection, and Remediation Conference and Exposition*, Houston, Texas, (pp. 33-47). Water Well Journal Publishing Co.

Novick, N.J., R.E. Payne, J.G. Hill, and T.L. Douthit, 1995. A Tiered Approach to Demonstrate Intrinsic Bioremediation of Petroleum Hydrocarbons in Groundwater. *Proceedings of the 1995 Petroleum Hydrocarbons and Organic Chemicals in Ground Water: Prevention, Detection, and Remediation Conference and Exposition*, Houston, Texas (pp. 493-508). Water Well Journal Publishing Co.

Odencrantz, J.E., A.J. Valocchi, B. E. Rittmann, 1990. Modeling Two-Dimensional Solute Transport with Different Biodegradation Kinetics. *Proceedings of the 1990 Conference on Petroleum Hydrocarbons and Organic Chemicals in Ground Water: Prevention, Detection, and Restoration in Houston, Texas*, (pp. 355-368). Water Well Journal Publishing Co.

Pollock, D.W., 1989. Documentation of Computer Programs to Compute and Display Pathlines Using the Results From the U.S. Geological Survey Modular Three-Dimensional Finite-Difference Ground-Water Flow Model, USGS Open File Report 89-391, 188 pp.

Rehfeldt, K.R., J.M. Boggs, and L.W. Gelhar, 1992. Field study of dispersion in a heterogeneous aquifer. 3. Geostatistical analysis of hydraulic conductivity. *Water Resources Research,* 28(12), 3309-3324.

Rifai, H.S., and P.B. Bedient, 1990. Comparison of Biodegradation Kinetics with and Instantaneous Reaction Model for Groundwater. *Water Resources Research*, **26**(4), 637-645.

Rifai, H.S., 1989. Numerical Techniques for Modeling In Situ Biorestoration and Biodegradation of Organic Contaminants in Ground Water. Doctoral Dissertation, Rice University.

Rifai, H.S., P.B. Bedient, J.T. Wilson, K.M. Miller, and J.M. Armstrong, 1988. Biodegradation Modeling at an Aviation Fuel Spill Site, *ASCE Journal of Environmental Engineering*, 114, 5, 1007-1029, 1988.

Rifai, H.S., and P.B. Bedient, 1987. Bioplume II - Two Dimensional Modeling for Hydrocarbon Biodegradation and In Situ Restoration. *Proceedings of the 1987 Conference on Petroleum Hydrocarbons and Organic Chemicals in Ground Water: Prevention, Detection, and Restoration*, Houston, Texas (pp. 431-450). Water Well Journal Publishing Co.

Stauffer, T.B., C.P. Antworth, R.G. Young, W.G. MacIntyre, J.M. Boggs, L.M. Beard, 1994. Degradation of Aromatic Hydrocarbons in an Aquifer During a Field Experiment Demonstrating the Feasibility of Remediation by Natural Attenuation, AL/EQ-TR-1993-0007,AL/EQ, 139 Barnes Drive, Tyndall AFB, FL.

Tabak, H. S., S. Desai, and R. Govind, 1990. Determination of Biodegradation Kinetics of RCRA Compounds Using Respirometry for Structure-Activity Relationships (EPA/600/D-90/136). United States Environmental Protection Agency.

Toze, S. G., Power, T. R., & Davis, G. B., 1995. Relating BTEX Degradation to the Biogeochemistry of an Anaerobic Aquifer. In R. E. Hinchee, J. T. Wilson, & D. C. Downey (Ed.), Intrinsic Bioremediation (pp. 117-125). Columbus, Ohio: Battelle Press.

Troy, M. A., Baker, K. H., & Herson, D. S., 1995. Evaluating Natural Attenuation of Petroleum Hydrocarbon Spills. In R. E. Hinchee, J. T. Wilson, & D. C. Downey (Ed.), Intrinsic Bioremediation (pp. 85-90). Columbus, Ohio: Battelle Press.

Walker, M. E., & Weers, L. C., 1994. The Role of Intrinsic Bioremediation in Closure of Sites After Cleanup Through In Situ Bioremediation: The Regulator's Perspective. Proceedings of the Symposium on Intrinsic Bioremediation of Ground Water in Denver, Colorado, EPA/540/R-94/515. (pp. 49-50). United States Environmental Protection Agency.

Ward, C. H., Thomas, J. M., Fiorenza, S., Rifai, H. S., Bedient, R. B., Wilson, J. T., & Raymond, R. L. 1989. In Situ Bioremediation of Subsurface Material and Ground Water Contaminated with Aviation Fuel: Traverse City, Michigan. Proceedings of the 1989 A&Wma/EPA International Symposium in Cincinnati, Ohio, (pp. 83-96).

Weidemeier, T.H., R.N. Miller, J.T. Wilson, D.H. Kampbell, 1995. Significance of Anaerobic Processes for the Intrinsic Bioremediation of Fuel Hydrocarbons. In: *Proceedings of the NGWA Conference on Petroleum Hydrocarbons*, Houston, Texas.

Wiedemeier, T. H., Guest, P. R., Henry, R. L., & Keith, C. B. 1993. The Use of Bioplume II to Support Regulatory Negotiations at a Fuel Spill Site Near Denver Colorado. Proceedings of the 1993 Petroleum Hydrocarbons and Organic Chemicals in Ground Water: Prevention, Detection, and Restoration in Houston, Texas, (pp. 445-459). Water Well Journal Publishing Co.

Wiedemeier, T.H., J.T. Wilson, R.N. Miller, and D.H. Kampbell, 1994. United States Air Force Guidelines for Successfully Supporting Intrinsic Remediation With an Example from Hill Air Force Base. In: *Proceedings of the NGWA Conference on Petroleum Hydrocarbons*, Houston, Texas.

Weidemeier, T.H., P.R. Guest, R.L. Henry, and C.B. Keith, 1992. The Use of BIOPLUME II to Support Regulatory Negotiations at a Fuel Spill Site Near Denver, Colorado. In: *Proceedings of the NGWA Conference on Petroleum Hydrocarbons*, Houston, Texas.

Wilson, J.L., and W.R. Linderfelt, 1994. Field Tracer Experiment Design Problems at the Borden Site. In: *Proceedings from the Second Tracer Workshop*, University of Texas at Austin.

Wilson, B. H., Wilson, J. T., Campbell, D. H., Bledsoe, B. E., & Armstrong, J. M., 1994. Traverse City: Geochemistry and Intrinsic Bioremediation of BTX Compounds. Proceedings of the Symposium on Intrinsic Bioremediation of Ground Water in Denver, Colorado, EPA/540/R-94/515. (pp. 94-102). United States Environmental Protection Agency.

Wilson, J. T., Pfeffer, F. M., Weaver, J. W., Kampbell, D. H., Wiedemeier, T. H., Hansen, J. A., & Miller, R. N., 1994. Intrinsic Bioremediation of JP-4 Jet Fuel. Proceedings of the Symposium on Intrinsic Bioremediation of Ground Water in Denver, Colorado, EPA/540/R-94/515. (pp. 60-72). United States Environmental Protection Agency.

Wilson, J. T., Sewell, G., Caron, D., Doyle, G., & Miller, R. N., 1995. Intrinsic Bioremediation of Jet Fuel Contamination at George Air Force Base. In R. E. Hinchee, J. T. Wilson, & D. C. Downey (Ed.), Intrinsic Bioremediation (pp. 91-100). Columbus, Ohio: Battelle Press.

Wisconsin Department of Natural Resources Emergency and Remedial Response Section, 1993. RRP Issues Guidelines on Natural Biodegradation. *Release News*, **3**(1)

Young, S.C., M.J. Neton, J.Dorsch, and C. Olson, 1994. Depositional Processess in Alluvial Environments and Their Impact on the Hydraulic Structure of Aquifers: Volume 1 - Sedimentology and Depositional Processes. R.S. Kerr Environmental Research Laboratory, Ada, Oklahoma.

This page intentionally left blank

APPENDIX A
MONTHLY POTENTIOMETRIC MAPS

Figures A-1 through A-17 show the potentiometric contours generated from water-level measurements collected in the shallow A-wells during the MADE-2 experiment. Figures A-18 through A-36 show the potentiometric contours generated from water-level measurements collected in the deep B-wells during the MADE-2 experiment.

Figures A-1 and A-18 show the A and B wells that were sampled on June 19, 1990. On this date, several wells to the east of the site were sampled. This permits an interpretation of the potentiometric surface from a bigger perspective than is possible in the following months (Figures A-2 through A-17 and A-19 through A-34).

All the maps were generated by using a standard kriging algorithm available in SURFER™ software. In addition, the algorithm was allowed to estimate and implement a linear drift that is inherent in the potentiometric surface. In general, incorporating a linear drift in the scheme to interpolate potentiometric surfaces will not significantly change the interpolated map at locations where data are available (ie., the interpolated data reproduce the observed data). However, implementing a linear drift allows the algorithm to incorporate the underlying slope of the potentiometric surface, which reduces the tendency for interpolation schemes to predict "bulls-eye" effects in areas where data are sparse.

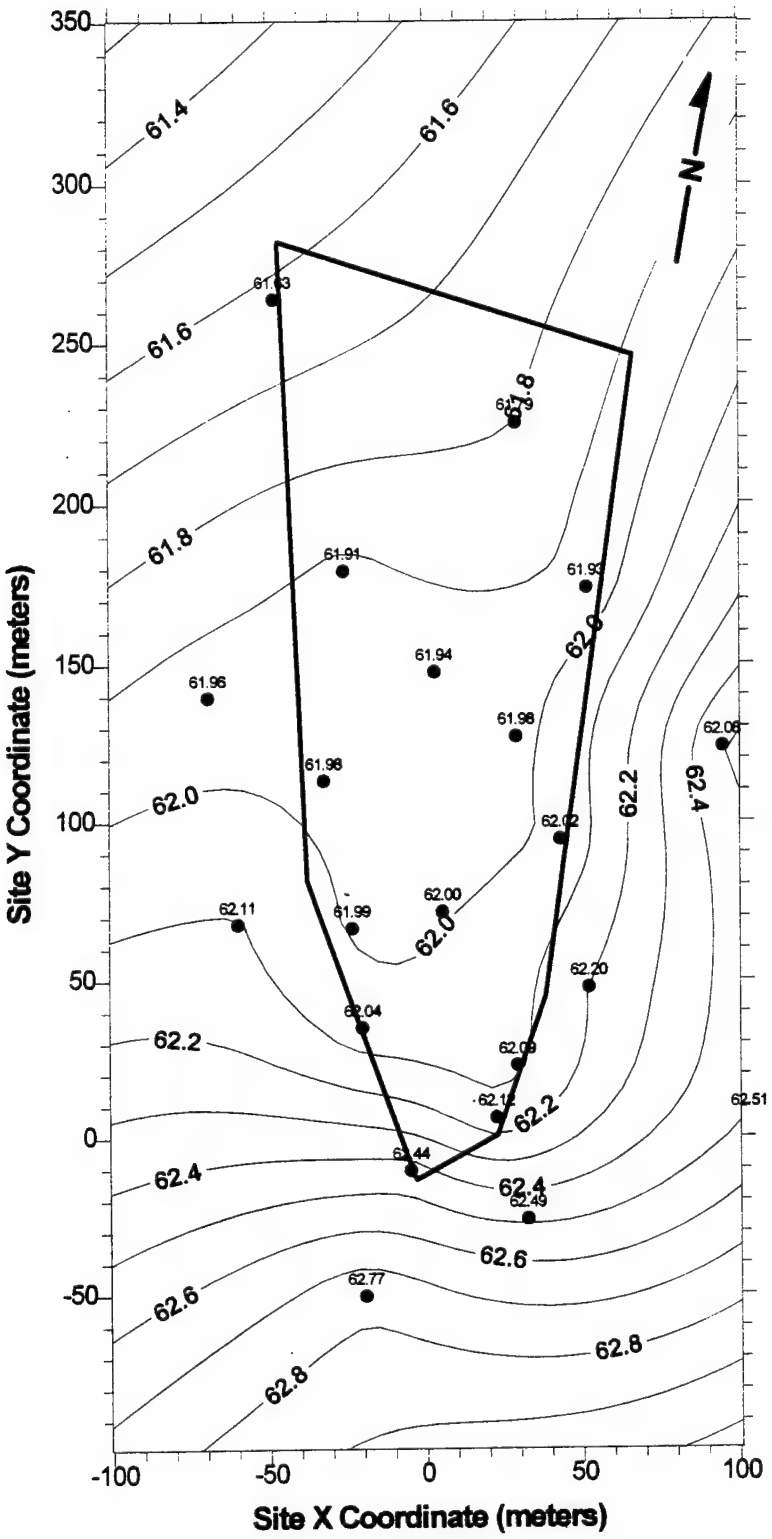

Figure A- 1. Potentiometric Surface Based on Water Levels Measured in A Wells on 06/19/90.

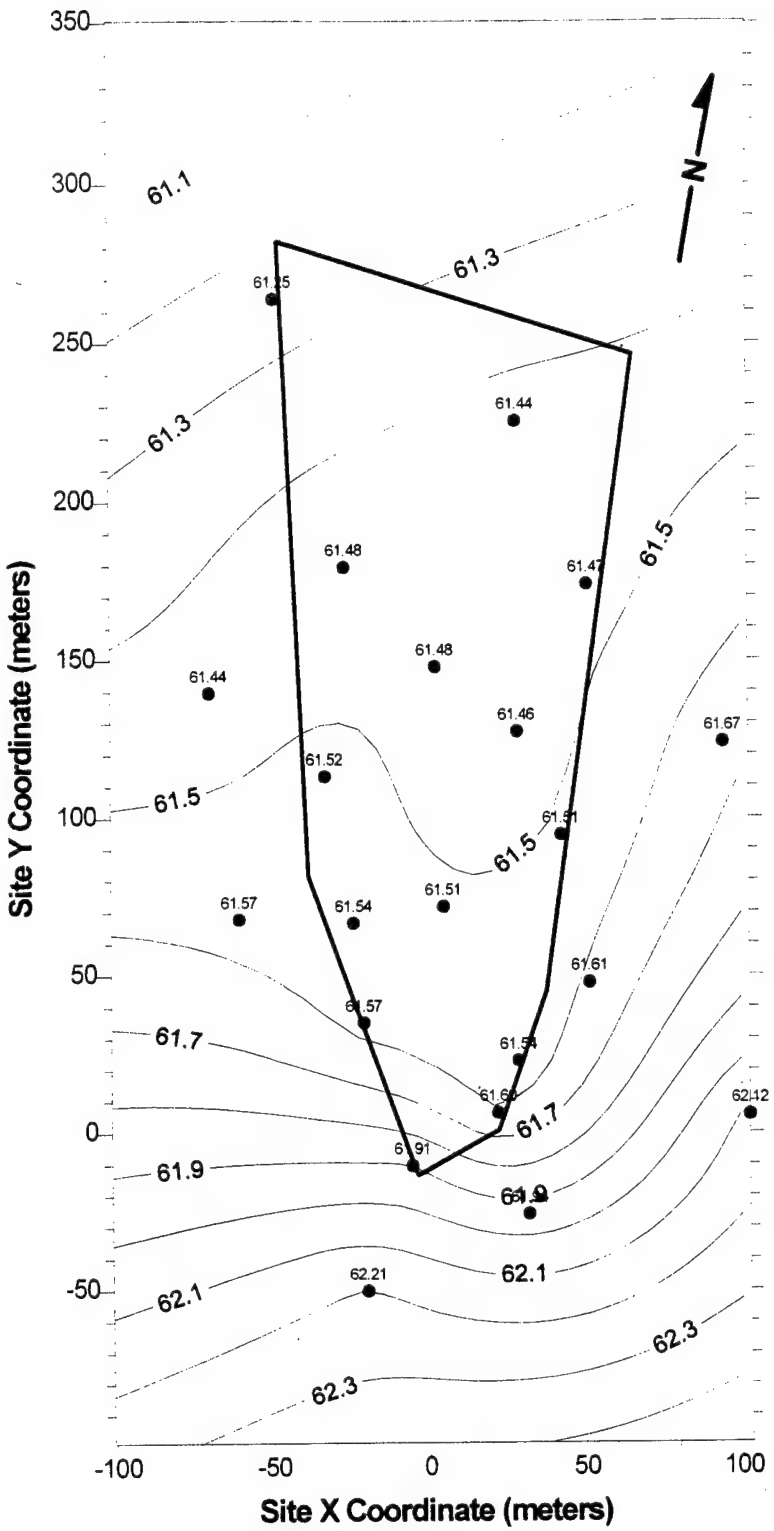

Figure A- 2. Potentiometric Surface Based on Water Levels Measured in A Wells on 07/23/90.

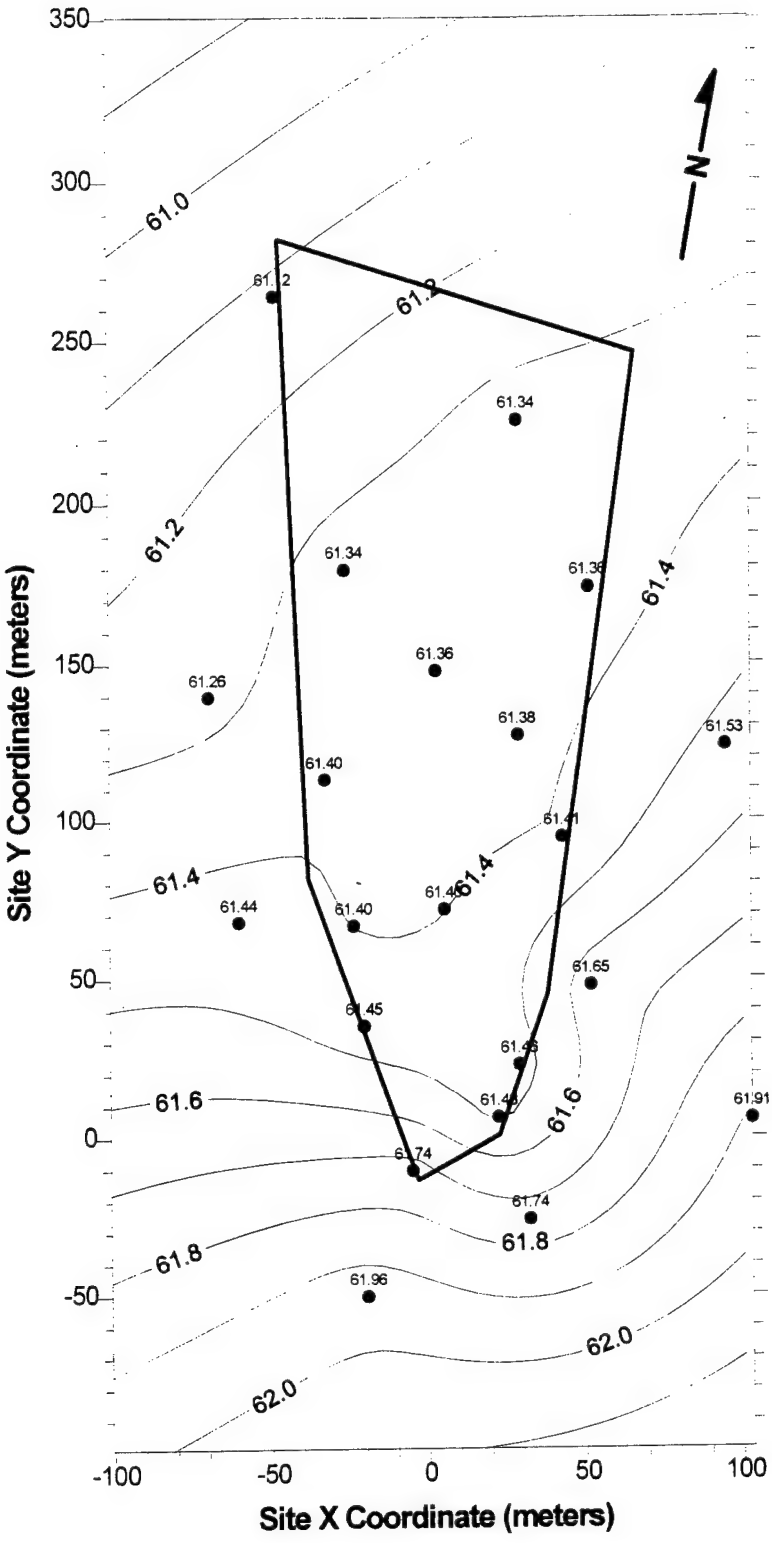

Figure A- 3. Potentiometric Surface Based on Water Levels Measured in A Wells on 08/13/90.

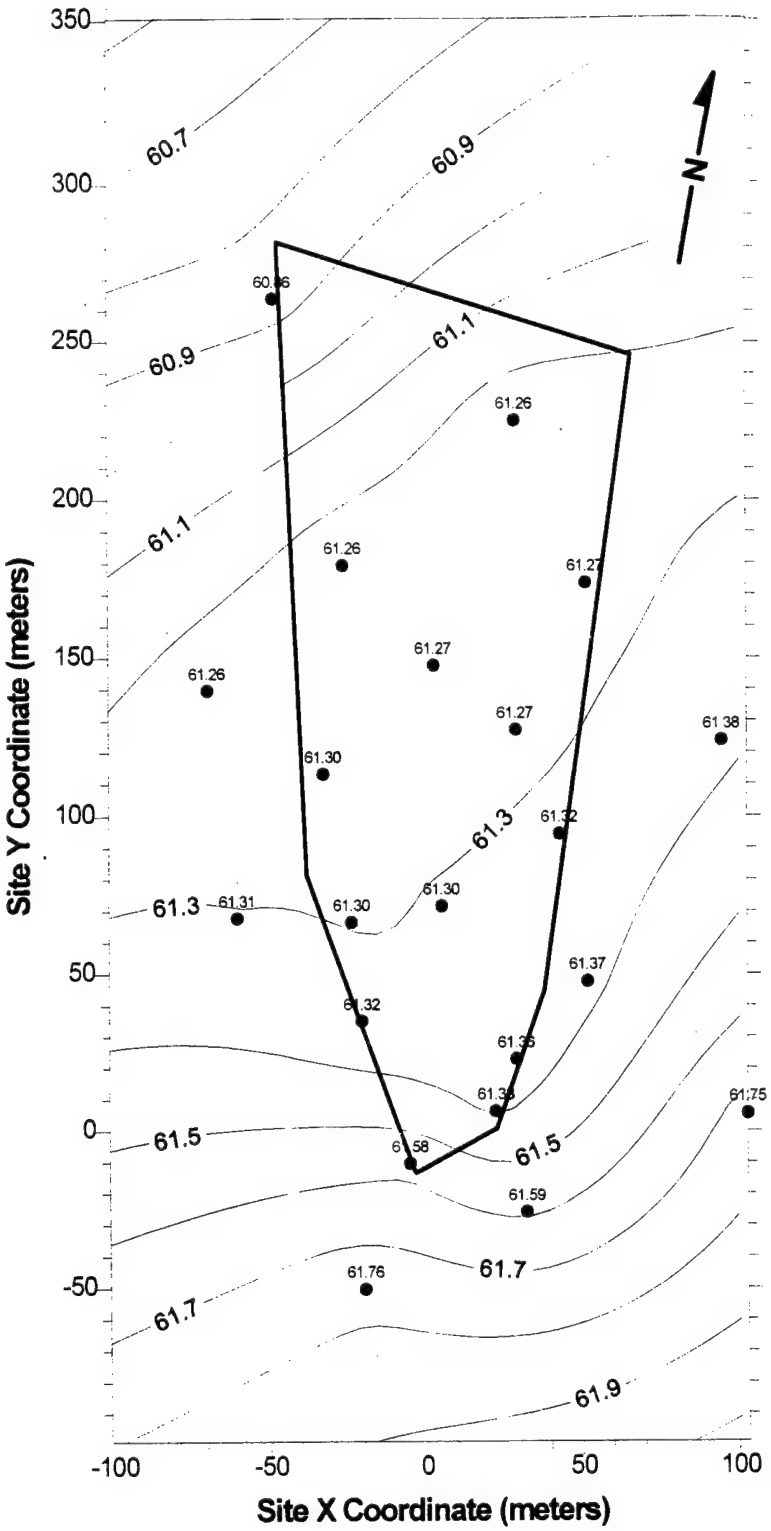

Figure A- 4. Potentiometric Surface Based on Water Levels Measured in A Wells on 09/17/90.

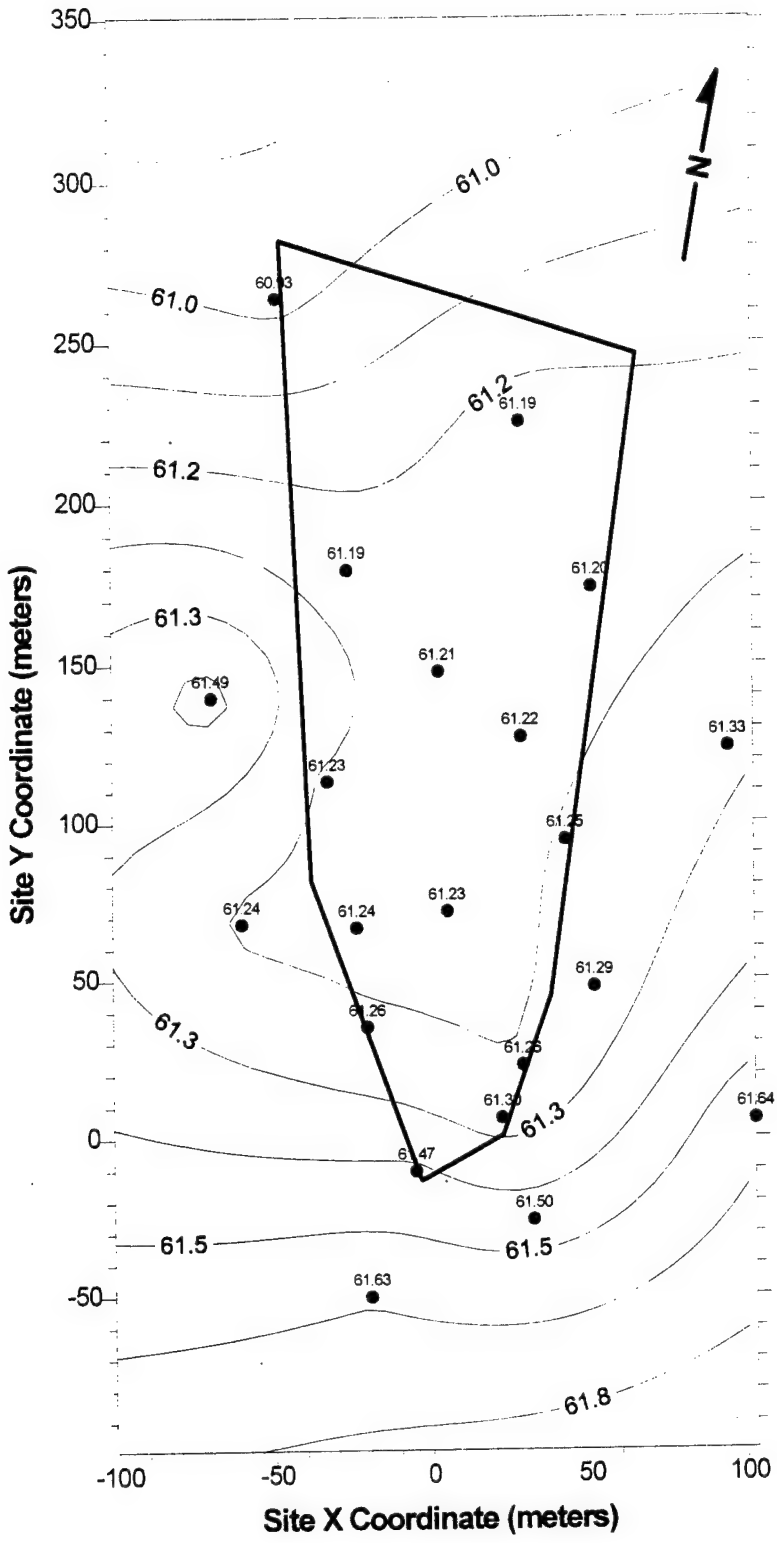

Figure A- 5. Potentiometric Surface Based on Water Levels Measured in A Wells on 10/15/90.

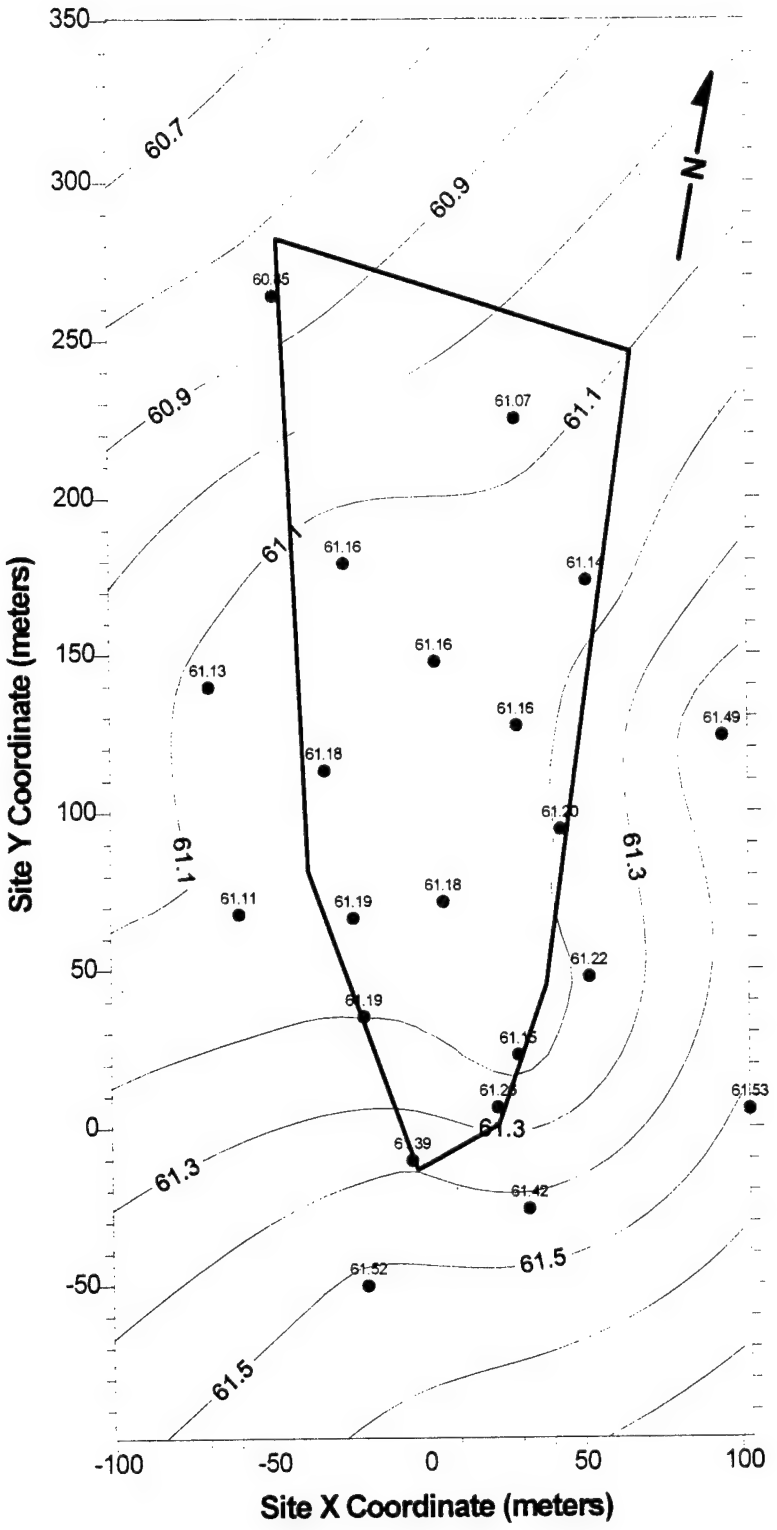

Figure A- 6. Potentiometric Surface Based on Water Levels Measured in A Wells on 11/07/90.

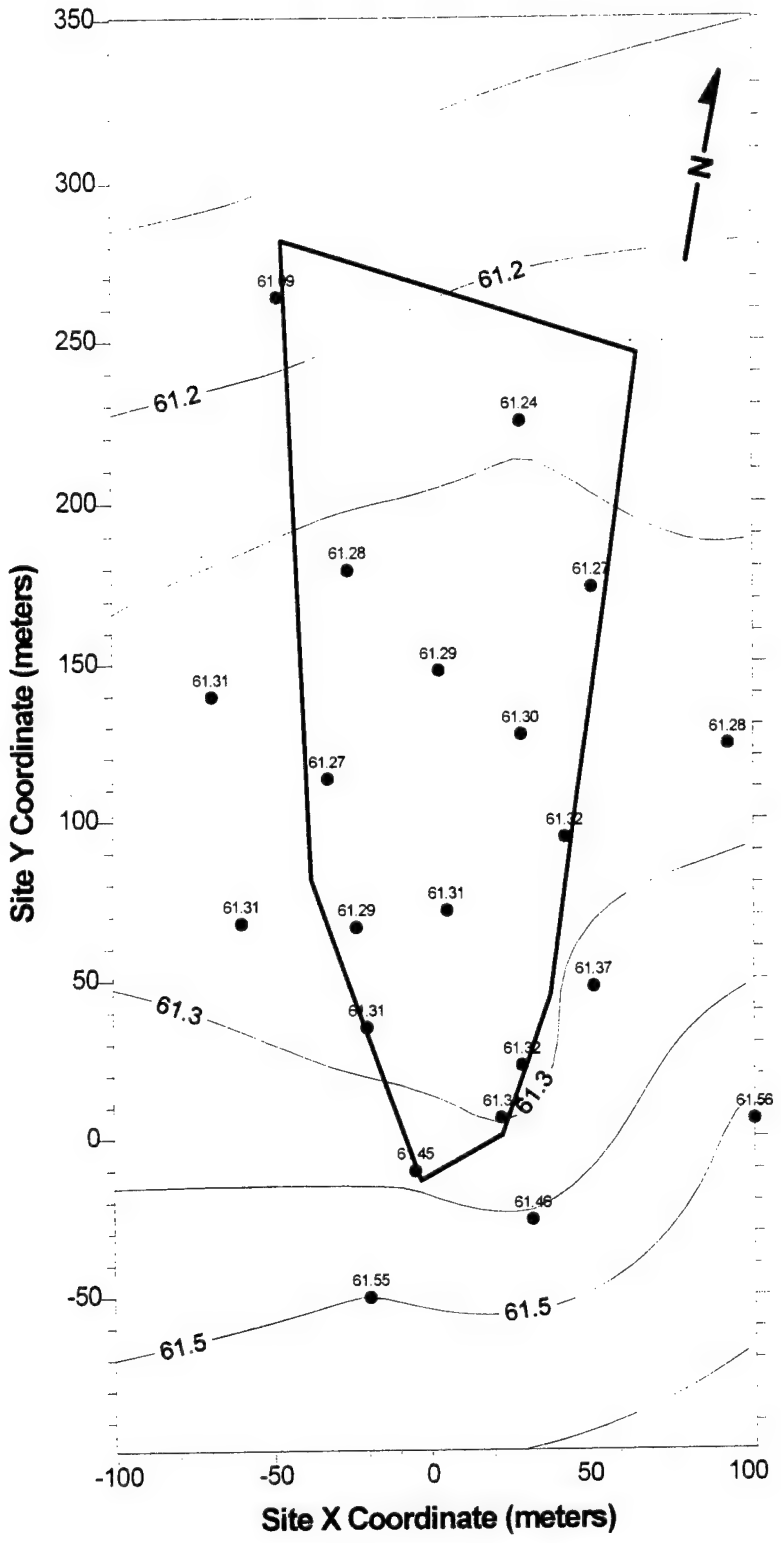

Figure A- 7. Potentiometric Surface Based on Water Levels Measured in A Wells on 12/05/90.

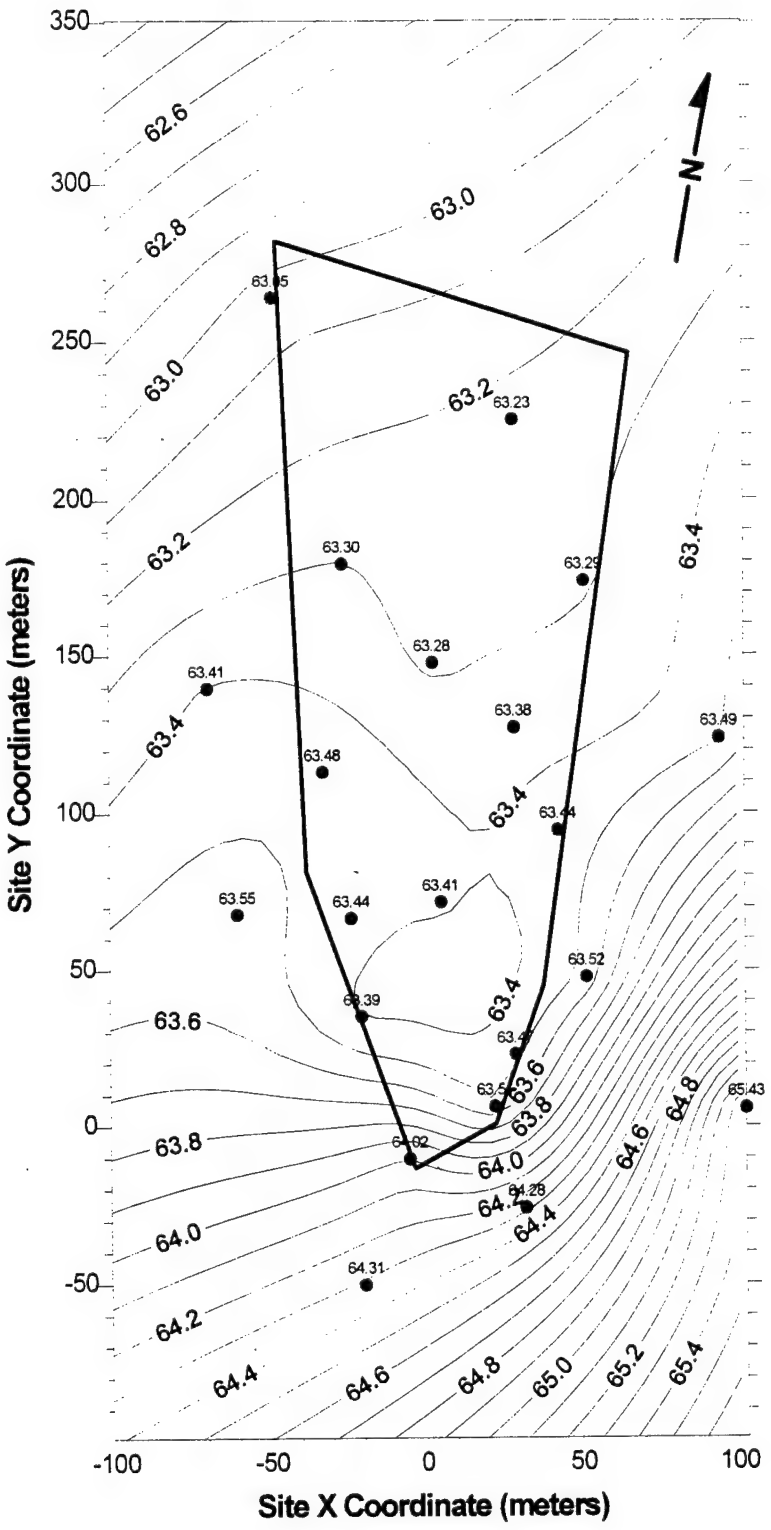

Figure A- 8. Potentiometric Surface Based on Water Levels Measured in A Wells on 01/08/91.

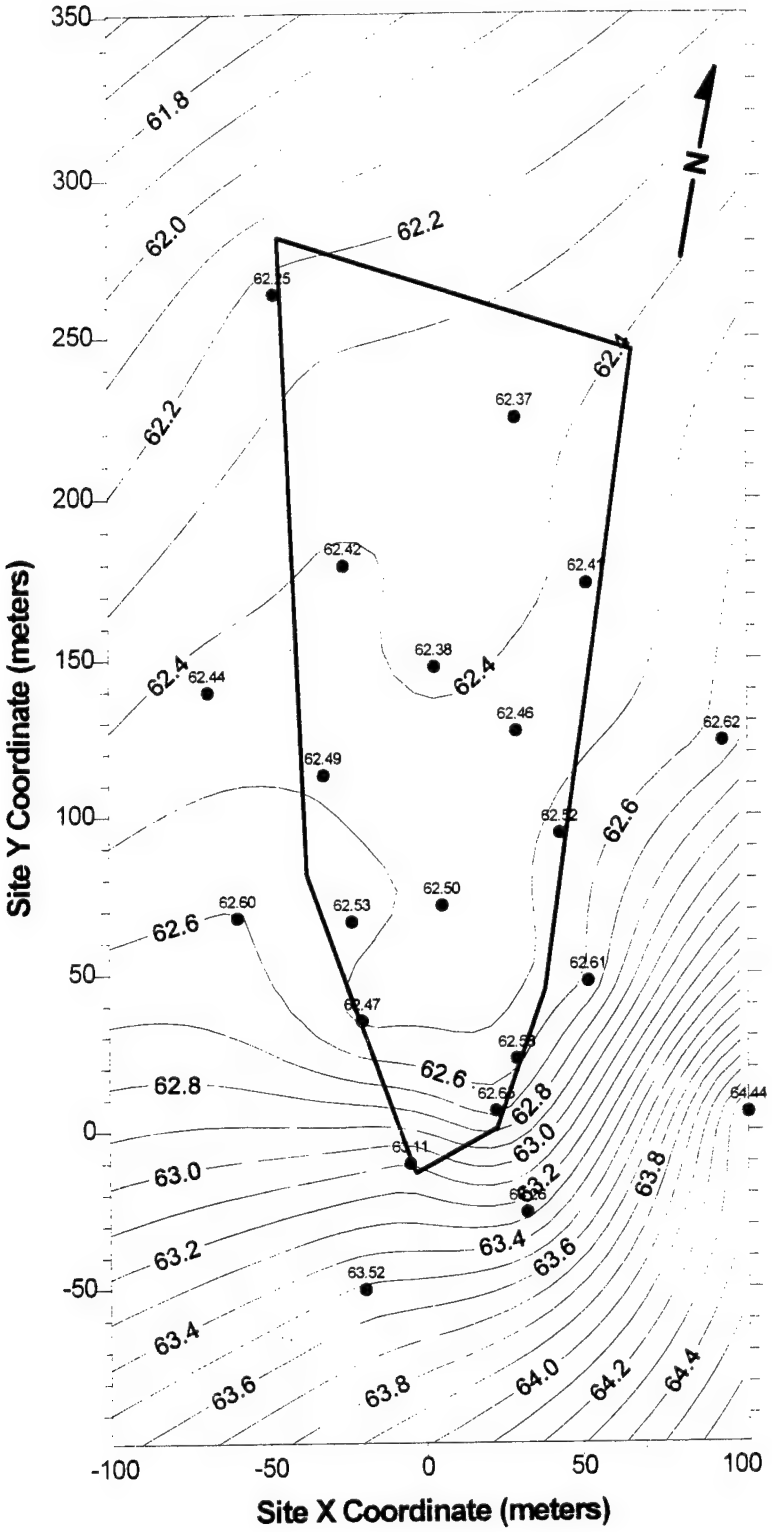

Figure A- 9. Potentiometric Surface Based on Water Levels Measured in A Wells on 02/08/91.

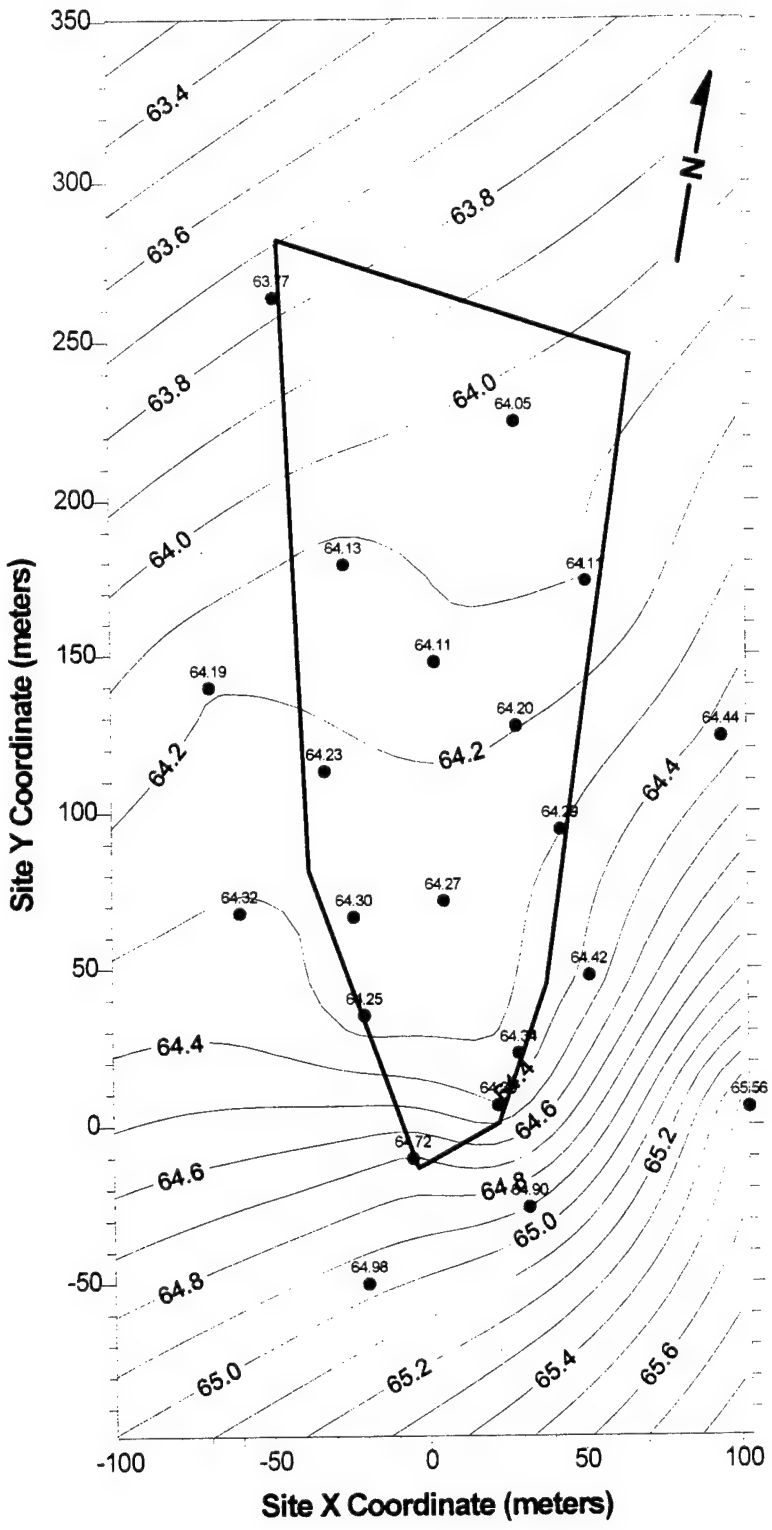

Figure A- 10. Potentiometric Surface Based on Water Levels Measured in A Wells on 03/08/91.

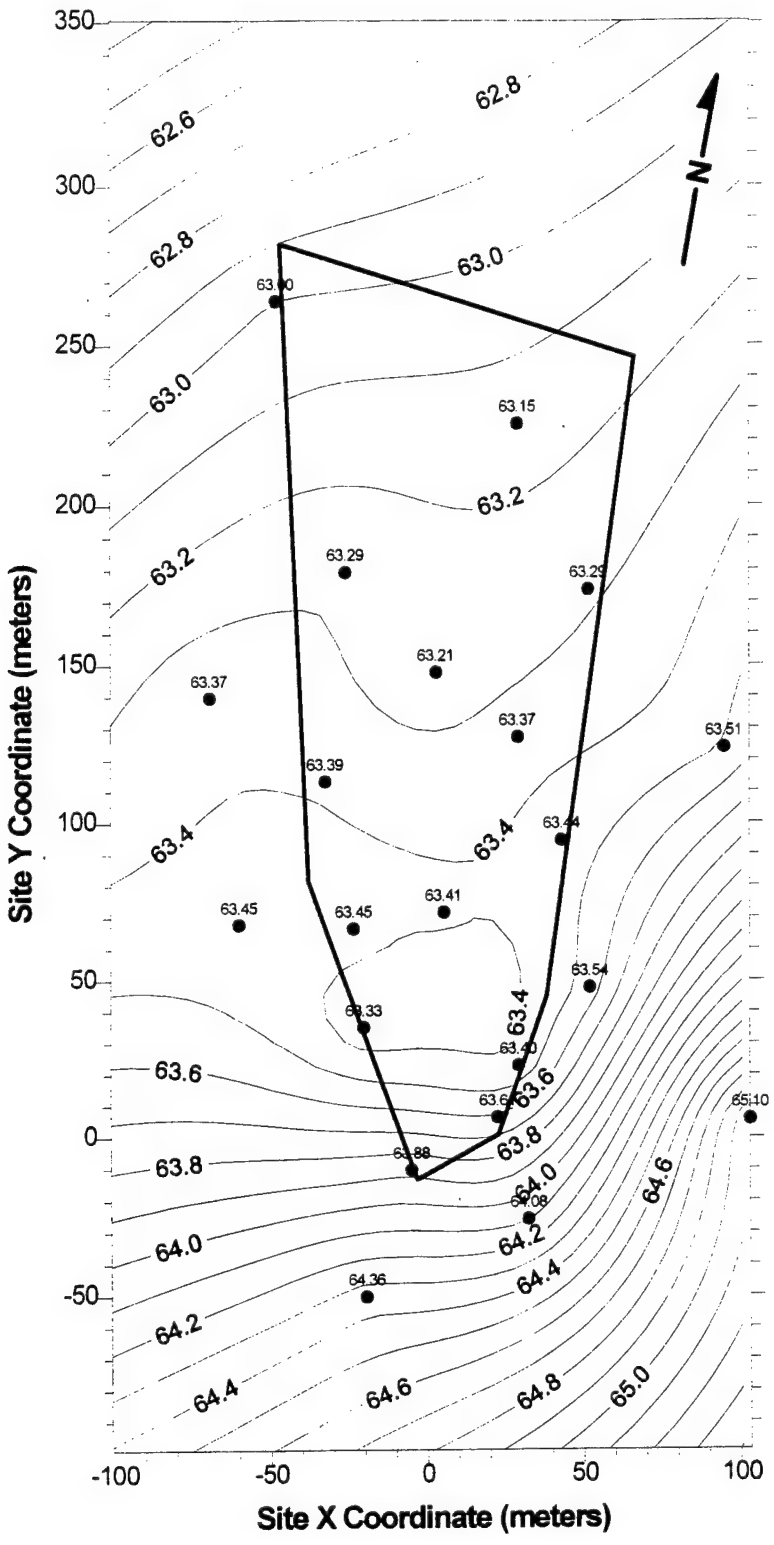

Figure A- 11. Potentiometric Surface Based on Water Levels Measured in A Wells on 04/04/91.

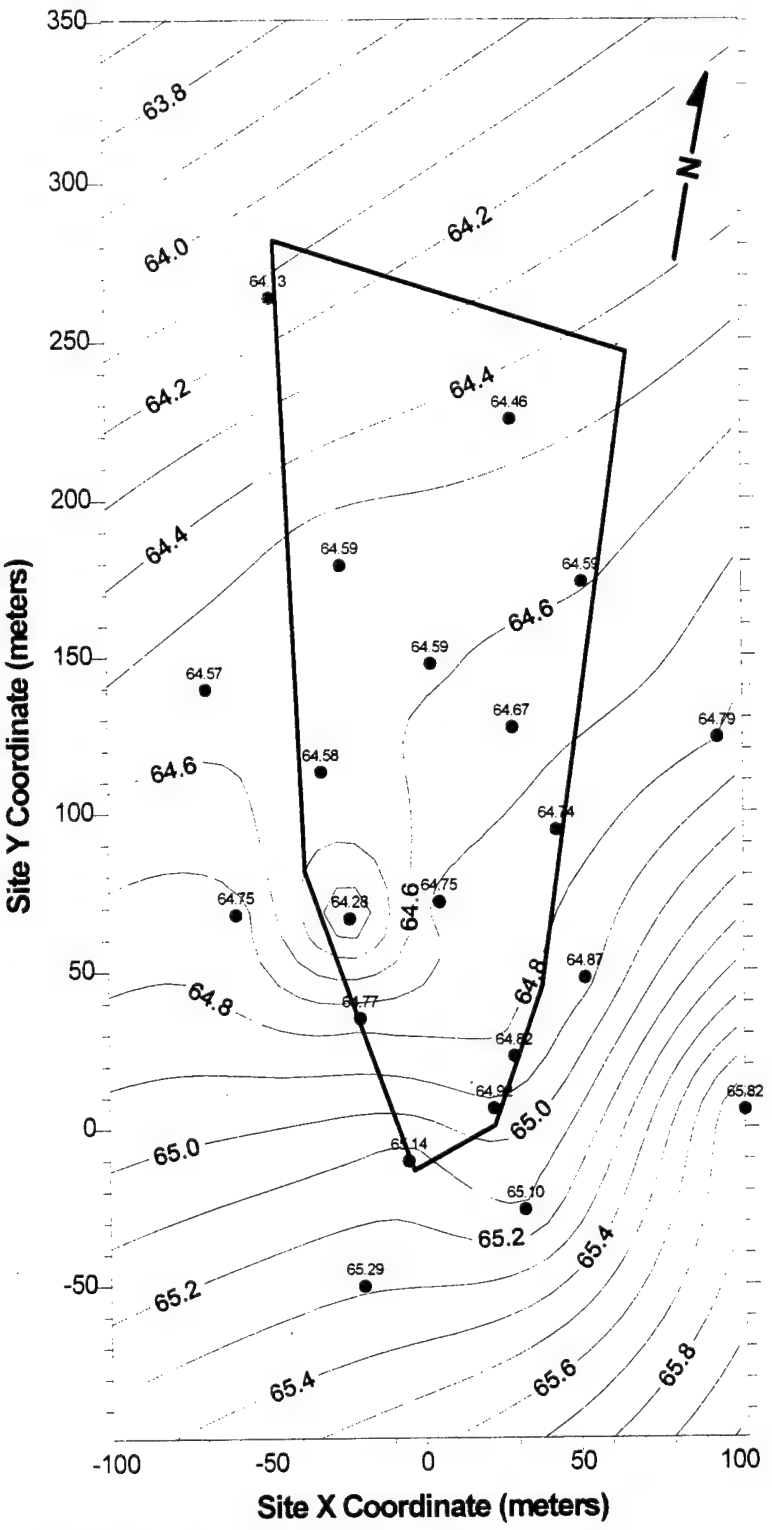

Figure A- 12. Potentiometric Surface Based on Water Levels Measured in A Wells on 05/10/91.

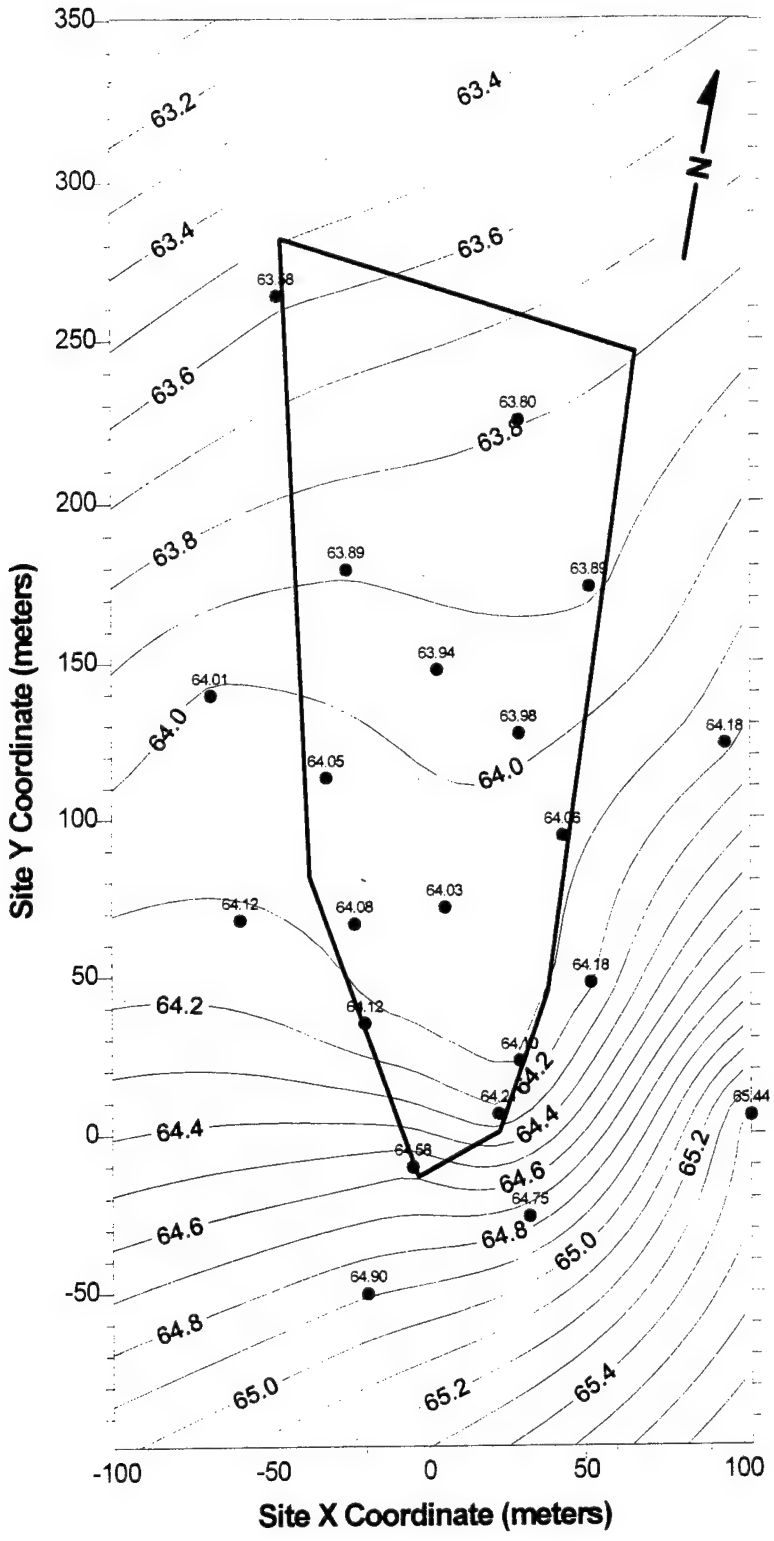

Figure A- 13. Potentiometric Surface Based on Water Levels Measured in A Wells on 05/20/91.

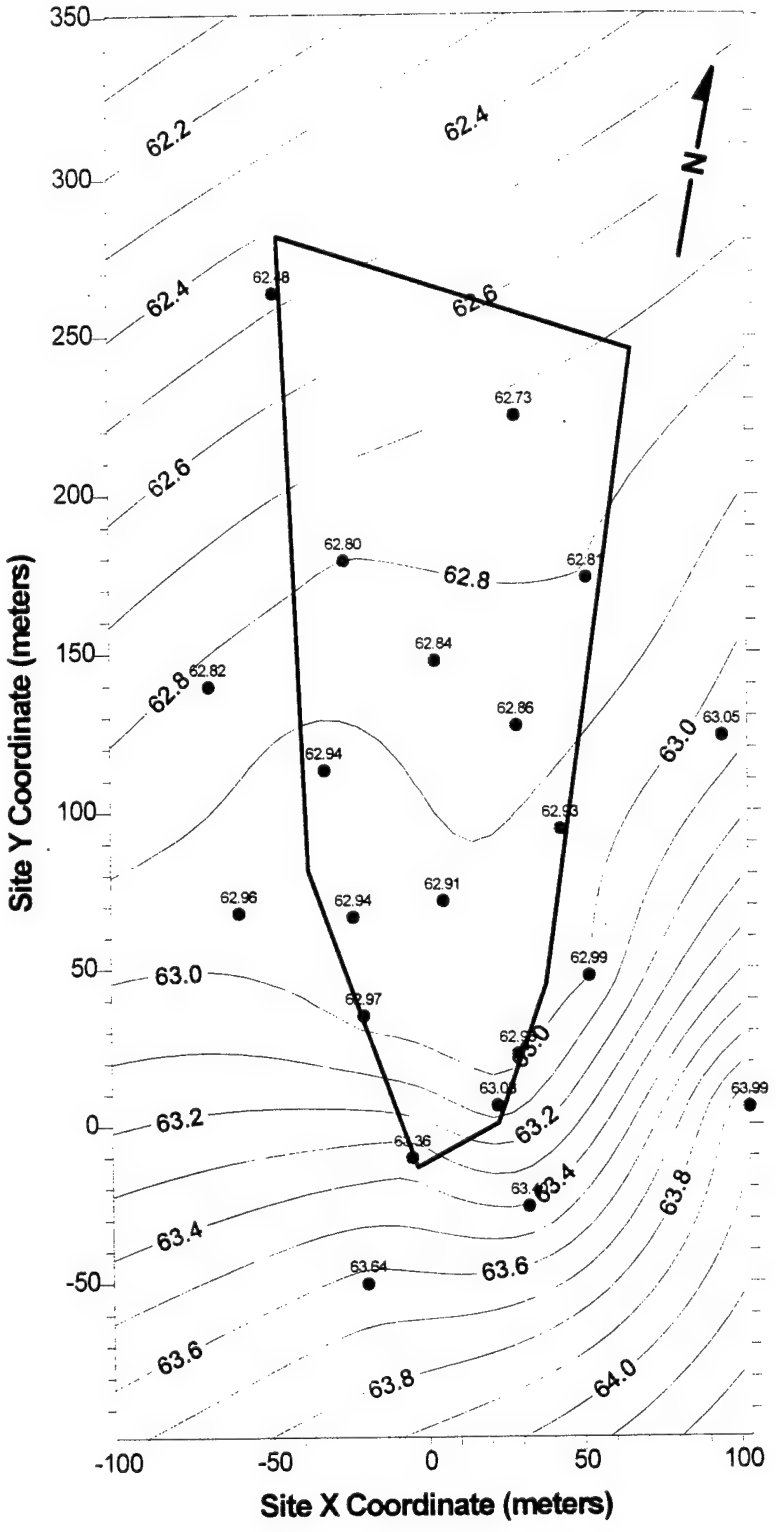

Figure A- 14. Potentiometric Surface Based on Water Levels Measured in A Wells on 06/13/91.

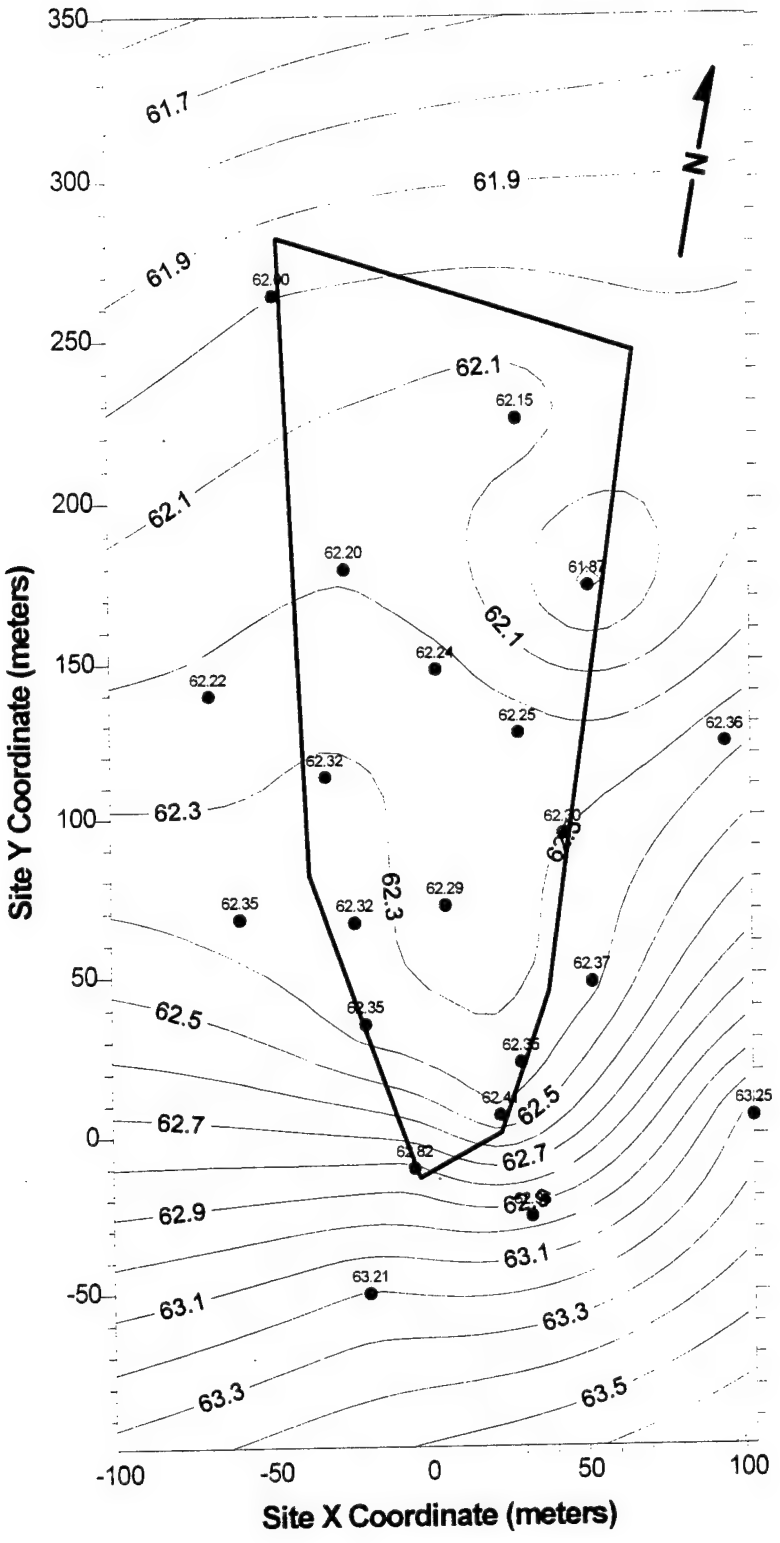

Figure A- 15. Potentiometric Surface Based on Water Levels Measured in A Wells on 07/09/91.

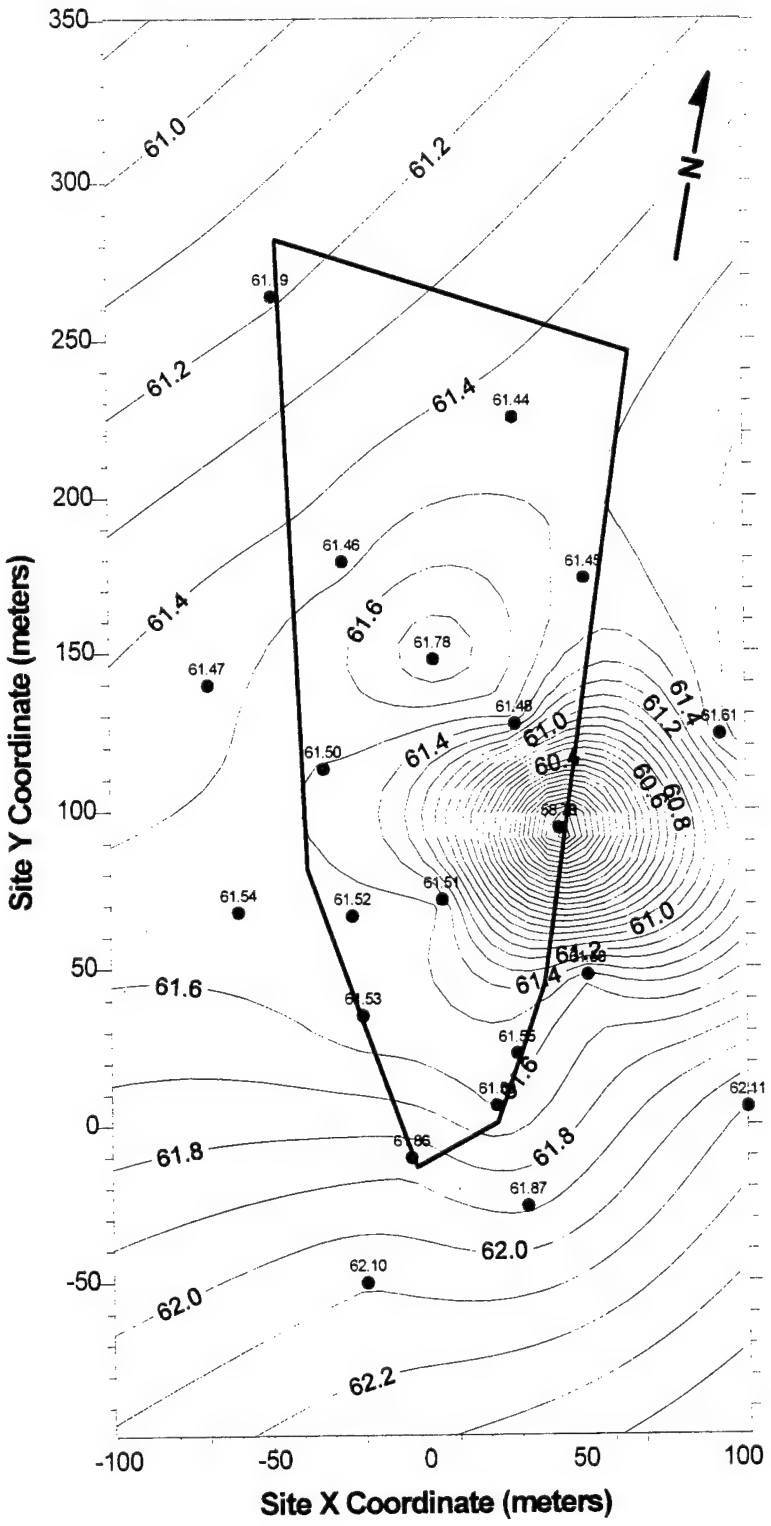

Figure A- 16. Potentiometric Surface Based on Water Levels Measured in A Wells on 08/19/91.

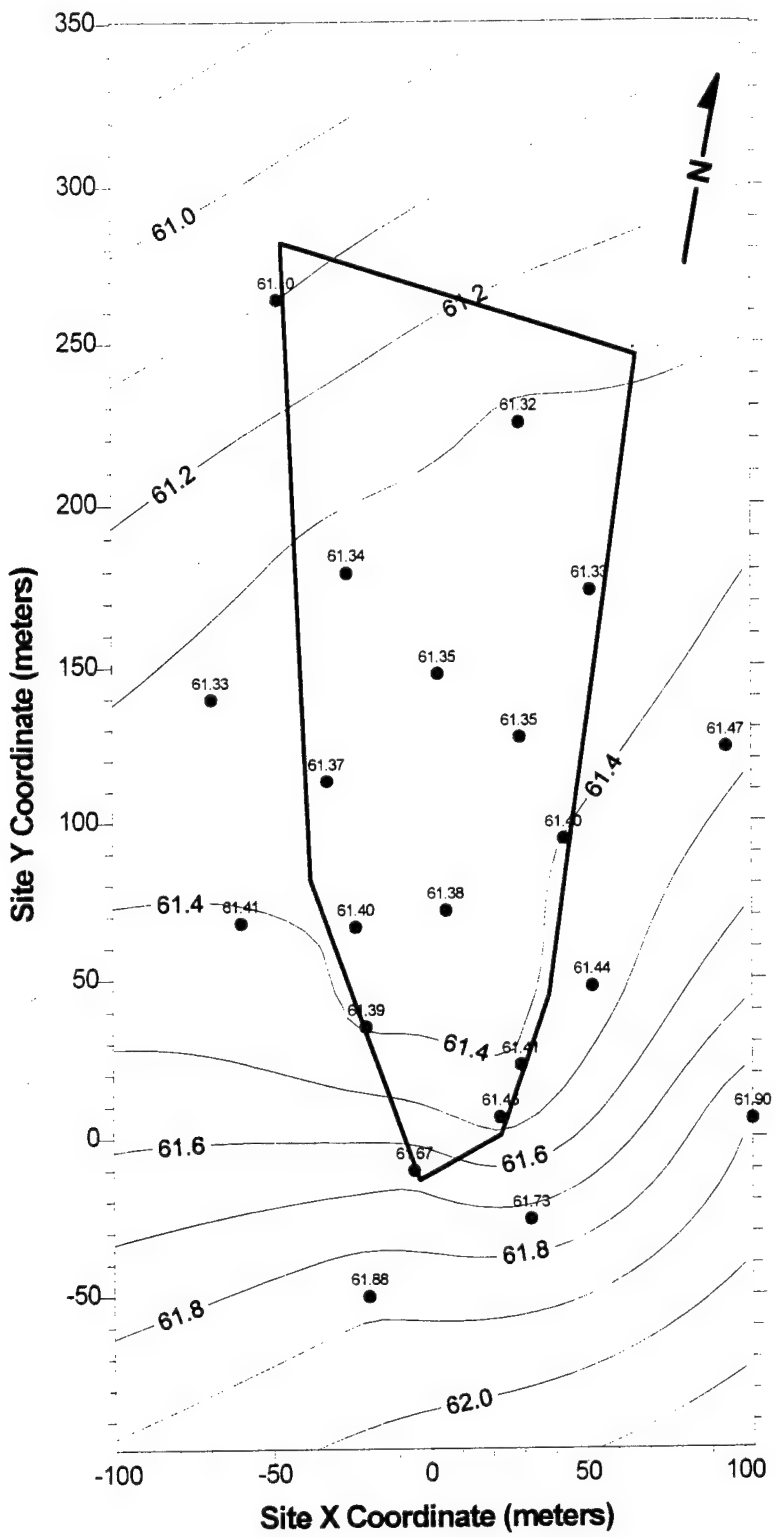

Figure A- 17. Potentiometric Surface Based on Water Levels Measured in A Wells on 09/11/91.

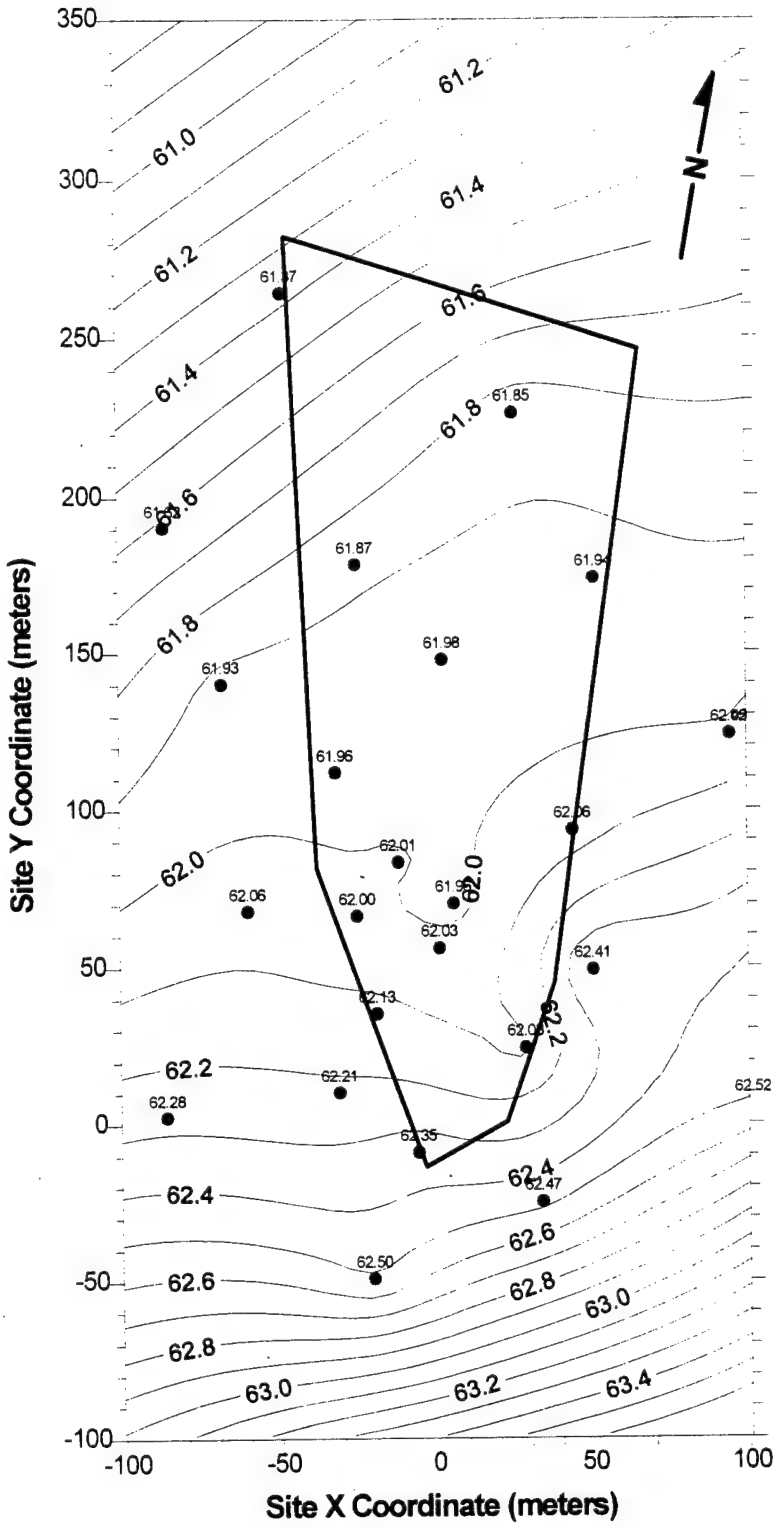

Figure A- 18. Potentiometric Surface Based on Water Levels Measured in B Wells on 06/19/90.

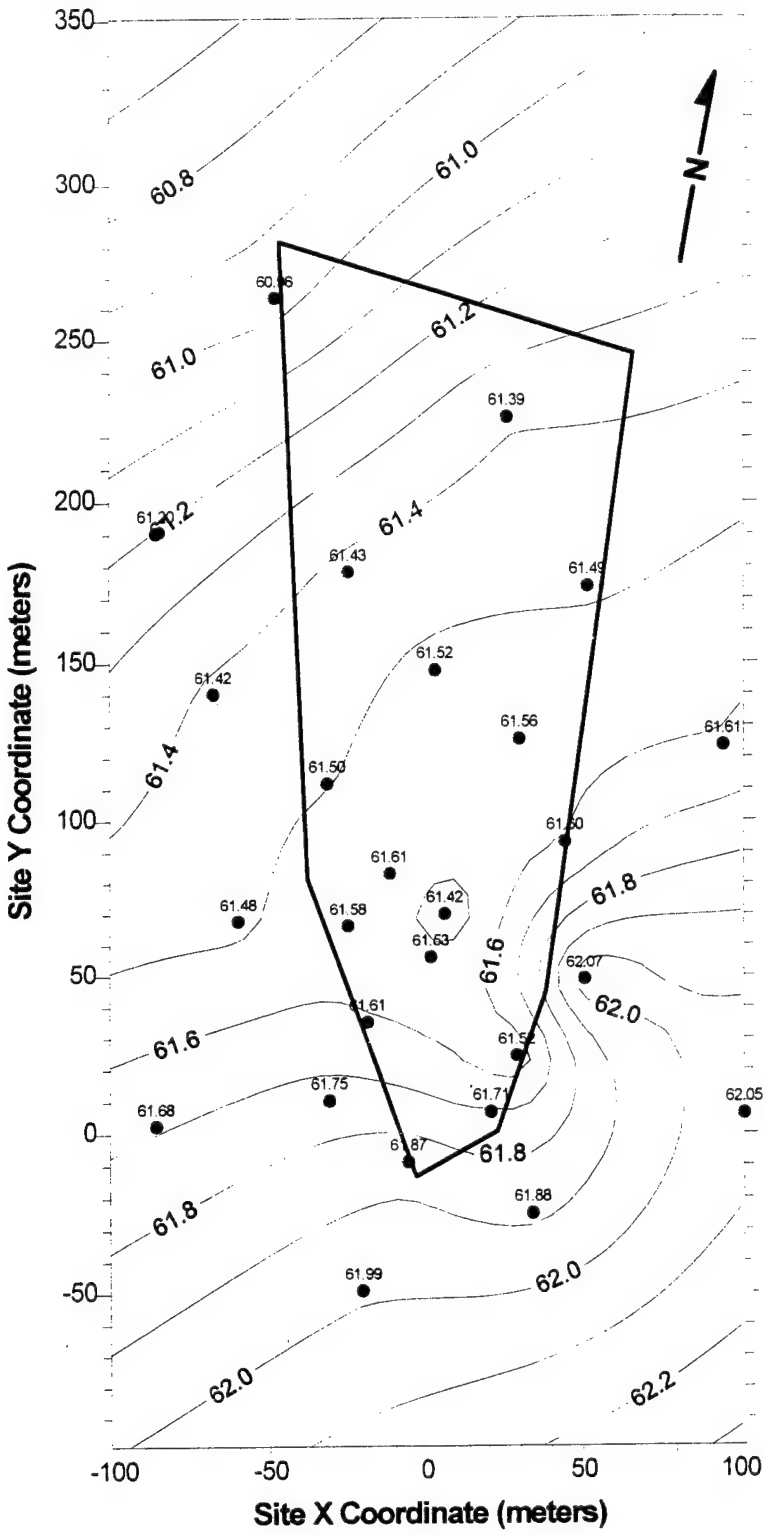

Figure A- 19. Potentiometric Surface Based on Water Levels Measured in B Wells on 07/23/90.

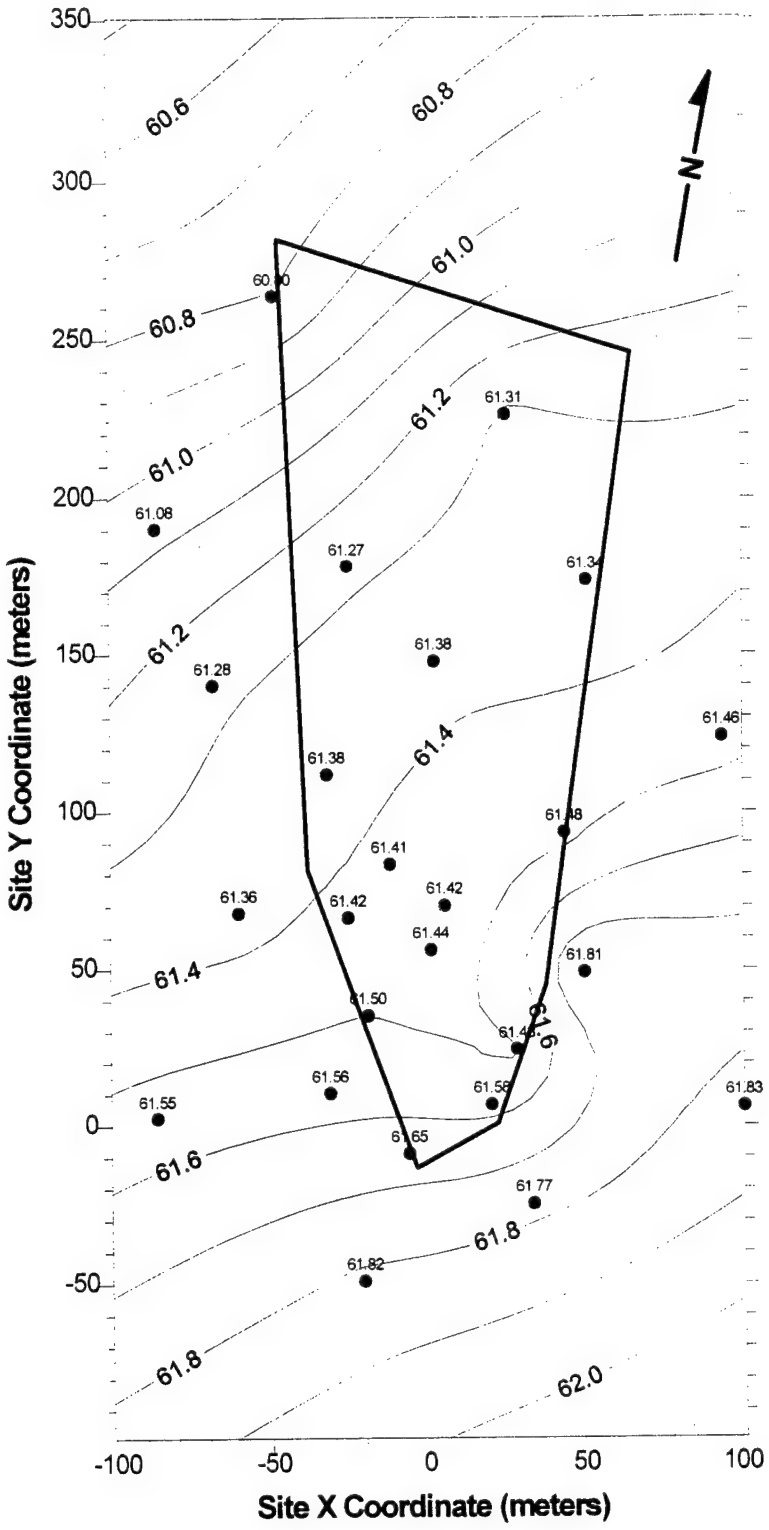

Figure A- 20. Potentiometric Surface Based on Water Levels Measured in B Wells on 08/13/90.

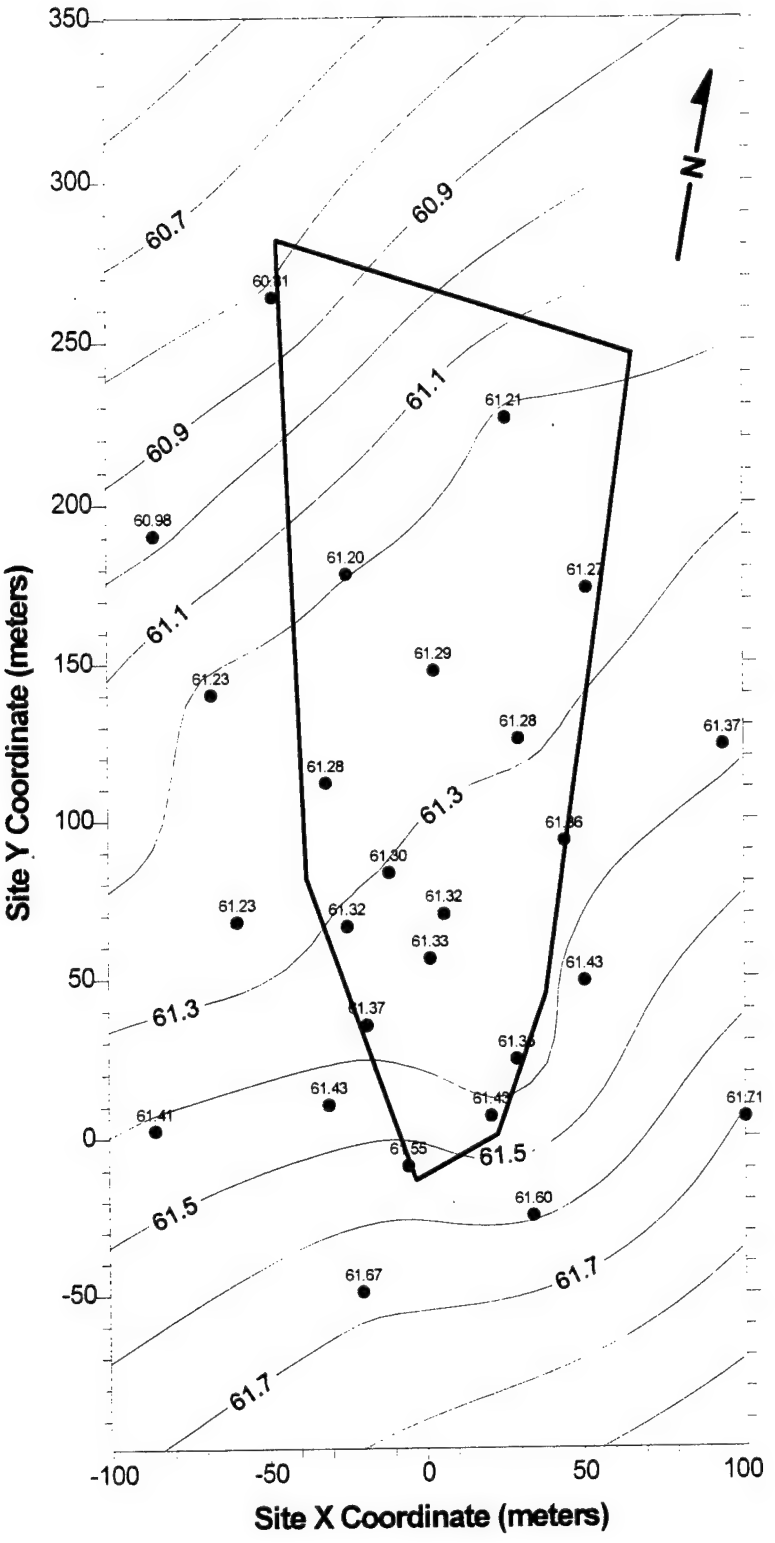

Figure A- 21. Potentiometric Surface Based on Water Levels Measured in B Wells on 09/17/90.

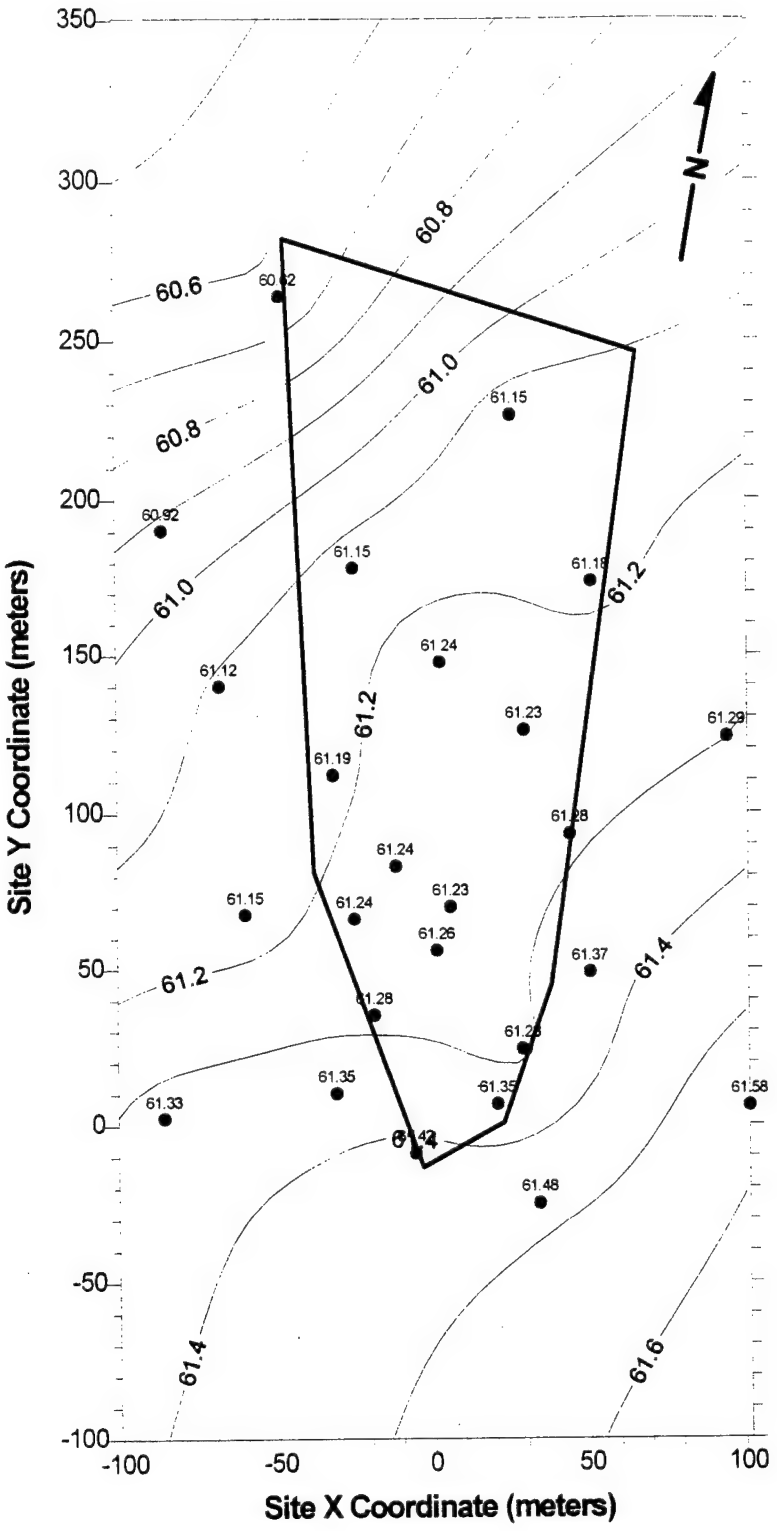

Figure A- 22. Potentiometric Surface Based on Water Levels Measured in B Wells on 10/15/90.

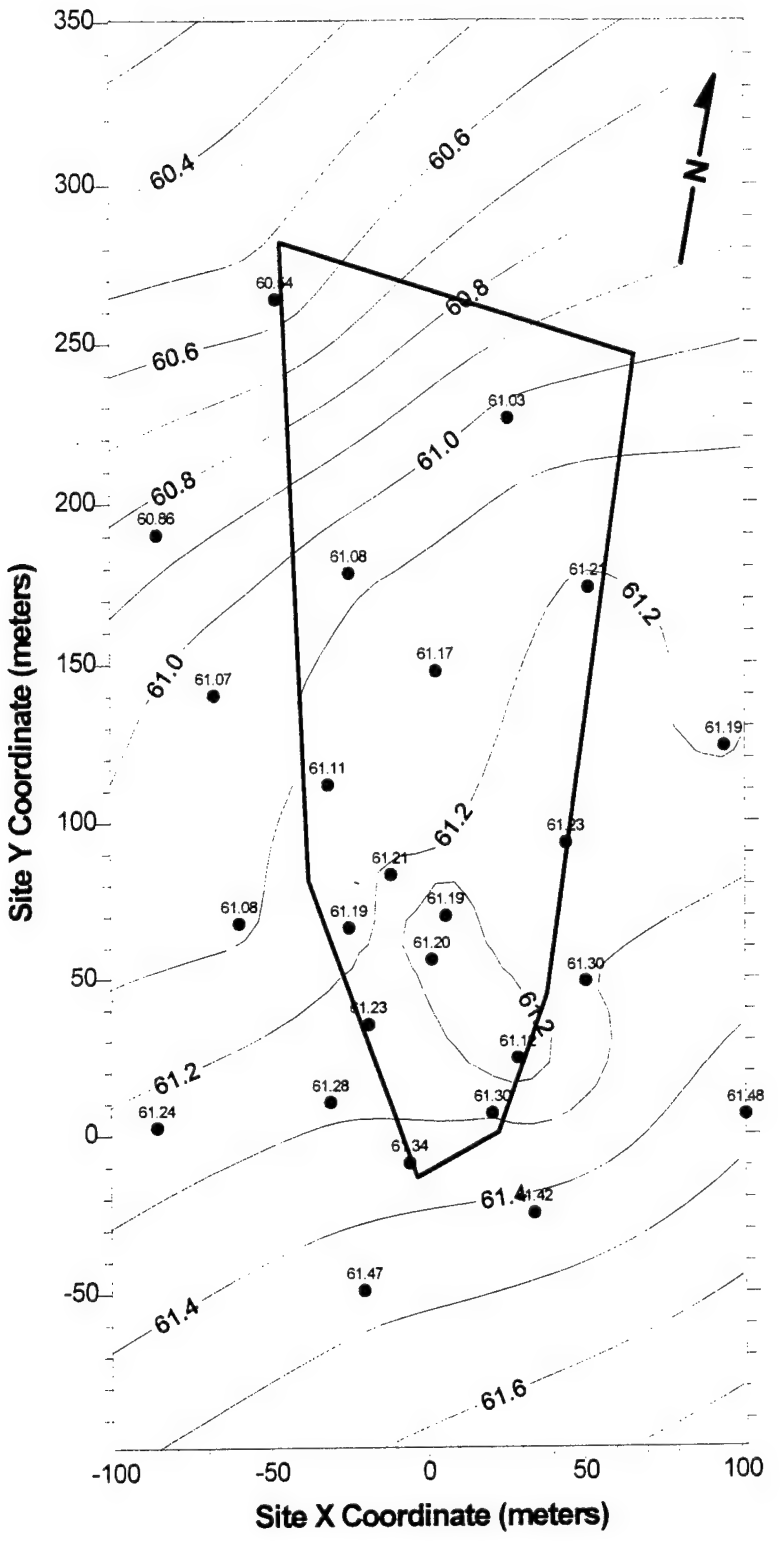

Figure A- 23. Potentiometric Surface Based on Water Levels Measured in B Wells on 11/07/90.

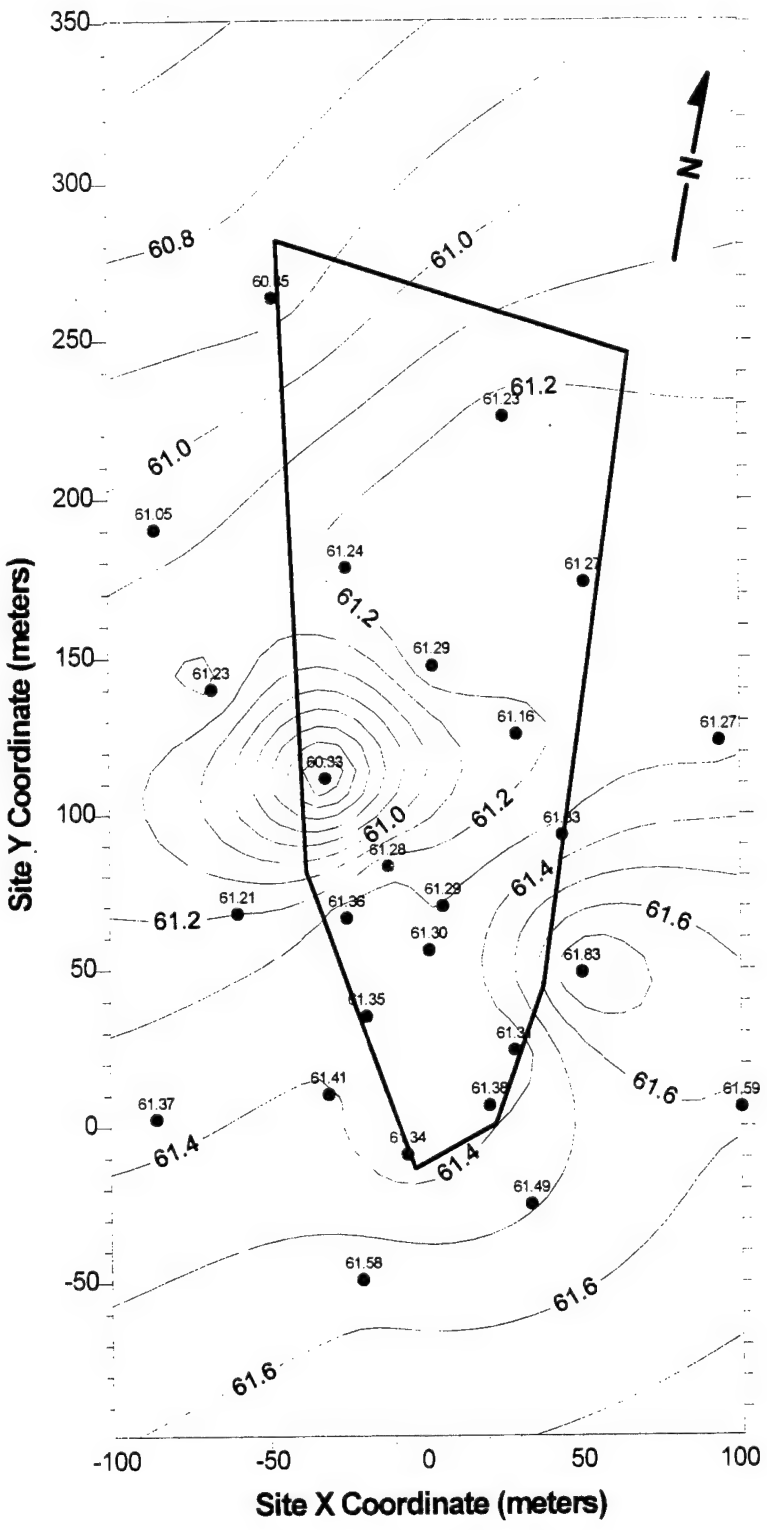

Figure A- 24. Potentiometric Surface Based on Water Levels Measured in B Wells on 12/05/90.

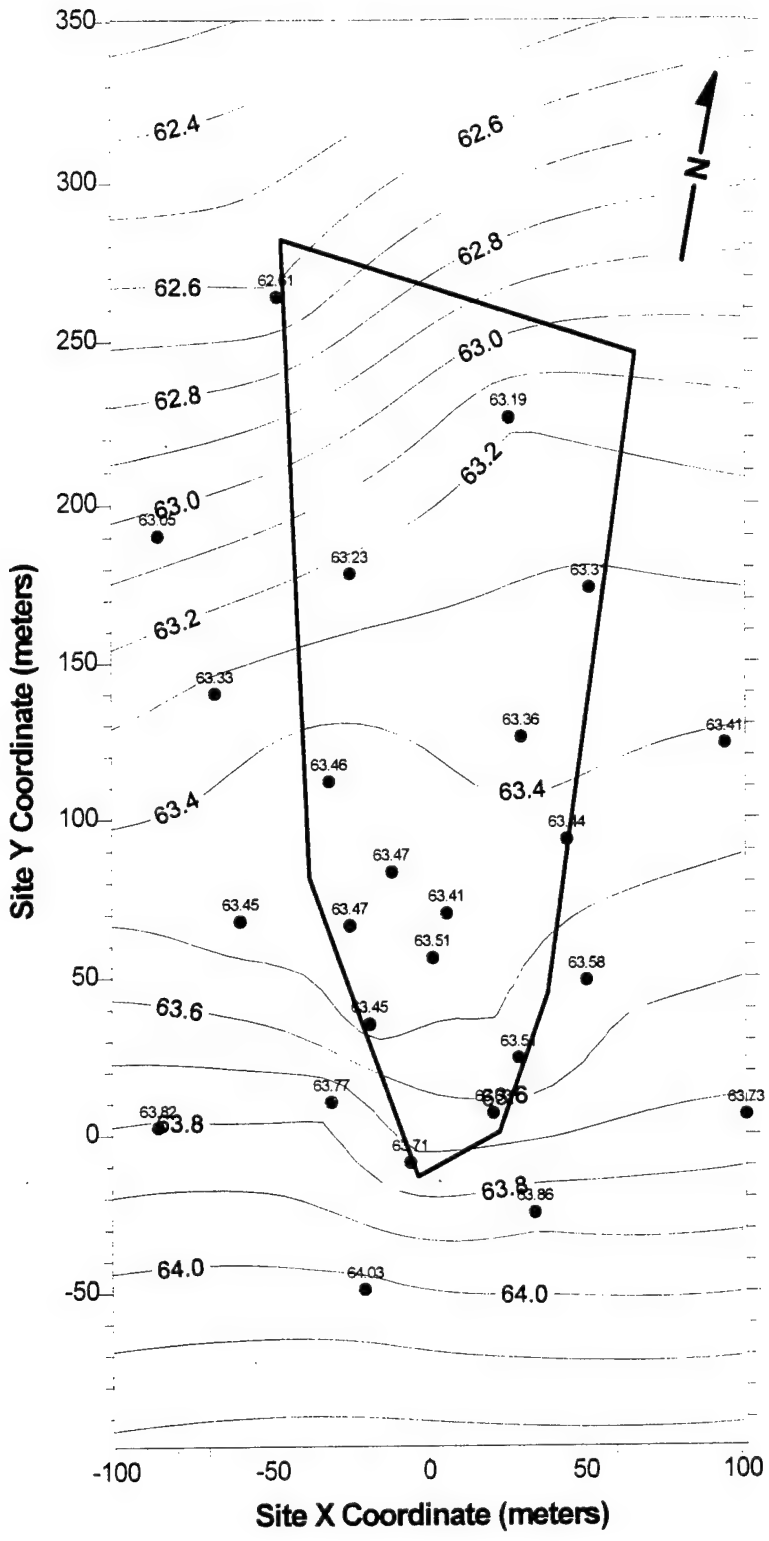

Figure A- 25. Potentiometric Surface Based on Water Levels Measured in B Wells on 01/08/91.

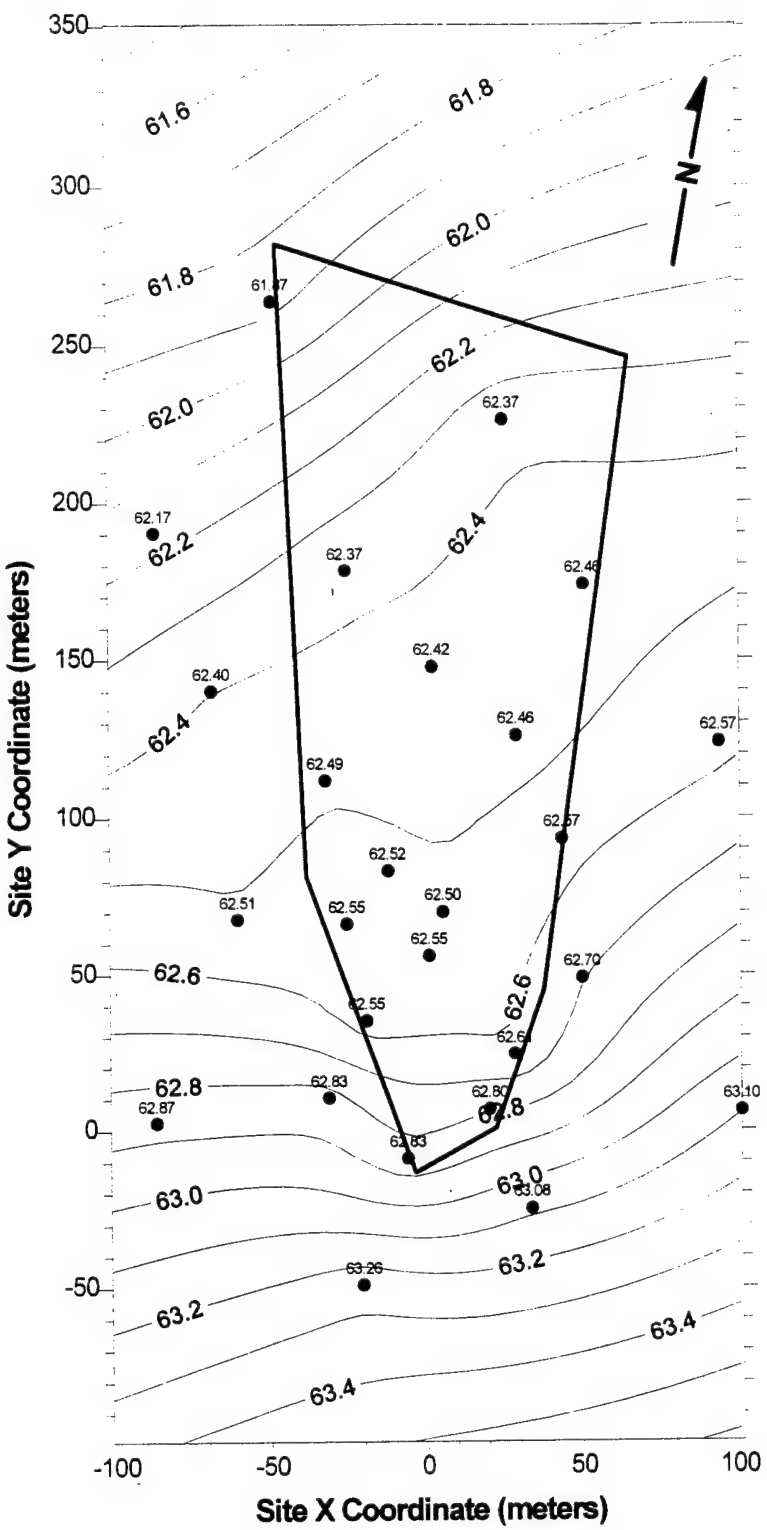

Figure A- 26. Potentiometric Surface Based on Water Levels Measured in B Wells on 02/08/91.

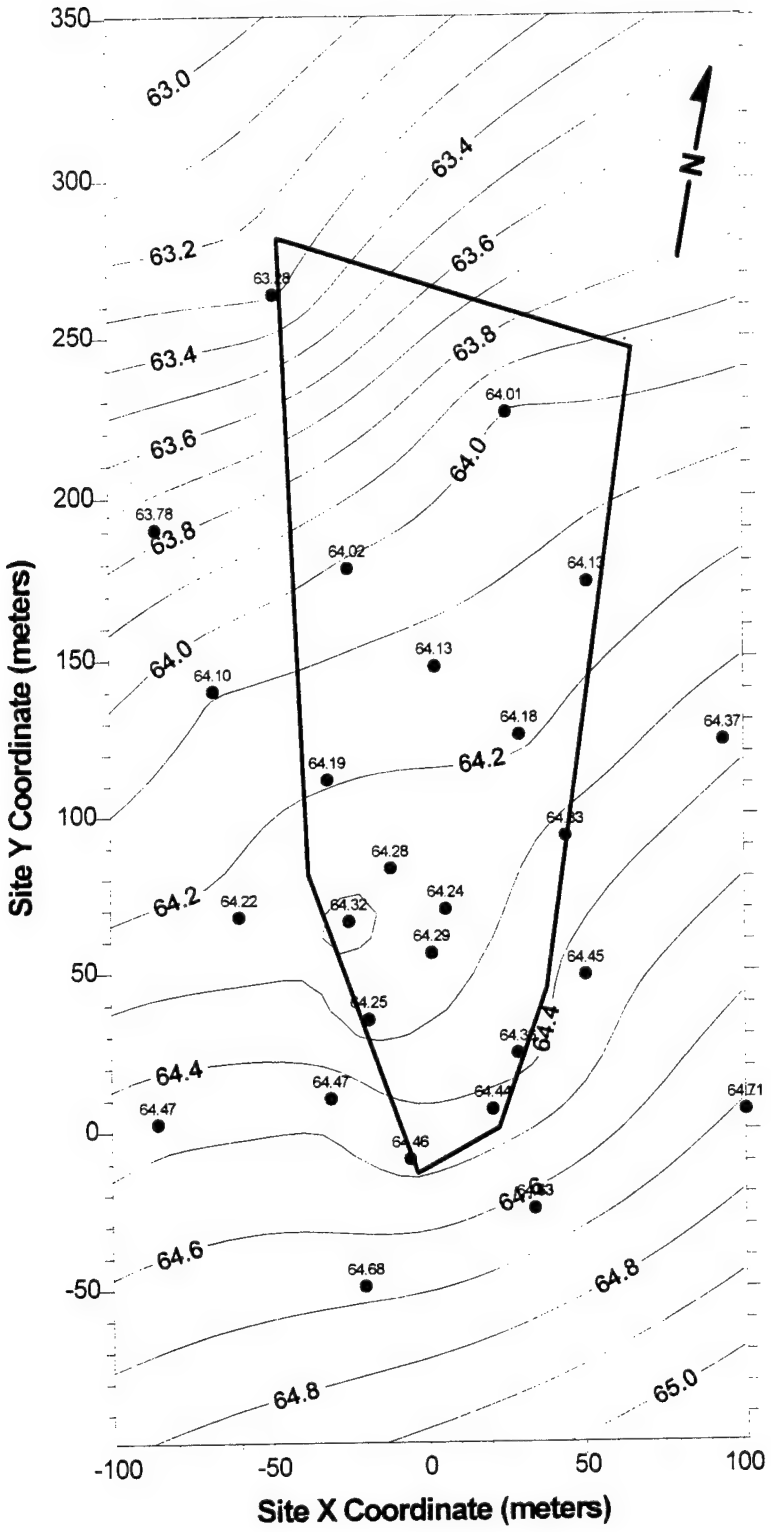

Figure A- 27. Potentiometric Surface Based on Water Levels Measured in B Wells on 03/08/91.

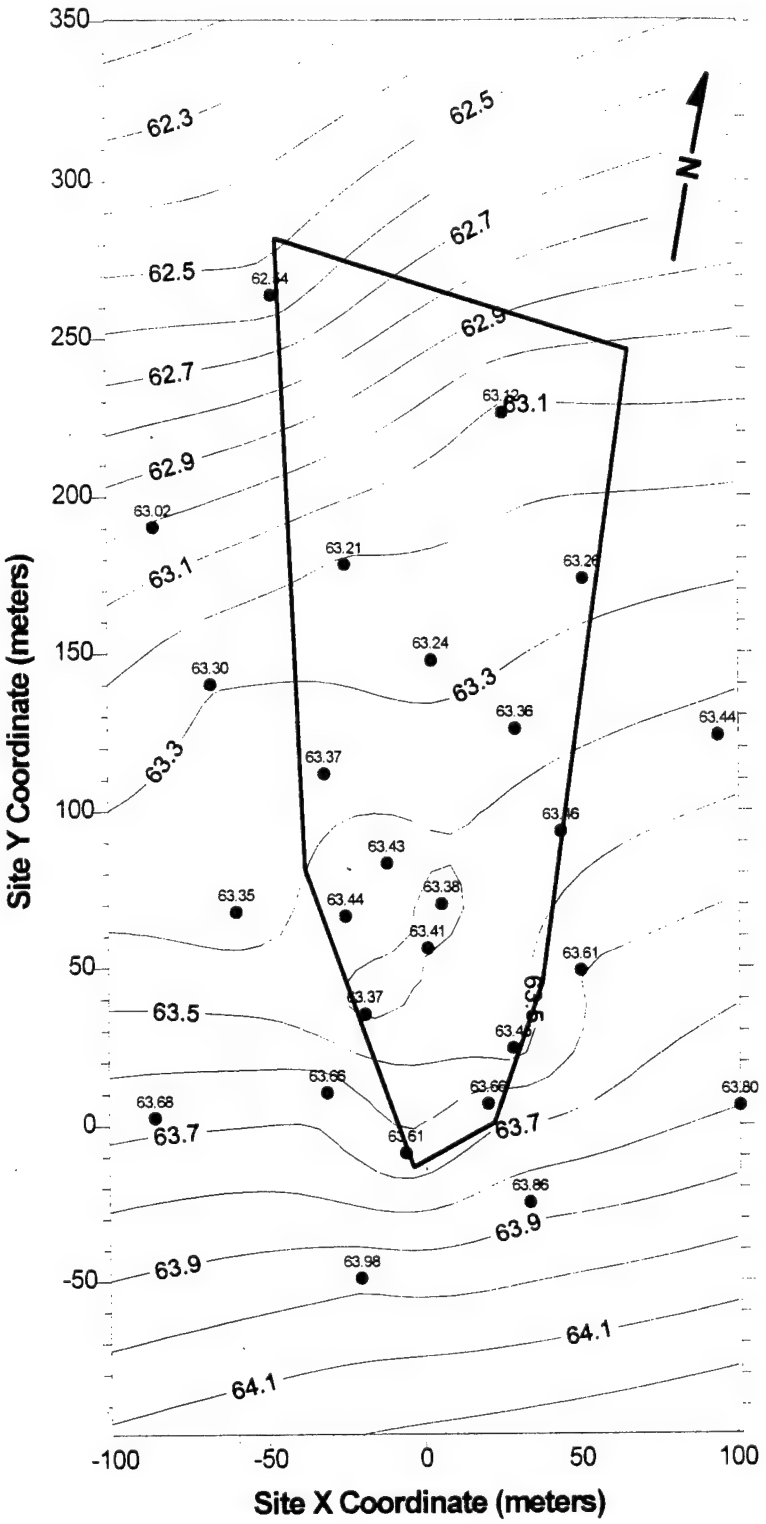

Figure A- 28. Potentiometric Surface Based on Water Levels Measured in B Wells on 04/04/91.

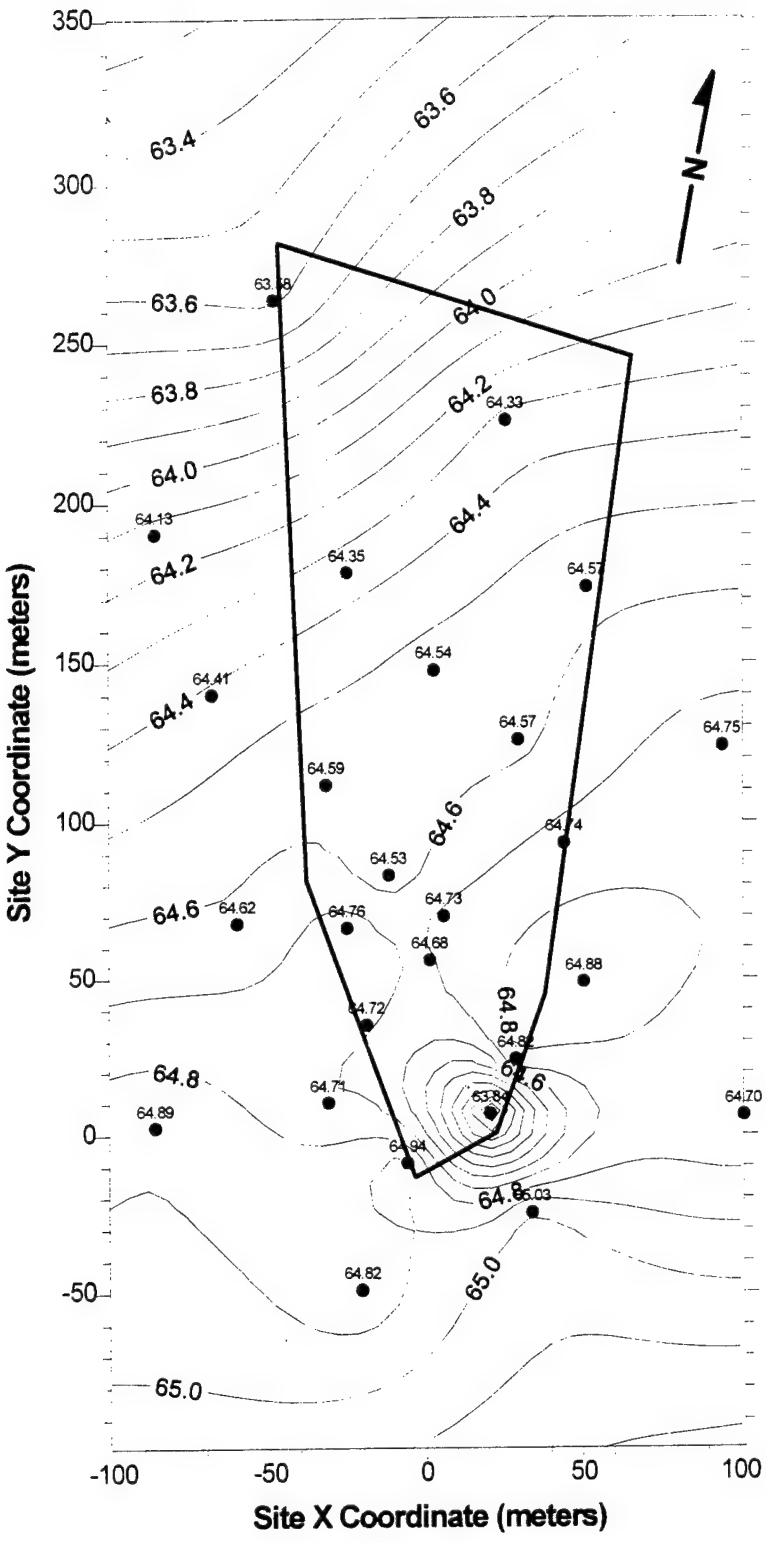

Figure A- 29. Potentiometric Surface Based on Water Levels Measured in B Wells on 05/10/91.

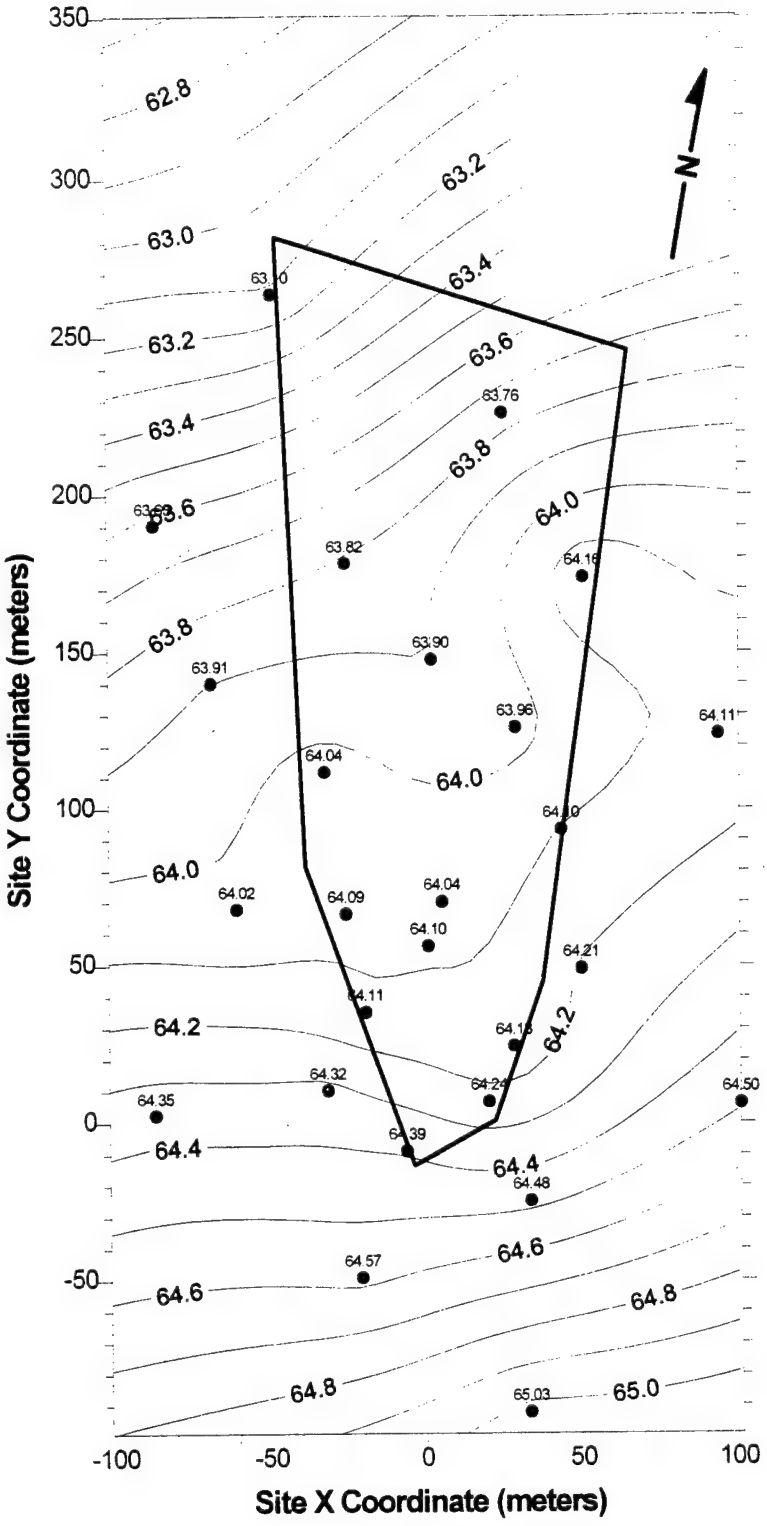

Figure A- 30. Potentiometric Surface Based on Water Levels Measured in B Wells on 05/20/91.

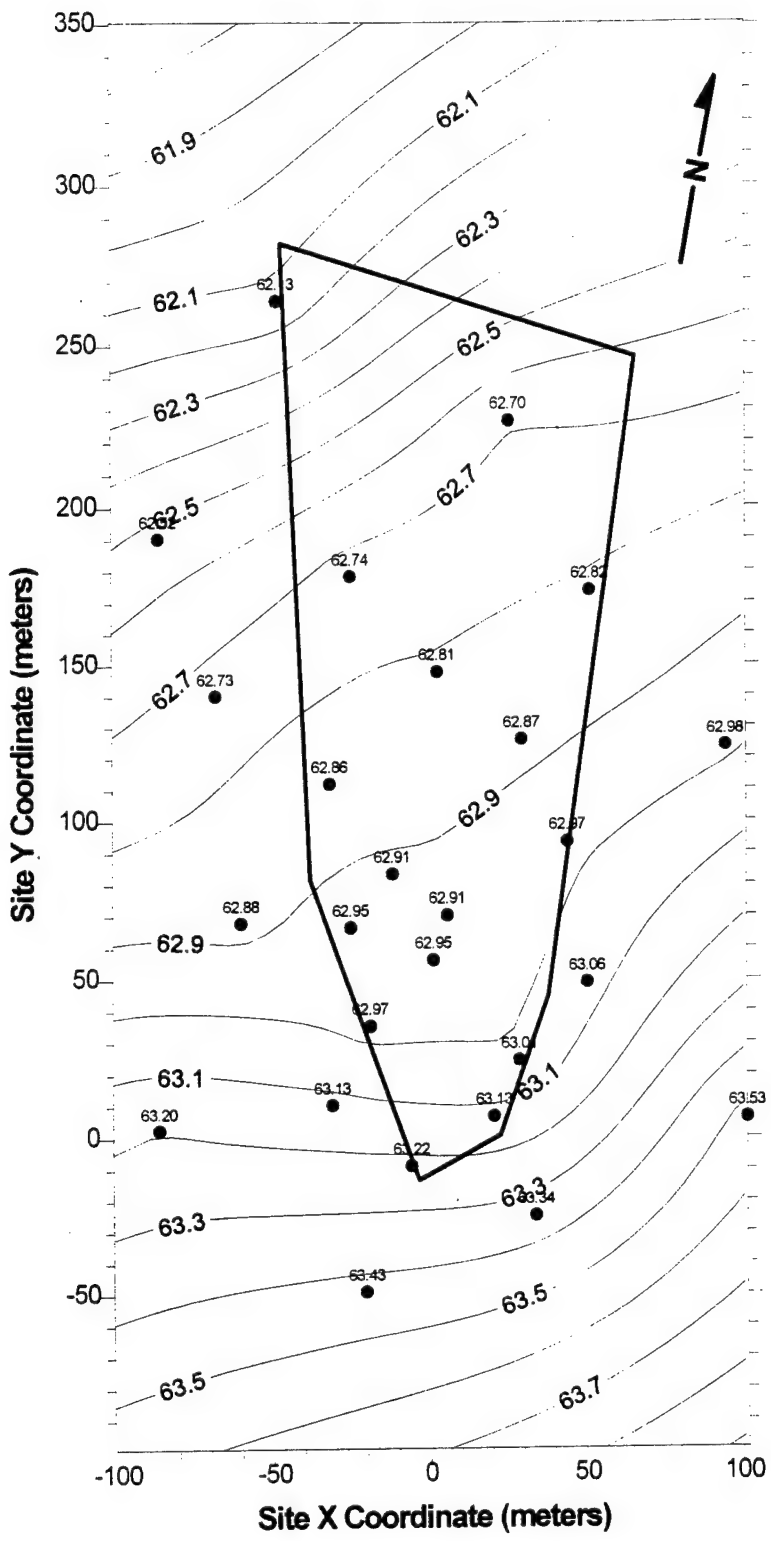

Figure A- 31. Potentiometric Surface Based on Water Levels Measured in B Wells on 06/13/91.

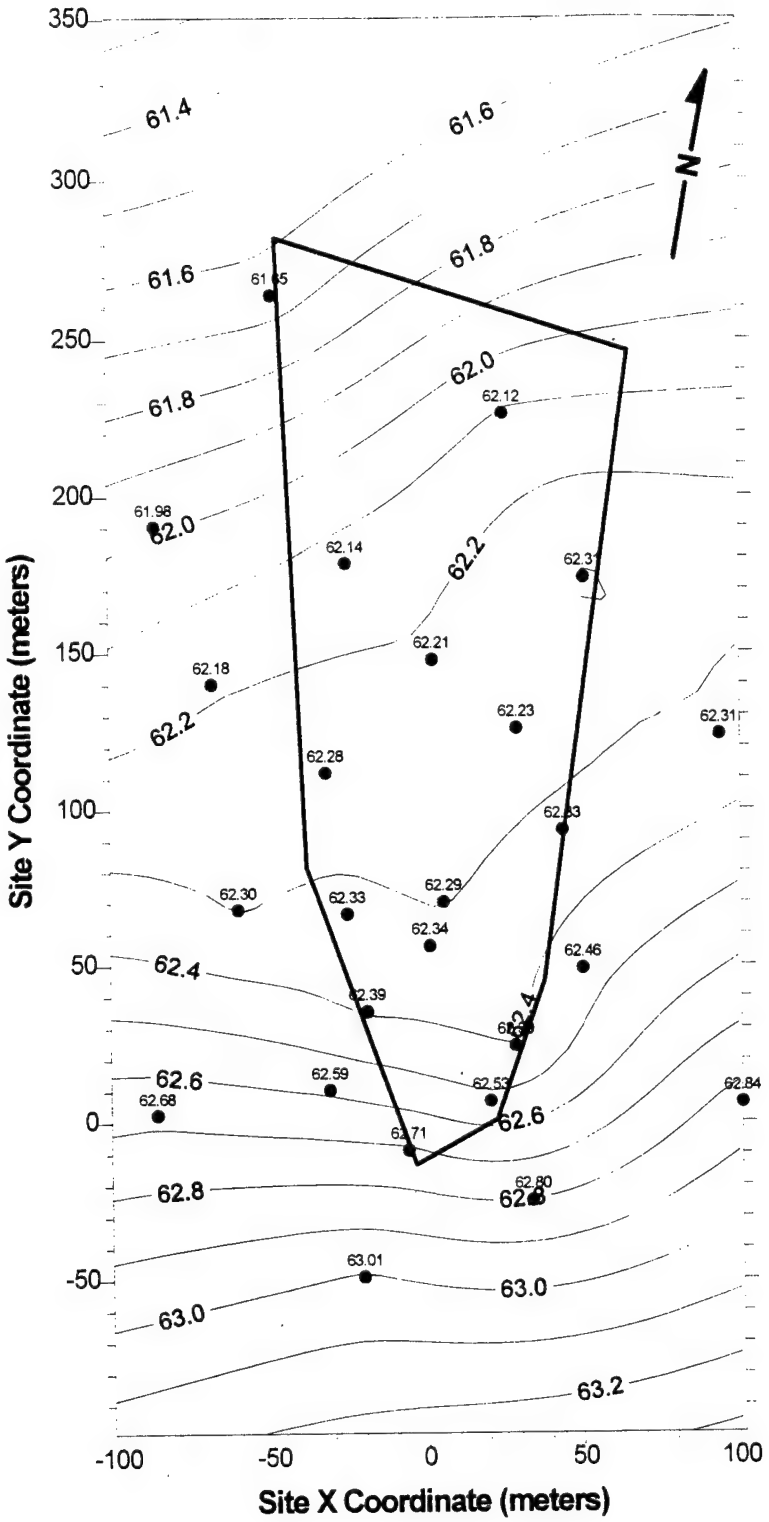

Figure A- 32. Potentiometric Surface Based on Water Levels Measured in B Wells on 07/09/91.

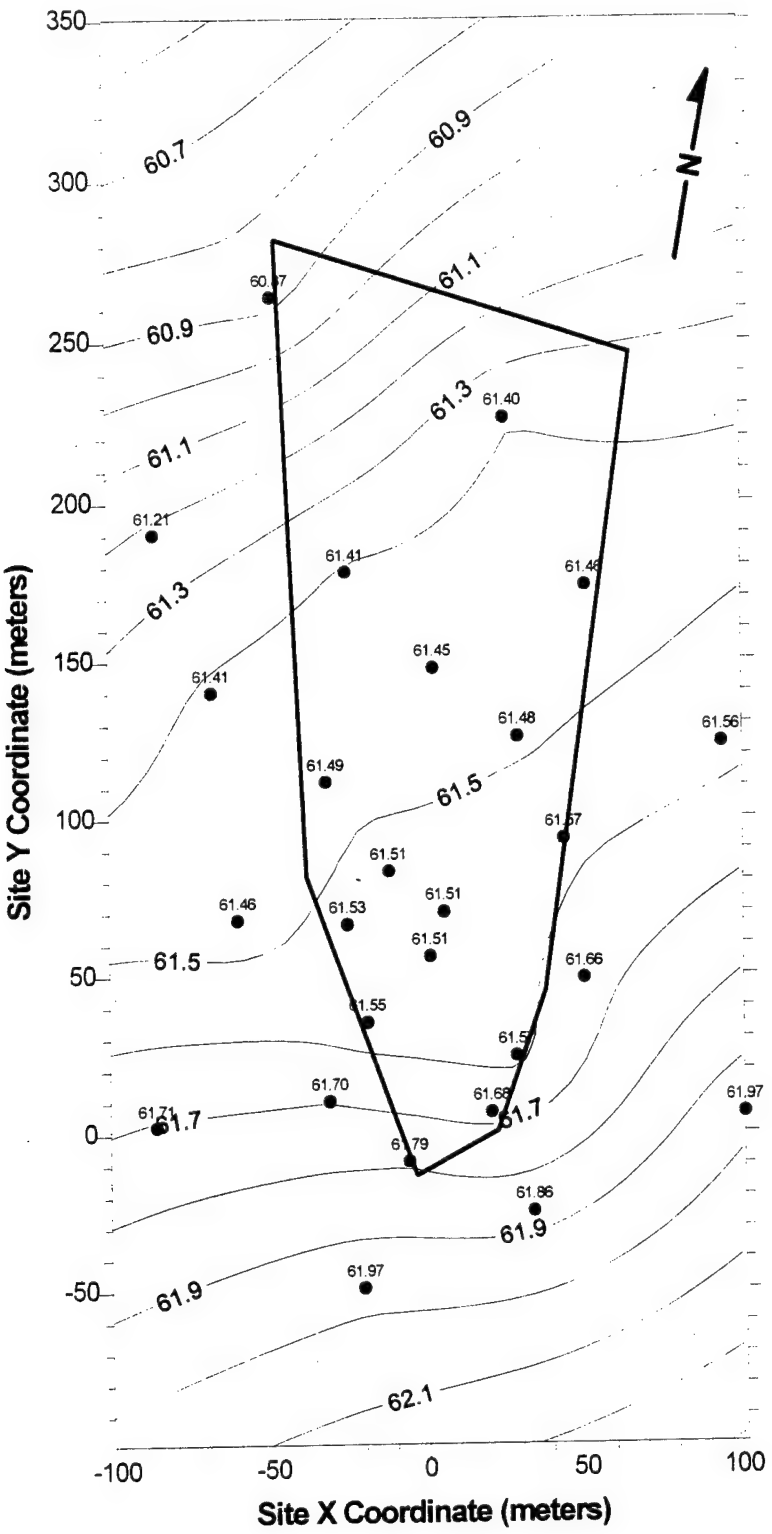

Figure A- 33. Potentiometric Surface Based on Water Levels Measured in B Wells on 08/19/91.

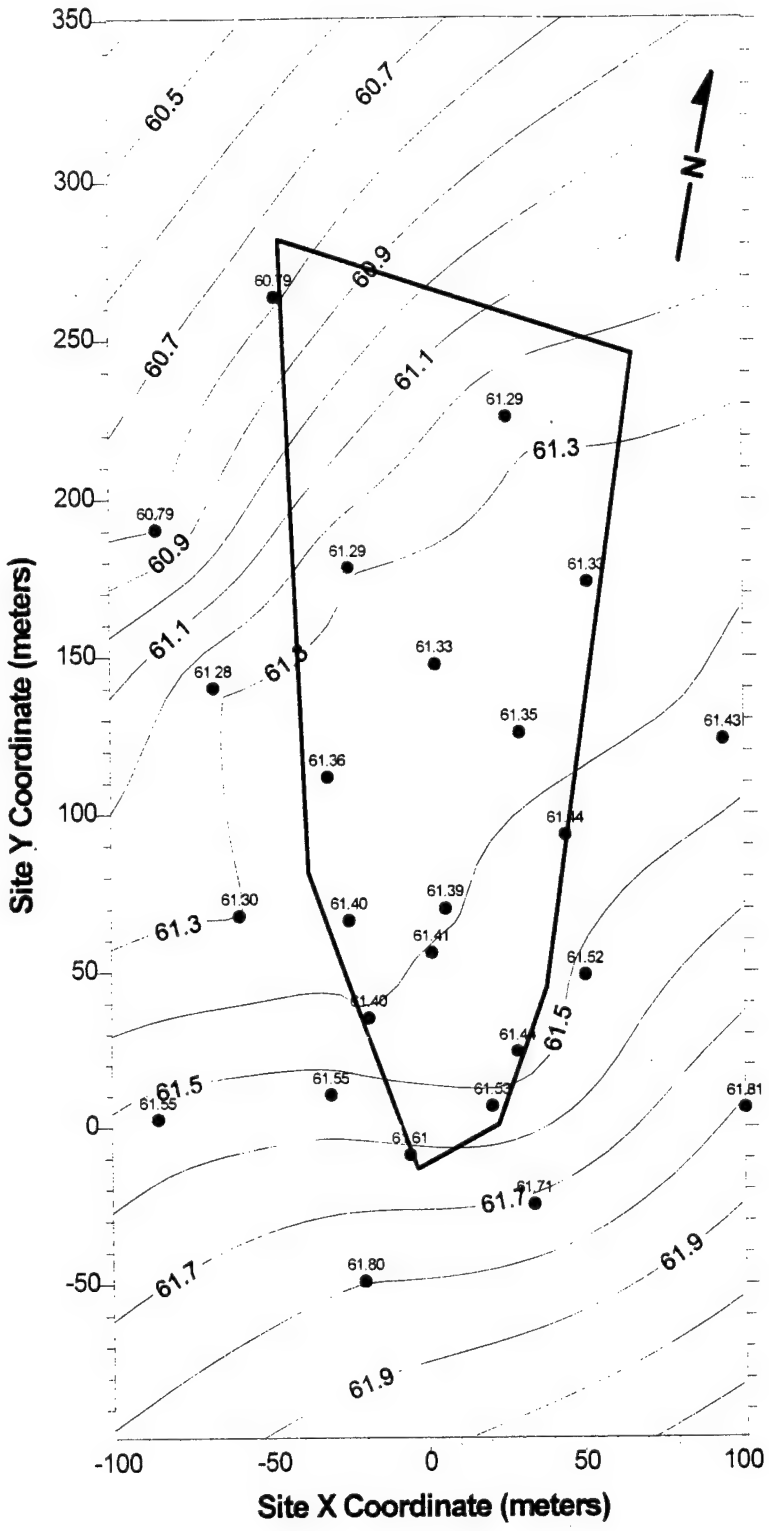

Figure A- 34. Potentiometric Surface Based on Water Levels Measured in B Wells on 09/11/91.

(The reverse of this page is blank.)

APPENDIX B
FLOW MODEL CALIBRATION METHODOLOGY

1.0 INTRODUCTION

This appendix describes the sequence of modifications to the hydraulic conductivity field and boundary conditions that was implemented to calibrate the steady-state flow model for the MADE-2 experiment. Eleven major steps in the process (designated simulations 1 to 11 in this appendix) are documented here. One additional simulation (designated simulation 12 in this appendix) examining the effect of anisotropy in the flow model is also considered. Numerous intermediate simulations incorporating minor boundary or conductivity adjustments will not be discussed. Figures for each simulation illustrating the simulated head contours, the simulated particle track and locations during snapshots 1-4, tritium concentration contours for snapshot 4, and center-of-mass locations of the tritium plume for snapshots 1-4 are included. Figures illustrating the evolution of the hydraulic conductivity field are also included.

Figure B-1 shows the overall decrease in the mean absolute error (MAE) and the root mean squared (RMS) error of head residuals as calibration progressed. Because the main objective of the project was to evaluate the Bioplume II model, the principal goal of flow model calibration was to develop a groundwater velocity distribution that would closely mimic the velocity distribution estimated from the observed tritium plume advance. The error in simulated plume position based on particle tracking is used as the error criterion for the velocity distribution. This value is determined by calculating the distance between the tritium center of mass for snapshots 1-4 documented by Stauffer et al. (1990), and the simulated position of a particle tracked from the injection location. Figure B-2 shows the overall decrease in the velocity error as calibration progressed.

2.0 SIMULATIONS 1-11

Simulation 1, shown in Figure B-3, was the initial steady-state model. Prescribed head boundary conditions for simulation 1 were obtained by averaging observed groundwater elevations, both deep and shallow, over the 16-month period of the MADE-2 experiment and extrapolating to the boundaries of the model. The initial hydraulic conductivity field (Figure B-4) was developed by vertically averaging conductivity measurements for all samples in each well and then interpolating the results as outlined in section IV.C.2.a. A recharge value of 10 inches per year (approximately 15 percent of annual precipitation) was used for simulations 1 through 8. Figure B-3 shows that the simulated groundwater flow direction is significantly different from that indicated by the observed plume. The assumption of steady-state conditions, errors in the kriging estimate of boundary heads, the smallness of the modeled area, and/or possible anisotropy could

have contributed to this problem. Similar results from transient modeling suggest that the steady-state assumption was valid.

To change the simulated groundwater flow direction to better match than that indicated by the observed plume, adjustments were made to the prescribed boundary heads. Figure B-5 shows the results using the adjusted prescribed head boundaries. The general groundwater flow direction is much closer to the observed, but the rate of flow is much too low, indicating the need for higher hydraulic conductivities.

For simulation 3, a new conductivity field equal to twice the original vertically integrated conductivities was used. Figures B-6 and B-7 are the new conductivity field and the simulation 3 model results, respectively. Some improvement in the flow rate due to the increase in hydraulic conductivity was noted, but groundwater flow was still too slow for snapshots 3 and 4.

Analysis of the three-dimensional hydraulic conductivity data indicates interconnected zones of higher conductivity which may be acting as preferential channels for tracer movement. To simulate groundwater moving preferentially through the higher conductivity zones, the aquifer thickness was divided into even increments with conductivity measurements vertically averaged for each increment. The maximum conductivity thus calculated for each well was then assigned as the hydraulic conductivity at the well location. Simulations 4 through 7 used this approach to calculate conductivity fields. Figure B-8 shows the conductivity field developed for simulation 4 using four vertical increments with a thickness of 3 meters each.

Simulation 4 (Figure B-9) shows some improvement over simulation 2, but the rate of flow is still much too low in the far field. Conductivity estimates for simulation 5, shown in Figure B-10, were based on six vertical increments of 2 meters each. Simulation 5 (Figure B-11) shows only minor improvement over simulation 4. For simulation 6, 12 vertical increments were used for calculating the conductivity field (Figure B-12). The model results for simulation 6 are shown in Figure B-13. Since the simulated particle locations for snapshots 3 and 4 are still short of the observed center-of-mass locations, a hydraulic conductivity field developed using 24 vertical increments of 0.5 meters each was tested. Figures B-14 and B-15 show the resulting conductivity field and model output for simulation 7.

Particle tracking indicated that simulated flow velocities were reasonably close to those of the observed plume from the injection point out to about 200 meters (MADE-2 coordinates), beyond which the particle track deviates to the west. The tritium plume, however, starts to curve toward the east between 150 meters and 200 meters. Two methods were tested for turning the simulated flow more toward the east. First, a narrow low-conductivity strip was inserted across the model along the northern edge of the abandoned meander channel to act as a flow barrier. This method influenced the simulated flow direction, but resulted in unrealistic head contours. The second approach was based on the lack of well control for conductivity in the northwest

corner of the model area and the location of the meander channel. Since there are no flowmeter wells in the northwest corner of the model area, the fan of conductivity values in that area (see Figure B-14) has no data support and is probably an artifact of the interpolation algorithm. Conductivity zones northwest of the meander channel should probably parallel the channel and decrease in value away from the channel. The conductivity field for simulation 7 was modified based on this concept and the result is shown in Figure B-16. The results of simulation 8 are shown in Figure B-17. The simulated flow direction in the far field is much closer to that of the observed tritium plume, although simulated flow closer to the injection point has moved slightly off the observed tritium plume centerline.

Simulation 9 (Figure B-18) is the result of minor adjustments to the simulation 8 conductivity field, an increase in precipitation recharge to 17 inches/year (approximately 25 percent of annual precipitation), and new boundary head values based on the average of the observed heads for the shallow wells. Prescribed head boundaries were obtained by extrapolating the observed head information to the model boundaries and then modifying the resulting values to properly orient the simulated flow along the observed path of the tritium plume. Simulation 9 shows a marked improvement in the hydraulic head calibration measures, the simulated flow direction, and the simulated position for the tracked particle for snapshot 2. It does, however, adversely affect the simulated positions of the tracked particle for snapshots 3 and 4, indicating the need for higher conductivity beyond the snapshot 2 center of mass location.

Additional minor adjustments to the hydraulic conductivity field resulted in simulation 10, shown in Figure B-19. Particle tracking demonstrates that simulated flow closely follows the center of the observed tritium plume out to about 200 meters (MADE-2 coordinates), at which point the observed plume starts to curve more sharply to the east than the simulated particle track. The overall position error for the four snapshots has also decreased significantly. This was the final simulation using the original 6.096 meters (20 feet) by 7.62 meters (25 feet) grid spacing. Bioplume II simulations using these results indicated that grid refinement was required to avoid excessive numerical dispersion.

The refined grid, with a 1.524 meters (5 feet) grid spacing in both directions, was used for simulation 11 (Figure B-20). Because the refined grid was smaller than the original grid, new prescribed head boundaries were interpolated from the simulation 10 model results. The conductivity field used for simulation 11 (Figure B-21) was developed by some minor modification of the simulation 10 conductivity field. Particle tracking demonstrates that simulated flow closely follows the center of the observed tritium plume out to about 200 meters (MADE-2 coordinates), at which point the observed plume starts to curve more sharply to the east than the simulated particle track. The main goal of calibration for this flow model was to develop a groundwater velocity distribution throughout the transport domain that would closely mimic the velocity distribution estimated by monitoring the tritium plume during the MADE-2 experiment.

Since the simulation 11 results met this criterion in the region of interest for the Bioplume II modeling, it was determined to have met the calibration requirements for the flow model.

3.0 ANISOTROPY

Comparison of the regional flow direction at the MADE site to the transport direction of the tritium plume suggests the possibility of anisotropic conditions. Based on this observation, simulation 12 (Figure B-22) was designed to test the effect of anisotropy on the flow model results. An anisotropy factor of three was used. Prescribed head boundaries were obtained by extrapolating the average of the observed heads for the shallow wells to the model boundaries. Precipitation recharge was set at 17 inches/year (approximately 25 percent of annual precipitation). The hydraulic conductivity field used was the same as that used for simulation 8.

Particle tracking shows that including anisotropy does help turn the simulated flow direction toward that of the observed tritium plume. However, since anisotropy at the site is most likely associated with the abandoned meander channel, applying an anisotropy factor to the whole model is probably inappropriate. Because Bioplume II does not allow for a variable anisotropy factor, this approach was not used.

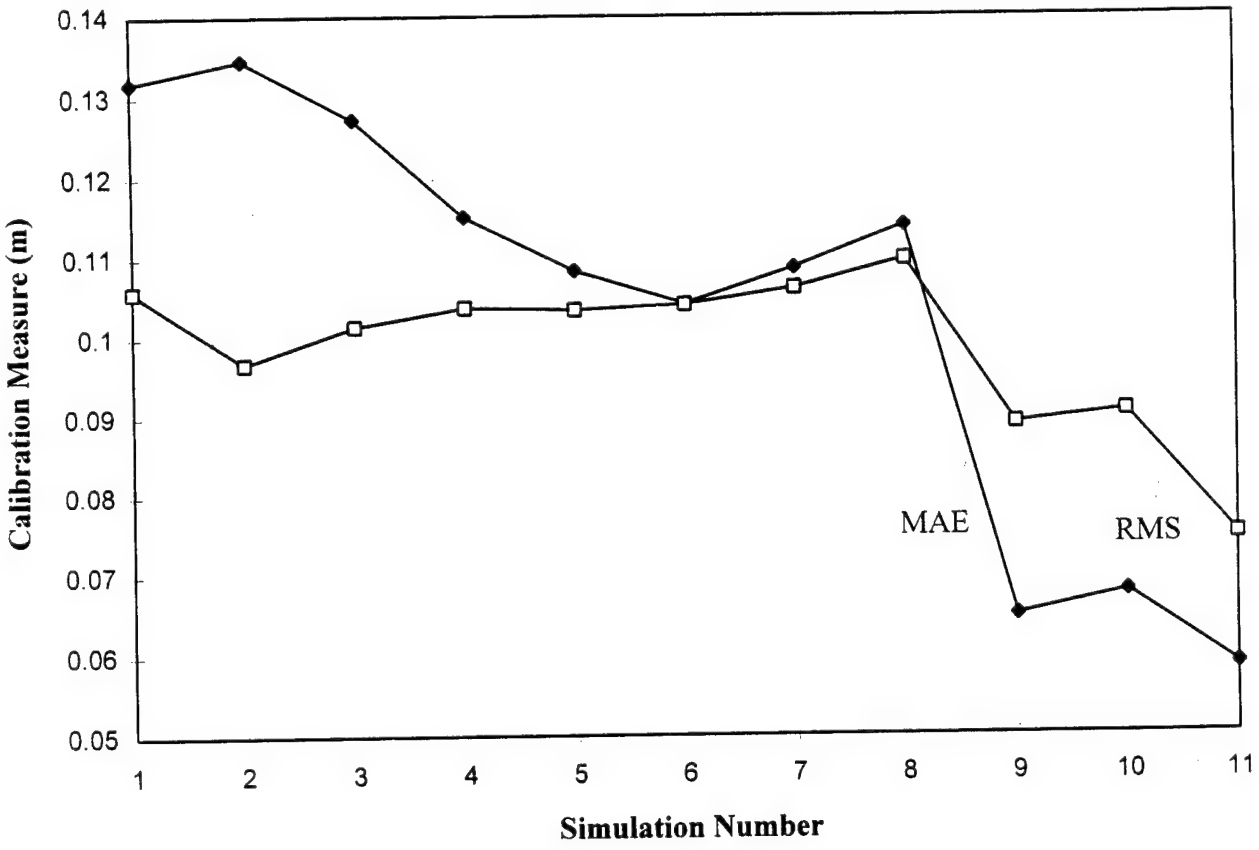

Figure B-1. Head Calibration Error for Simulations 1 through 11.

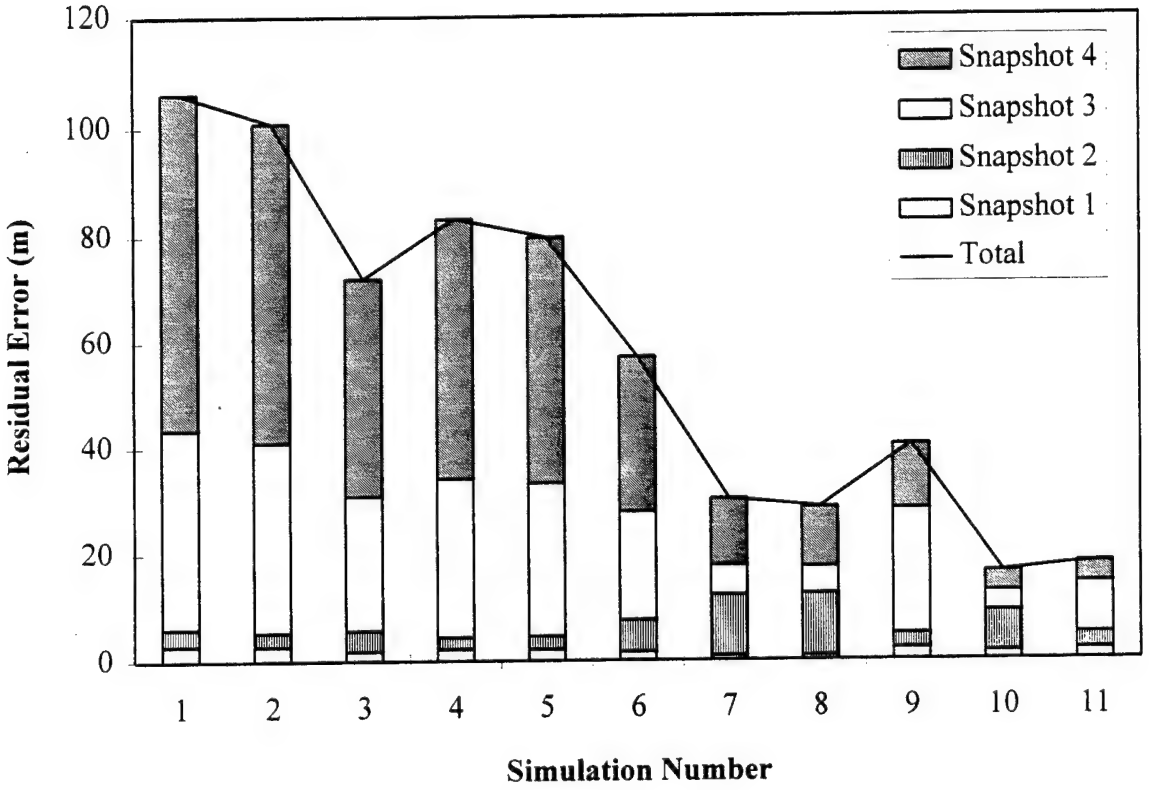

Figure B-2. Residual Error in the Simulated Plume Position Based on Observed Tritium Center of Mass Locations.

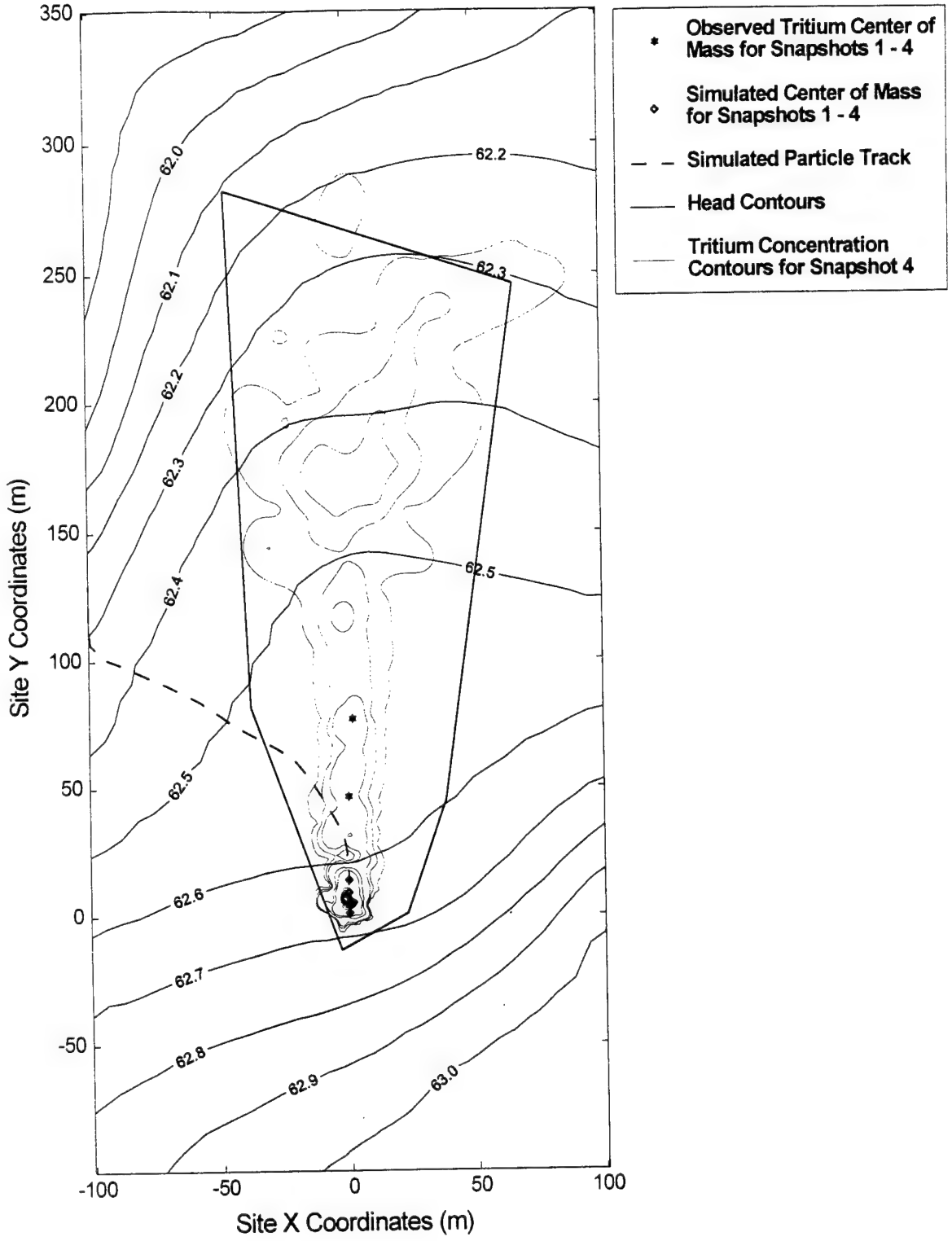

Figure B-3. Simulation 1 : Steady-State Simulated Heads (m amsl) Resulting from the Initial Assumptions for Hydraulic Conductivities and Boundary Conditions.

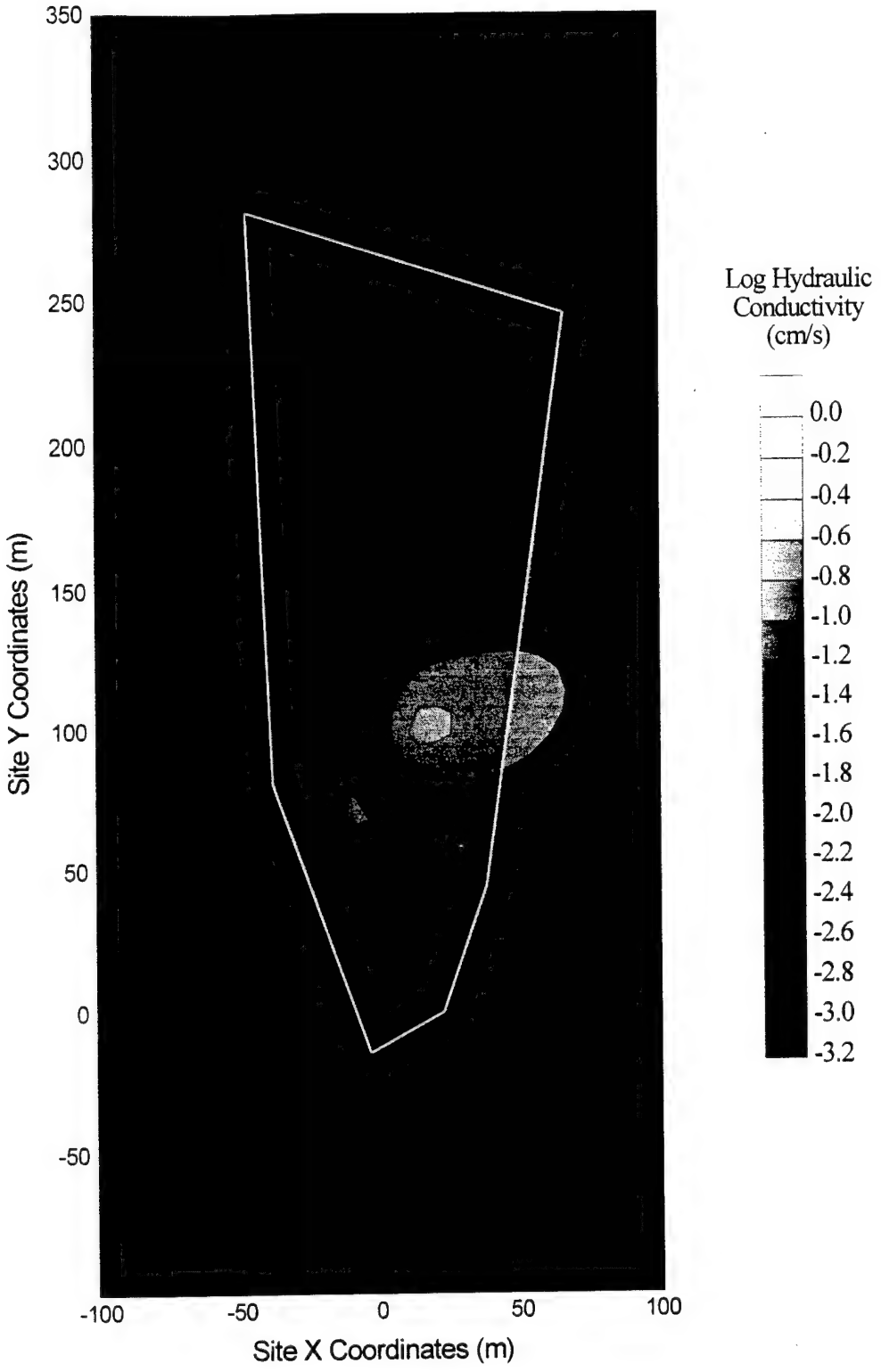

Figure B-4. Initial Hydraulic Conductivity Field (Used for Simulations 1 and 2).

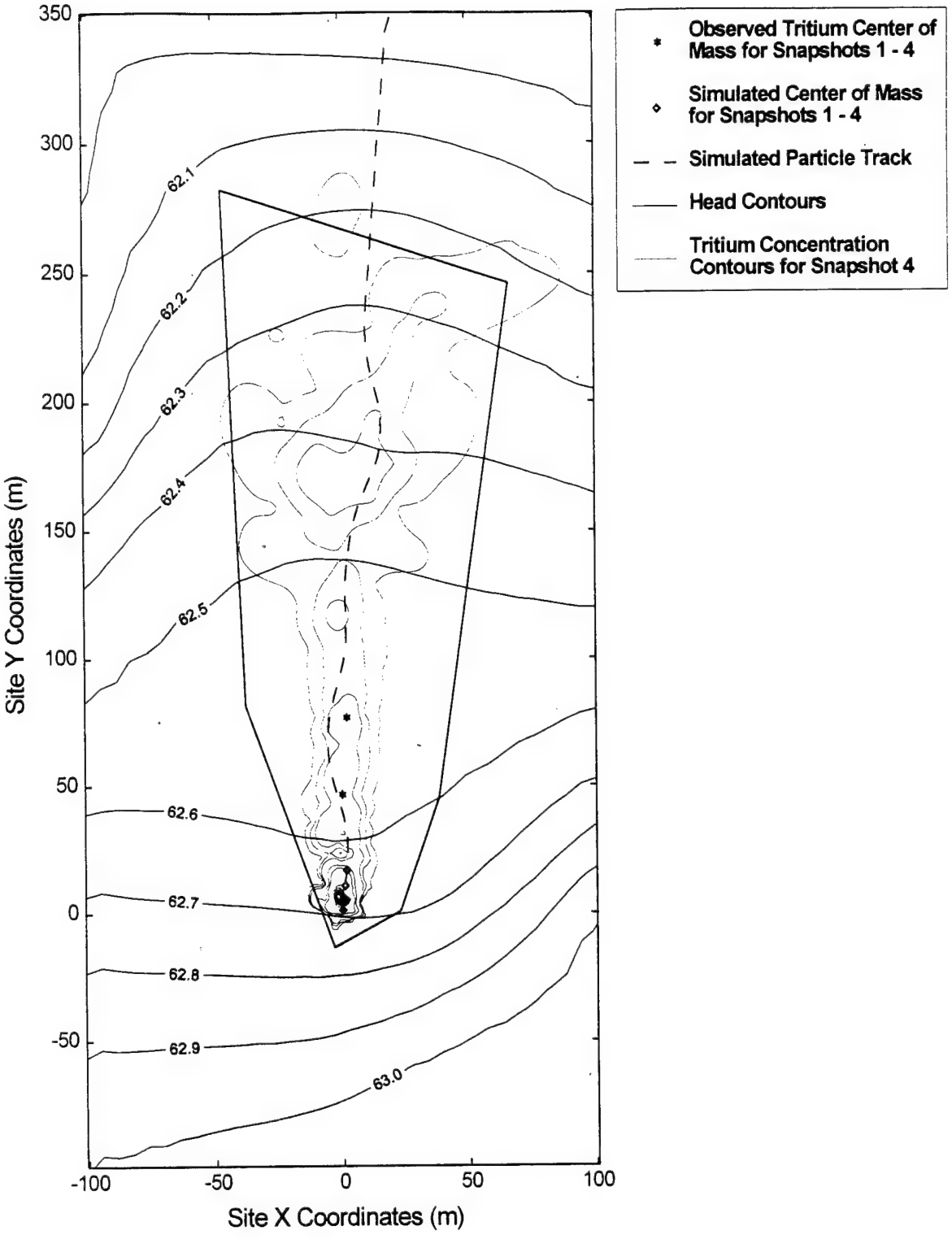

Figure B-5. Simulation 2 : Steady-State Simulated Heads (m amsl) Resulting from the Modification of Simulation 1 Prescribed Head Boundaries.

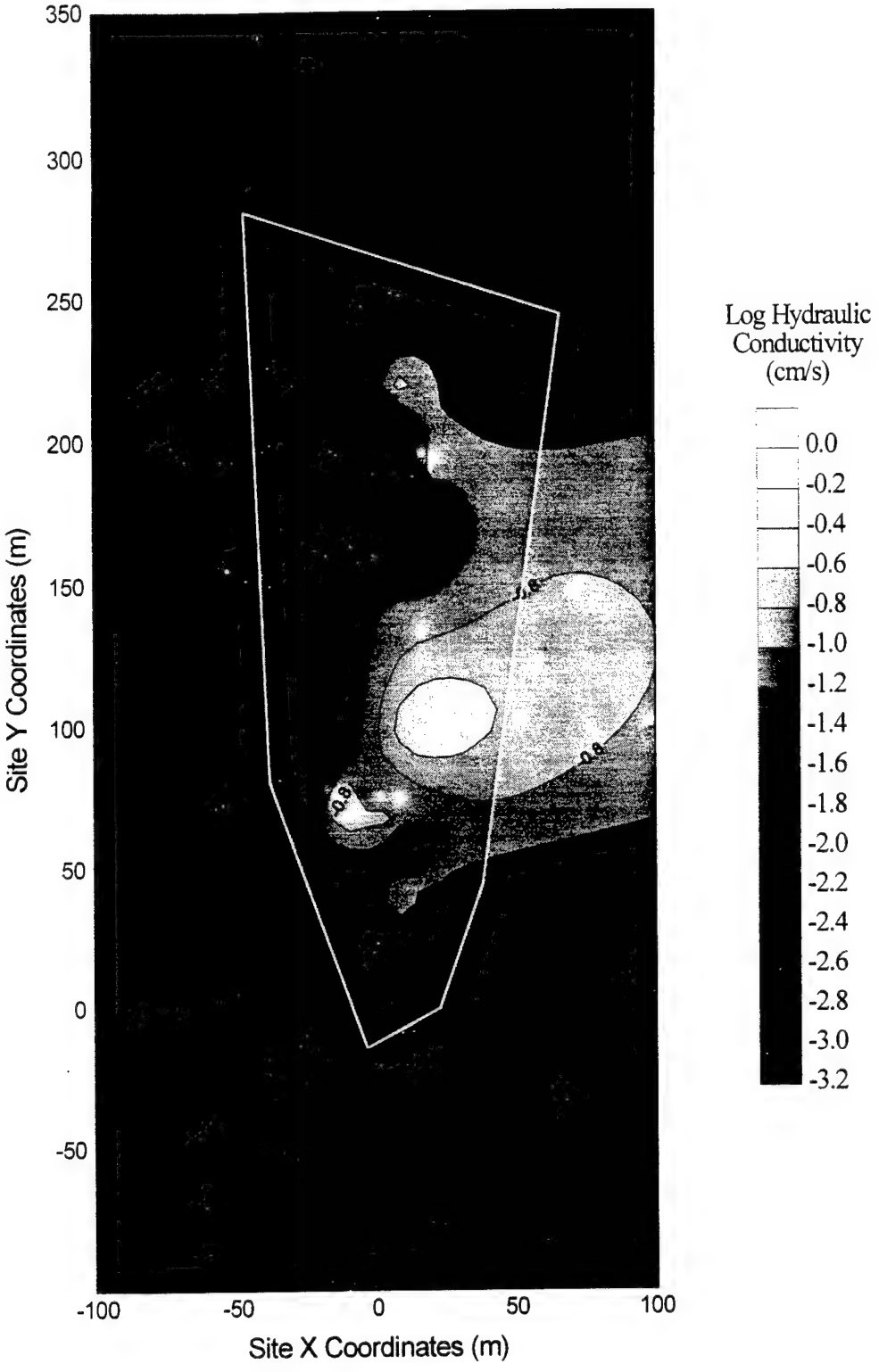

Figure B-6. Hydraulic Conductivity Field Equal to Two Times the Vertically Averaged Values (Used for Simulation 3).

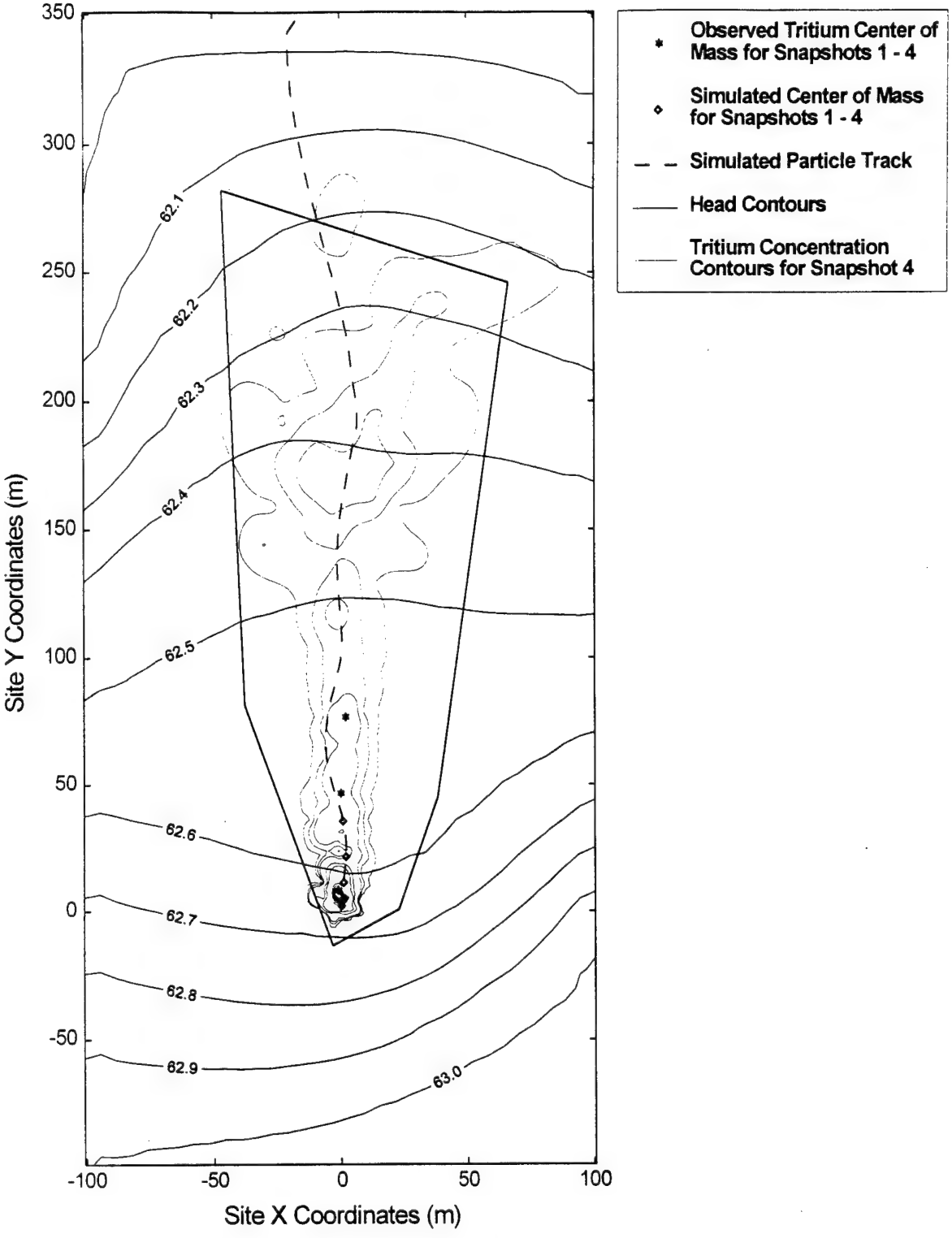

Figure B-7. Simulation 3 : Steady-State Simulated Heads (m amsl) with New Hydraulic Conductivities (2 x original).

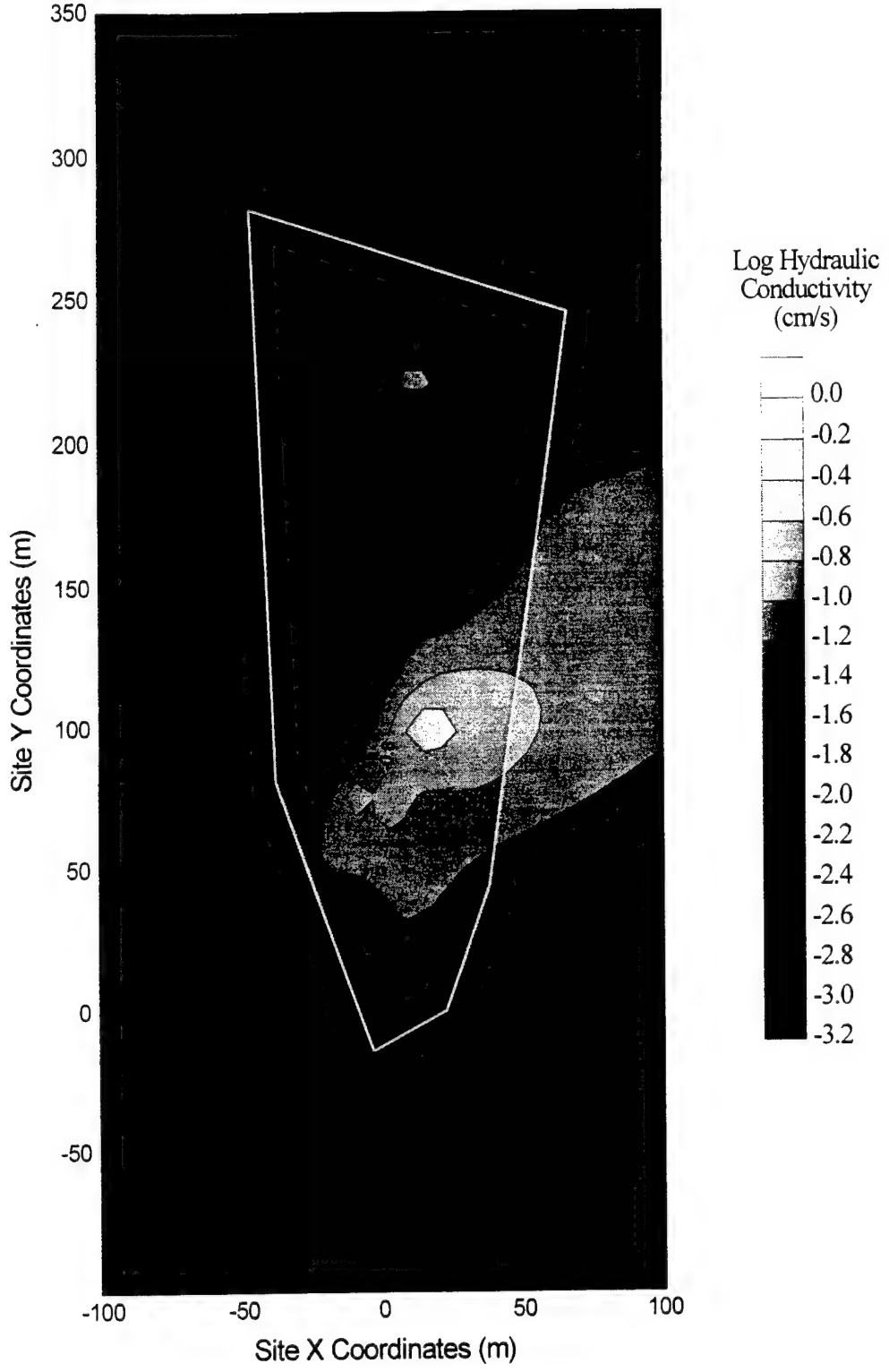

Figure B-8. Hydraulic Conductivity Field Based on Four 3-meter Thick Vertical Increments (Used for Simulation 4).

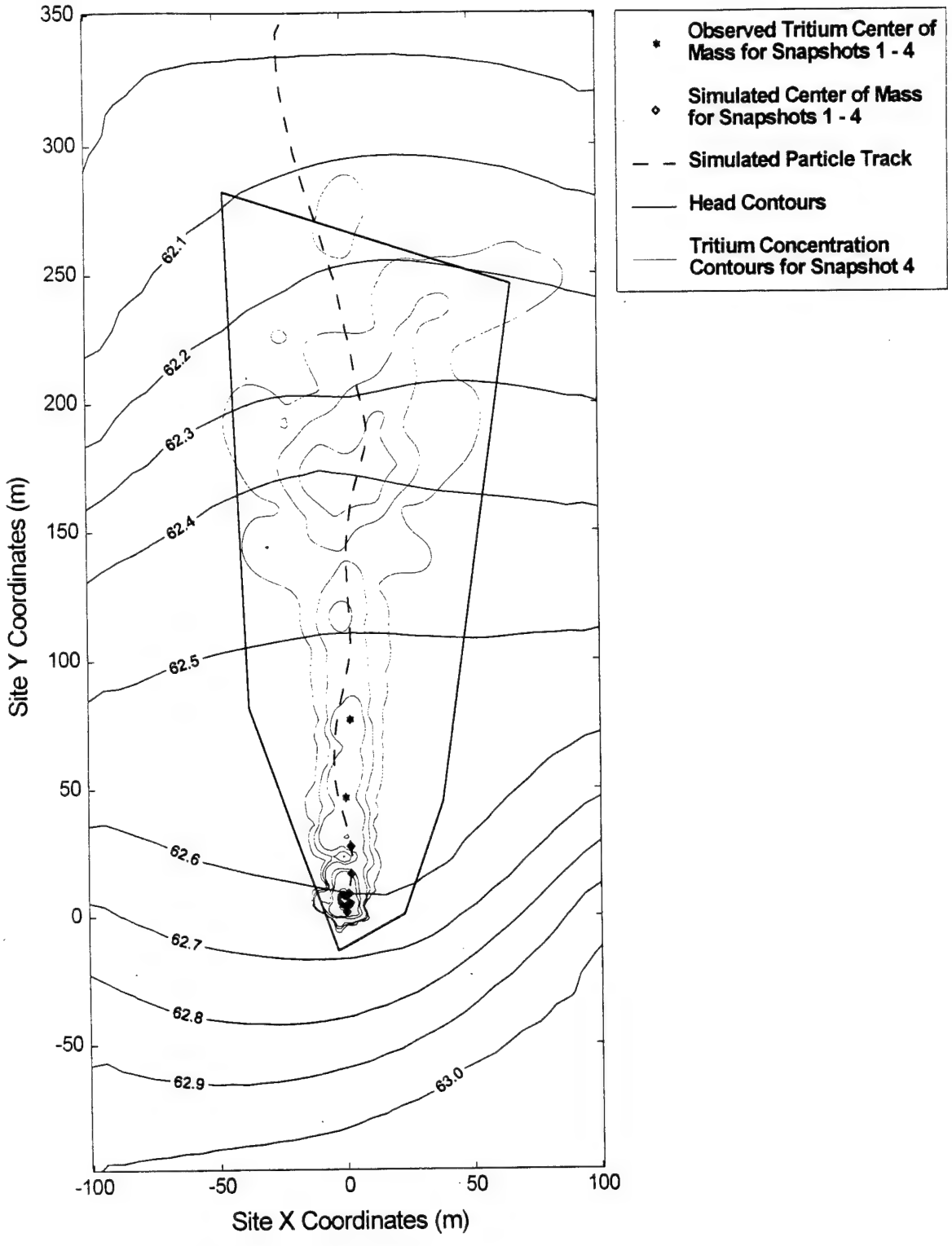

Figure B-9. Simulation 4 : Steady-State Simulated Heads (m amsl)
(Hydraulic Conductivity Field Shown in Figure B-8).

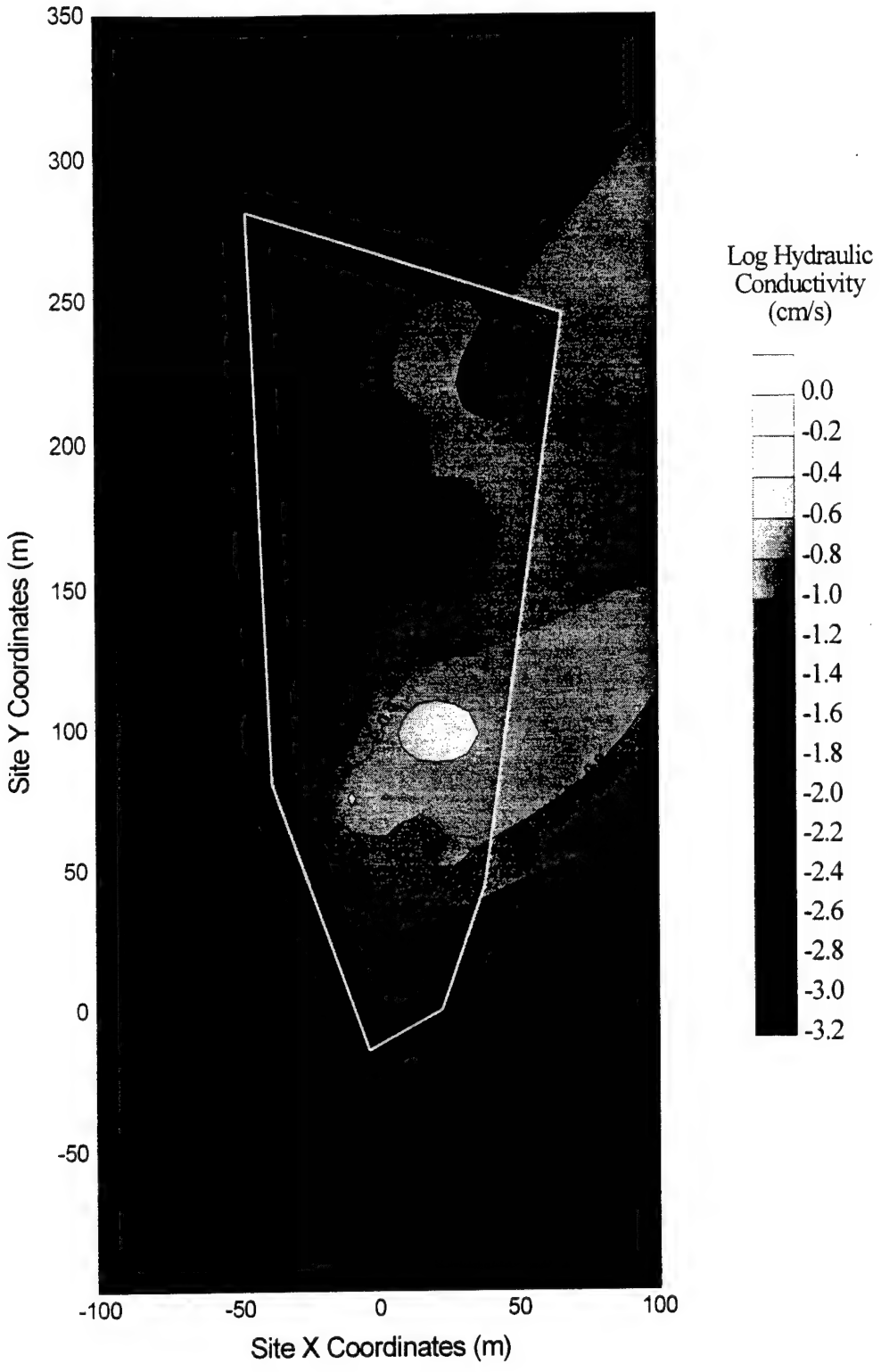

Figure B-10. Hydraulic Conductivity Field Based on Six 2-meter Thick Vertical Increments (Used for Simulation 5).

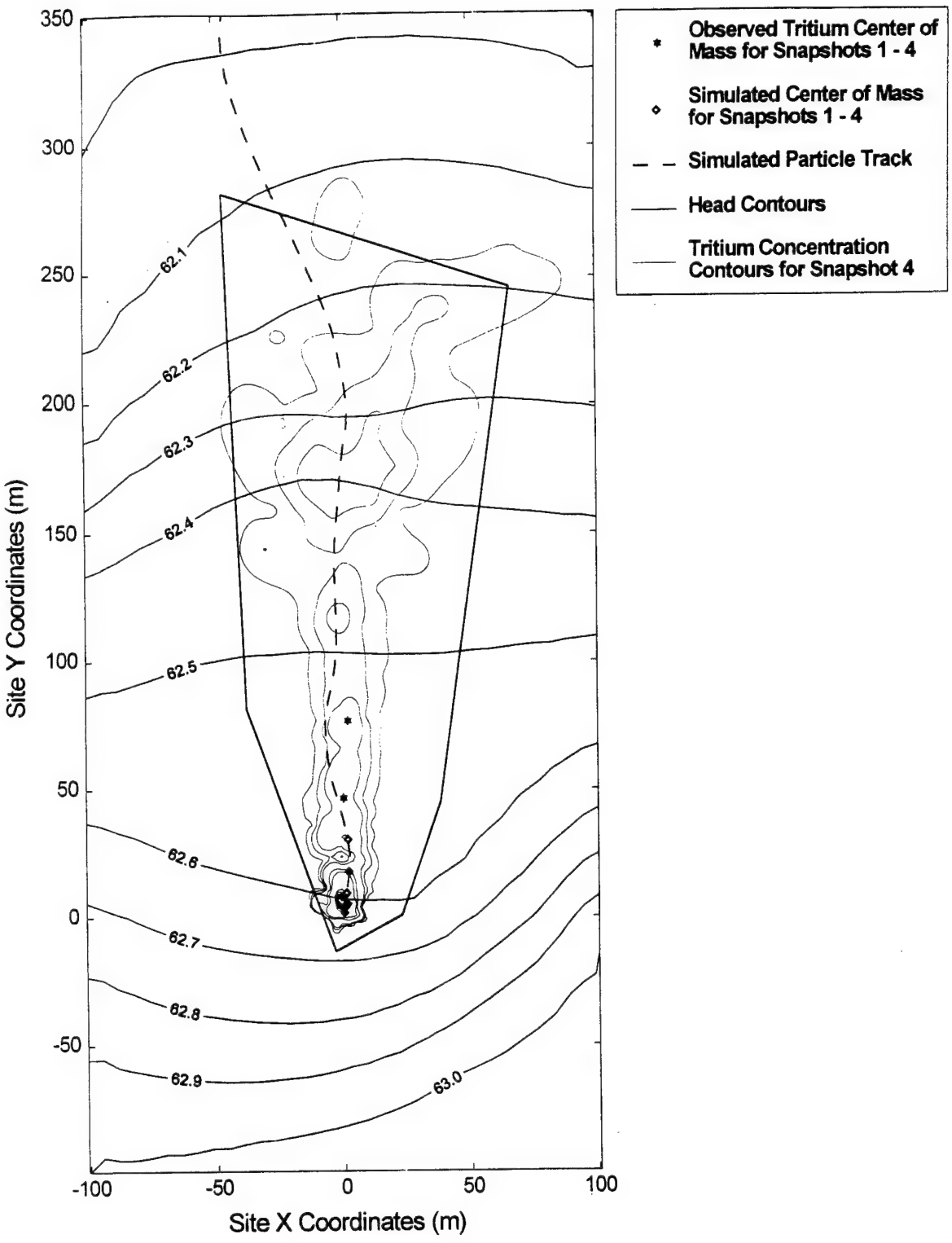

Figure B-11. Simulation 5 : Steady-State Simulated Heads (m amsl) (Hydraulic Conductivity Field Shown in Figure B-10).

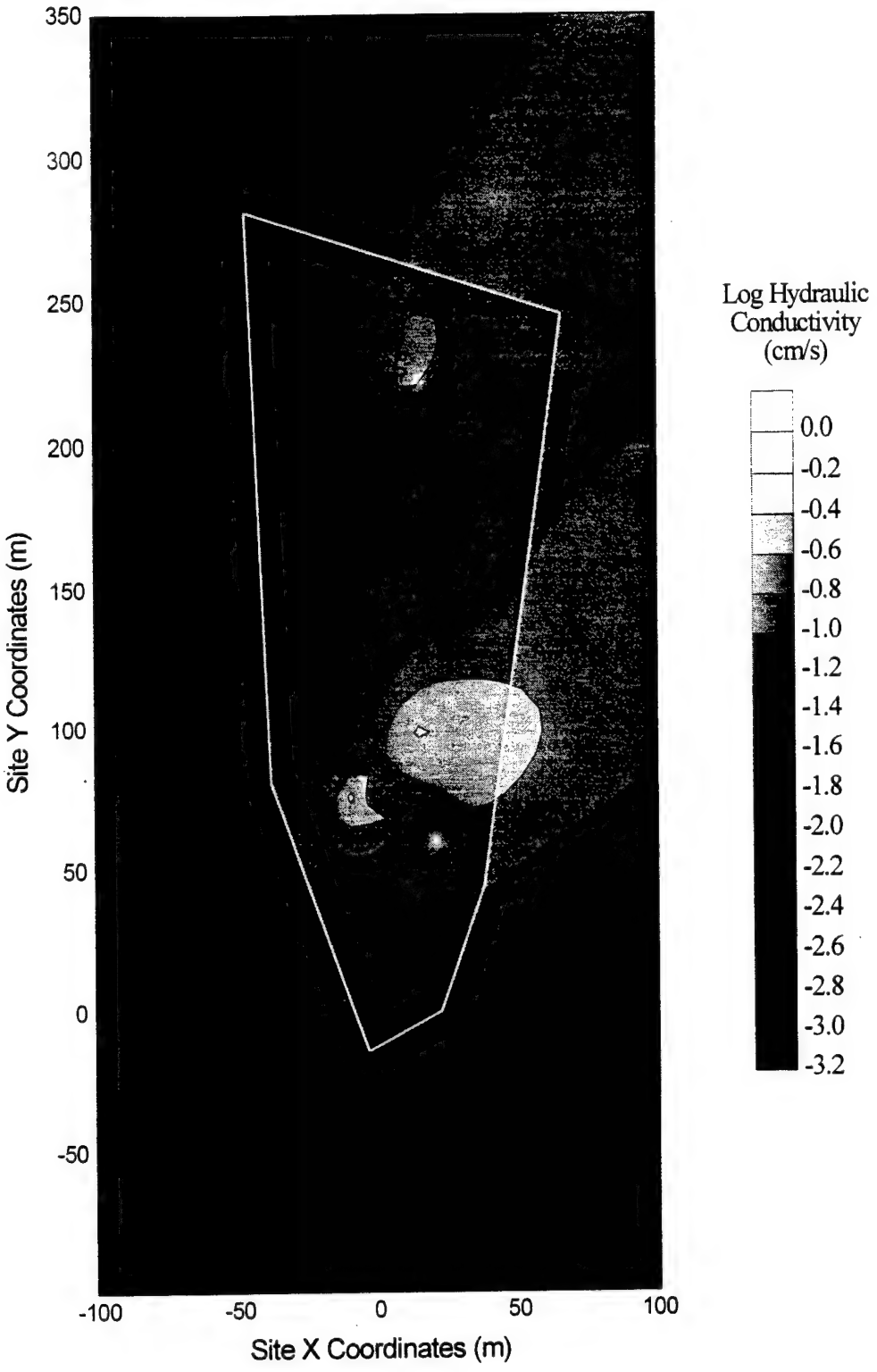

Figure B-12. Hydraulic Conductivity Field Based on 12 1-meter Thick Vertical Increments (Used for Simulation 6).

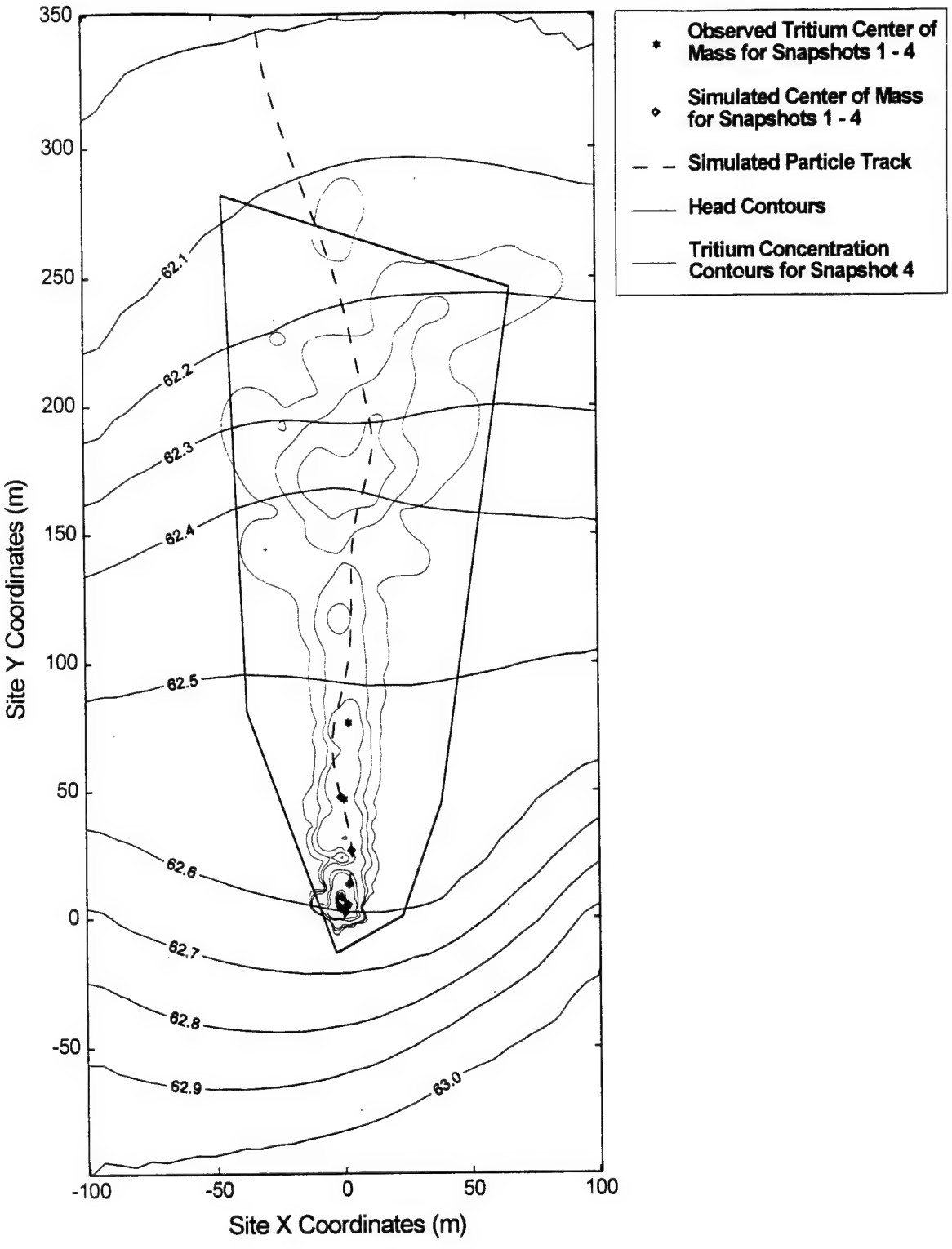

Figure B-13. Simulation 6 : Steady-State Simulated Heads (m amsl)
(Hydraulic Conductivity Field Shown in Figure B-12).

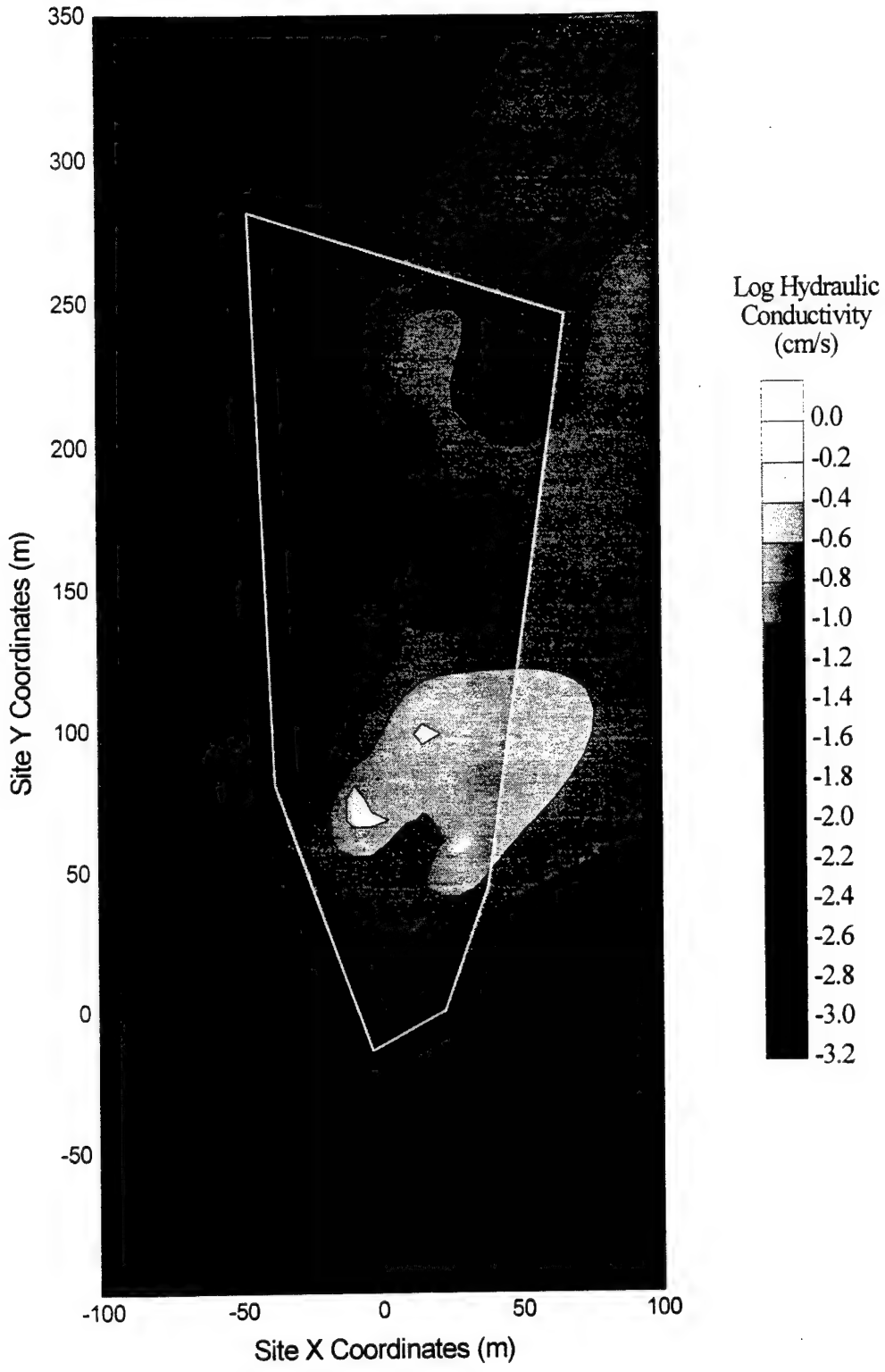

Figure B-14. Hydraulic Conductivity Field Based on 24 0.5-meter Thick Vertical Increments (Used for Simulation 7).

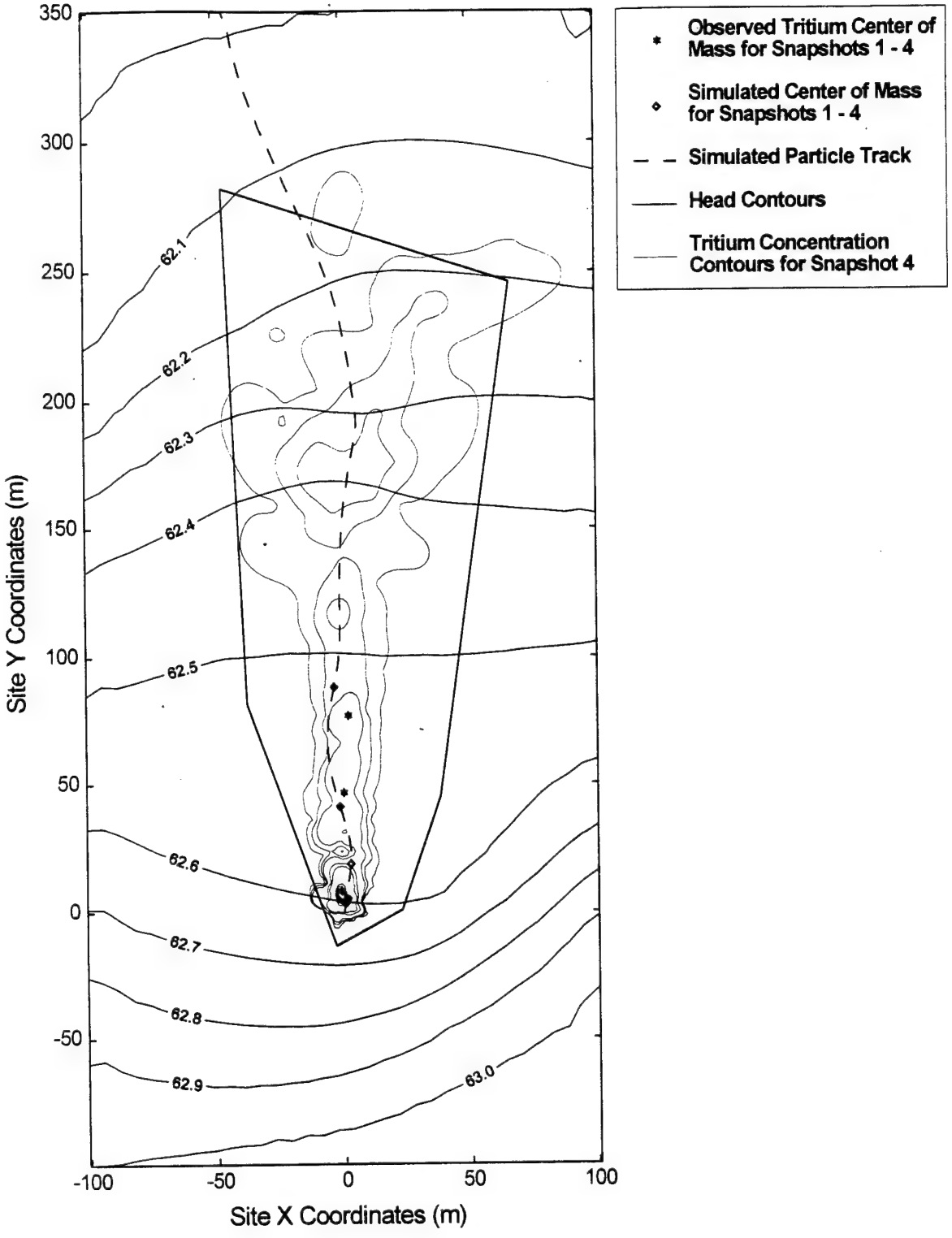

Figure B-15. Simulation 7 : Steady-State Simulated Heads (m amsl)
(Hydraulic Conductivity Field Shown in Figure B-14).

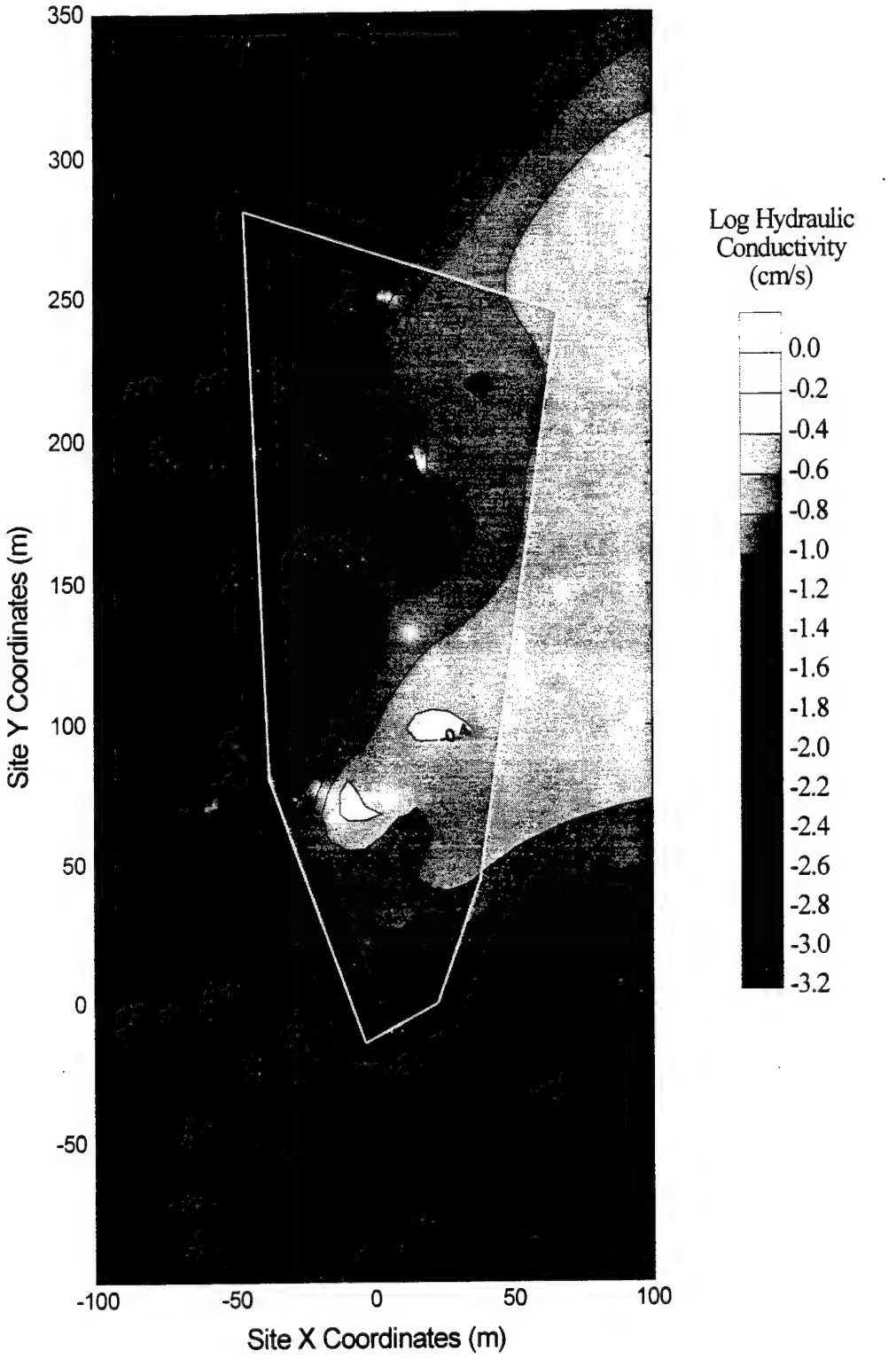

Figure B-16. Hydraulic Conductivity Field Based on 24 0.5-meter Thick Vertical Increments and Modified in the Northwest Corner (Used for Simulation 8.

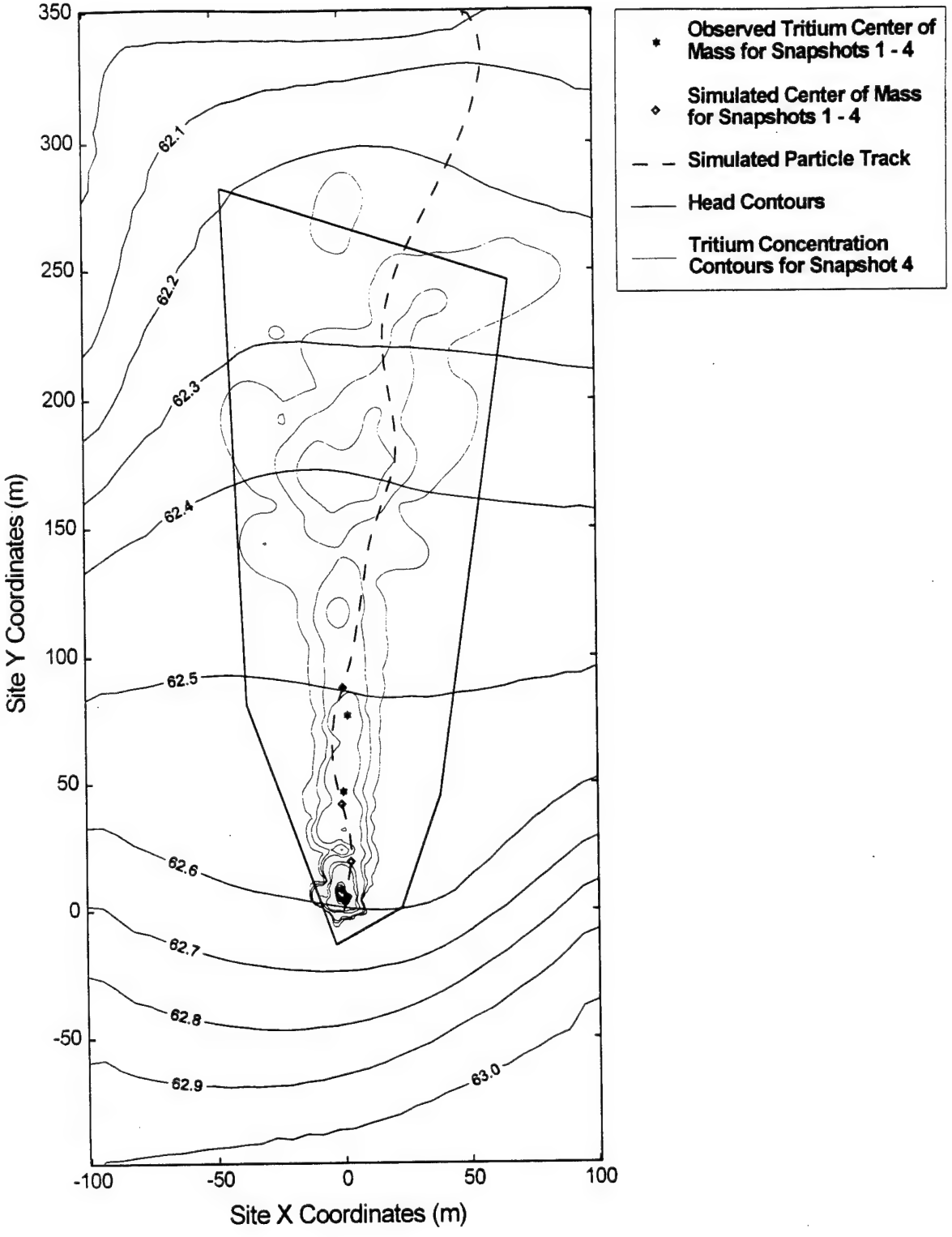

Figure B-17. Simulation 8 : Steady-State Simulated Heads (m amsl) (Hydraulic Conductivity Field Shown in Figure B-16).

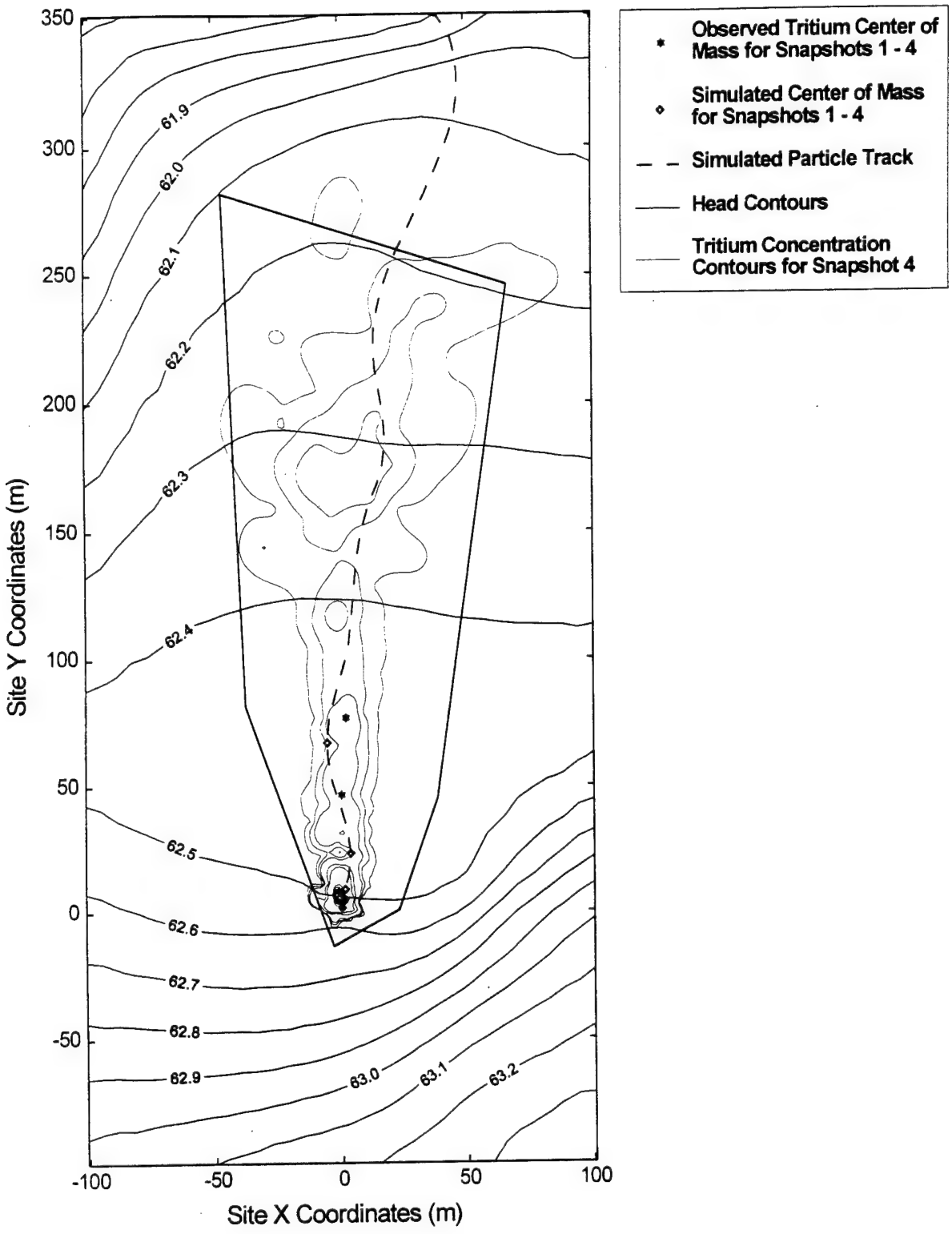

Figure B-18. Simulation 9 : Steady-State Simulated Heads (m amsl).

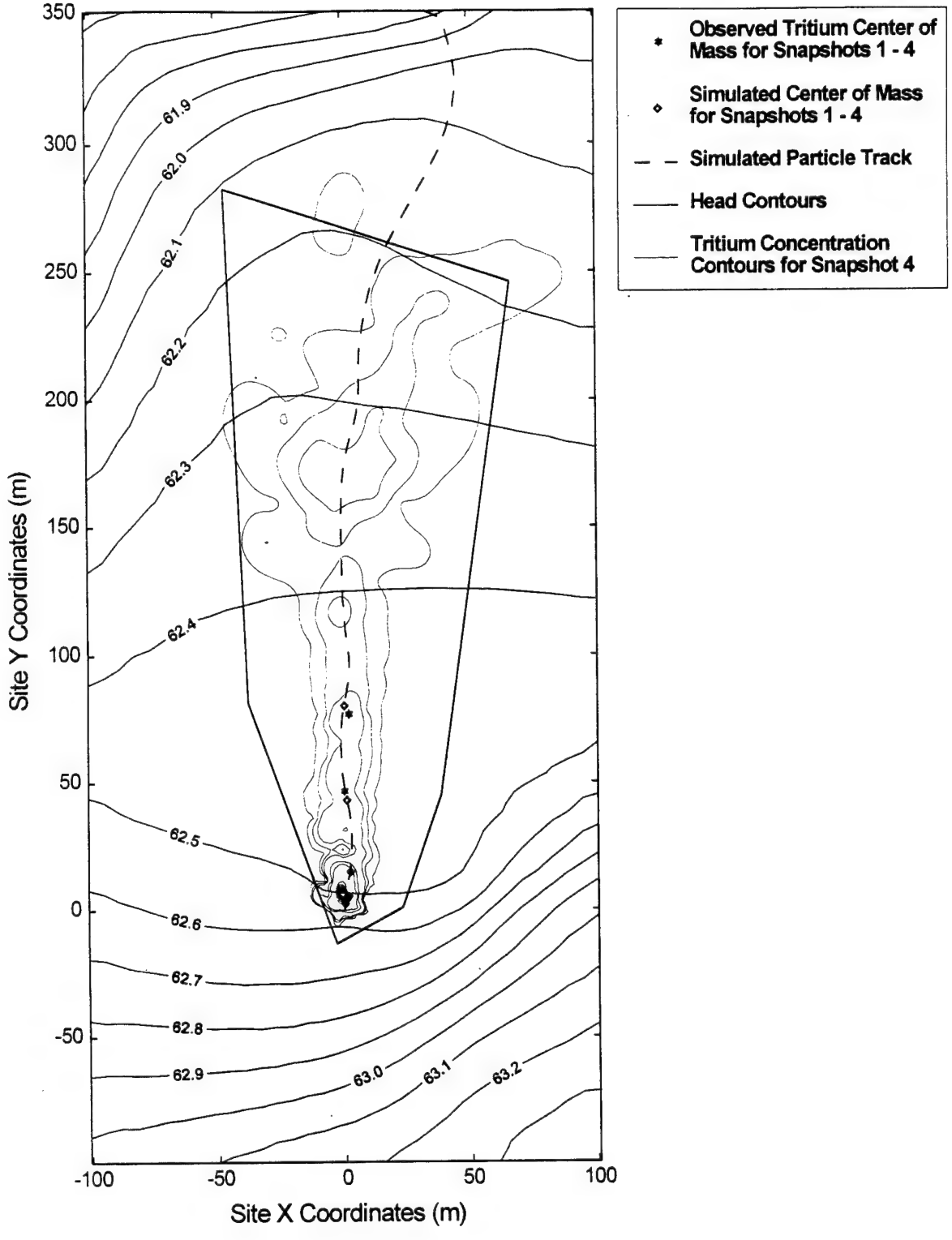

Figure B-19. Simulation 10 : Steady-State Simulated Heads (m amsl).

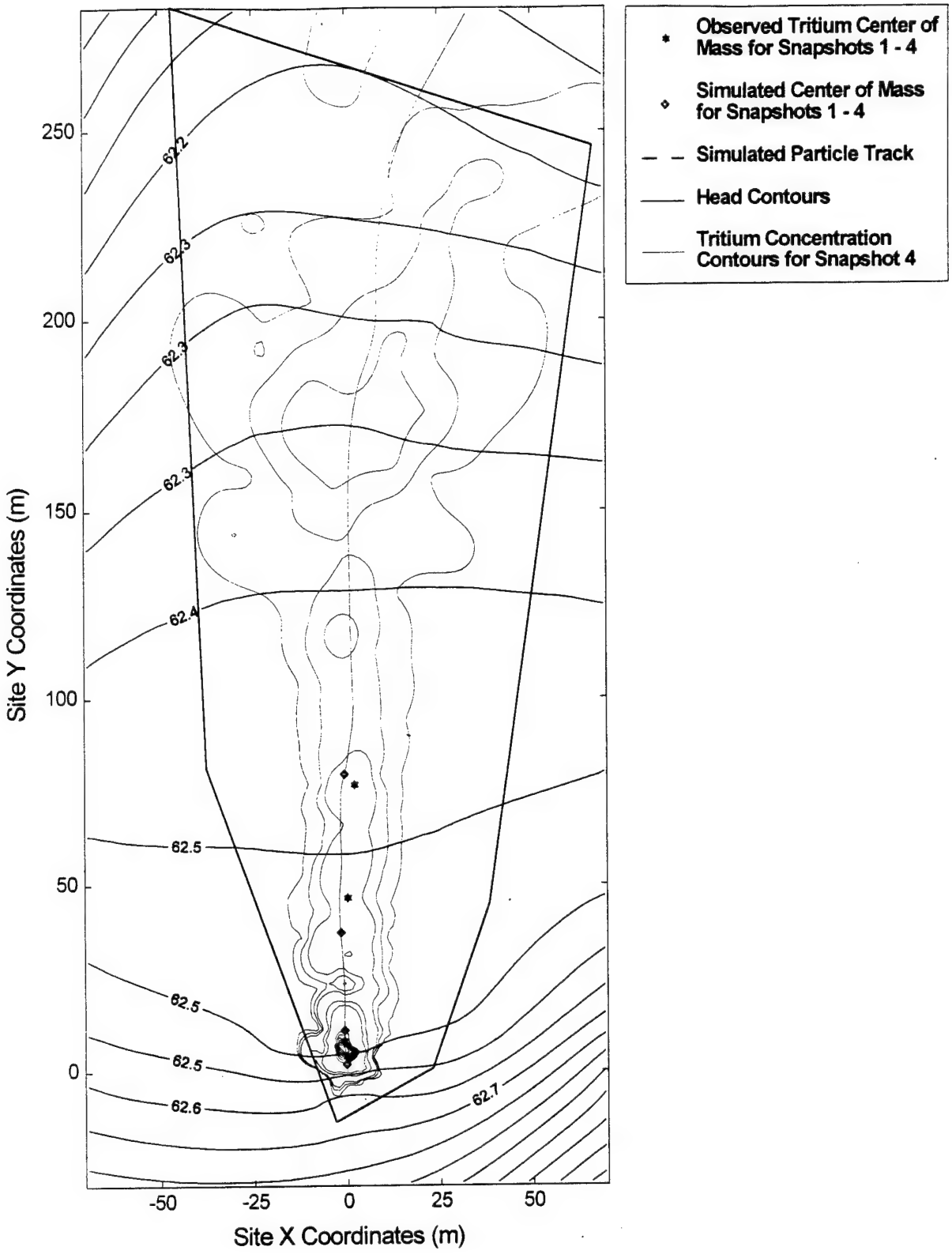

Figure B-20. Simulation 11 : Steady-State Simulated Heads (m amsl) from Refined Grid Model.

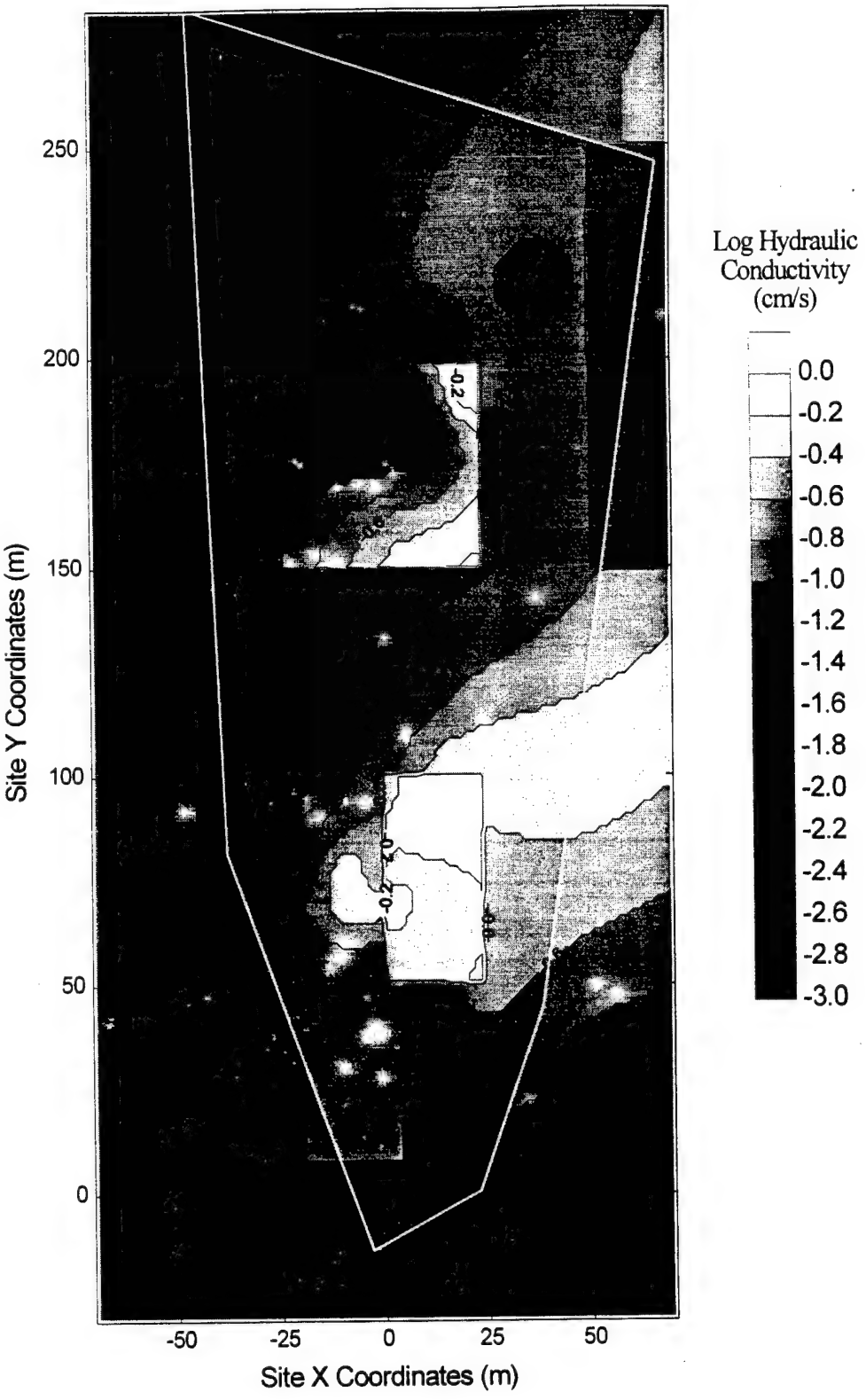

Figure B-21. Final Hydraulic Conductivity Field.

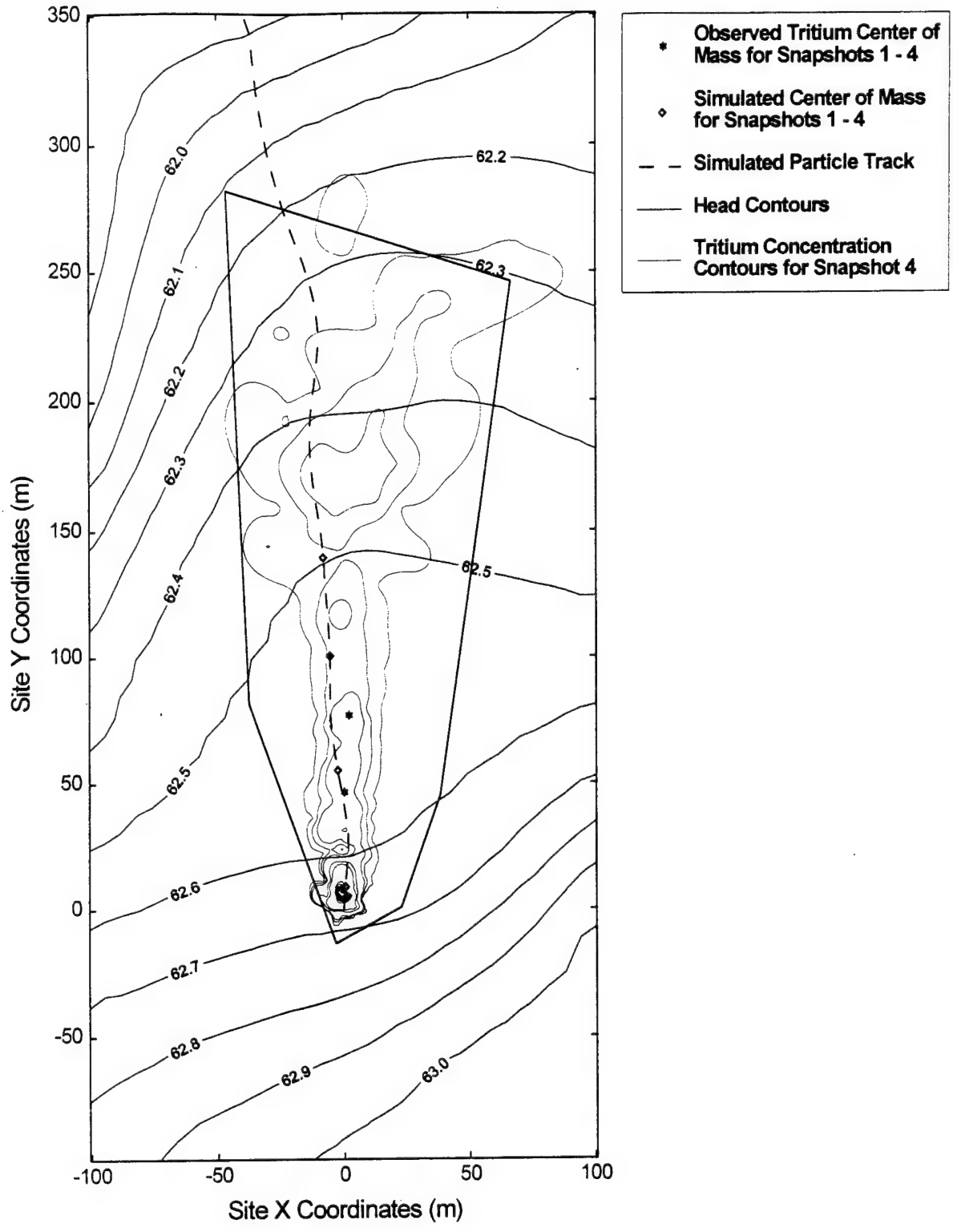

Figure B-22. Simulation 12 : Steady-State Simulated Heads (m amsl) (Anisotropy Factor of Three).

APPENDIX C
INTERPOLATED VERTICALLY AVERAGED PLUMES

Figures C-1 through C-5 show the contoured vertically averaged tritium concentration data collected at Snapshots 1 through 5, respectively. These figures also contain the MLS data locations used to generate the maps. The legend explains which locations were used to interpolate the contour maps. A well or MLS had to have at least five sampling locations in the vertical direction to be vertically averaged and used for map interpolation. Those wells or MLS that had less than five vertical sampling locations were not included in the map interpolation and are marked by the X symbol on the map. The standard kriging algorithm used in SURFER™ mapping software was used to interpolate the irregular data onto a regular grid for contouring. A linear variogram was used in the kriging process.

Figures C-6 through C-10 show the corrected, vertically averaged, cumulative organic tracer concentration contour maps. These figures also contain the MLS data locations used to generate the maps. The concentration data were corrected according to the suggestions of Stauffer *et al.* (1994). In addition, because Bioplume II can simulate only one organic compound at a time, the concentration of all four organic tracers was summed at each sample location to determine a combined "cumulative" organic tracer concentration for that location. Finally, all the concentration data from each MLS were vertically averaged to accommodate comparison to Bioplume II results. The symbols marking the sampling locations on the map have the same meaning as discussed above for the tritium maps.

Figure C-11(a) shows the areal distribution of interpolated combined organics plume as a function of concentration. The plot shows the significant increase in areal distribution at Snapshots 3 and 4. Figure C-11(b) shows the distribution of combined organics mass as a function of concentration. This figure indicates that, at Snapshot , only 20 percent of the mass of the plume is contained within the 500 ug/L contour. However, at Snapshot 4, over 90 percent of the mass of the plume is contained by the 500 ug/L contour. These plume dynamics may have a big influence on the types and rates of natural attenuation processes that act on the contaminants. Figure C-12(a) shows a comparison of estimated vertical distribution of the interpolated tritium plume. The graph shows the comparison of the three values. The "injected" value shows the total tritium activity at each snapshot (1 to 4). These activity values remain the same through time because the small amount (6.7 percent) of radioactive decay that occurs during the experiment is not accounted for in these values. The "vertically averaged" values for each snapshot represent the activity that is calculated when the vertically averaged concentrations are assumed to be fully mixed throughout the thickness of the aquifer (which is assumed to be 11 meters). The "thickness-adjusted" activity is the same as the "injected" activity because the aquifer thickness used to calculate the total pore volume enclosed by the plume is adjusted so that the "thickness-adjusted" activity is the same as the "injected" activity. The numbers on top of

each bar indicate the aquifer thickness used to calculate the total activity. The purpose of this graph is to show how the vertically averaged plumes relate to the known injected activity for tritium. The thickness-adjusted values indicate that, with each successive snapshot, the aquifer thickness required to match the injected activity increases. This indicates that the plume is not fully mixed during the first half of the experiment and only at Snapshot 4 does the adjusted aquifer thickness of 10.3 meters compare to the average aquifer thickness estimated from field observations (11 meters). This analysis indicates that applying a vertically integrated model at sites with a relatively thin aquifer may have an impact on the appropriateness of the model. It is estimated that the simulated concentrations near the injection zone were two or three times smaller than the observed values for this reason.

Figure C-12(b) shows the results of the same analysis for the combined organics plume. Because the organics plumes were degraded through time, the injection mass was not valid as a comparison. Therefore, the total mass estimates from the moment analysis (Stauffer *et al.*, 1994) were assumed to be the "correct" value for comparison purposes. The same trend is observed for this combined organics plume, except that the difference between the mass estimated from the moment analysis and the vertically averaged plumes is not as great as for tritium. This may be caused by (1) the difference in the comparison value (known injected activity for tritium versus moment-estimated mass for organics), or (2) the dynamics of the plume development caused by the biodegradation of the organic tracers.

Figure C-13 compares the "adjusted-thickness" values for the organic and the tritium tracers. Although the adjusted thickness values may be different for the organic and tritium tracers for some snapshots, the increasing trend is the same for both tracers. This finding is confirmed by Figures 11 through 13 in Stauffer *et al.* (1994), which show that the plumes are not fully mixed throughout the aquifer.

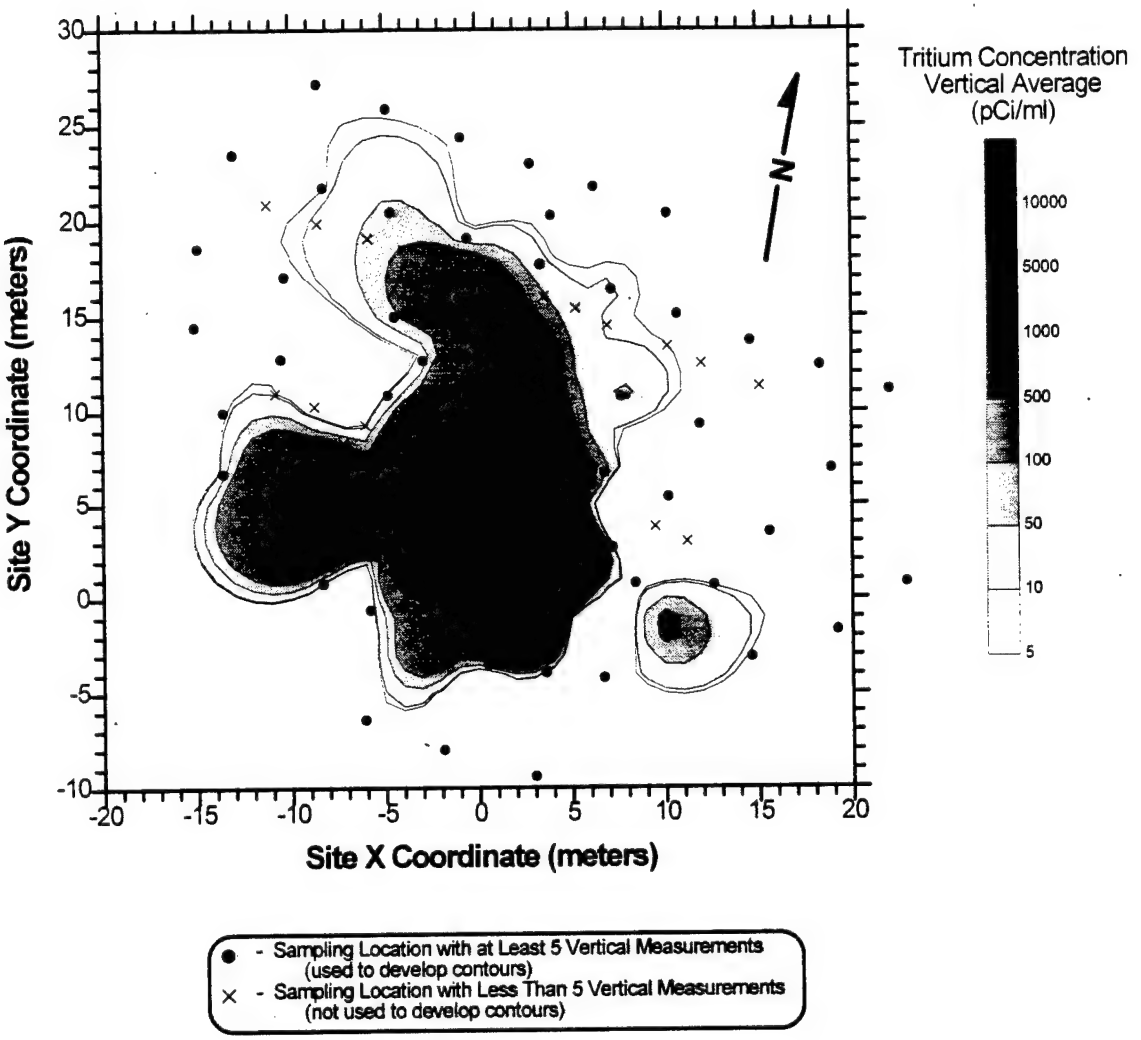

Figure C-1. Vertical Average of Observed Tritium Concentration (Snapshot 1, 27 Days After Injection).

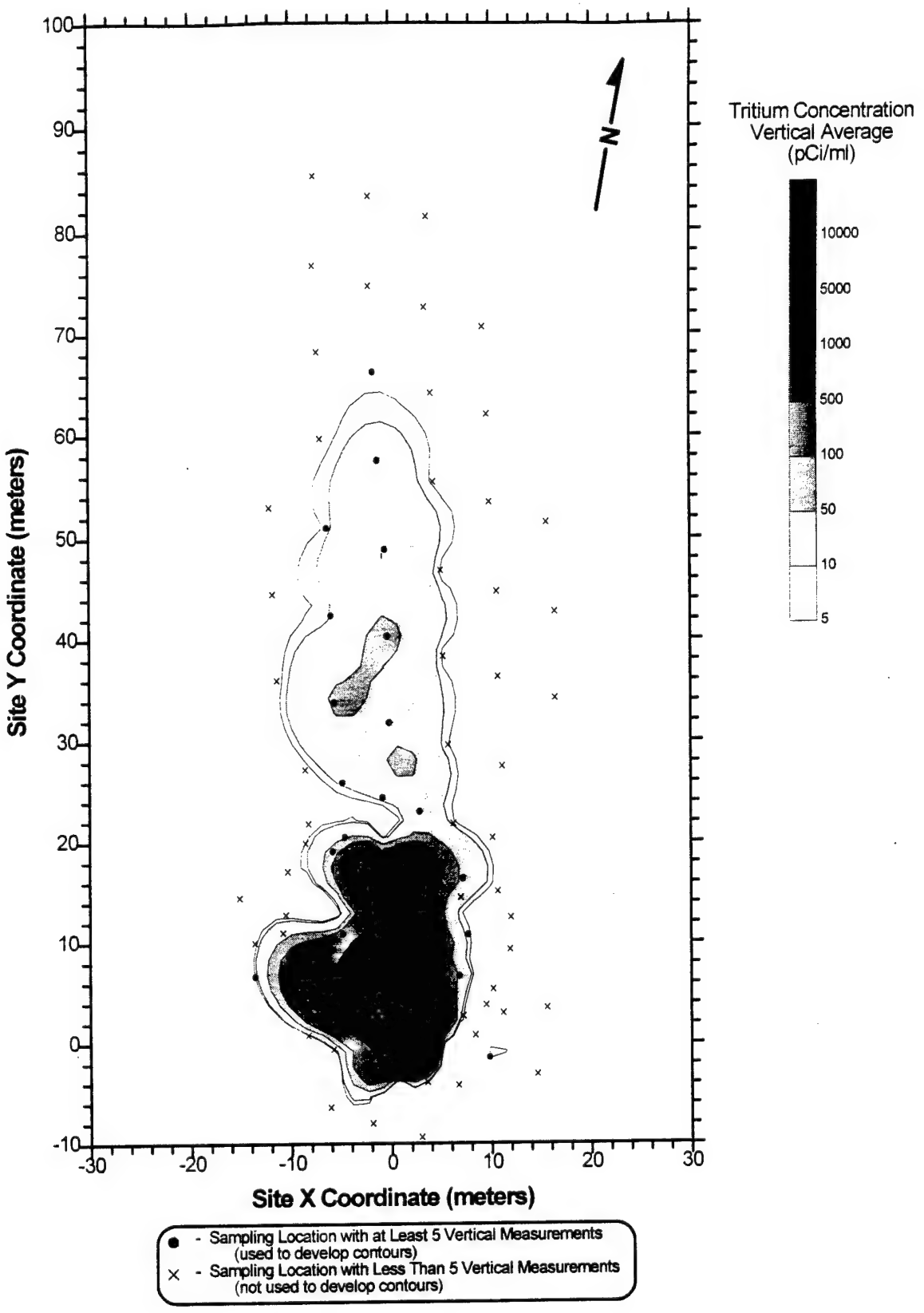

Figure C-2. Vertical Average of Observed Tritium Concentration (Snapshot 2, 132 Days After Injection).

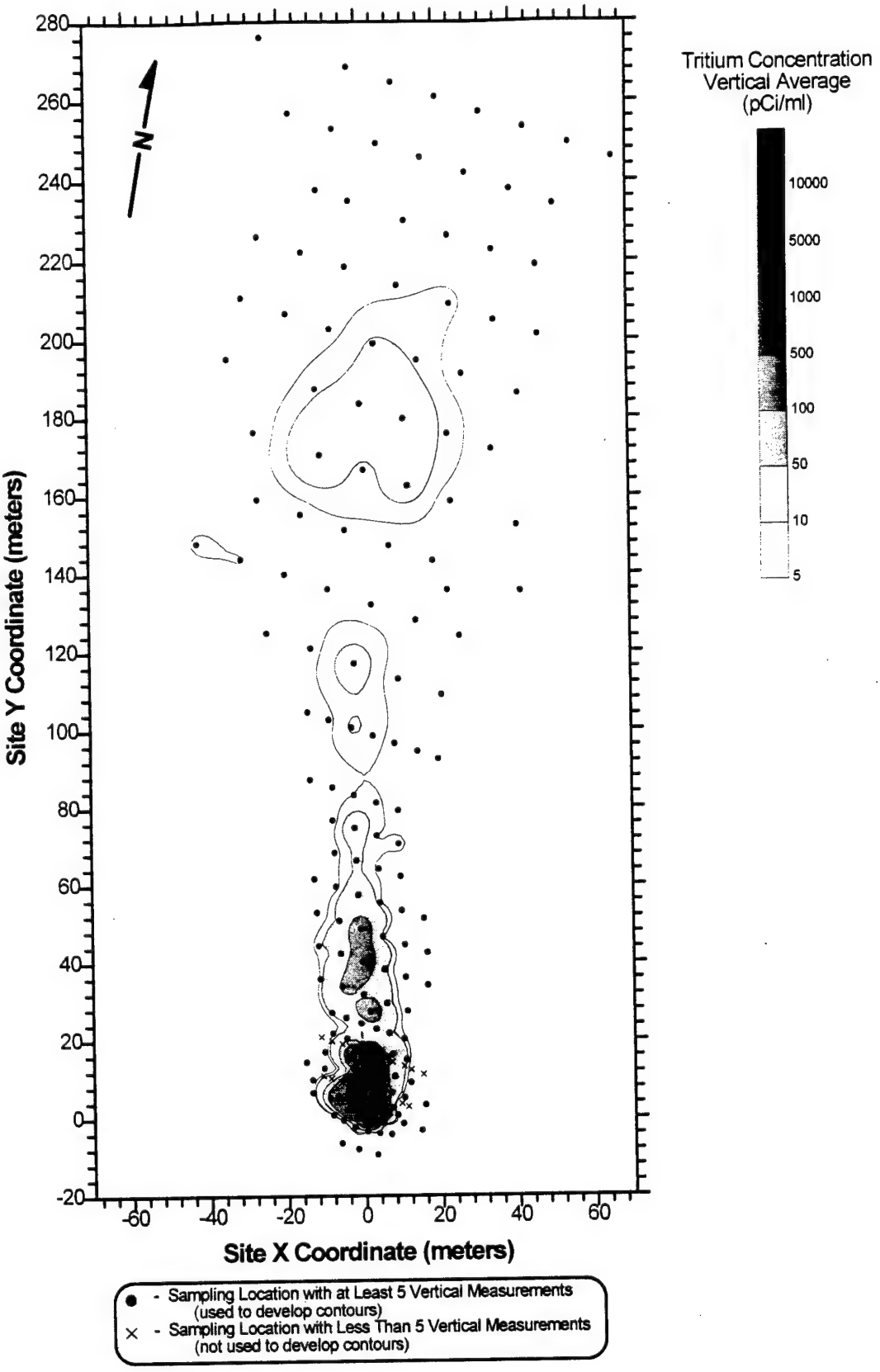

Figure C-3. Vertical Average of Observed Tritium Concentration (Snapshot 3, 224 Days After Injection).

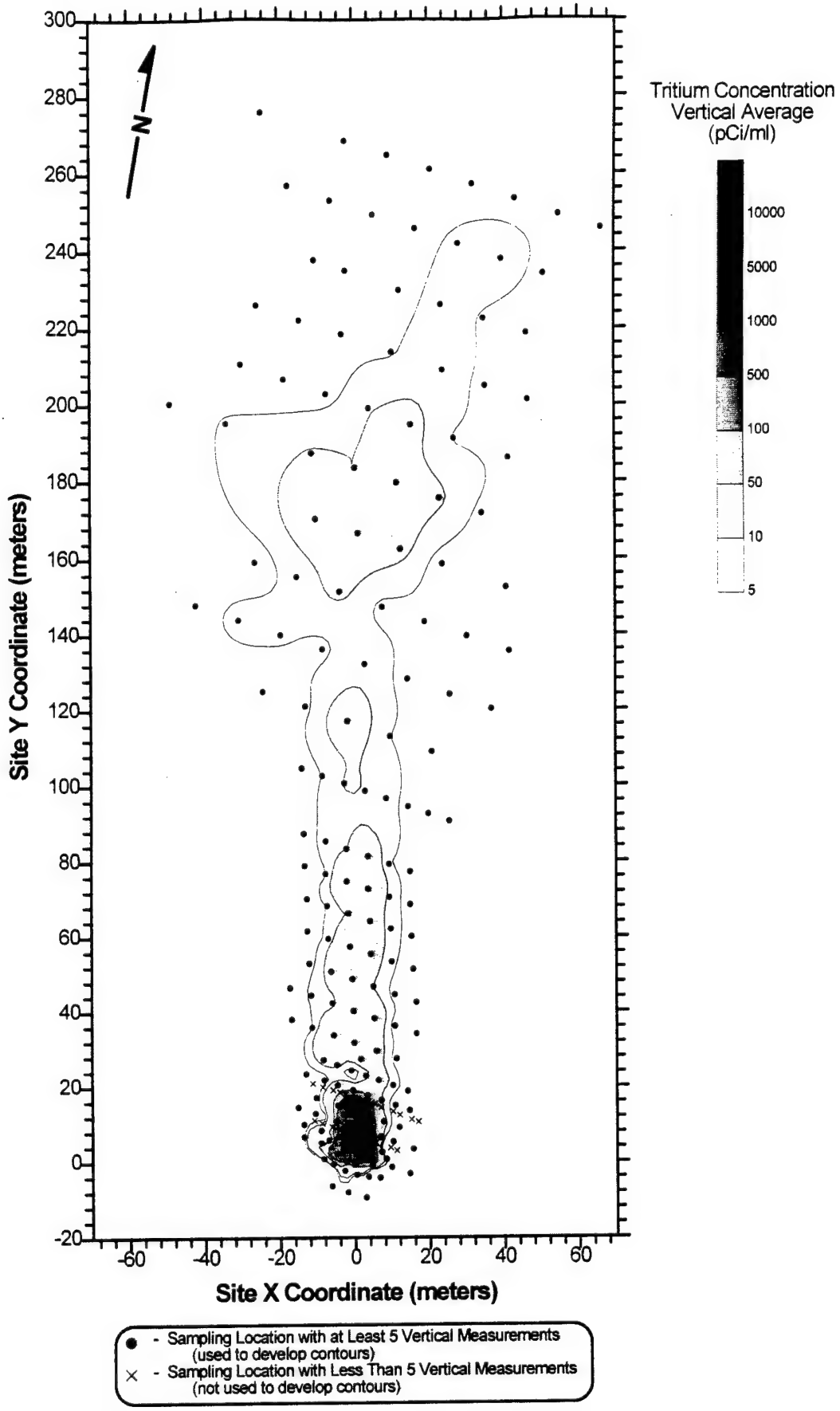

Figure C-4. Vertical Average of Observed Tritium Concentration (Snapshot 4, 328 Days After Injection).

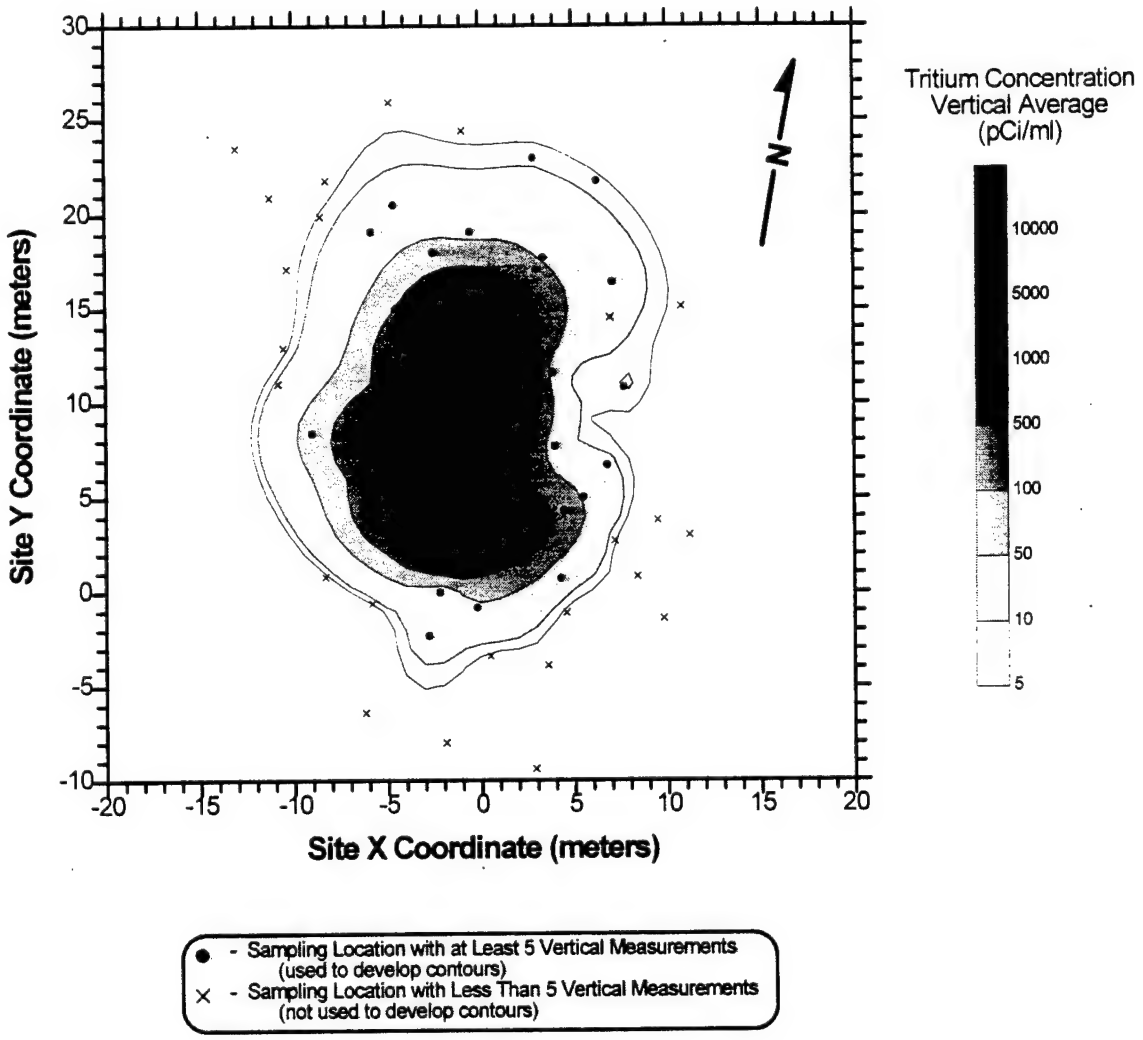

Figure C-5. Vertical Average of Observed Tritium Concentration (Snapshot 5, 440 Days After Injection).

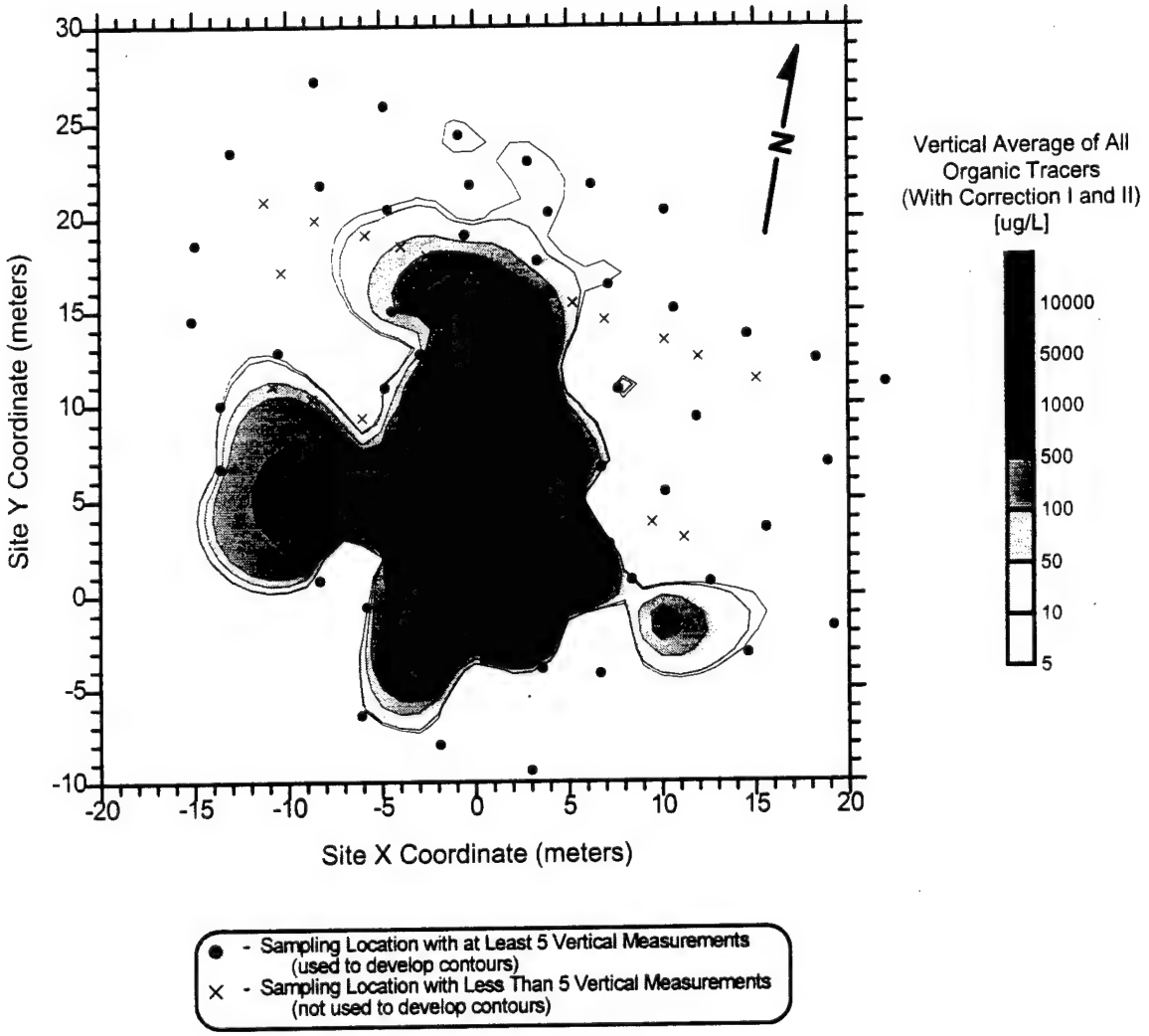

Figure C-6. Vertical Average of Observed Combined Organics Concentration (Snapshot 1, 27 Days After Injection).

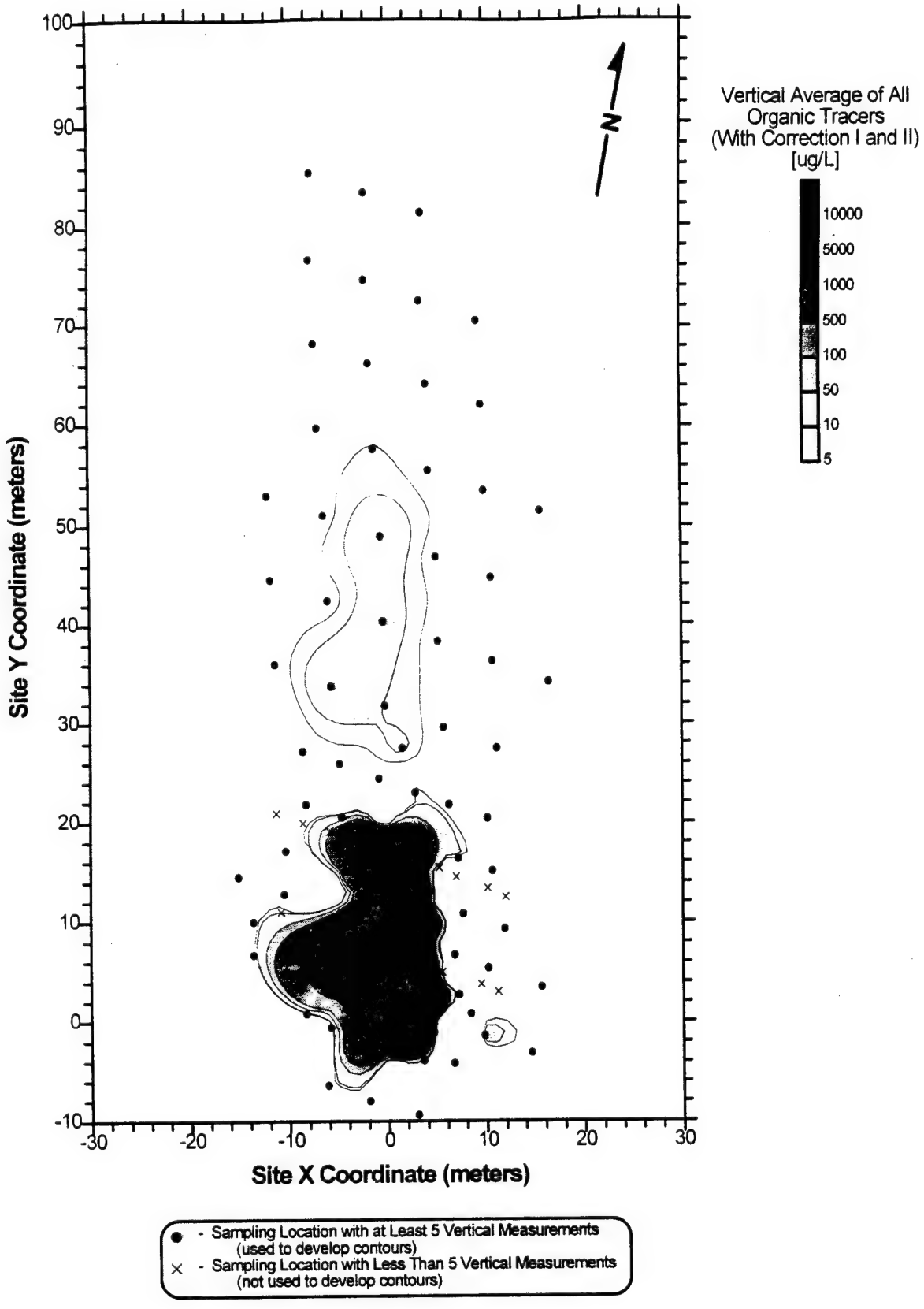

Figure C-7. Vertical Average of Observed Combined Organics Concentration (Snapshot 2, 132 Days After Injection).

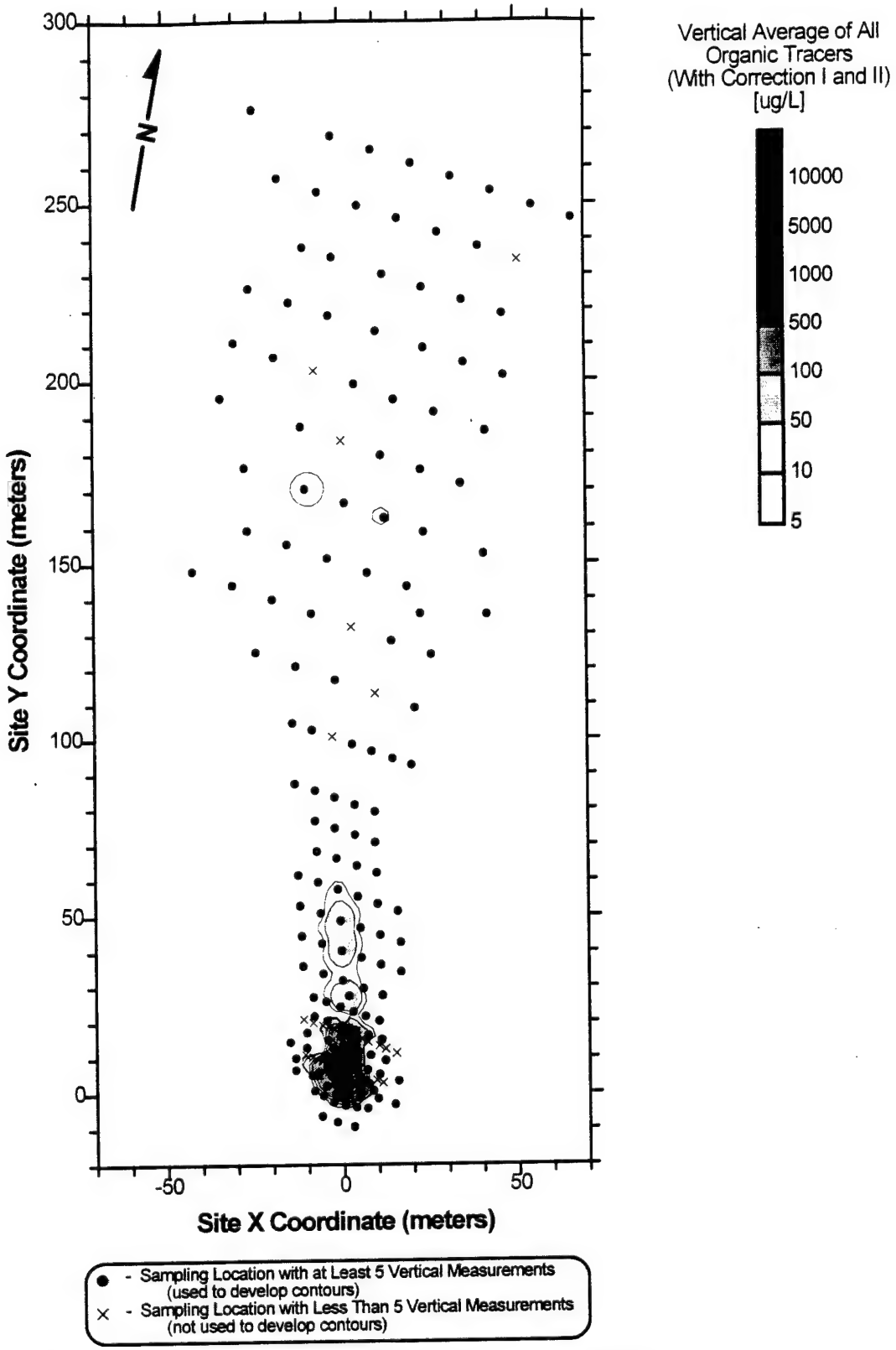

Figure C-8. Vertical Average of Observed Combined Organics Concentration (Snapshot 3, 224 Days After Injection).

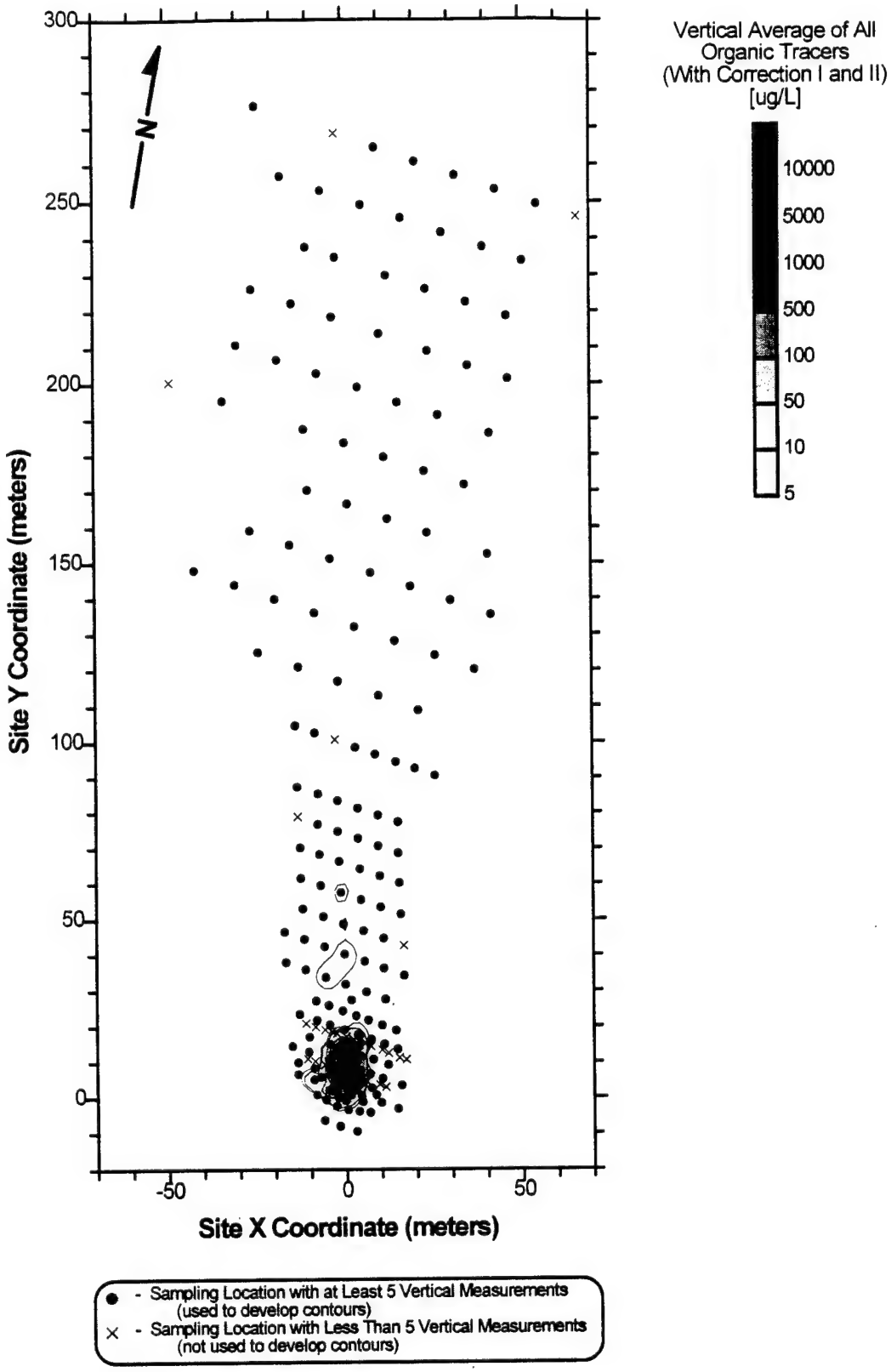

Figure C-9. Vertical Average of Observed Combined Organics Concentration (Snapshot 4, 328 Days After Injection).

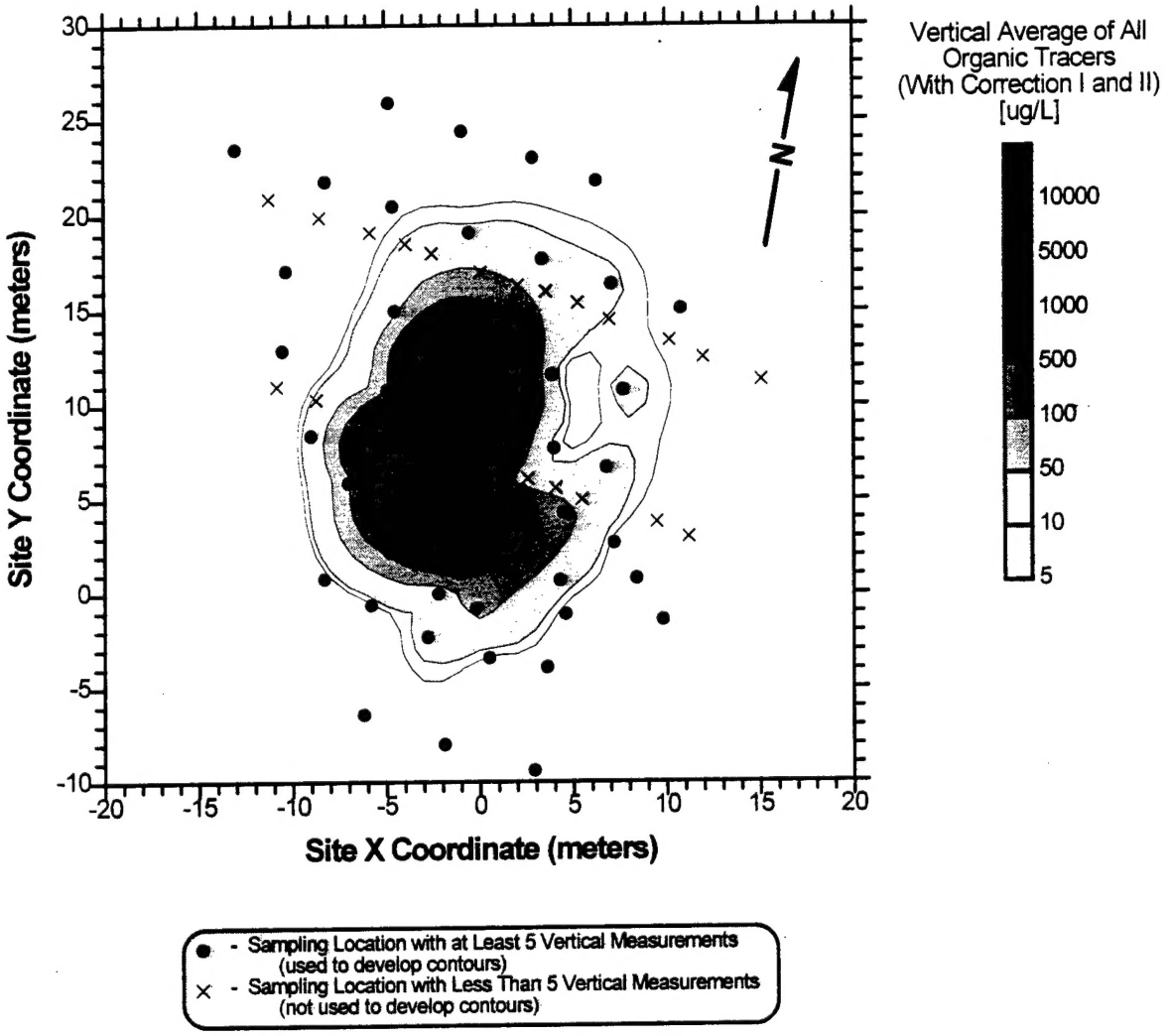

Figure C-10. Vertical Average of Observed Combined Organics Concentration (Snapshot 5, 440 Days After Injection).

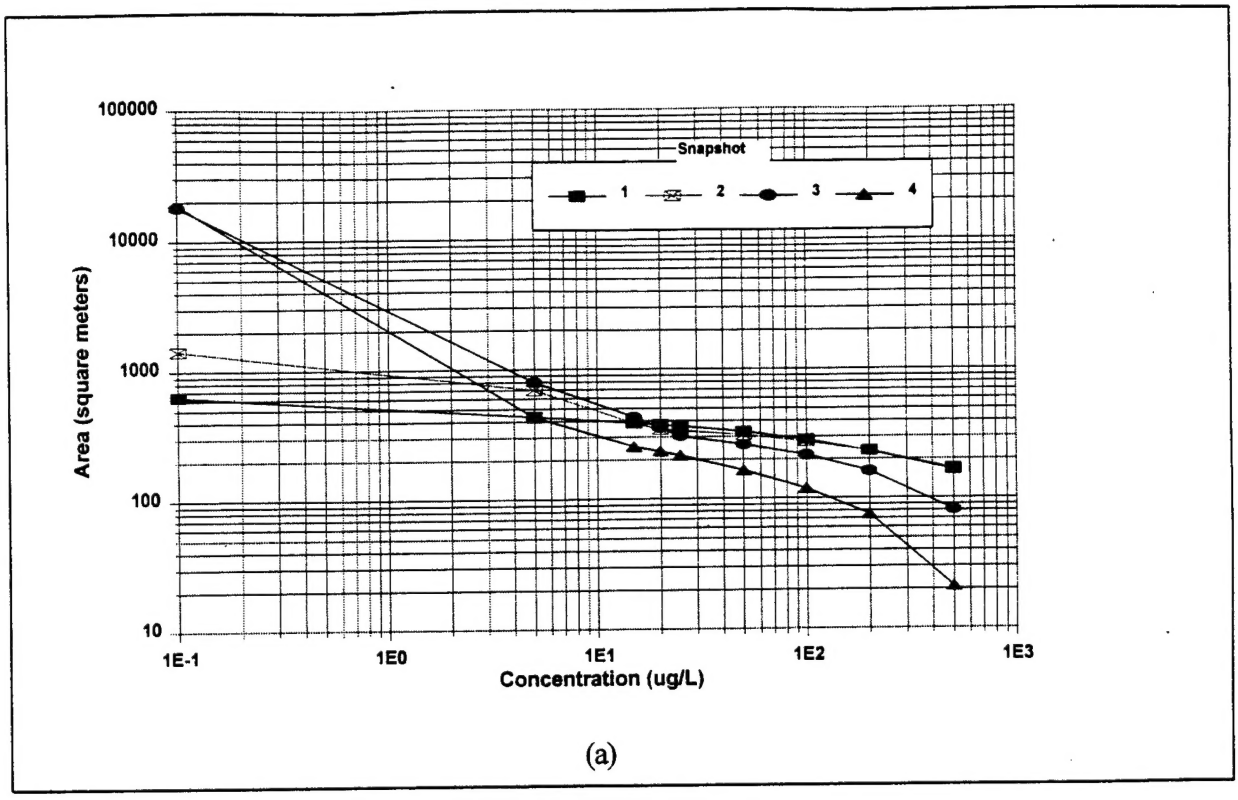

(a)

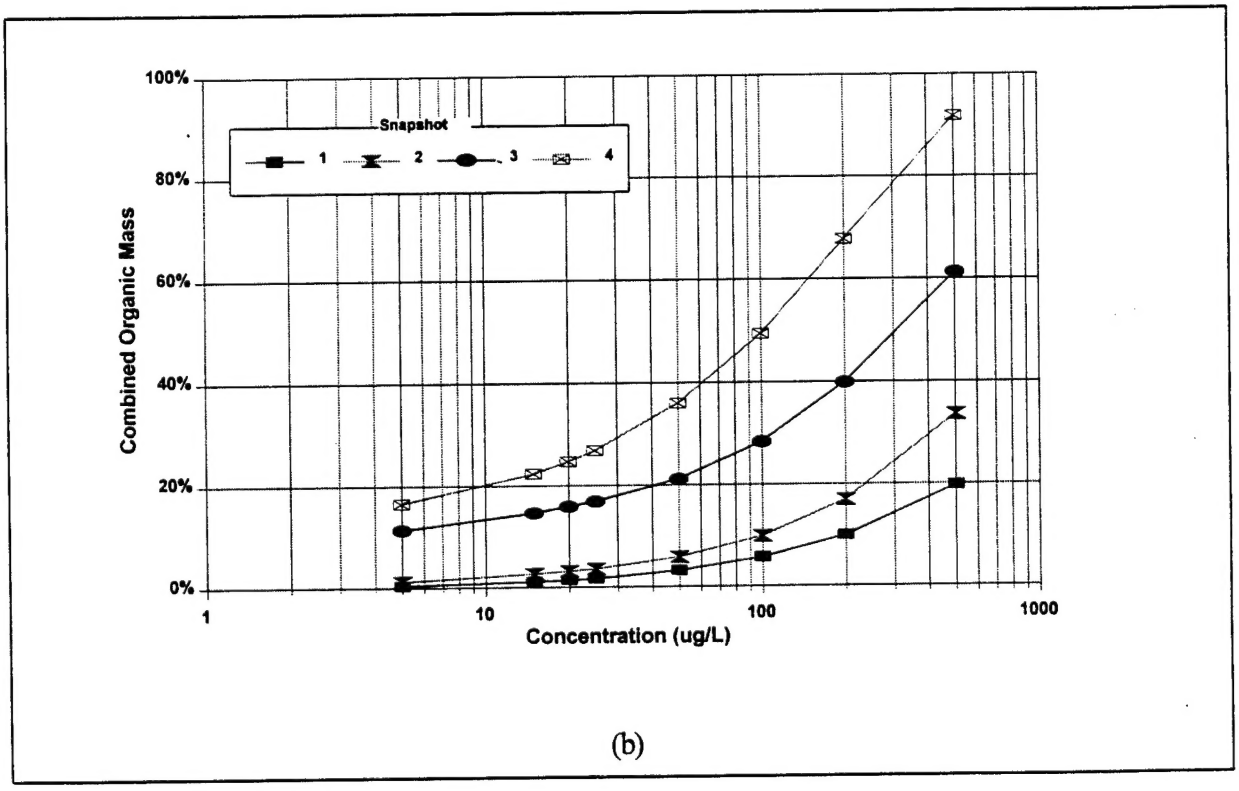

(b)

Figure C-11 (a). Areal Distribution of Interpolated Combined Organics Plume.
(b). Distribution of Combined Organics Mass as a Function of Concentration.

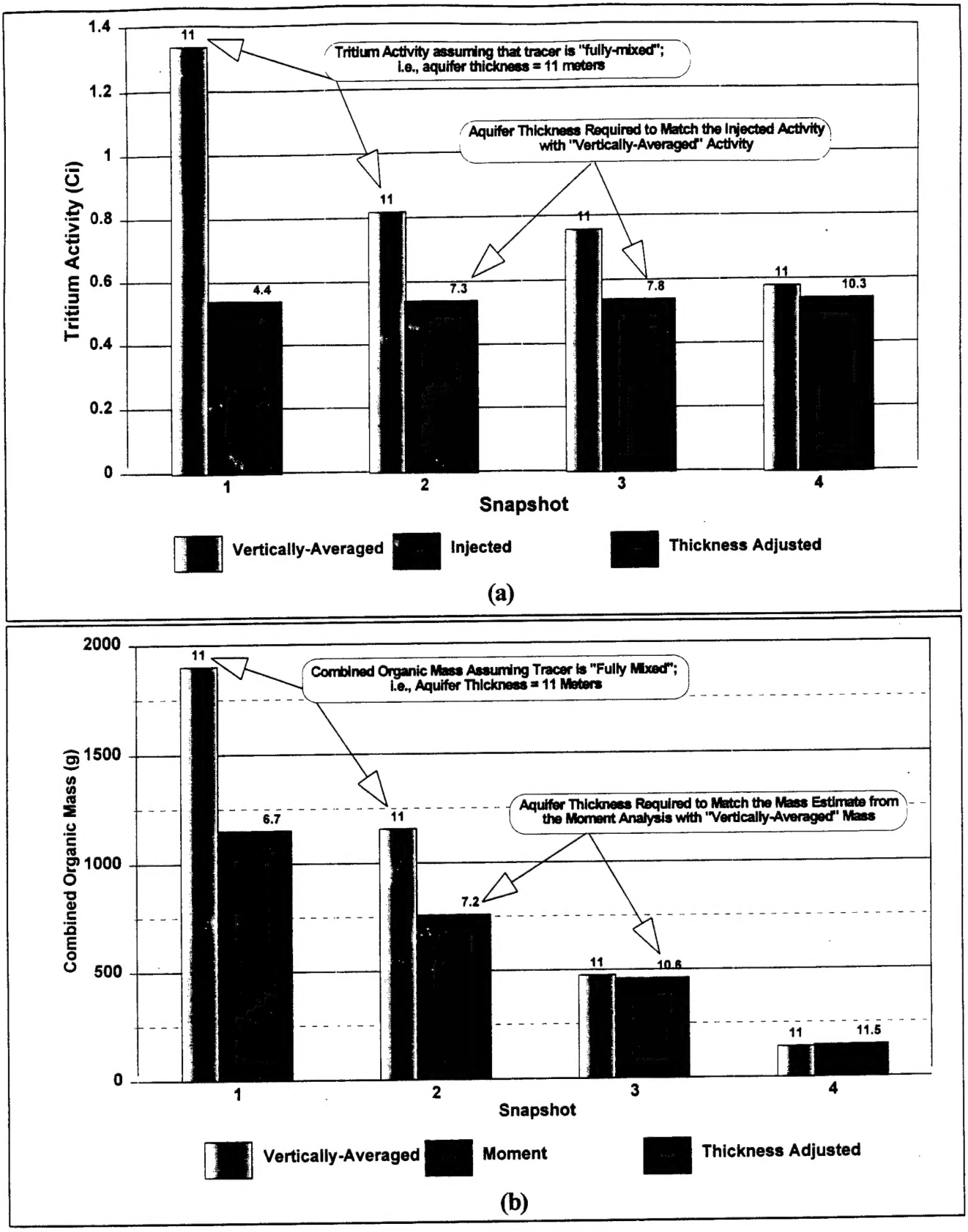

Figure C-12 (a). Vertical Distribution of Tritium Plume.
(b). Vertical Distribution of Combined Organics Plume.

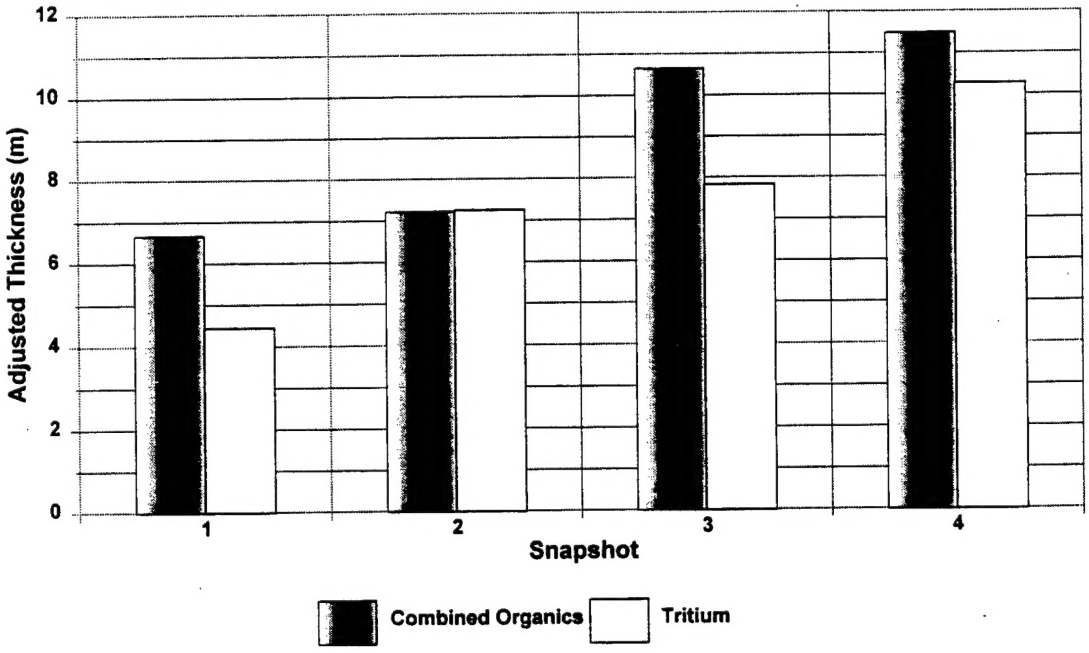

Figure C-13. Comparison of Adjusted Thickness Estimates for Tritium and Combined Organics Plumes.